DEVELOPMENT AND CHARACTERIZATION OF METAL-CERAMIC COMPOSITE CASTINGS THROUGH MICROWAVE HYBRID HEATING

A thesis submitted in the fulfillment of the requirement for the award of the degree of

DOCTOR OF PHILOSOPHY

IN

MECHANICAL ENGINEERING

Submitted by

SATNAM SINGH

Roll No. 951308003

Under the supervision of

Dr. Dheeraj Gupta
Associate Professor
MED, TIET, Patiala

Dr. Vivek Jain
Associate Professor
MED, TIET, Patiala

THAPAR INSTITUTE
OF ENGINEERING & TECHNOLOGY
(Deemed to be University)

DEPARTMENT OF MECHANICAL ENGINEERING

THAPAR INSTITUTE OF ENGINEERING & TECHNOLOGY, PATIALA-147004, INDIA

January – 2018

...DEDICATED TO MY FAMILY

CERTIFICATE

I, Satnam Singh, Roll. No. 951308003, hereby declares that the thesis entitled **"Development and Characterization of Metal-Ceramic Composite Castings through Microwave Hybrid Heating"** submitted to the Department of Mechanical Engineering at Thapar Institute of Engineering & Technology, Patiala, Punjab, for the award of the degree of **Doctor of Philosophy**, is a record of original bonafide research work carried out by me under the supervision of **Dr. Dheeraj Gupta** and **Dr. Vivek Jain**. All the requirements for the submission of this thesis have been fulfilled as per institute norms.

The results presented in this thesis have not been submitted elsewhere for the award of a degree or diploma.

25/01/18

Satnam Singh

Roll. No. 951308003

25/02/18

Dr. Dheeraj Gupta

Associate Professor

Department of Mechanical Engineering

Thapar Institute of Engineering & Technology

25/01/18

Dr. Vivek Jain

Associate Professor

Department of Mechanical Engineering

Thapar Institute of Engineering & Technology

Date: 25/01/18

Place: Thapar Institute of Engineering & Technology, Patiala-147004, Punjab, India.

ACKNOWLEDGEMENT

First and foremost, I wish to thank my supervisors **Dr. Dheeraj Gupta** and **Dr. Vivek Jain** for their valuable support, supervision, guidance and belief in me. I am thankful for the positive suggestions, and meticulous guidance that helped me to improve my scientific writing and carry out the new research. I feel really motivated and honored to work under their guidance throughout my entire Ph.D. work.

I wholeheartedly thank the doctoral committee members **Dr. S. K. Mohapatra** (Chairman, Board of Studies), **Dr. Ajay Batish, Dr. Kulvir Singh**, **Dr. Dheeraj Gupta** and **Dr. Vivek Jain** for the feedback and reviews that were given on my research proposal and progress monitoring presentations. Their guidance was beneficial for me to improve my research work. I am also thankful to **Dr. Tarun Nanda** and **Dr. Gagandeep Bhardwaj** our Ph.D. coordinators for their approachability and keeping me informed with all the relevant communication throughout E-mails.

A special thanks to the office of Mechanical Engineering Department for providing all the facilities required for research work. Thanks to all my lab mates, colleagues and friends for their support and a very special and sincere thanks to Mr. Sarbjeet Kaushal, Mr. Rohit Kumar, and Mr. Ripan Sarkar, who had helped me a lot during my research work. I am thankful to the office staff of the ME department at Thapar Institute of Engineering & Technology for their help and cooperation throughout my study.

I would like to thank my wife, Ms. Shilpa for his understanding and continuous support during my thesis work. I am very thankful to my daughter, Seerat Singh, for her love and patience which gave me encouragement and positivity during my work. It has not been easy and

I could not have completed it without their love and encouragement. I want to thank my younger brother Mr. Vikas Sarwara for help and support during my study period.

A huge thanks goes to my parents, Hony. Capt. (Retd.) Dharam Singh and Mrs. Amarjit Kaur and parents-in-law, Mr. Narender Singh and Mrs. Sudesh, who always encouraged me and stood by me. I thank all my family and relatives who had supported and cared for me during my research work. I wish to thank all those who have helped me directly or indirectly in this journey of my life.

Finally, I bow and thank the Almighty, without whom I could have not completed this journey of completing my research work for the highest degree in the engineering discipline.

Satnam Singh

ABSTRACT

The manufacturing sector of any country plays an important role in its economic development, but it consumes more than 30% of the energy resources. Within the manufacturing domain, the melting and casting of steel and iron consumes majority of the primary energy resources and responsible for 38% of CO_2 emissions worldwide. To handle such situations, technologists, researchers and academicians are continuously working towards efficient processing of materials such that production cost can be reduced and energy can be saved. The conventional manufacturing practices are getting obsolete due to higher energy consumptions; higher pollution levels, low productivity and formation of higher defects in developed component. The alternative or new processing methods are required to reduce production or manufacturing costs, processing times, and to enhance product quality. Further, the developed technology should be widely acceptable for all types of materials such as metal matrix composites, ceramics, alloys, and fiber reinforced plastics. In current scenario, the focus is on the development of energy efficient and green processing methods, which are sustainable. Thus, it is of prime importance for the researchers to investigate alternative processing methods/techniques, which have the potential to overcome/lower the deficiencies of conventional one. The developed techniques are expected to be highly energy efficient, reduces CO_2 or other unwanted toxic gas emission, and produces better quality products at an effective processing cost.

In mid of year 90’s, microwave heating effects were discovered and microwaves were successfully utilized in the cooking sector with the discovery of the microwave oven. During 1980-1990 the utilization of microwave ovens spread throughout the world and become the essential part of home appliances due to the better efficiency and lower processing time characteristics. However, at the same time some commercial applications of microwave heating

were also discovered such as drying of wood, processing of rubbers, chemical processing, etc. The continuous efforts of researchers led to the development of microwave sintering process, which has emerged as one of the most promising technology in the materials processing field. However, microwave sintering was confined to the ceramics and ceramic based composites in different forms. Processing of metallic powders/metals through microwaves was unsuccessful due to lower skin depth associated with such materials. However, researchers led to the development of microwave hybrid heating techniques to process such materials like metals in the form of powders. But, still processing of metallic based materials is a challenging task at lower frequencies.

Lately, a lot of work in the field of microwave joining of bulk metals and cladding of metallic based powders on metallic substrates was reported. The joining and cladding was achieved with partial melting of metallic powders which motivated the researchers to explore the potential of microwave heating in powdered metal casting and in situ casting processes. Still, the majority of the work is reported on sintering of metallic powders and provided an opportunity to investigate the potential of microwaves to melt metallic based powders.

In the present work, microwave energy is utilized for melting and casting of powdered metal-ceramic composites. The domestic microwave oven working at 2.45 GHz and 900 W maximum power is used as microwave applicator. Microwave hybrid heating was used with charcoal as a susceptor material; for melting the nickel based metal powder particles. For the development of various MMC's, commercially available EWAC 1004EN powder was selected as matrix material, which is approximately 97% nickel and ceramic reinforcements of silicon carbide (SiC), alumina (Al_2O_3) and tungsten carbide (WC-8Co) were selected. The matrix and reinforcements powders were premixed in a mechanical mixer to obtain homogeneously mixed

powders; with reinforcement volume fraction of 5% and 10%. The premixed powder was preheated to 200° C and placed in the graphite cavity; which is exposed to microwave radiations for optimum processing times. The cavity was allowed to cool under the atmospheric conditions for solidification of the castings. The developed castings were characterized using various relevant techniques to study the X-ray diffraction patterns (phase analysis), microstructural characterizations (using optical microscope and scanning electron microscope equipped with EDS), mechanical properties (microhardness, tensile strength and percent elongation) and functional characteristics (dry sliding wear behavior).

The XRD study of castings revealed the formation of various intermetallics which was due to higher processing time and intense heating by microwaves. On adding SiC reinforcement, intermetallic of Ni_2Si was observed, whereas pure EWAC casting revealed peak of intermetallic $FeNi_3$. Similarly, on adding alumina, nickel aluminide intermetallic peaks were observed, whereas Ni_4W major peak was observed in WC-8Co casting. All these intermetallics were favored due to the thermal degradation of reinforcements at higher temperatures. The EDS analysis revealed that the hard phases of chromium carbides, nickel carbide and cementite were precipitated along the grain boundaries. The microwave processed castings revealed the formation of equiaxed grains throughout the microstructures and this was due to the volumetric heating characteristics of microwaves. There was no evidence of dendritic transition from the cellular/equiaxed structures. The porosity content of developed castings was low, which is again due to the uniform heating profile obtained in MHH process.

The formation of various hard intermetallic compounds within the castings led to the higher average microhardness. The EWAC casting revealed average Vickers microhardness of 410±55 HV, whereas, the addition of 10% SiC led to microhardness of 980±208 HV, addition of

10% alumina led to microhardness of 985±80 HV and 10%(WC-10Co) reinforced casting revealed the microhardness of 1012±108 HV. Tensile tests revealed that EWAC casting possesses an average tensile strength of 330±15 MPa with average percent elongation of 33±2%. By adding the ceramic reinforcements the load carrying capacity increased, but hard phases of reinforcement restricted the plastic deformations thus producing lower elongations. By increasing the content of SiC to 10% volume fraction, the strength further increased by 26.67% (450±21 MPa) in comparison to EWAC casting with an average elongation of 10.5±2%. The average tensile strength of 10% alumina reinforced composite was 355±10 MPa, with percent elongation of 18±3%. The tensile strength of EWAC+10%(WC-8Co) composite increases to 508±6 MPa, which is 53.93% higher than EWAC casting and average percent elongation of 18±4%.

The functional characterization (in terms of dry sliding wear tests) results revealed lower wear rates in microwave processed MMC's in comparison to pure EWAC casting and this was due to higher microhardness and uniform dispersion of reinforcements. In comparison to the EWAC casting wear rate ($10.82x10^{-3}$ mg/s), the EWAC+10%(WC-8CO) casting revealed 12.8 times lower wear rate ($0.84x10^{-3}$ mg/s) under the 20 N load, 1.0 m/s sliding velocity and after 2000 m of sliding. The EWAC+10%SiC casting revealed 5.15 times lower wear rate ($2.1x10^{-3}$ mg/s) and EWAC+10% Al_2O_3 casting revealed 3.53 times less wear rate ($3.06x10^{-3}$ mg/s) in comparison to EWAC casting.

The overall results led to the conclusion that microwave energy was successfully employed in melting and casting of various MMC's with less energy consumption. The developed metal-ceramic composites can be used in many industrial applications where high strength and anti wear characteristics are required.

TABLE OF CONTENTS

LIST OF FIGURES

LIST OF TABLES

LIST OF ABBREVIATIONS

CMC	:	Ceramic Matrix Composite
CNT	:	Carbon Nano Tubes
CVD	:	Chemical Vapor Deposition
DSC	:	Differential Scanning Calorimetry
EDS	:	Energy Dispersive X-ray Spectroscopy
EM	:	Electro Magnetic
FGM	:	Functionally Graded Materials
GHz	:	Giga Heartz
GPa	:	Giga Pascal
HAZ	:	Heat Affected Zone
MHH	:	Microwave Hybrid Heating
MHz	:	Mega Heartz
MMC	:	Metal Matrix Composite
MPa	:	Mega Pascal
MS	:	Mild Steel
MW	:	Microwave
OM	:	Optical Micrograph
PJ	:	Peta (10^{15}) Joules
PMC	:	Polymer Matrix Composite
SEM	:	Scanning Electron Microscopy
SS	:	Stainless Steel
TD	:	Theoretical Density
UTS	:	Ultimate Tensile Strength
WC	:	Tungsten Carbide
XRD	:	X-ray Diffraction
YS	:	Yield Strength

LIST OF SYMBOLS

m	:	Meter
mm	:	Millimeter
λ	:	Wavelength
H	:	Magnetic field
E	:	Electric field
ε'	:	Real permittivity (dielectric constant)
ε''	:	Imaginary permittivity (dielectric loss factor)
ε_c	:	Complex permittivity
$\tan \delta$	:	Loss tangent
δ	:	Skin depth
σ	:	Electrical conductivity
f	:	Frequency
μ	:	Electrical resistivity
P	:	Power absorbed
μ_o	:	Magnetic permeability
μ''	:	Magnetic loss factor (Imaginary part)
E_{rms}	:	Root mean square of the electric field
H_{rms}	:	Root mean square of the magnetic field
P_o	:	Incident power
x	:	Distance within the material
α	:	Attenuation factor
m	:	Mass of material
C	:	Specific heat of material
Δt	:	Temperature difference
V	:	Volume of the material
t	:	Time of microwave exposure
T_C	:	Time taken in conventional heating
T_M	:	Time taken in microwave heating
μm	:	Micrometer

wt	:	Weight
min	:	Minutes
nm	:	Nanometer

CHAPTER 1

INTRODUCTION AND OVERVIEW

1.1 INTRODUCTION

The efficient processing of materials is one of the primary concerns for the technologists, researchers and academicians. There is a great need to reduce the energy requirements in processing of materials which allowed the researchers to come up with newer clean and green technologies. The newer developing processes should survive the present cut throat engineering environment and should be sustainable. The in-general requirements for any manufacturing processes/techniques to qualify for the efficient processing methods are as illustrated in Fig. 1.1.

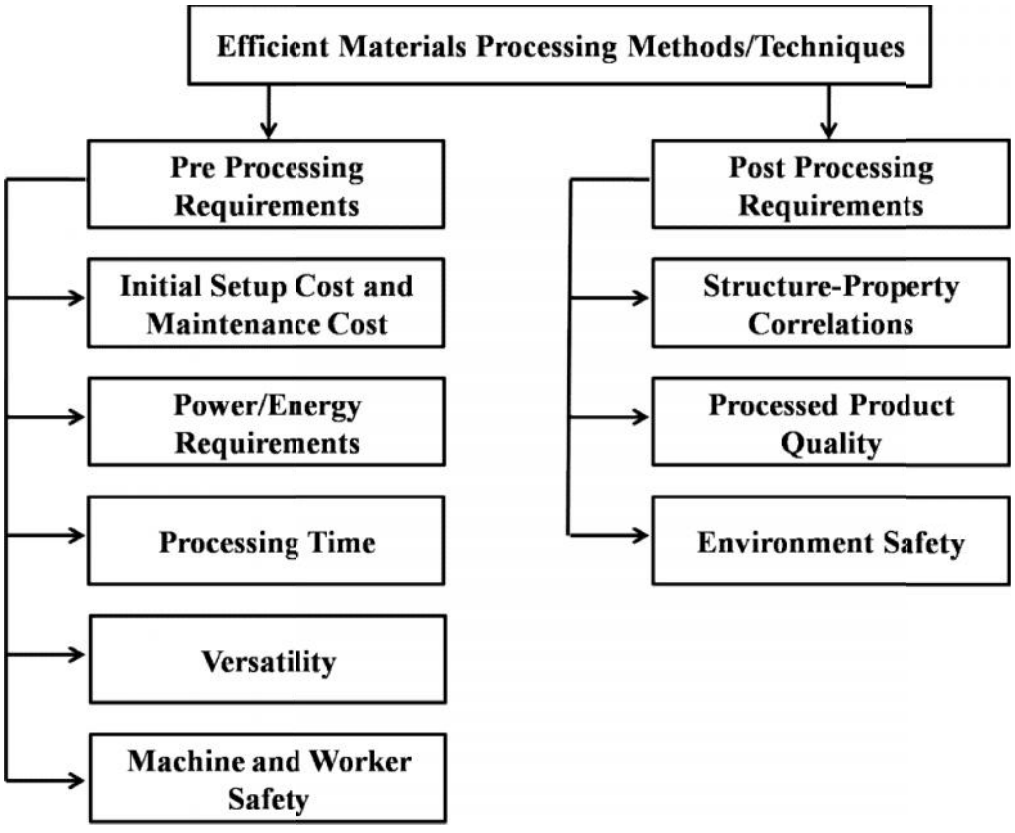

Fig. 1.1: General requirements of efficient materials processing methods

These requirements can be categorized into two parts, i.e. pre and post processing requirements. The pre-processing requirements describe the initial factors of any process which are responsible for the efficient processing. These factors include; initial setup cost, maintenance cost of the system, energy requirements for processing of materials, lower processing time, universal utilization of available materials (versatility) and safety of the workers. All these factors should contribute in such a way that economy of processing method can be attained. The post-processing requirements generally include the structure-property correlations of processed materials, quality of processed product (in terms of lower defects such as porosity) and impact on the environment.

It has been seen that the old manufacturing/processing methods are getting obsolete due to higher energy consumptions and lower efficiencies. It has been reported [Apostolos et al. (2013)] that energy efficiencies of such processes act as a driver for the manufacturing industries which are one of the major energy consumers worldwide. As per the authors [Reddy and Ray (2010)], industrial sector in India accounts for 36% of energy consumption and out of this 36%, the 66% consumption (year 2004-2005) is in iron and steel, pharmaceuticals, cement and paper industries. The contribution of heating and melting alone stands the highest with ~30% energy consumption.

Table 1.1 provides the estimate of total energy consumption in India from 1970-2005. It can be observed that from the year 1970 to 2005 the primary energy consumption has increased to 22040 PJ from 6274 PJ, with a growth rate of 3.7% per annum. However, for the same period of time the consumption of commercial energy grew by a rate of 4.6%. Similarly, commercial energy consumption in industries has increased from 1235 PJ for 1970-71 to 4283 PJ for 2004-05, with a steady growth rate of 3.6%.

Table 1.1: Total energy consumption in India (1970-2005) [Reddy and Ray (2010)]

Energy utilization (PJ or %)	Year					Growth rate per annum
	1970-71	1980-81	1990-91	2000-01	2004-05	
Primary energy consumption	6274	8884	13017	18668	22040	3.7
Commercial energy consumption	2488	3440	6721	9735	11852	4.6
Commercial share in %	39.7	38.7	51.6	52.2	58	
Commercial energy consumption by industries	1235	1418	2609	3596	4283	3.6
Industrial share in commercial energy consumption in %	49.64	41.22	38.82	36.94	36	

Table 1.2: Energy consumptions (PJ) by various manufacturing industries [Reddy and Ray (2010)]

Sector	Year			%total manufacturing
	1995	2000	2005	
Aluminium	202	260	351	12.2
Beverages and Tobacco	3	3	4	0.1
Cement	236	315	471	16.4
Chemicals	287	463	605	21.2
Copper	5	11	13	0.4
Food products	22	46	57	2
Iron and steel	595	702	733	25.6
Machinery	2	3	3	0.1
Mining	1	5	6	0.2
Other nonmetals	42	38	43	1.5
Paper	121	181	238	8.3
Textiles	65	245	339	11.8
Transport equipments	4	4	4	0.1
Total	1583	2274	2867	100.0

Table 1.2 shows the energy consumption in various manufacturing sectors. Iron and steel making alone contributes to the 25.6% of energy consumption, which is the highest among all the sectors. However, the second highest energy consumption is required in chemical industries. The review article by the authors [Apostolos et al. (2013)] reported the utilization of 33% of primary energy resources in the manufacturing sector and this manufacturing segment is responsible for 38% of CO_2 emissions worldwide. Further, the major part of the energy is utilized in primary manufacturing processes and it is mainly in the melting and casting of ferrous/non-ferrous materials. The energy consumption in any industry can be studied by energy audit process and it helps in determining the energy consumption patterns. These energy consumption patterns can help in understanding the manner, in which energy is utilized and it also helps in the selection of areas where energy conservation can be possible. The typical energy consumption pattern for a foundry is represented in Table 1.3.

Table 1.3: Distribution of energy consumption in foundry [Arasu and Jeffrey (2009)]

S. No.	Sections	Energy Consumption (%)
1	Melting	70
2	Molding and core making	10
3	Sand plant	6
4	Lightning	5
5	Compressor	5
6	Others	4

The melting of materials involves the 70% of energy in any foundry practices and it is the major energy consuming process among all. The energy consumption study provides the scope for improvement in this area; so that effective energy utilizations can be incorporated to bring down the energy consumption requirements.

The casting of materials is one of the oldest and widely used methods of materials processing [Salonitis et al. (2016)]. Melting and casting of iron and steel is considered as one of the major processes carried out throughout the world and is the main factor contributing to the high energy requirements with higher emission of pollutants. The casting processes can be classified into various categories as shown in Fig. 1.2.

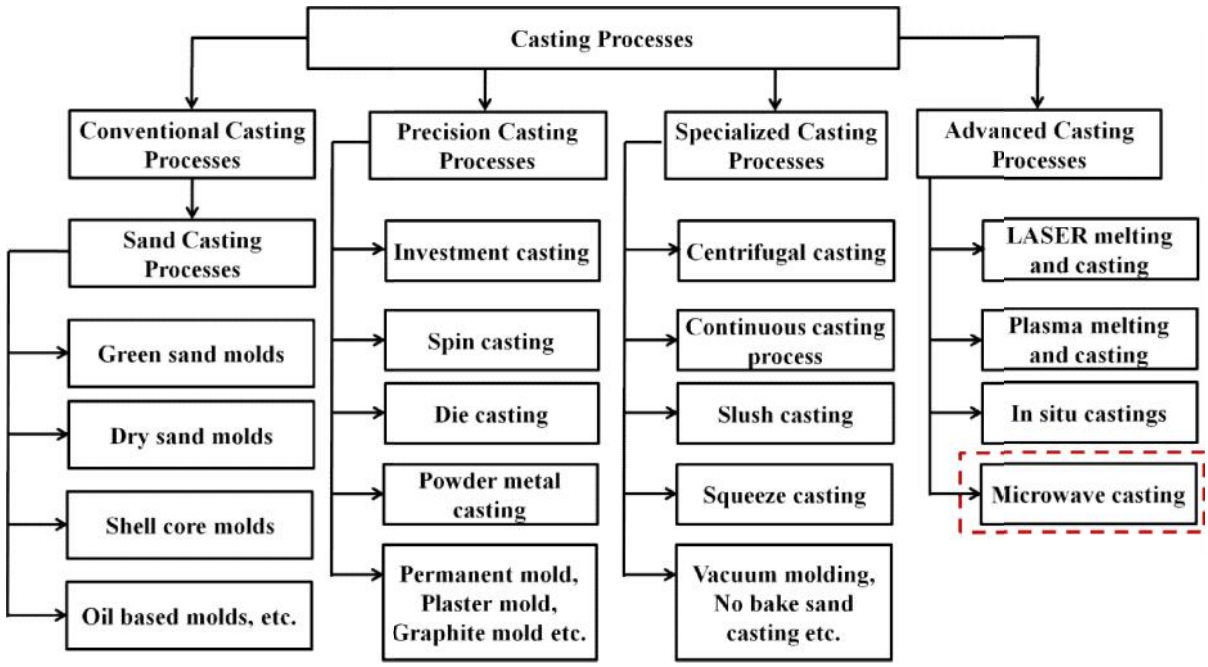

Fig. 1.2: Broad classification of casting processes

The conventional casting processes are one of the oldest and widely used manufacturing processes; which are still in practice for many industries. The basic operations of the conventional casting process include sand mold preparation (cope, drag and cheek), pattern making, gating system design, core making, melting of metal, pouring and solidification of castings, and inspection of castings. Over the years, the casting operation remains the same, but a lot of work has been carried out in the mold design. To acquire the basic properties of strength, permeability and collapsibility; green sand molds are modified with various binders and new

mold are used such as loam mold, compo mold, cement bonded molds, oil based molds, etc. In the dry sand molding, molds are created by adding binders to the un-bonded sand, which is formed to the mold and baked. These dry sand molds are extensively used to acquire the close tolerances and to produce a better surface finish. Still, conventional casting processes are used for obtaining various castings in the field of material science, automotive applications, aerospace, marine applications etc.

These casting processes were further improved to produce the near shape castings, net shape castings and precision castings. In recent times, significant research work [Guo et al. (2014) and Aguilar et al. (2011)] has been carried out to develop such casting processes. The main aim of precision casting processes is to obtain intricate shapes with high accuracy and close dimensional tolerances. This process allowed the less utilization of secondary manufacturing processes and finally yields castings which can be utilized directly. The precision casting processes include the investment casting processes, die casting process, permanent mold casting, spin casting, powder metal casting (sintering), etc. The die casting processes are widely used in manufacturing of various automotive parts and are one of the highly automated processes in the manufacturing industries. Another process known as powder casting or sintering is one of the fastest growing technology in the material processing domain. Sintering allowed the development of various alloys, composites and advanced materials which were not feasible to produce through the conventional processes. It further allowed the high temperature processing of ceramics in various fields of manufacturing, thin coatings, claddings, etc. To further minimize the wastages and to lower the processing times, specialized casting processes were developed such as continuous casting processes, slush casting, squeeze casting process, vacuum molding

etc. These processes allowed processing of complex shape castings with better dimensional tolerances, higher production rates and quality castings.

To further explore the benefits of materials processing technologies in the challenging environment of engineering, research was carried out in the advanced casting processes. The main aim was to reduce the energy consumptions, to obtain quality products, to reduce processing times and to minimize the environmental pollution, which is still the problem for conventional casting processes. The laser casting and cladding processes have emerged as one of the novel routes in materials processing and having commercial applications since 1970 [Gedda and Powell (2005)]. These processes have made significant advancements and are the best available methods for materials processing in terms of claddings, joining, welding, precise manufacturing, etc. The main concern in laser processing of materials is the high initial cost involved in the equipment, higher maintenance cost, safety issues and lower rate of performance (i.e. Deposition of materials in clads, machining and melting). The development of high thermal stresses due to intense heating involved in smaller areas which can lead to thermal cracking and the transition of microstructures from one form to another. Further, plasma was utilized in the processing of materials involving the coating, melting and casting; but again cost is the critical factor for sustainable growth. In-situ casting processes were studied by many researchers [Mohanavel et al. (2015) and Ya et al. (2015)] and reported the utilization of process for processing various composites and alloys.

In current scenario, the focus is on the development of energy efficient and green processing methods, which are sustainable. Thus, it is of prime importance for the researchers to investigate alternative processing methods/techniques, which have the potential to overcome/lower the deficiencies of conventional one. The developed techniques are expected to

be highly energy efficient, reduces CO_2 and unwanted emissions, and produces better quality products at an effective processing cost.

Recently, a significant work has been carried out in the area of processing ceramic materials through microwave energy and this is the thrust area where very less work has been reported on melting and casting of metallic materials. Microwave heating technology allows many advantages which cannot be obtained through conventional heating processes. Microwaves were extensively used in the communication systems during the World War II, but sooner the heating effects were discovered [Spencer (1945)]. This discovery allowed microwaves to be utilized in the field of thermal heating of materials and since then many commercial applications have been developed in the microwave heating process. Microwaves have been extensively utilized in the processing of food materials, processing of ceramic materials, processing of polymers, synthesis of various compounds, enhancements in chemical reactions, minerals processing, medical applications, etc. The domain of microwave materials processing has increased many folds and based upon the processing temperatures the MW processes has diversified over a wide range. The various applications of MW radiations in materials processing technologies are presented in Fig. 1.3.

In recent years the focus has been shifted towards the processing of metal-based materials. Attainment of high temperatures in MW materials processing has created new opportunities in this novel field which are still to be exploited in near future.

1.2 MICROWAVE ENERGY AS ALTERNATE HEATING SOURCE

Heating of materials is involved in almost all the manufacturing industries through various sources such as burning of fossil fuels, resistive heating, induction heating, frictional

heating, etc. The effective utilization of any process depends upon the controlling of heating process and this control can impart better microstructures and structure properties correlations [Xu et al. (2014)].

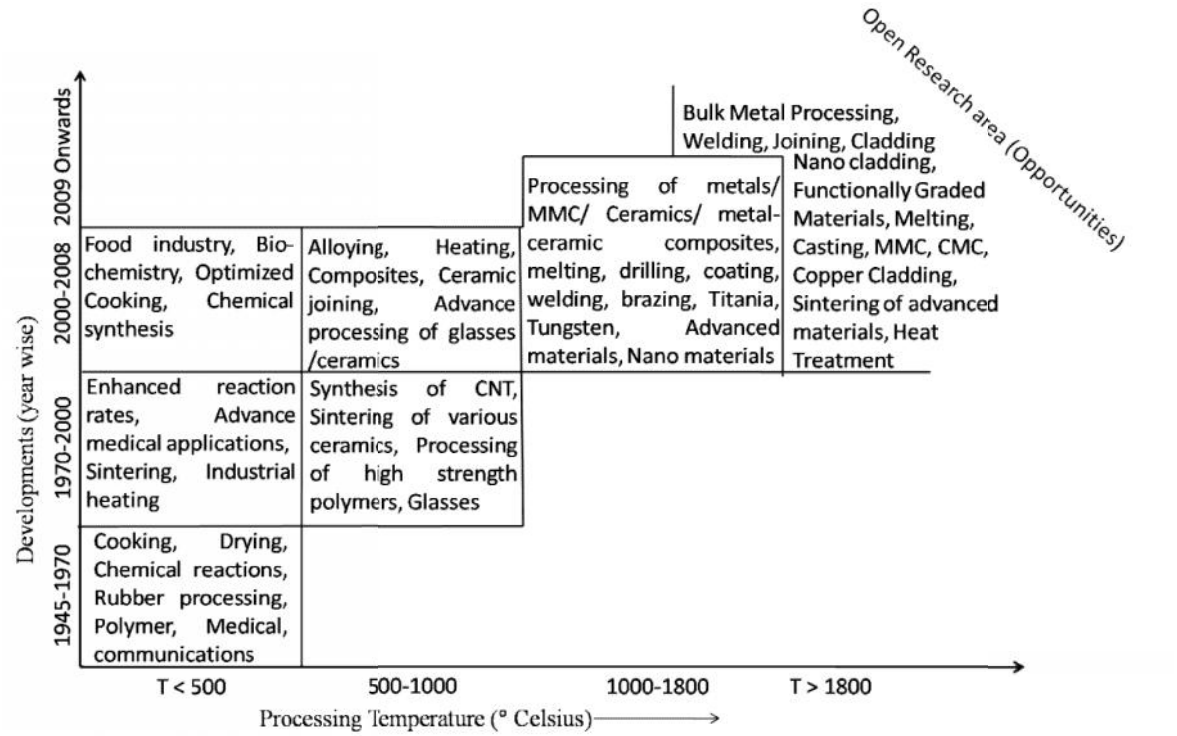

Fig. 1.3: Developments in the domain of MW materials processing over the years

The study of heating effects and its influence on the properties of the processed materials plays a significant role in the selection of materials processing technologies. In the conventional heating of materials, the heat is generated at the surfaces which propagates through the materials and reaches the core via conduction, convection or radiations. Thus, heat flows from outside to the inside of the body in conventional processes and depends upon various thermal properties of materials. The heating through microwave radiations is completely different from conventional; as microwaves get absorbed in the materials and gets transformed into heat at the atomic levels [Oghbaei and Mirzaee (2010)]. The heat generated within the materials is then propagated towards the outside surface. Both the conventional and microwave heating technologies have

their own advantages and disadvantages. But microwave heating being volumetric, intense and rapid has an upper hand over the conventional heating processes. The numerous advantages of microwave heating allowed this heating technology to be used in many commercial applications. The first commercial application in the field of heating was in the form of microwave ovens which are the essential part of every kitchen. Further, microwaves were successfully employed in the sintering of various ceramic materials [Agrawal (2006)]. Depending upon the materials and the microwave absorption profile, heating throughout the inner and outer surfaces of materials can take place. This type of heating is known as volumetric heating. Authors [Gupta and Wong (2005)] have reported that due to volumetric heating in microwave processing of materials, rapid heating with higher heating rates were possible. The basic comparison between the conventional and microwave heating mechanisms is shown in Fig. 1.4 which shows the direction of heat flow.

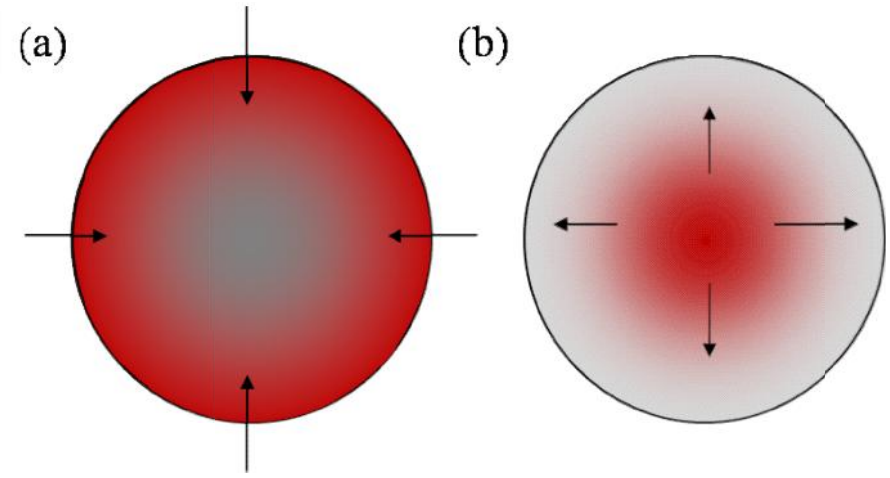

Fig. 1.4: Heat flow mechanism in (a) Conventional and (b) Microwave heating process

The industrial applications of microwaves were started in the field of food processing through the development of microwave ovens [Spencer (1945)]. During the years 1980-1990 the utilization of microwave ovens spread throughout the world and become the essential part of home appliances. However, at the same time some commercial applications were also discovered such as drying of wood, processing of rubbers, chemical processing, etc. [Thostenson and Chou

(1999)]. But, lately microwave sintering has emerged as one of the most promising technology in the materials processing field. However, microwave sintering was confined to the ceramics and ceramic based composites in different forms till the year 2002, but now literature on microwaves used in the processing of metal based materials is increased up to 10% as shown in Fig. 1.5.

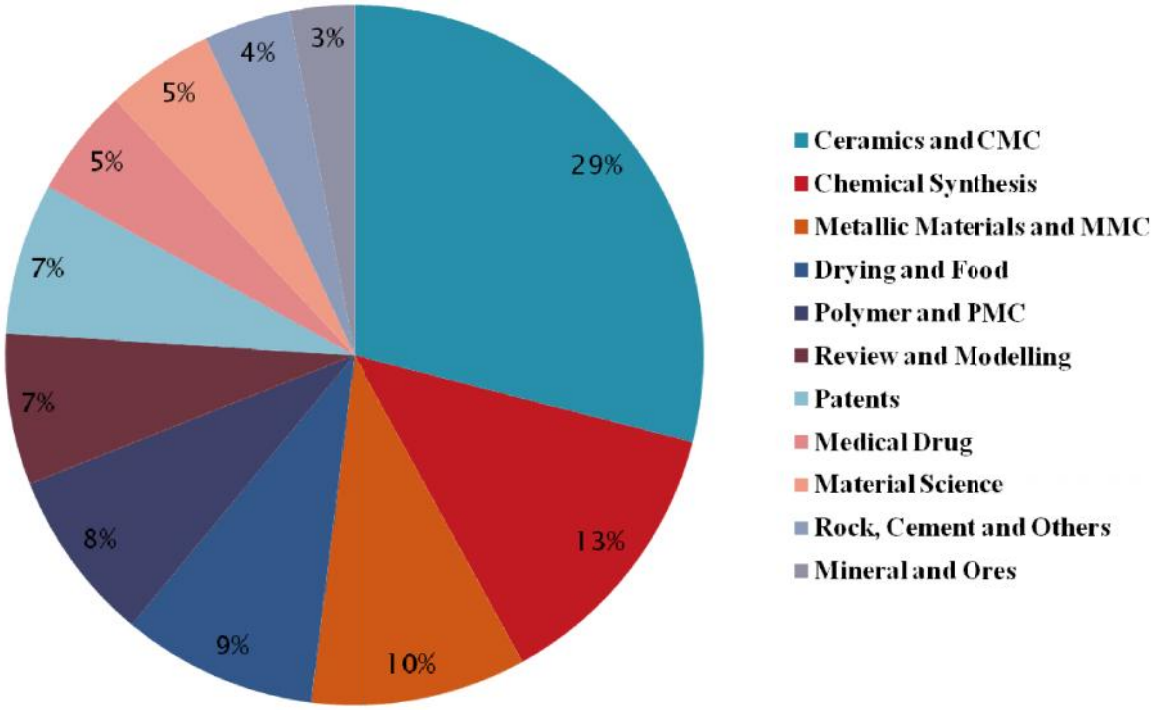

Fig. 1.5: Available literature in the field of microwave processing of materials [Mishra and Sharma (2016)]

The majority of the work has been carried out in the domain of microwave sintering of ceramics and CMC materials and this may be due to the fact that most of the ceramics and ceramic based materials are good absorbers of the microwaves at room temperatures. Due to better absorption of microwaves in the ceramic materials, rapid heating with higher heating rates (> 400°C/min) was observed; which led to the lowering of processing time and energy requirements [Agrawal et al. (2001)]. In addition to the volumetric heating achieved by microwaves, the ambient surroundings of the objects are not affected which results in ultra fast

heating and cooling rates. A comparative study showing the significant reduction in processing time and better mechanical properties of WC based ceramic composite sintered parts was reported by Author [Agrawal (1998)] and is presented in Table 1.4. The results reported that lower sintering temperatures and 9 times lower sintering time with the better bending strength of the microwave processed materials was observed.

Table 1.4: Comparison of conventional and microwave sintering process [Agrawal (1998)]

Parameters	**Sintering Methods**	
	Microwave processing	**Conventional**
Sintering temperature (˚C)	1300	1450
Total cycle time (minutes)	90	720-840
Sintering time (minutes)	10	60
Density (%TD) *(TD: Theoretical Density)*	99.5	99.7
Bending strength (MPa)	1800	1700

In another research work [Agrawal (2001)] reported that microwave processing led to the reduction of sintering time by a factor of 10. This reduction in time can minimize the grain growths and also the fine initial microstructure can be retained without using any grain growth inhibitors which eventually help in achieving high mechanical strength.

The heating rates obtained in the microwave processing are usually very high as compared to conventional processes and owing to which the cycle time reduces in the same manner from days to minutes. Further, the microwave sintering process is simple and one step method which involves a huge amount of energy savings [Clark and Sutton (1996)]. The energy savings in microwave processing of various materials in comparison to other conventional processes are shown in Table 1.5.

Table 1.5: Comparison of conventional and microwave processing of ceramics [Clark and Sutton (1996)]

Energy Saving					
Materials	Conventional Drying ($x10^6$ kW.h/yr)	Microwave Drying ($x10^6$ kW.h/yr)	Conventional Firing ($x10^6$ kW.h/yr)	Microwave Firing ($x10^6$ kW.h/yr)	TotalEnergy Savings ($x10^6$ kW.h/yr)
Brick and tile	56.10	28.05	198.90	19.90	207.06
Electrical porcelain	3.52	1.76	12.48	1.25	12.99
Glazes	16.63	8.30	58.97	5.89	61.37
Pottery	1.96	0.98	6.94	0.69	7.23
Refractories	10.87	5.40	38.53	3.85	40.08
Sanitary ware	25.04	12.52	88.76	8.88	92.40
Advance ceramics	1.30	0.65	4.60	0.46	4.79
Total	115.42	57.66	409.18	40.92	425.92

These advantageous characteristics of microwave heating are well known in the field of ceramic and ceramic based materials, but limited research is carried out in the field of metallic based materials processing through MW energy. The main reason for this limited research is that metallic based materials being conductive in nature and they cannot be heated effectively using by using low frequency (2.45 GHz) microwave radiations. This is due to the lower skin depths associated with bulk metallic materials (a few microns) at a common microwave frequency of 2.45 GHz. Hence bulk metals will reflect most of the microwaves incident upon them [Thostenson and Chou (1999); Bykov et al. (2001); Leonelli et al. (2008)]. This reflection can cause arcing problem which may cause damage to the equipment. Due to the above said reasons very limited work has been reported in the processing of metals through microwave energy. The initial work on microwave interaction with metal powders was reported in US patent [Nishitani (1979)] and it was reported that on adding a few percentage of electrically conducting powders such as aluminum, the heating rates of the refractory ceramics could be enhanced enormously. The heating rates of various metal based powders and minerals were first reported [Walkiewicz et al. (1988)] in 1988, when exposed to the 2.45 GHz frequency microwaves. The results are reported in Table 1.6. It was reported that pure metal powders can couple effectively with

microwaves and can be moderately heated in excess of 700 ºC in a few minutes without arcing using a commercial microwave oven.

Table 1.6: Microwave heating characteristics of various materials [Walkiewicz et al. (1988)]

Material	**Resistivity (Ω-m)**	**Heating Characteristic (ºC/min-temperature reached in specified time at 1 kW and 2.45 GHz)**
Metal Powders	**10^{-8}-10^{-6}**	**Moderately Heated**
Al		577ºC/6 min
Co		697/3
Cu		228/7
Fe		768/7
Mg		120/7
Mo		660/4
Sulfide Semiconductors	**10^{-5}-10^{-3}**	**Easily Heated**
FeS_2		1019/6.75
PbS		956/7
$CuFeS_2$		920/1
Mixed Valent Oxides	**10^{-4}-10^{-2}**	**Easily Heated**
Fe_3O_4		1258/2.75
CuO		1012/6.25
NiO		1305/6.25

On the other hand, metal sulfides and oxides were easily heated with heating rates higher than pure metals and temperatures above 1200°C. Some results of Fe alloy heating through microwave oven was reported by Narsimhan et al. (1995). It was reported that within 30 minutes of microwave exposure, temperature of 370°C was attained. The fallacy that metals cannot be heated with microwaves was removed by the investigators from Penn State University [Roy et

al.(1999)], USA, and reported the successful processing of Fe-Ni alloys with superior properties than conventional processing. It was reported that metal in the form of powders can easily and effectively heated by microwaves. The sintered densities were higher than the conventional processed parts which enhances the mechanical performance. After the initial research on sintering of some metallic powders, a lot of work was carried out in the field of sintering of pure metallic powders [Saitou, (2006); Prabhu et al., (2009)], alloys of metallic based powders [Leonelli et al. (2008); Upadhyaya et al. (2007); Chhillar et al. (2008); Mondal et al. (2009)] and sintering of MMC's [Rajkumar and Aravindan (2009, 2011 and 2013)]. From year 2000 onward, the domain of microwave processing has shifted from ceramics to processing of metallic based powders and bulk metals processing. In recent years MW was successfully employed in the development of metallic based powder claddings on the bulk steels [Gupta et al. (2012), Zafar and Sharma (2015, 2016), Hebbale and Srinath (2016 and 2017)] and it was reported that clads were formed by metallurgical bonding with the substrate. The joining of various similar or dissimilar bulk metals was carried out using microwaves [Srinath et al. (2011a and 2011b)] and it was reported that microwave processed joints were free from the defects such as porosity and exhibit good mechanical properties.

1.3 MOTIVATION

Nickel and nickel based alloys plays an important role in the modern engineering world. It was discovered by the Swedish chemist Axel Fredrik Cronstedt in 1751. It has been reported that [Reck et al. (2008)] nickel is widely used in alloyed form in stainless steels with a 68% consumption annually. Out of this the industrial machineries are the largest consumer of nickel based steel with a 25% consumption, 22% in construction and 21% in transportation. The

estimated consumption of nickel in India (2011) was 40 kt, which was around 3% of the total nickel consumption of the world and is shown in Table 1.7.

Table 1.7: Details of nickel consumption worldwide

Country	Consumption (kt)
India	40
Europe	406
South Korea	85
North America	133
Japan	171
China	655
Rest of world	112
Brazil	30

Source internet*: http://metalpedia.asianmetal.com/metal/nickel/resources&production.shtml*

However, the utilization of nickel based material has increased many folds in the industrial applications. Apart from production of stainless steels, nickel is widely used in the manufacturing of non ferrous alloys, alloy steels, plating applications, foundry applications, used in batteries, claddings, coatings and other specific applications such as nickel super alloys for turbines and aerospace applications. Fig. 1.6 shows the percentage of nickel used in various applications [Source: *http://metalpedia.asianmetal.com/metal/nickel/application.shtml*].

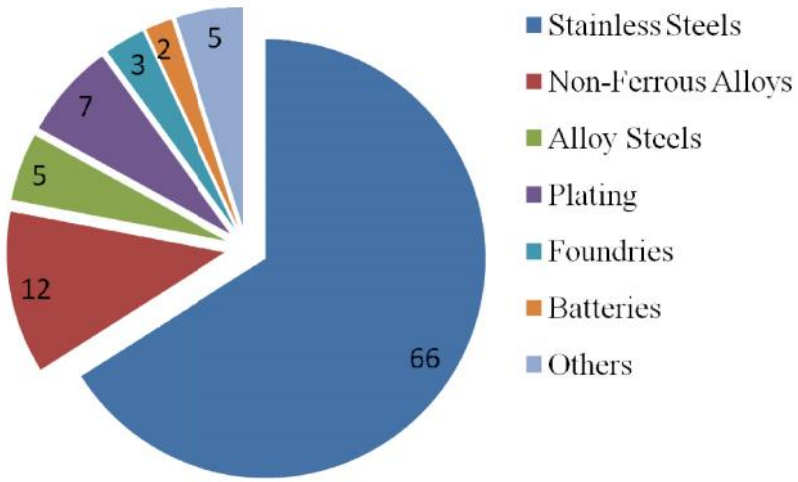

Fig. 1.6: Utilization of nickel in various applications

In recent years a lot of work has been reported on coatings and claddings of nickel based materials/nickel based MMC's [Gupta and Sharma (2014)]. It is a well known fact that nickel based materials have better corrosion, high temperature oxidation resistance, greater toughness, better mechanical properties at higher and lower temperatures with a wider range of magnetic and electronic properties. The nickel based steels are well suitable for many machine components due to the above said properties but still it is quite difficult to process the nickel based materials. The main reason behind this is the higher melting point of nickel (~1500°C). Many advanced techniques were developed lately; however, laser material processing has gained a lot of attention and emerged as one of the pioneer's material processing technology [Malinauskas et al. (2016); Mincuzzi et al. (2012) and Shi et al. (2016)]. The lasers are extensively used in the processing of biomedical materials, cladding/joining and selective melting of materials, but authors [Gupta and Sharma (2012)] have reported that initial investment and maintenance costs restrict the effective utilization. On the other hand utilization of nickel based materials is increasing at a significant pace. The advanced applications of nickel based materials in the field of aerospace, nuclear, automobile, mechanical, thermal, etc. allowed nickel-ceramic based composites as a substitute for the conventional monolithic metals [Zhen at al. (2014) and Kumar et al. (2017)]. The unparalleled performance and characteristics of metal‑ceramic (mainly nickel based) composite materials such as higher working temperature ranges, higher thermal stability, higher wear, and corrosion resistance, allowed metal ceramic composites in cut-throat engineering applications [Rajan and Pai (2014)]. The lack of ductility and aggregation in sintered pure ceramic materials further allowed metal- ceramic composites to grow extensively in high end aerospace, turbines and machine tools applications. There is huge demand from the industry to develop such materials having high structure‑property correlations. It is well known fact that the properties and performance of materials directly depends upon the

microstructures of the materials. The laser processing allowed the development of many nickels based composite claddings/materials, but again the initial set-up cost, thermal stresses, thermal cracking in the processed materials led to poor mechanical and metallurgical characteristics. This is the dominant area where microwave heating technology is found to be useful and profitable. The MW heating helps in the mitigation of defects like porosity, cracking, microstructure dislocations, etc. and suppression of these defects allows refinement in properties [Gupta et al. (2012)]. Also, the efficiency of the MW heating process is high as it reduces the processing time and energy consumptions. MW processing also helps in saving the environment as no pollution occurs while processing the materials. All these characteristics are inherent features of microwave heating and allowed regular innovations in this field. The various developments in the field of MW processing of metals are shown in Fig. 1.7, which represents the year wise chronological developments in this novel field.

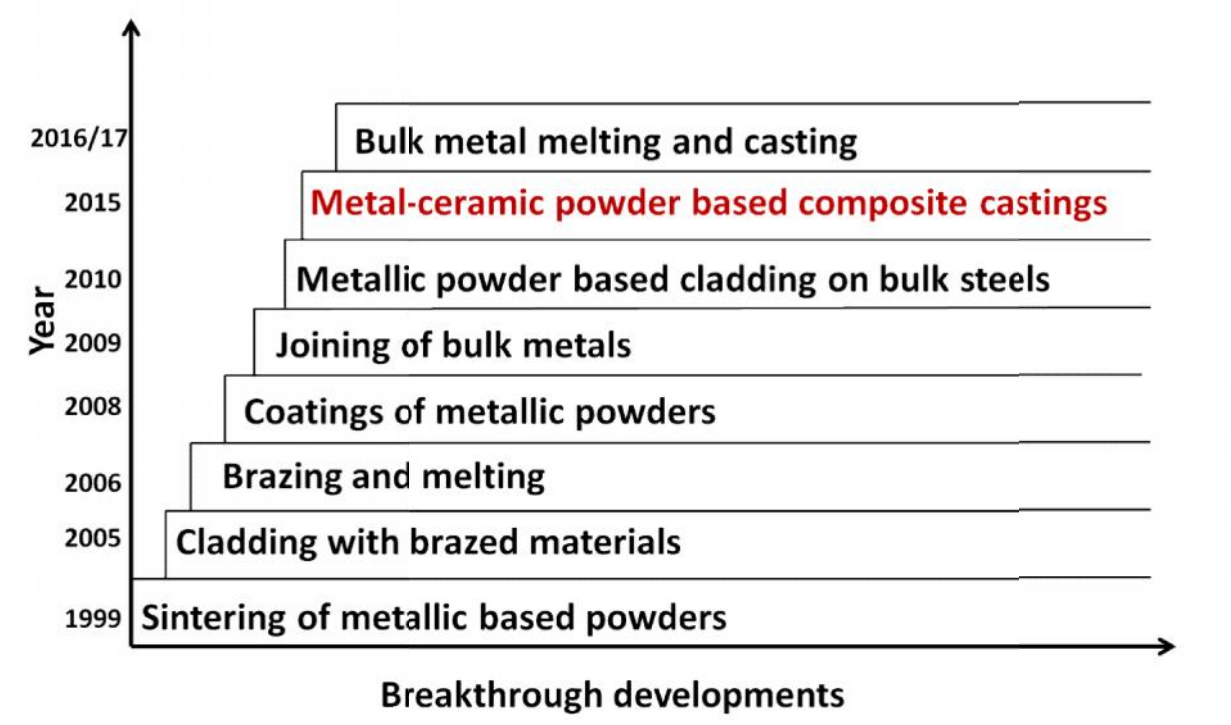

Fig. 1.7: Developments in the field of metal based materials processing through MW heating

The fruitful developments in the sintering of metallic based powders created the spark in the field of metal based materials processing through microwaves and researchers are now progressing towards the melting and casting industry [Lingappa et al. (2018)]. It was reported that in microwave joining [Srinath et al. (2011), Singh et al. (2017)] and cladding process [Gupta and Sharma (2014), Kaushal et al. (2015, 2016 and 2017), Zafar and Sharma (2015, 2016)] that partial melting of metal powders were observed which eventually led to the metallurgical bonding. Partial melting of nickel powders shows that it is possible to achieve melting temperatures through microwaves. This motivated for the development of metallic powder based castings through the microwave heating process. In the present literature survey, no work has been reported on the development of metal-ceramic MMC's castings through microwave melting and casting process. So, it is worth attempting to develop a new process for casting of metallic based powders MMC's through microwave energy. The developed process would be efficient, environment friendly and capable of producing small scale MMC's castings.

1.4 THESIS OVERVIEW

The work presented in the thesis has been organized into the following chapters:

Chapter 1: In this chapter a brief introduction to the understanding of the need of efficient materials processing technologies has been presented. The requirement of energy in manufacturing sectors and mainly in foundries is highlighted. A brief history of microwave heating, heating mechanism and various applications of microwave heating are highlighted. The breakthrough developments in different areas and common difficulties encountered in processing metallic materials through microwaves are highlighted. Motivation of the work has been outlined which focuses on the new microwave casting process for developing MMC's.

Chapter 2: In this chapter a comprehensive literature review of microwave processing of materials has been presented. The focus was on the high temperature applications of microwave heating. Identification of research gaps and opportunities, problem identification, objectives, scope of the present work and the methodology adopted for the presented study has been discussed.

Chapter 3: In this chapter the interaction between the various types of materials and microwaves has been highlighted. The mechanism for melting of metallic powders through microwave hybrid heating has been presented. The complete theory of microwave casting process has been discussed in detail.

Chapter 4: Provides the information on the materials used in this study and the experimental procedures for the development of MMC's through microwave hybrid heating process. The various characterizations of selected materials used in the present study are also introduced; and feasibility results of the microwave casting process have been reported. The various parameters for the casting of metallic powders have been optimized. Initial experimental trial results have been presented in the chapter.

Chapter 5: Results of the metallurgical, mechanical characterizations of Nickel based castings and Nickel based MMC castings are discussed. The results of tensile strength and percentage elongation of various EWAC (Ni) based castings are reported and results are compared to get the overview of the strengthening of composites by adding various reinforcements. The fractrography analysis was carried out to study the modes of failure.

Chapter 6: The dry sliding wear behavior of microwave processed castings has been reported. The results of fractographic analysis of wear tests are reported in the present chapter which

reveals the mechanisms involved in weight loss. The effect of various parameters on the wear has been discussed with proper justifications through SEM and EDS characterizations.

Chapter 7: Concludes the findings of the research work carried out in this study and provides the recommendations for possible future work in this area. Major contributions of the investigation have been outlined.

The list of references, appendix and visible outputs from the present research work in terms of including published research papers, conference attended and patent details are provided at the end of the thesis.

1.5 SUMMARY

The energy consumption in materials processing technologies is of serious concern and level of CO_2 emissions are increasing at an alarming rate. The maximum amount of energy consumption throughout the world is in the melting and casting of metals. It was stressed that there is a need to develop manufacturing processes which are energy efficient, consumes less time, yields better quality products and are environmentally friendly.

The conventionally available and widely used methods for casting of metals are discussed with their advantages and limitations. A brief overview of casting industry and energy consumption in various processes has been presented in the present chapter. The processing of various materials through electromagnetic energy (laser) is a fascinating approach with few attractive characteristics (low dilution, rapid cooling, low HAZ) of laser processed products. However, some defects like solidification cracks, porosity and cracking in laser processed materials significantly affect the product quality. The recent trends in materials processing through microwave energy have been briefly discussed. The developments taking place in the

microwave processing of metals have been discussed. Comparative analysis in terms of energy consumptions and processing times of conventional and microwave processing of ceramics is highlighted. The unique characteristics, benefits and major challenges of microwave processing of materials are presented. Motivation for the present work through literature has been stated. The organization of the thesis is presented in the chapter.

CHAPTER 2

LITERATURE REVIEW AND PROBLEM FORMULATION

The effective processing of materials plays an important role in deciding the cost and utilization of advanced materials in various engineering applications. Higher manufacturing costs will certainly constraints the effective exploitation of materials in various applications. Further, the continuous pressure from governments to minimize the energy consumptions and pollution levels has directed the researchers to develop novel material processing technologies. These technologies on one hand will help in reducing the manufacturing costs and on the other hand will help in lowering the consumption of energy. For any country, the manufacturing sector is the backbone of its economic growth. But, the manufacturing sector itself consumes the maximum share of the energy produced. Among the manufacturing sector, melting and casting of materials along contribute 70% of energy consumptions. This problem can be solved by developing novel material processing technologies which are efficient, cost effective and can process a variety of materials. In recent years, a lot of work has been carried out in this direction and resulted in many advanced materials processing techniques such as Laser processing, induction heating and melting, plasma heating and melting, etc. The hybridization of various processes was also carried out to improve the efficiency and quality of product produced. But there are some inherent limitations of these processes, either they are developed for specific materials or involves very high initial cost. But microwave heating has emerged as a cost effective solution for processing of a variety of materials. Fig. 1.7 in chapter 1 provides the breakthrough developments in microwave heating technology in the domain of metal based materials. Over the years, the domain of microwave heating is expanded over the wide range of

temperatures and in some recent works melting of metallic powders through microwave energy has been reported. Before going for the detailed literature review in this novel field of microwave materials processing; it is important to understand the microwaves and its heating mechanisms.

2.1 INTRODUCTION TO MICROWAVES

The spectrum of electromagnetic waves spread over a wide range of frequencies and within this range microwaves lies between 300 MHz to 300 GHz frequency bandwidth with wavelength of 1 *m* to 1 *mm*, respectively. Microwaves are coherent, polarized and can be transmitted, absorbed, or reflected depending on the interaction with the selected materials type [Sutton (1989)]. During World War-II microwaves were extensively used for tele-communication systems, radar detection, tracking, and electronic warfare. The heating effects of microwaves were accidentally discovered by Percy Spencer when a candy bar in his pocket was melted while he was experimenting on the MW generator. He filed the patent on heating of foodstuffs using microwaves in 1945. The heating through microwaves were initially focused on low-temperature applications such as heating of foodstuffs, curing of resins, wood drying, drying of materials, etc. [Appleton et al (2005) and Das et al. (2009)]. These earlier developments in microwave heating were appreciated due to lower-energy consumptions and rapid-heating process, which lowered the processing time significantly. These characteristics of microwave heating process attracted many researchers, and novel field of microwave sintering was explored with many advantageous characteristics. The microwave sintering process has emerged as one of the best methods to process various materials and allowed huge energy savings. Thus, the utilization of MW in various materials processing applications has been increased many folds over the decades [Clark and Sutton (1996); Katz (1992); Mishra and Sharma (2016)] as shown in Fig. 1.3. The common frequencies used for commercial and domestic heating applications are

0.915 and 2.45 GHz. The most of domestic microwave ovens in many countries work on 2.45 GHz frequency. But, higher frequency microwave and millimeter wave furnaces ranging from 1 to 30 GHz were developed for various materials processing [Link et al. (1999), Luo et al. (2004) and Rhee (2003)]. Microwave heating offers certain advantages which are unparalleled match for the conventional heating techniques. This allowed microwave heating to expand its domain in many medical treatment processes, non-destructive testing, power transmission, commercial heating of materials, materials processing, etc. Still a broad open area is left where microwaves can be successfully employed. In India, the domestic microwave oven works at 2.45 GHz frequency as shown in Fig. 2.1, which represents the spectrum of EM energy.

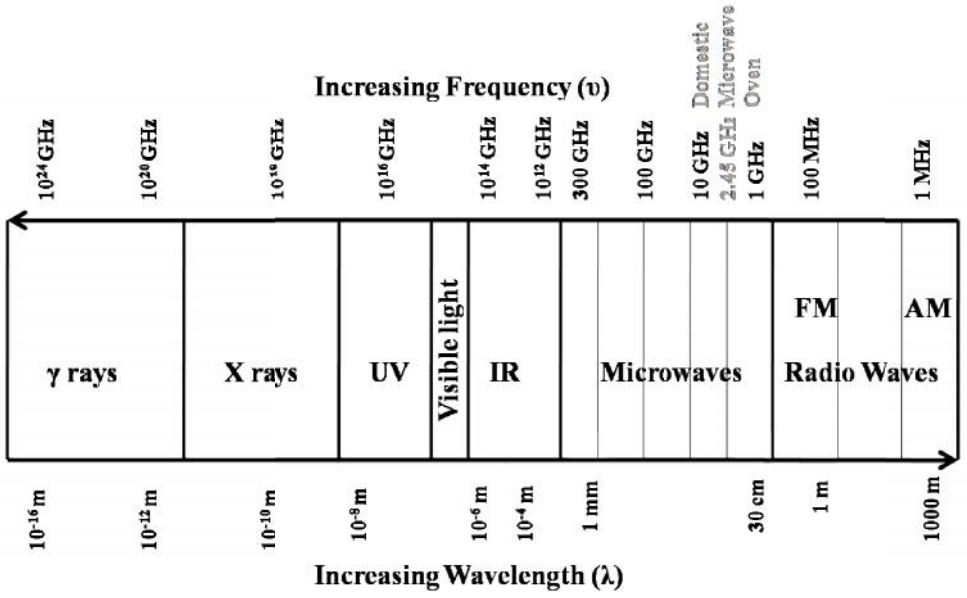

Fig. 2.1: EM spectrum showing the microwaves bandwidth

2.2 MICROWAVE MATERIALS INTERACTION

The sudden increase in the processing of materials through microwave energy is on the brighter side of this novel heating and materials processing technology. But on the other hand, it is also true that all the known engineering materials cannot interact and hence processed

effectively with microwaves. This limits the material domain which can be processed directly by microwave radiations [Clark et al. (2000)]. This is due to the fact that different materials possess different electrical, dielectric and magnetic properties and based upon these properties microwave absorption behavior changes. It is remarkable that researchers are continuously working on expanding the domain of microwave heating in materials processing; starting from the heating of foodstuffs to the development of microwave manufacturing processes involving metallic materials [Mishra et al. (2006); Luo et al. (2004) and Huang and Hwang (2001)]. The various processes such as microwave cladding process [Pathania et al. (2015); Zafar and Sharma (2014)], microwave joining of bulk metals [Bansal et al. (2013); Srinath et al. (2011c); Singh et al. (2017)], and microwave casting of metals [Bist et al. (2014)] are recently targeted by researchers. These efforts motivate the researchers to further explore in this fascinating field; which is full of uncertainties.

There are various factors which affect the microwave-materials interactions, but materials physical properties are one of the major factors in deciding the effective coupling of materials with microwaves. Depending upon the interaction of materials with microwaves; materials can be categorized into microwave absorbing and non-absorbing materials. The physical properties of materials allow the variation of magnetic field (H) and electrical field (E) within the materials and decide their coupling behavior with microwaves. Depending upon the absorption behavior of microwaves, the materials are categorized into three main groups as shown in Fig 2.2 [Mishra and Sharma (2016)], which also show the variation of energy absorbed per unit volume.

- **<u>Group 1: Transparent materials / Low loss insulators</u>**

  There are certain materials that allow microwaves to pass through them easily, and without causing any changes in the E and H field. This causes no interaction between

materials and microwaves and hence no absorption of microwave energy takes place. Such types of materials are known as transparent materials. In some cases, limited heating may occur, but maximum of the microwave radiations passes through without any loss. This may be due to the negligible loss tangents and high skin depths associated with the materials. Some typical examples of microwave transparent materials involve quartz, teflon, thin plastic sheets, etc. Fig. 2.2 shows that for such type of materials there is no change in *E* and *H* field when microwaves pass through the materials.

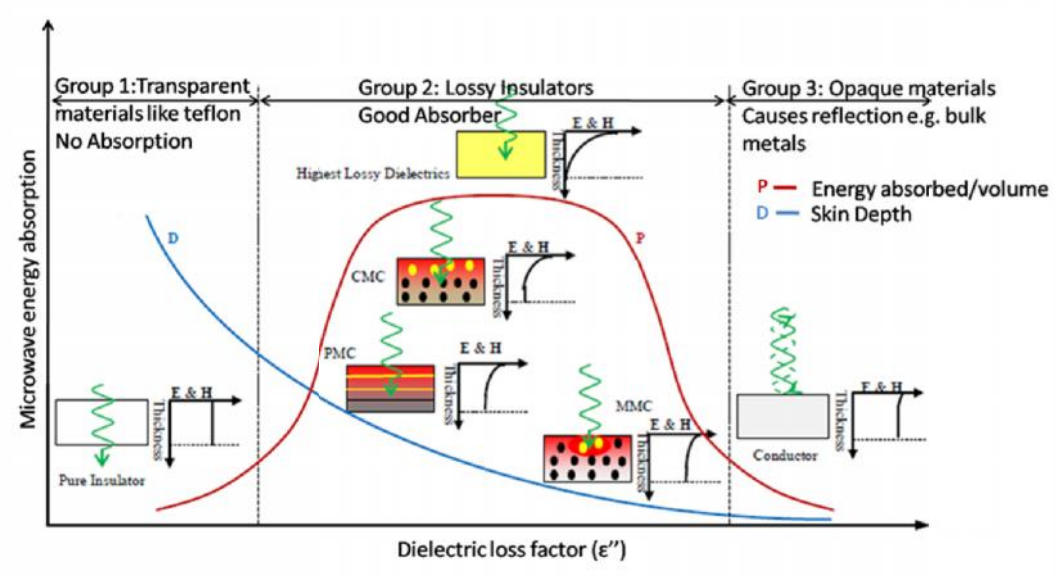

Fig. 2.2: Categorization of materials based on microwave-materials interaction [Mishra and Sharma (2016)]

- **<u>Group 2: Microwave absorbing materials / Lossy insulators</u>**

  The materials with high to moderate dielectric loss factors which absorbs the microwaves and convert them into heat are called lossy insulators. Though high dielectric loss factor may affect the microwave absorption, but it is not necessary that high dielectric loss factor always led to higher efficiency in absorbing microwave power. The skin depths associated with the materials also plays an important role in the absorption of microwaves. If size of materials is comparable to the skin depth associated then efficient

heating through microwave absorption can take place. Such materials can effectively converts the absorbed microwaves into heat at lower frequencies and lower temperatures. Typical examples of such materials include water, silicon carbide, ceramics, carbon fibers, graphite, charcoal, etc. It is also possible to alter the dielectric properties of the transparent materials by the addition of some filler materials such that combination allows microwave absorption. Such materials are termed as mixed absorber materials. The best example of these materials includes multi-phase materials in which one phase acts as transparent or opaque to the microwave energy but other phases allows microwave absorption. This phenomenon can be seen in various metal matrix composites, ceramic matrix composites, and polymer matrix composites containing fillers of CNT, carbon black, copper, silver, and alloys which can modify the dielectric properties.

- **Group 3: Opaque materials/ No loss materials**

  There are some materials which act as opaque to the microwave energy and when irradiated with microwaves, they reflect microwaves back. The reflection of MW occurs mainly due to a lower penetration depth of microwaves which is further due to lower skin depths associated with such materials. However, in some cases surface heating may take place due to some penetration of microwave radiations, but maximum of the radiations are rebounded. Such reflecting materials are known as opaque, and bulk metals are one of the best examples.

The effect of skin depths on microwave absorption of materials is shown in Fig. 2.3. Thus, MW can be reflected, transmitted and/or absorbed depending upon the type of material and skin depths associated with them. The microwave energy absorbed by the materials will

penetrate within and gets converted to heat, which in turn raises the temperature of the materials. Due to the direct conversion of MW energy into thermal energy, the characteristic heating of microwaves allows interior parts of the material to be heated first than its surface. The heat loss from the surface to the surroundings also affects the heating and inner parts are at higher temperatures as shown in Fig. 2.4.

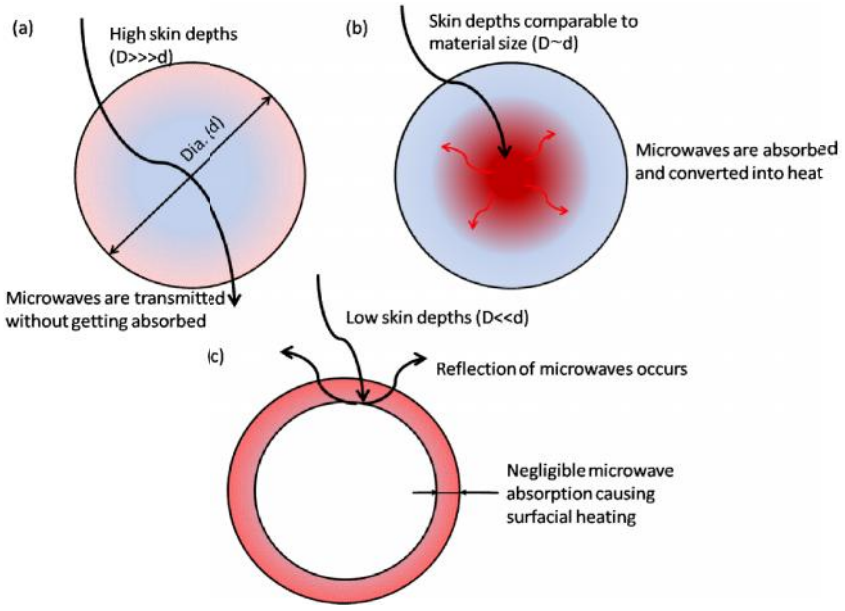

Fig. 2.3: Effect of skin depth on microwave absorption of materials having (a) high skin depths, (b) skin depth comparable to material size, and (c) low skin depths

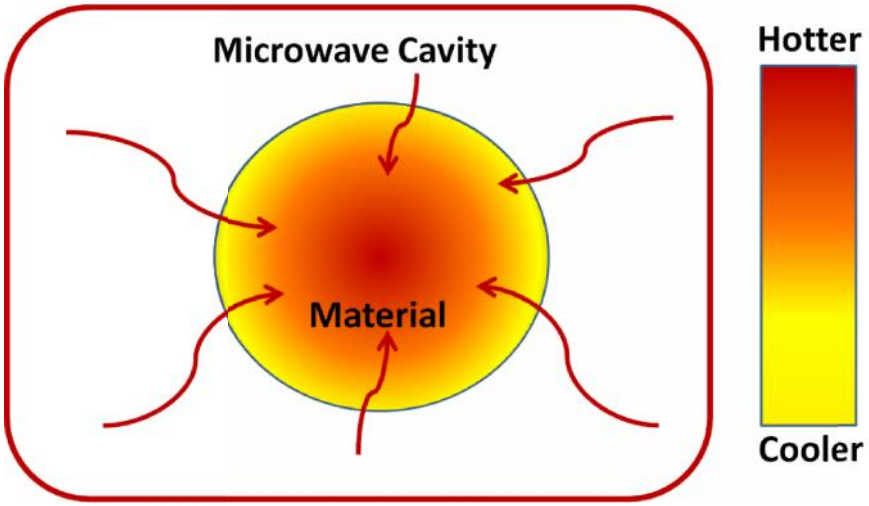

Fig. 2.4: Heating profile of materials with microwave energy

The effective heating of materials through microwaves is governed by mainly two fundamental properties of materials i.e. the dielectric constant, ε', also known as the real permittivity of the materials and dielectric loss factor. The first property of dielectric constant defines the ability for electromagnetic energy to penetrate within the material when irradiated. For most of the materials, the value of dielectric constant can be practically treated as a constant and there are no significant effects of the changing temperature of the materials and the frequency of the electromagnetic radiations. The second fundamental material property is the dielectric loss factor, ε'', also known as the dielectric loss or imaginary permittivity. It is the measure of the ability of the material to store/retain electromagnetic energy when irradiated with microwaves. Any materials with a high dielectric loss factor do store the energy effectively, and this can result in the conversion of a significant portion of the energy to thermal energy within the materials. Another parameter known as complex permittivity (ε_c) allows the fusing the two permittivity's values into a single parameter, which comprised of the real and imaginary permittivity parts as shown by equation (2.1).

$$\varepsilon_c = \varepsilon_0(\varepsilon' - j\varepsilon''), (\text{F m}^{-1}) \tag{2.1}$$

The equation (2.1) can be rewritten in term of a quantity called loss tangent 'tan δ', which is illustrated in equations (2.2-2.3).

$$\varepsilon_c = \varepsilon_0\varepsilon'(1 - j\tan\delta) \tag{2.2}$$

Where,

$$tan\,\delta = \frac{\varepsilon''}{\varepsilon'} \tag{2.3}$$

The loss factor mainly indicates the degree of heating the materials with microwave energy. A low-loss material, with a low value of ε'', is capable of storing electromagnetic energy well but does not absorb much of the stored energy. In such cases, the real part of materials permittivity,

ε' is significant and the imaginary part is so small that can be neglected. In case of a lossy material, with a high value of ε'', larger portion of the electromagnetic energy is absorbed instead of storing it all. The absorbed energy is converted into thermal energy within the material through several dissipation mechanisms. Since these materials absorb a larger portion of any incident electromagnetic energy, they are heated more readily than a low-loss material.

2.2.1 Mechanisms of Heating by Microwaves

Microwave heating applicators consists of three main parts; source, transmission lines and applicator [Thostenson and Chou (1999)]. The microwave source (vacuum tubes, magnetrons, klystrons, etc.) generates the electromagnetic radiations, which are transferred to the applicator heating area through transmission lines. Depending upon the load (materials to be heated) either microwaves are directly absorbed or reflected by materials kept in the cavity. The theoretical analysis of microwave heating can be analyzed and governed by using appropriate boundary conditions to the Maxwell equations (equation 2.4) [Thostenson and Chou (1999); Zhu et al. (2007); Geedipalli (2007)] shown below:

$$\nabla \times E = \frac{\partial B}{\partial t}, \nabla . B = 0$$

$$\nabla \times B = \frac{\partial D}{\partial t} + I, \nabla . D = \rho \qquad (2.4)$$

The Maxwell equations can be solved analytically/numerically with the required boundary conditions for the distribution behavior of the electric field and magnetic field within the microwave applicator. These distribution results decide the location for placement of load for efficient heating inside the applicator. Depending upon the type of applicator i.e. single mode or multi mode; the favorable sites can be obtained depending upon the electrical or magnetic field strengths. The initial heating behavior of materials can be judged by the fundamental properties of dielectric constant and dielectric loss factor, but the various phenomena which convert the

absorbed MW energy into heat energy are also important. The various phenomena which occur within the materials and allow the heating of materials via microwave energy route are discussed by many authors in details [Torres and Jecko (1997); Pozar (2009)]. Depending upon the type of material, i.e. magnetic / non-magnetic, the various heat generating phenomena are involved. In the lossy dielectric materials, the five primary modes of energy dissipation are:

(a) Electronic Polarization, (b) Ionic or atomic Polarization, (c) ionic conduction, (d) dipole (orientation) polarization, (e) Maxwell– Wagner polarization [Thostenson and Chou (1999)]

In case of dielectric materials, the microwaves penetrate and propagate which causes the generation of internal electric fields. This generated electric field causes the local charge (bound charge and free charge) to move (translational motions and rotational motion) and results in polarization [Thostenson and Chou (1999); Roy et al. (1999)]. The internal, elastic, and frictional forces resist this motion and generate heat. The developed internal heat is volumetric in nature as the process occurs throughout the volume of materials. The interaction (penetration and propagation) of microwave within the materials is mainly dependent on dielectric properties (ε', ε'' and $\tan\delta$). For processing of non magnetic materials such as Al, Cu, Ceramics, water, etc., the phenomenon of dipolar loss and conduction loss are predominant. In case of magnetic materials such as Fe, Ni, Steel powder, W, etc., the phenomenon of hysteresis losses, Eddy current losses and residual losses (domain wall resonance and electron spin) are predominant. While processing the materials by microwave energy, the interaction of both the magnetic as well as electric fields occurs. Processing of magnetic materials by microwaves involves heating by magnetic field through the phenomena of ‘electron spin’, ‘domain wall movement’ and ‘orientation of domains’ within the material; whereas the role of electric field is to impart the motion to the free electrons. The total heat generation for any magnetic metallic material

includes various losses such as conduction losses (due to electric fields) and magnetic losses (hysteresis loss, eddy current loss, domain wall resonance and electron spin resonance). Thus, the absorbed microwave power in a material is the dissipated power due to the magnetic fields and electric field of microwave energy; which represent the total energy converted into heat within the material. It is very difficult to find the percentage contribution of electric and magnetic fields leading to various losses in overall heating of materials. To overcome this problem, another parameter, i.e. power dissipation is used as the measure for effective microwave heating. Further, the power dissipation in any material depends upon the depth up to which the microwave radiations are absorbed. The penetration behavior of microwaves varies in accordance to the type of materials and associated properties. For non-metallic materials the penetration of microwaves is defined by the term 'Penetration Depth' (It is the distance from the surface of material at which the incident microwave incident power drops to 1/e (36.8%) of the surface value) which is mathematically expressed in equation (2.5) [Mishra and Sharma (2016a)].

$$D_P = \frac{1}{\omega \sqrt{\left(0.5\,\mu_0\,\mu'\,\varepsilon_0\,\varepsilon' \left\{\sqrt{\left(1+\left(\frac{\varepsilon''_{eff}}{\varepsilon'}\right)^2\right)}-1\right\}\right)}} \tag{2.5}$$

Whereas in case of metallic based materials the penetration of microwaves under the normal conditions is negligible and hence corresponding depth is termed as 'Skin Depth'. The skin depth (δ) is relatively simple with the least number of parameters and is mathematically expressed by equation (2.6) [Mishra and Sharma (2016b)].

$$D_s(\delta) = \frac{1}{\sqrt{\pi\, f\, \mu\, \sigma}} = 0.029\ (\rho\ \lambda_0)^{0.5} \tag{2.6}$$

Where, δ is the skin depth (m), σ is the electrical conductivity (S m^{-1}), f is the frequency of the microwaves (GHz), μ is the electrical resistivity (Ω m), and λ_0 (m) is the incident wavelength.

This shows that the power absorbed during the microwave radiations depends on the electromagnetic characteristics and thickness (volume characteristics) of the materials irradiated. For thin sections of materials, the estimated power absorbed per unit volume (W m^{-3}) is represented by equation (2.7) [Saltiel and Dutta (1999) and Kubel (2005)].

$$P = 2\pi f \varepsilon_0 \varepsilon'' E_{rms}^2 + 2\pi f \mu_0 \mu'' H_{rms}^2 \quad (2.7)$$

Where, P is the power absorbed (W m^{-3}), μ_0 is magnetic permeability of air (H m^{-1}), μ'' is the imaginary component of the magnetic permeability (H m^{-1}) and known as magnetic loss factor, E_{rms} is the root mean square of the electric field (V m^{-1}) and H_{rms} is the root mean square of the magnetic field (A m^{-1}).

In case of non-magnetic materials the $2\pi f \mu_0 \mu'' H_{rms}^2$ term can be neglected as μ'' is negligible. For thick sections the power absorbed can be predicted by using Lambert Law as expressed in equation 2.8 [Mishra and Sharma (2016a)].

$$P_x = P_0 e^{(-2\alpha x)} \quad (2.8)$$

Where, P_0 is the incident power (W) at the surface of material, x is the distance (m) at which power is to be determined and α is called the attenuation factor (dB m-1).

But, the material properties get altered as the temperature changes and in such cases, it becomes highly cumbersome to estimate the power absorption. To estimate the power absorption up to some extent, an energy balance equation as expressed in equation 2.9 [Ayappa et al. (1999); Mishra and Sharma (2016a)] can be used.

$$\sum mC\Delta t = 2\pi f \varepsilon_0 \varepsilon'' E_{rms}^2 V t \quad (2.9)$$

Where, m is the mass of material (kg), C is the specific heat (J $kg^{-1}K^{-1}$) of material, Δt is the temperature difference (°C), V is the volume of the material (m^3) and t is the time of microwave exposure (s).

The penetration and propagation of incident microwave can significantly be enhanced by altering the dielectric properties (*ε''* and *tanδ*) of materials which are temperature dependent. This can be carried out through indirect heating or infrared heating and the corresponding technique is named as microwave hybrid heating (MHH).

2.2.2 Microwave Heating Methods

Microwaves are directly or indirectly used in many industrial and materials processing applications; however, with the passage of time newer technologies are emerging in this field. The newer developments and research are collaborating with microwave heating processes and helping in expanding the domain in the field of materials processing. The heating methods through microwaves are divided into four categories, i.e. direct microwave heating, microwave hybrid heating, selective heating and microwave assisted heating. Some of the heating methods are shown in Fig. 2.5.

- **Direct Microwave Heating**

  The direct heating of materials is employed mainly for the materials which are microwave absorber (lossy insulator). These materials directly couple with the microwave radiations, absorb and convert microwave energy into heat energy as shown in Fig. 2.5 (a). Typical material examples are water, foodstuffs, some ceramics, etc. Though, heating can occur at rapid rates, but the uniformity in direct heating of materials is a critical issue. The generation of heat within the core with higher processing times can

seriously damage the materials by producing hot spots. Authors [Krigsmann (1997), Manickavasagan et al. (2006), Spotz at al. (1995)] have reported many issues while exposing materials (such as SiO_2, ZrO_2, alumina etc.) directly to microwaves and these includes thermal instabilities, non-uniform heating and cracking.

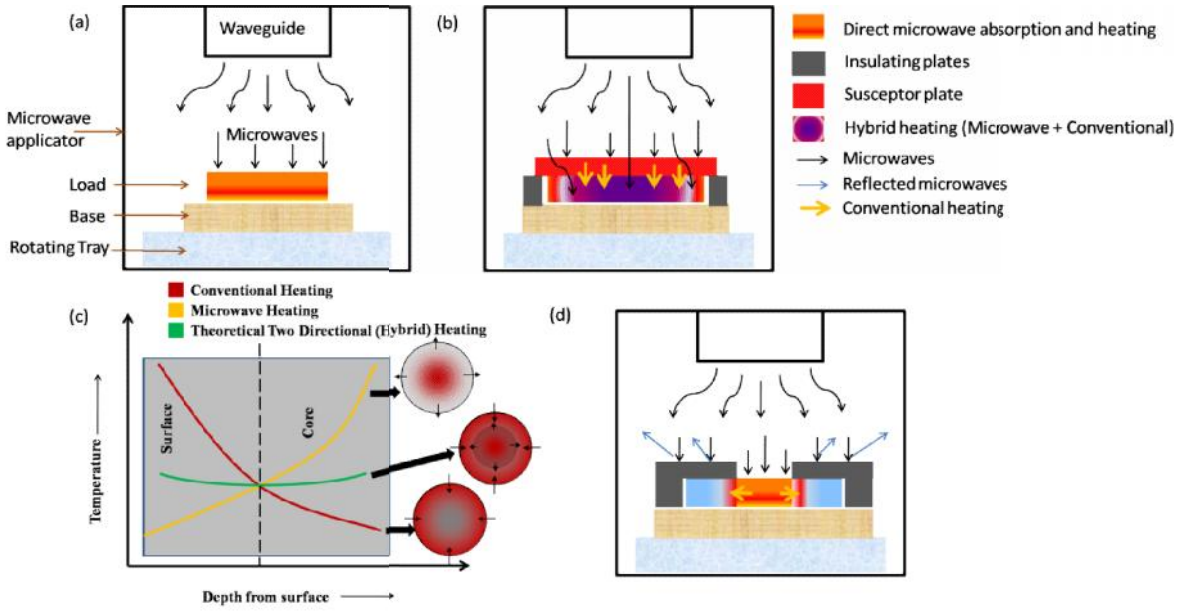

Fig. 2.5: (a) Direct microwave heating, (b) Microwave hybrid heating, (c) Effect of microwave hybrid heating on temperature profile and (d) Selective microwave heating

- **Microwave Hybrid Heating (MHH)**

Microwave hybrid heating is a method of indirect heating which may be employed to overcome the difficulties in heating of low microwave absorbing material like metal and most ceramic. The MHH technique utilizes an additional material (susceptor) in the microwave cavity that readily absorbs MW radiations at room temperatures. The susceptor materials couples with microwaves at room temperature and gets heated up rapidly. The generated/developed heat is transferred to the metallic/non coupled materials via conventional modes of heat transfer. This elevates the temperature of the poor

microwave absorbing materials and enables them to couple with microwaves at higher temperature. A schematic representation of microwave hybrid heating is shown in Fig. 2.5 (b). The heating profiles shown in Fig. 2.5 (c) shows the flattening of profile in MHH whereas profile is conventional and microwave heating is not uniform. On reaching the critical temperature states, the non absorbing materials start coupling with microwaves directly [Aravindan and Krishnamurthy (1999); Clark et al. (2000)], whereas; conventional heating still continues from susceptor. A suitable separator material is also required, which performs the function of separating susceptor from processed materials and also acts as a heat transfer media from susceptor to load. The MHH allows bi-directional heating of materials i.e. heat is transferred from outer side to the inner side through conventional modes and from inner to outer direction in microwave heating due to absorption of radiations within the material. The schematic representation of heat flow within the materials in MHH process is shown in Fig. 2.6.

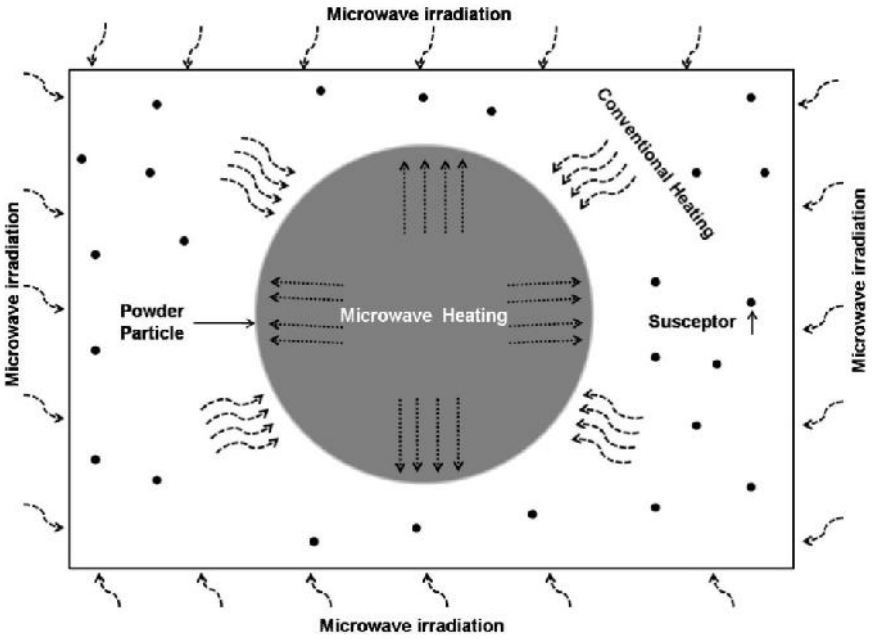

Fig. 2.6: Schematic representation of heat flow in microwave hybrid heating process [Gupta, (2012)]

- **Selective Heating**

  This type of heating is a part of direct microwave heating method, where heating is to be carried out at a selected location of load placed in the microwave applicator. The best example of selective heating is in the case of joining of materials, where microwave radiations are allowed to fall on joint regions and other parts are kept away from exposure by the use of masking materials. The schematic of selective heating is shown in Fig. 2.4 (d). It is highly effective when heating is to be carried out at particular locations and this has been used for localized doping/heating of materials [Livshits et al. (2011); Jerby et al. (2015)].

- **Microwave Assisted Processing of Materials**

  In recent years microwaves have been united with other technologies in the field of materials processing, such that the advantages of microwave heating can be coupled for efficiency and properties improvement. Extensive work has been reported on the microwave assisted plasma technique for manufacturing of carbon fibers [Pauleau et al. (2004) and Whittaker and Mingos (1995)]. Presently, microwave assisted technologies are used in many industrial applications researchers [Porada et al. (2015)] are working on combined laser assisted microwave processing in the field of material processing. This allows the integrity of other processes with efficient microwave heating process [Jerby et al. (2013)] which helps in the cost reduction and advantageous characteristics of both the techniques can be coupled. Research on microwave plasma assisted CVD has been utilized in the processing of many materials and enhance the importance of microwaves in many industrial applications.

2.3 MICROWAVE PROCESSING OF METALLIC MATERIALS

A brief review of the available literature in the field of microwave processing of metallic materials in the form of sintering, joining, claddings, melting and casting are presented in the following sections.

2.3.1 Microwave Sintering of Metals/Metallic Alloys/Metal based Composites

In principle, sintering is the process of compacting loose powder particles by heat or pressure to form bulk objects without reaching melting temperatures. In nature, sintering occurs naturally in the formation of mineral deposits. As a manufacturing process, sintering is used to process metals, ceramics, plastics, composites and other materials. In conventional sintering process a green body (unsintered powder compact) is sintered using resistant heating methods such that the application of thermal energy causes the atoms of the materials to diffuse along the boundaries. This diffusion caused the fusion of particles to form a single solid object. Sintering of materials in conventional way generally requires 0.6-0.7 T_m (melting temperature) for diffusion and requires high holding times for proper fusion of particles. Sintering is a very complex phenomenon and the sintering temperatures for various materials will be determined by the microstructures requirements. Higher temperatures lead to higher densities but promote high grain growth. The proper sintering temperatures may be determined by using some characterization techniques such as DSC (Differential Scanning Calorimetry) and dilatometry; which can detect the temperature of various phase transformations.

Sintering through microwave energy is a novel method explored and it has been applied successfully in processing of various materials. The absorption of microwaves within the materials lead to the electric and magnetic field components to interact directly with the materials; and dielectric and magnetic losses in the materials leads to self heating of materials in

microwave sintering. This self heating through microwave energy is volumetric in nature and allows rapid heating throughout the materials [Sharma et al. (2001)]. In a patent [Spencer (1945)] it was revealed that microwave processing of food was highly efficient process. It was reported that to bake a potato microwave requires the expenditure of about 240 kW-sec in comparison to 72,000 kW-sec for electric oven. A review on the processing of materials in the domain of high temperatures has been reported [Clark et al. (2000)]. Benefits of microwave processing in terms of uniform, rapid heating with high heating rates and reduced processing times, improved physical and mechanical properties, and unique properties which were not available in conventional heating were discussed. In the available review articles by the authors [Yahaya et al. (2013); Agrawal (2010a); Kim et al. (2012); Oghbai and Mirzaee (2010)]; the economic aspects of using microwaves were highlighted and in comparison to conventional heating, huge amount of energy and time savings were reported in sintering of metallic based powders. Over the last two decades, extensive research was carried out on the heating aspects of microwave energy in the area of processing of ceramics, ceramic composites and polymeric composites. Several studies on the processing of ceramics and composites using microwave energy have reported [Link et al. (1999); Sharma et al. (2001); Cheng et al. (2001); Sharma et al. (2002); Fisher et al. (2003); Binner et al. (2007); Agrawal et al. (2010b); Gupta and Wong (2005); Wong and Gupta (2007) and Fang et al. (2009)] that the microwave sintered products are, produced at a shorter sintering time, at lower temperature and at low cost when compared to conventional sintered products. Properties of microwave sintered products were far better from the conventionally sintered products. Till the year 2000, most of the research was conducted on the microwave sintering of semiconductors, inorganic, ceramics and polymeric materials. The lack of research on microwave sintering of metals was due to the fact that metals reflect microwave radiations and hence cause arching during microwave heating. This resulted in limited

investigations on metal sintering through microwave energy. Walkiewicz et al. (1988) exposed various materials to a 2.45 GHz microwave field, and reported modest heating in the range from 120 ºC for Mg to 768 ºC for Fe. Sheinberg et al. (1990) heated copper powder coated with CuO to 650 ºC but did not report any sintering. Narasimhan et al. (1995) succeeded in heating Fe-alloys in a microwave oven only up to 370 ºC in 30 minutes. Till 1995, the major conclusion of the researchers on microwave processing of metallic materials was that no sintering of pure metal or alloy powders can be carried out.

Further, research has been carried out on sintering of various metallic based powders by Roy et al. (1999). It was reported that powered metal green bodies can be sintered successfully within 30 minutes of exposure with a higher modulus of rupture than conventionally processed alloys. The samples of microwave processed Fe-Ni alloy resulted in 60% high modulus of rupture. Other sample with a composition of Fe + Cu (2%) + graphite (0.8%) was processed in a microwave field at 1200 ºC for 30 minutes. The characterization results revealed excellent density. Cobalt metal powder was pressed into pellets, and microwave sintered in pure H_2 at 1 atmospheric pressure at various temperatures ranging from 900 ºC to 1200 ºC for 10 minutes. The density reached 8.70 g/cm^3 at 900 ºC to 8.88 g/cm^3 at 1000–1050 ºC, and very near theoretical density of 8.89 g/cm^3 at 1100–1200 ºC. The encouraging results of Roy et al. (2009) allowed the researchers to expand their work in the domain of metal based materials processing. Anklekar et al. (2001) successfully sintered the PM copper steel using microwaves at 2.45 GHz and 2.0 kW power in a commercial microwave oven. It was reported that microwave sintering of susceptor coated powders produced better microstructures with minimum porosity as compared to conventional sintering. Peelamedu et al. (2002) reported the synthesis and sintering of $NiAl_2O_4$ from NiO +Al_2O_3 powder mixture in just 15 min in a 2.45 GHz microwave field. Sethi et al. (2003) investigated the sintering behavior of Cu-12Sn Bronze using microwave and

conventional heating. It was reported that higher coalescence was observed in microwave sintered bronze due to the 'microwave effects'. Further, less time was required for microwave sintering and characterization results revealed uniform structures and better mechanical properties. No swelling was observed in microwave sintering of bronze. The theory and experiments on electromagnetic losses during processing of powdered metal was studied by Luo et al. (2004). Takayama et al. (2004) experimentally studied the sintering behavior of Cu powder by millimeter wave and reported that even at lower temperatures, volumetric heating was observed. Sintering of Tungsten and its alloys using microwave energy at 2.45 GHz and with 6 kW power was reported by Agrawal et al. (2004). Commercially available tungsten particles in varying size of 0.03 to 0.7 µm was used for sintering. The samples were sintered between 1400 ºC to 2000 ºC in 10 to 20 minutes in a hydrogen atmosphere and soaking time of 10 to 30 minutes. The reported results showed that the sintered samples achieved full densification at 1350 ºC with much finer microstructures than achieved with conventional method. The experimental work carried out by Mondal et al. (2013) on sintering of W-Cu alloys using microwaves revealed that the processing times were reduced in comparison to the conventional furnace method. The comparisons of processing time show reduction by a factor of five ($T_C/T_M \approx 5$) in microwave heating and results are presented in Fig. 2.7 (a). The work carried out by Panda et al. (2006) on sintering time, densification and microstructure of various steels reported about 90% savings in time and hence saving in energy consumptions. The results are presented in Fig. 2.7 (b), which shows time profile for both the methods for processing of austenitic and ferritic stainless steels. Time saving with a factor of ten was achieved ($T_C/T_M \approx 10$). Gupta and Wong (2005) reported the enhanced mechanical properties of metal based powders using two-directional microwave assisted rapid sintering. Experiments were carried out using microwave coupled SiC heating, with 900 W, 2.45 GHz frequency microwave oven.

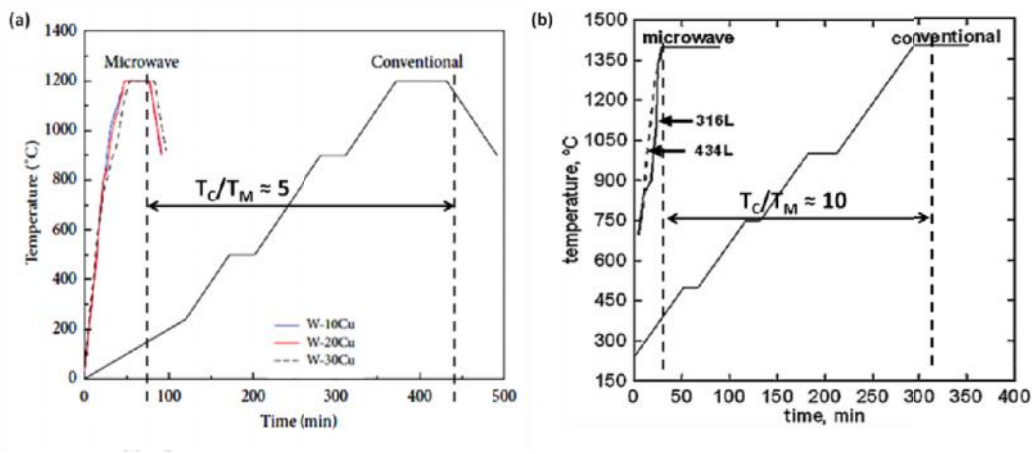

Fig 2.7: Temperature versus time profile in conventional and microwave sintering process for (a) W-Cu alloys and (b) steels (316L and 434L) [Mondal et al. (2013) and Panda et al. (2006)]

Billets of aluminium powder of 7–15 μm size range were microwave sintered for 30 minutes. Magnesium powders of 60–300 μm size range were microwave sintered for 25 minutes and lead-free viromet 349 solder alloy (Sn: 91.4, Cu: 0.5, Ag: 4.1, In: 4) were subsequently sintered using the two-directional sintering approach under ambient condition within 10 minutes. The results of mechanical testing revealed the higher ultimate tensile strength of microwave processed powders in comparison to the conventional processed powders. Wong and Gupta (2006) processed magnesium based nano SiC reinforced composites using microwave sintering. Result of mechanical characterizations revealed the improvement in microhardness, 0.2 %YS, UTS and ductility with the addition of nano-size SiC particulates and the use of the microwave sintering process.

Successful sintering of Fe, Co, Ni, Cu and 316L stainless steel powders was carried out through microwave radiation by Saitou (2006). The metal powders were sintered using single mode microwave applicator and the obtained results were compared with conventional sintering process. The sintering temperatures were reported in the range of 775 ˚C to 1400 ˚C in H_2 and N_2 atmospheres respectively within 30 minutes of exposure. The microwave processed samples

promoted greater shrinkage than conventional sintering. Microwave sintering of Al/Ti composite and Al/ (Ti+SiC) hybrid composites were successfully reported by Thakur et al. (2007). The comparison of power consumption and heating time for conventional sintering and microwave sintering on W-Ni-Fe alloy was reported by Upadhyaya et al. (2007), and are presented in Fig. 2.8. The results clearly revealed time and power savings by a factor of 7 and 4, and support the microwave processing in terms of lower power consumptions and reduced processing timings.

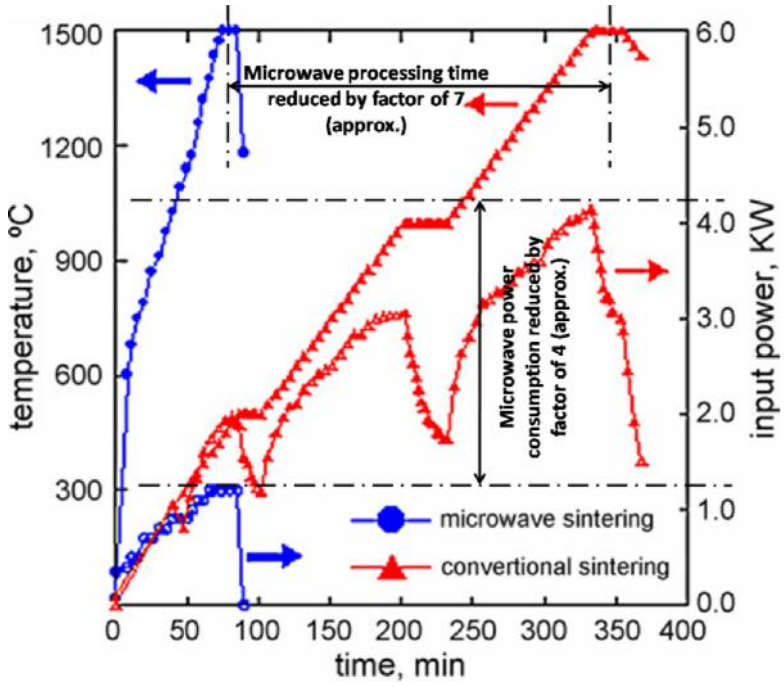

Fig. 2.8: Comparison of power consumed and processing time in conventional and microwave sintering of W-Ni-Fe alloy [Upadhyaya et al. (2007)]

The optical micrographs reported by Upadhyaya et al. (2007) and Panda et al. (2006) are shown in Fig. 2.9. The formation of finer microstructures was reported due to uniform heating rates in addition to lower processing time and temperature conditions during microwave processing, which were absent in conventional heating. The effect of heating mode on mechanical properties of W-Ni alloy is presented in Table 2.1, which indicates that microwave processed sample exhibits better properties than conventional one.

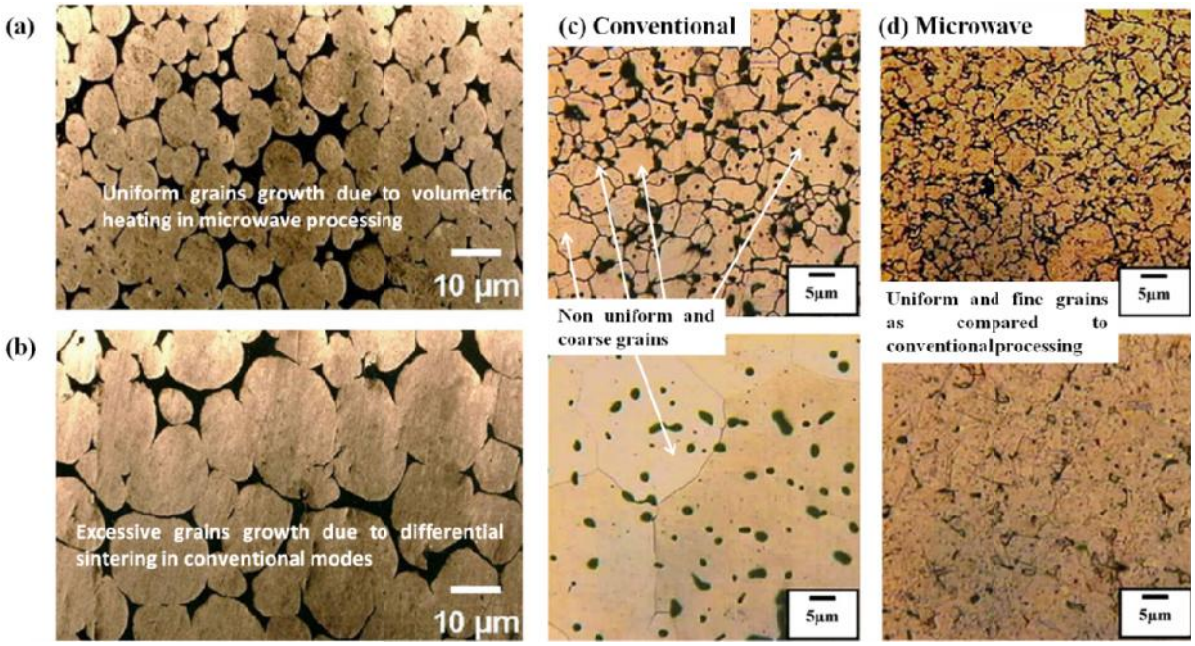

Fig. 2.9: Optical micrographs showing uniform and finer grain formation in (a & d) microwave processed component and (b & c) conventional processed components [Upadhyaya et al., (2007) and Panda et al., (2006)]

Table 2.1: Effect of heating mode on mechanical properties of Tungsten-Nickel alloy (Upadhyaya et al., 2007)

Attributes	Heating mode	
	Conventional	Microwave
Avg. W grain size (µm)	17.3±0.8	9.4±0.5
Bulk hardness, HV_2	210±15	295±10
W grains microhardness, $HV_{0.05}$	398±8	407±5
Matrix microhardness, $HV_{0.005}$	120±11	95±6
Tensile strength (MPa)	642±23	805±14
Elongation (%)	3.5±0.8	11.2±1.1

Padmavathi et al. (2008a) have reported sintering of aluminum and its alloys at 630 ºC in 1 hour in 2.45 GHz microwave applicator at 6 kW. It was reported that microwave sintering allowed enhanced densification in shorter time (50%) and lower sintering temperature than

conventional sintering with better properties. Report on the sintering of commercially available molybdenum powder was made by Chillar et al. (2008). The microwave sintering experiments were carried out using a 6 kW, 2.45 GHz, multimode microwave furnace. Samples were successfully sintered to above 98% TD (Theoretical Density) at 1600 °C –1700 °C in less than 5 minutes, whereas in conventional sintering samples were heated to 1400 °C for 10 hours which resulted in 98% TD. However, in microwave sintering, nearly 99% TD was obtained at 1400 °C in just 30 minutes. Thus the reported results indicate that microwave sintering is much faster than conventional sintering. Leonelli et al. (2008) reported the near-net-shape and net-shape manufacturing of green metal parts (AISI 420 with polymeric binder) through microwave assisted sintering. Sintering of the green compacts was carried out using a multimode cavity at 2.45 GHz, and alumina powder as insulation material. Results revealed that after 15 minutes of microwave exposure, samples were uniformly sintered. The TiN reinforced aluminium MMC were produced by Venkateswarlu et al. (2010) by using microwave sintering process. Hybrid heating technique was used with SiC as a susceptor to sinter the Al-TiN composites under inert environment of argon. It was reported that the presence of TiN particles at grain boundaries of MMC plays a significant role in improving the densification and hardness values. Developed composites were tested for dry sliding wear behavior and results revealed improvement in wear resistance of the composites due to the presence of TiN particles. Further, the wear results of microwave sintered samples were superior to the Al-TiN samples made by hot pressing technique. Comparative evaluation of processing time and properties of microwave and conventional sintered 90W–7Ni–3Cu alloy was carried out by Mondal et al. (2010). It was reported that microwave sintering required about 75% less processing time in comparison to conventional method and microwave sintering yields better physical and mechanical properties in terms of densification parameter, microstructures and hardness. Rajkumar and Aravindan

(2009) developed copper–graphite composites using microwave hybrid heating. Copper–graphite composite samples were manufactured through powder metallurgy route using microwave energy. The 5 *wt %* Copper–graphite composites were post-heat treated at 600 °C for 10, 20, and 30 minutes at the constant microwave power of 400 W using a 3.2 kW and 2.45 GHz microwave multimode applicator. Microstructural results revealed crack free composites with uniform distribution of graphite particles in the matrix phase. The SEM images of some of the developed composites are presented in Fig. 2.10.

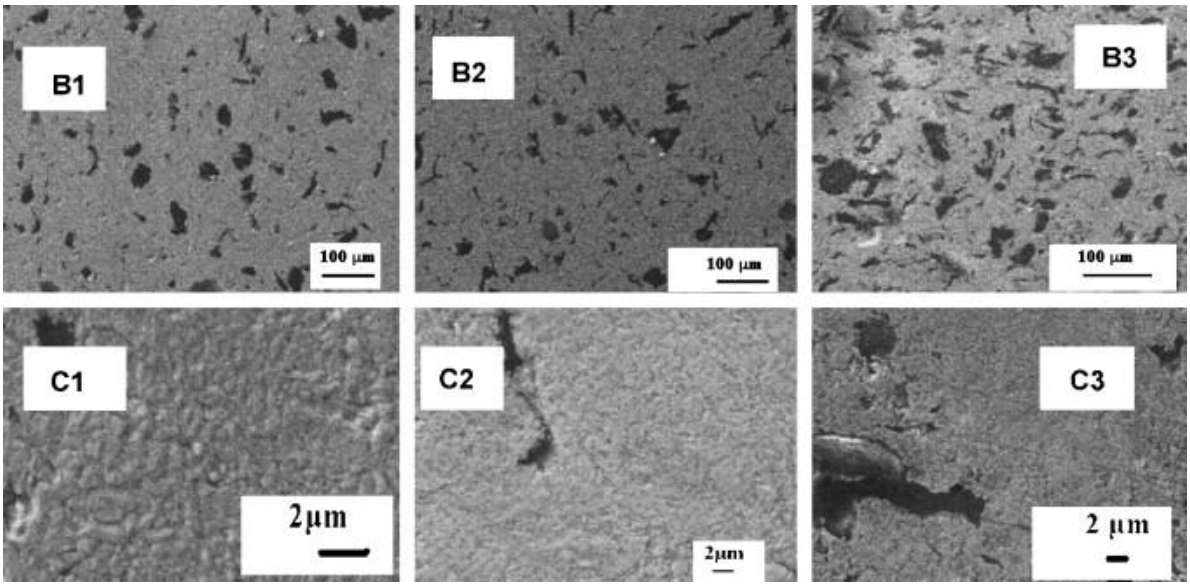

Fig. 2.10: Typical SEM images of copper–graphite composite, (B1) copper-10% graphite, (B2) copper-20% graphite, (B3) copper-30% graphite, (C1) copper-10% graphite, (C2) copper-20 % graphite and (C3) copper-30 % graphite [Rajkumar and Arvindan (2009)]

Rajkumar and Aravindan (2011) carried out microwave sintering of copper-TiC-graphite hybrid composites and revealed the uniform dispersion of reinforcements in the copper matrix. The uniformity in the microstructures was due to volumetric and rapid heating in microwave processing, further, no cracks were observed in the sintered composite specimens. The SEM images of sintered composite are shown in Fig. 2.11.

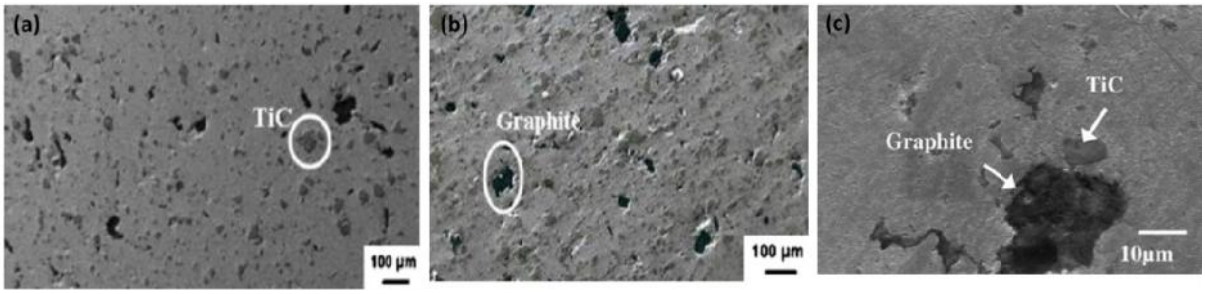

Fig. 2.11: SEM images showing the uniformity in the dispersion behavior of reinforcements in microwave sintered (a) Cu-TiC(10%)-Gr(5%) sample, (b) Cu-TiC(15%)-Gr(5%) and (c) enlarged image of hybrid composite [Rajkumar and Arvindan (2011)]

The development of nano graphite reinforced copper composites through microwave sintering for tribological applications was carried out by Rajkumar and Aravindan (2013). The microwave power of 640 W was used with controlled heating rate of 12 °C/min was maintained. Uniform distribution of nano graphite was observed for 15% volume fraction and further increase in content led to the agglomeration of particles. Demirskyi et al. (2011) reported the sintering of nickel powder through microwave energy. Sintering was carried out without any use of susceptor material and it was reported that microwave heating allowed the formation of liquid phases during microwave sintering.

Liu et al. (2012) reported the sintering of W-Fe-Ni alloy by the microwave sintering process. It was reported that the increase in sintering temperatures from 1250 °C to 1500 °C, the relative densities and mechanical properties of 93W-4.9Ni-2.1Fe alloy were significantly improved. This increase in sintering temperatures allowed reduction of pores in the alloy and gradually eliminated the porosity. Tungsten grains and matrix phase became more homogeneous at higher temperatures. Development of WC-8Co composites via microwave sintering was carried out by Bao et al. (2012). It was reported that mechanical properties of the alloy can be enhanced with lower processing cycles using microwave energy. Microwaves were further used for development of Functionally Graded Materials (FGM) by layer by layer sintering such as

development of W/Cu FGM by Liu et al. (2012) for fusion reactor applications. It was reported that the five-layered W/Cu FGM (W30% + Cu70%/W50% + Cu50%/W70% + Cu30%/W90% + Cu10%/W100%, volume fraction) was fabricated by a microwave sintering method within 30 minutes of processing. Results of characterizations showed that the graded structure was retained even when the microwave sintering temperature was as high as 1300 °C (well above the melting temperature of Cu) and the fine microstructure of W in each layer was maintained due to the short sintering time associated with the microwave processing. Demirskyi et al. (2013) compared the grain growth and properties of titanium nitride sintering processed through microwaves and conventional route. It was reported that fully dense materials with a sub-micron grain size of 170 *nm* was obtained using microwave sintering and 240 *nm* grain size by using conventional sintering. The overall improvement of the mechanical properties, was observed in case of microwave sintering such as an increase in hardness (from 18 to 20 GPa), fracture toughness (from 2.9 to 3.4 MPa $m^{1/2}$). This was due to the grain refinement obtained by the microwave sintering process. Microwave sintering of bulk Ni-Al_2O_3 functionally graded materials was carried by Bykov et al. (2014). The developed FGM is shown in Fig. 2.12.

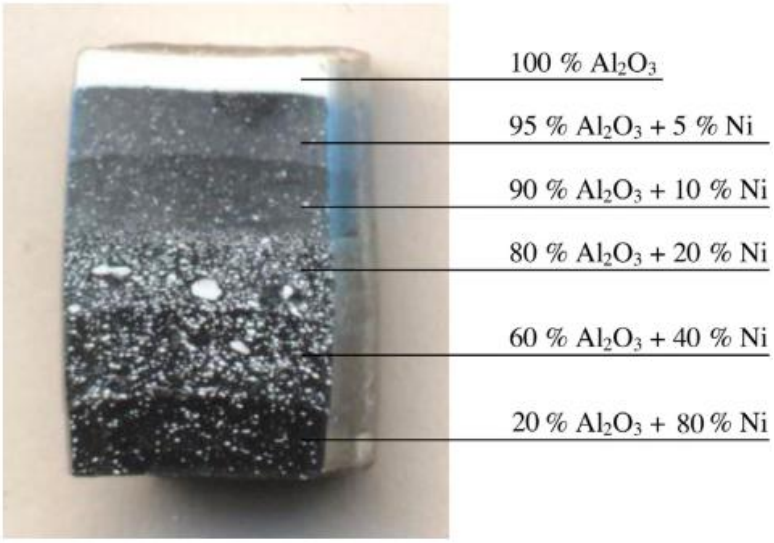

Fig. 2.12: Microwave sintered Ni- Al_2O_3 functionally graded material [Bykov et al. (2014)]

The composite FGM samples were prepared from the alumina powder, having a particle size of 2 μm and nickel powder of 2.5μm. Six layered samples with composition of pure Al_2O_3, Al_2O_3+5%Ni, Al_2O_3+10%Ni, Al_2O_3+20%Ni, Al_2O_3+40%Ni and Al_2O_3+80%Ni were obtained using microwave heating. Microwave power of 5 kW at a frequency of 24 GHz was used for processing. It was reported that the multi-layer component was free from cracks and delamination. Jerby et al. (2015) utilized the microwaves for development of additive manufacturing of 3D structures by stepwise consolidation of metal powders. Metal layers were developed by localized heating using microwaves. Imam et al. (2016) have reported the sintering of Ti-6Al-4V powders through microwave energy. Microwave sintering was reported as one of the best low cost and energy efficient process for near-net shape powder parts. Ghasali et al. (2017) reported the sintering of Al-SiC-TiC hybrid composites by using microwave and conventional process. Microwave sintering of samples resulted in improved mechanical properties with significantly reduced sintering time and energy. Veronesi et al. (2016) carried out the microwave assisted synthesis of high entropy alloys. Rapid microwave heating of the metallic powders mixture compact was carried out in single mode 2.45 GHz applicator. Microwave heating was carried out in the presence of SiC susceptor to attain hybrid heating. Microstructural investigations of HEA revealed the dendritic structure of iron rich and copper rich inter dendritic regions. Veronesi et al. (2017) reported the microwave processing of high entropy alloys at 2.45 GHz and 5.8 GHz. It was reported that microwave processing required the shortest time and lowest specific energy consumptions, thus leading to the most efficient cost saving technique. The literature on microwave sintering has revealed a tremendous amount of energy savings, shorter processing times, lower sintering temperatures coupled with improved mechanical properties in comparison to the conventional process. Some of the comparisons are shown in Table 2.2.

Table 2.2: Properties comparison of alloys/composite properties processed through microwave heating and conventional processes

S. No.	Alloy/ Composite	Parameter	Processing Mode		Conclusion
			Conventional	Microwave	
1	W-Ni-Fe [Upadhyaya et al. (2007)]	Tensile Strength (MPa)	642±23	805±14	Better mechanical properties, Refine microstructures, Lower processing time and power consumption in microwave processing
		Elongation (%)	3.5±0.8	11.2±1.1	
		Avg. W Grain Size (µm)	17.3±0.8	9.4±0.5	
		Processing Time (Min.)	~350	~80	
2	W-30Cu [Mondal et al. (2013)]	Sintered Density (% Theoretical)	~92	~99.98	Better Micro-structure, properties and six times lower power consumption in microwave heating
		Sintering Time	~480	~80	
		Avg. Grain Size (nm)	499 ± 75	302 ± 63	
		Electrical Conductivity (%IACS)	40.0 ± 0.3	43.1 ± 0.7	
		Hardness (HV_5)	258 ± 8	322 ± 9	
3	Al-Mg-Si-Cu [Padmavathi et al. (2011)]	Processing Time (min)	T	58% lower than T	Lower processing time which restricted the formation of intermetallics in microwave processing
		XRD Analysis	Formation of intermetallics	Absence of intermetallics due to insufficient time for diffusion	
4	WC/Co [Breval et al. (2005)]	Soaking Time (Min.)	100	12	Lower processing time and better corrosion properties of microwave sintered samples
		Rockwell A hardness (GPa)	175.5	177.6	
		Corrosion Loss (in HNO_3, 48 hr, wt%)	1.16	0.20	
5	434L Stainless Steels [Panda et al. (2006)]	Processing Time (Min.)	~350	90% reduction in processing times (~40-50)	Microwave processing allowed lower processing time and higher density
		Densification Parameter	0.61	0.63	

2.3.2 Microwave Joining of Metals

As shown in the previous sections, researchers have reported successful sintering of many metallic materials, including development of alloys and composites. But few researchers have reported the brazing/joining of bulk metallic materials. Again, this is due to the lower skin depth associated with the bulk metals. Sieroes and Rego (1995) joined, a thin steel sheet of thickness 0.1-0.3 mm through localized arcing in a 2 kW multimode magnetron. It was reported that by using a higher power magnetron (5 kW) and controlled argon gas flow in the weld sections, plasma was generated to melt the interfaces of thicker sheets. The work reported by Sallom et al. (2005) has brazed Gamma TiAl with Ag-based filler metal. Agrawal et al. (2006) have successfully joined regular steel and cast iron parts through microwave energy within 2-3 minutes; using a braze powder at the faying surfaces. Development of perfect joint was reported with microstructural characterizations. Laurent et al. (2008) successfully reported the brazing of super alloy by using the brazed material of the same composition of base material to maintain the homogeneity. To reduce the melting point temperatures the addition of Si and B material were preferred and joint was irradiated through microwaves by using suitable susceptor. The Indian patent filed by Srinath et al. (2009) sparked the work on joining of bulk metallic parts using microwave hybrid heating techniques. The authors have successfully developed the process and carried out the joining of bulk metallic pieces (steels) with fusion of the parent metals in a domestic microwave oven at a frequency 2.45 GHz and power 900W within 5-10 minutes. Srinath et al. (2011a) investigated a new and novel approach for metallurgical joining of high thermal conductivity materials (copper) using microwave heating. It was reported that joining of copper using conventional techniques possesses many problems due to high conductivity nature. The joining of copper metal in bulk form was carried out using domestic microwave oven at 2.45 GHz and power of 900 W. The microwave hybrid heating was facilitated by charcoal as a

susceptor material. The joining of two plates of copper was carried out by introducing a sandwiched layer of copper powder of 0.5 mm thickness. Characterizations of the joints were carried out through microstructure study, elemental analysis, phase analysis, microhardness survey, porosity measurement, and tensile strength. A uniform, dense joint was obtained with good metallurgical boning and an interface with fused zone is shown in Fig. 2.13. Weld zone shows no sign of micro-cracking; however, some pores are clearly visible at the weld interface.

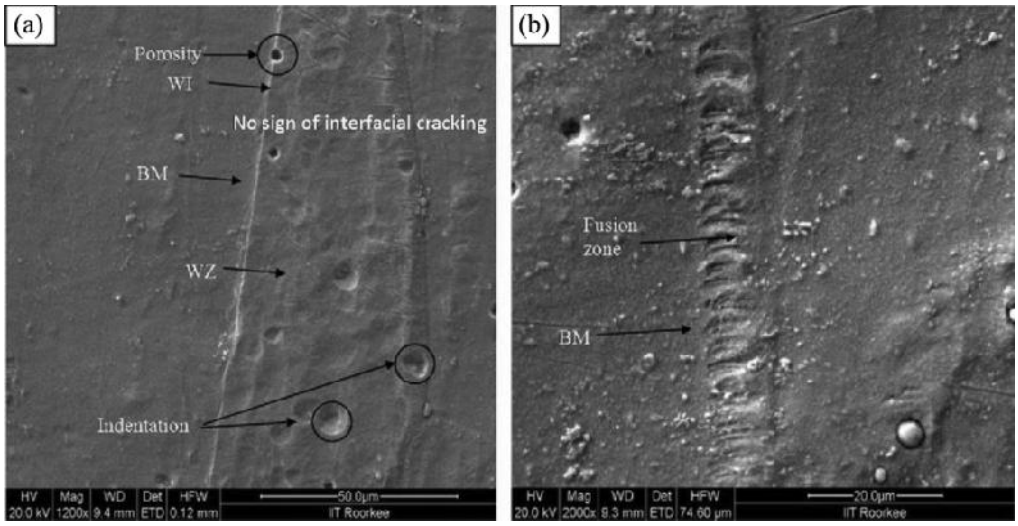

Fig. 2.13: SEM micrographs of microwave processed copper joint. (a) Weld interface. (b) Fused zone [Srinath et al. (2011a)]

The hardness of the joint area was observed to be 78 ± 7 HV, while the porosity in the joint was observed to be 1.92%. The copper joints reported to be exhibited approximately 29.21% elongation with an average ultimate tensile strength of 164.4 MPa. Further, Srinath et al. (2011b) have extended the range of metallic materials for joining, and investigated for joining of bulk stainless steel (SS-316) by using a multimode microwave applicator at the frequency of 2.45 GHz and power of 900 W. The result showed that the joining was effected through fusing and metallurgical bonding of a sandwich layer between the bulk pieces. Heating in the sandwich layer was selectively induced by exposing it to control microwave radiation for a predetermined period (360 s). Porosity measurement in the joint area revealed negligible porosity (0.78%).

Evaluation of the tensile properties of the joints showed an ultimate tensile strength in the order of 309 MPa with an elongation of 11.50%. The joining of dissimilar materials using microwave hybrid heating process was carried out by Srinath et al. (2011c). The microwave joining of stainless steel (SS-316) to mild steel (MS) in bulk form was successfully carried out using a multimode applicator working at 2.45 GHz and 900 W power levels. Complete fusion of the interface layer and metallurgical bonding with bulk interfaces was reported due to the volumetric heating throughout the joint. The formation of metallic carbides ($Cr_{23}C_6$) and cementite (Fe_3C) were confirmed during microwave heating of the joint. The ultimate tensile strength of 346.6 MPa with an elongation of 13.58% was reported because of complete melting of the interface layer and complete bonding with the bulk interfaces. Bansal et al. (2014) carried out the joining of stainless steel plates (SS-316) using microwave hybrid heating. SS-316 powder of 50 μm average particle size was used for joining. The schematic of microwave hybrid heating process used for joining of materials is shown in Fig. 2.14. The microwave processed SS-316 joint and the microstructure of joint is shown in Fig. 2.15 (a-d). The results of various characterizations revealed the formation of relatively low porosity (0.94%) in the joint region and joint exhibit ultimate tensile strength of 425 MPa with an elongation of 9.44% which was approximately 82.5% of the base material strength.

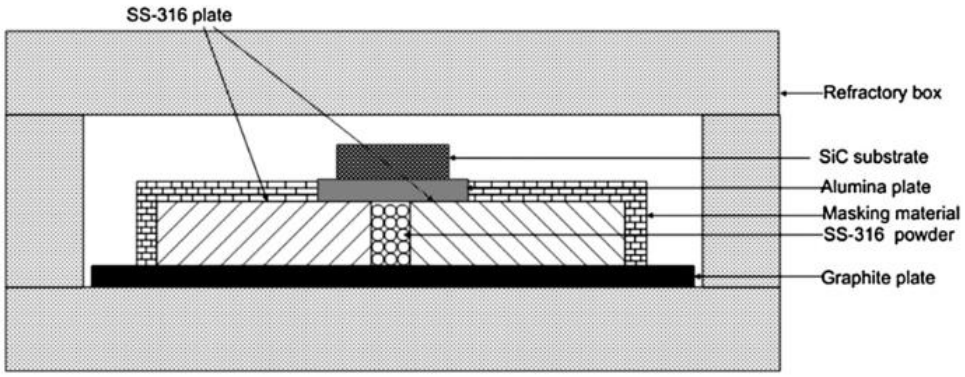

Fig. 2.14: Schematic representation of MHH process for joining of SS-316 plates [Bansal et al. (2014)]

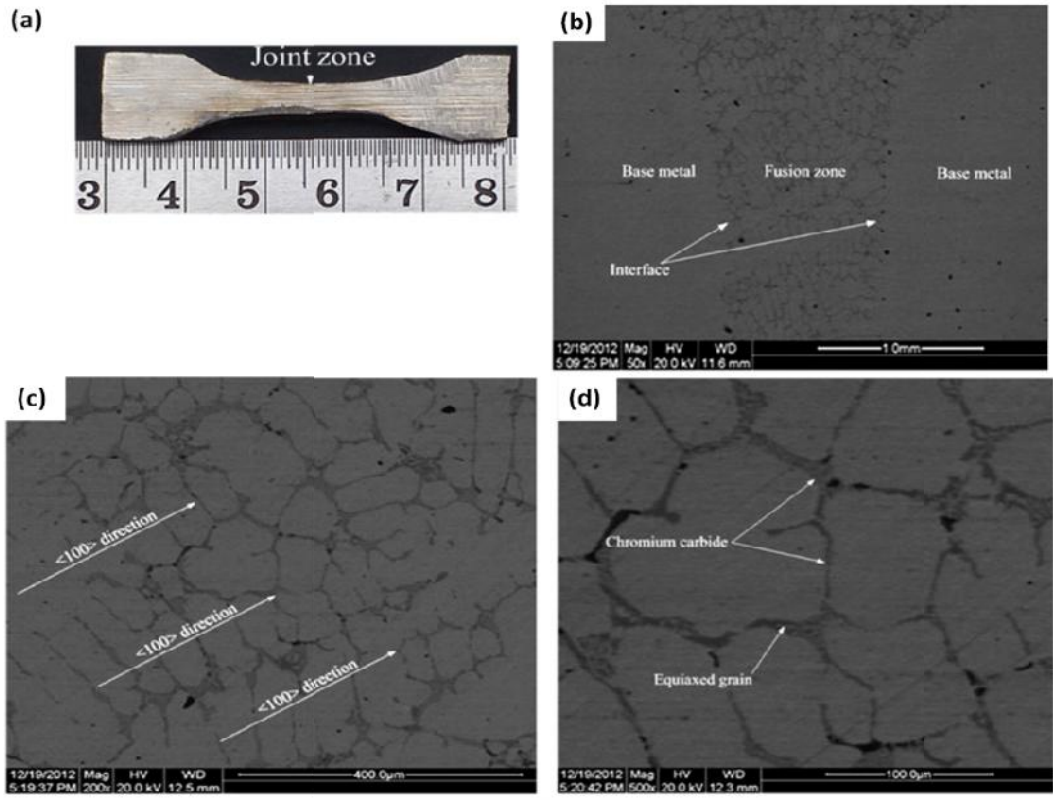

Fig. 2.15: (a) SS-316 microwave processed joint, (b) Joint region, (c) Microstructure showing columnar dendritic growth and (d) Formation of equiaxed grain in weld region [Bansal et al. (2014)]

Bansal et al. (2015) studied the structure property correlations of microwave joined Inconel 718 alloy. It was reported that microwave heating retarded the microstructural transformation of equiaxed grains to dendritic due to volumetric heating associated with microwaves. Singh et al. (2017) reported the preliminary results on joining of Hastelloy through microwave energy. It was reported that within 480±10 seconds of microwave exposure, metallurgical bonded joints were obtained. The reported tensile strength of the microwave processed joints was~82% of base Hastelloy material.

The literature on microwave joining of metallic based materials revealed the potential of microwave energy in materials joining; and maximum of the results reported that microwave processing led to lower porosity defects, lower processing energy and high strength of joints. The formation of equiaxed structures in many reported results were due to the uniform heating

obtained by microwave energy. Further, selective heating leads to the very less less effected zones in the materials.

2.3.3 Microwave Processed Metallic Based Coatings on Metallic Substrates

The work on processing of metallic based cladding/coatings on bulk metals through microwave energy is relatively a new domain in materials processing technologies. Very few studies have been reported in this area (before year 2010). A U.S. patent filed by Wilhelm (1988) reported the PVCD coating of metallic copper waveguide using microwaves. A 6 m long waveguide was coated at 2.45 GHz and 0.5 kW power. Nickel- Titanium (NiTi) plate of 1.2 mm thickness was successfully clad on AISI 316L stainless steel substrate by a microwave-assisted brazing process reported by Chiu et al. (2005). Brazing was conducted in a commercial multimode microwave oven at 2.45 GHz and power levels of 500–1700 W. All the experiments carried out at ambient conditions using a copper-based brazing material in tape form. The results of microstructure study revealed the formation of metallurgical bonding formed via inter-diffusion between the brazing filler and the adjacent materials. The overall study revealed the potential of microwave-assisted brazing and it was reported that this process is simple, economical, and feasible process for cladding NiTi on 316L stainless steel for enhancing cavitation erosion resistance. The work reported by Borneman and Saylor (2008) in the patent for coating of friction reducing alloys powder CuNiIn (150 microns) on Ti-6Al-4V substrate through microwave radiation at preferred frequencies of 2.45 GHz. The results revealed dense coatings on metallic based powders on titanium based material. The scanned images of the developed coating are shown in Fig. 2.16.

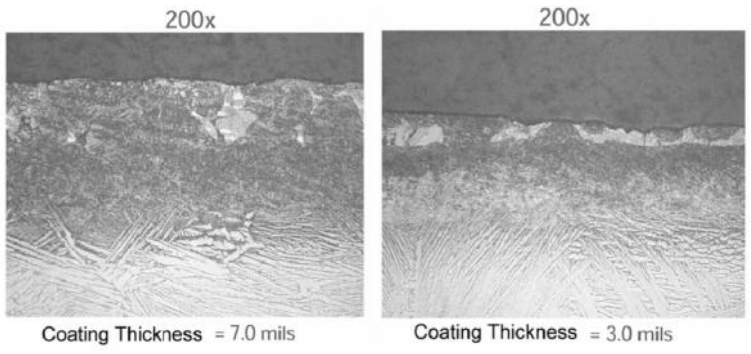

Fig. 2.16: Scanned images of microwave processed metallic based coatings on titanium alloy [Borneman and Saylor (2008)]

Cammarota et al. (2009) reported a novel two phase technique to develop thick NiAl coatings on Ti substrate. Microwaves at 2.45 GHz were used to ignite the self propagating high temperature synthesis of NiAl powders to form coating. The coating was processed at 1200 W and microwave assisted SHS required only 30 seconds. In a patent filed by Gupta and Sharma (2010), a novel process for surface engineering known as microwave cladding was reported for metallic and nonmetallic powders on bulk metallic substrates. The authors claimed that processing of cladding using microwave radiations is a cost-effective method and requires very less energy and processing time. It was reported that clad processed by microwave heating possesses lower defects like porosity and solidification cracks which may contribute to enhanced mechanical properties of developed clads. The experimental work carried out by Gupta and Sharma (2011) investigated the sliding wear performance of cermet clad (WC10Co2Ni) developed through a novel approach of microwave hybrid heating on SS-316 steel substrate. Clads were developed by domestic microwave oven at frequency 2.45 GHz and 600–900 W power within 60 seconds. It was reported that within 360 seconds of microwave exposure, the powders were semi melted and formed metallurgical bonding with the substrate. The porosity levels were relatively low (0.89%) and clads exhibited 84 times higher wear resistance than SS-316 steel. The schematic approach to develop cladding using MHH is shown in Fig. 2.17.

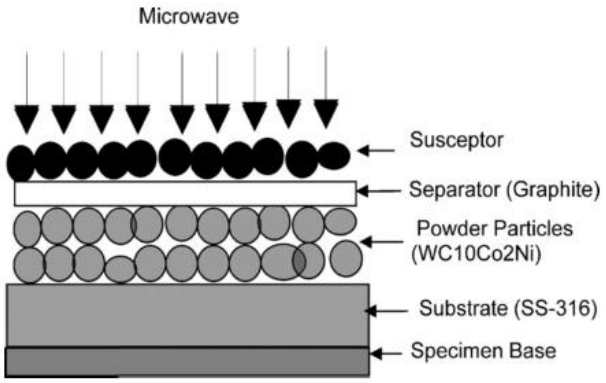

Fig. 2.17: Schematic representation of the MHH process for developing claddings [Gupta and Sharma (2011)]

The microwave processed cladding was ~2mm thick and revealed partial diffusion of substrate material. The average Vickers microhardness of clad was 1064 ± 99 HV due to the formation of hard intermetallics. The microstructures revealed skeleton like carbides dispersed uniformly in the clad as shown in Fig. 2.18.

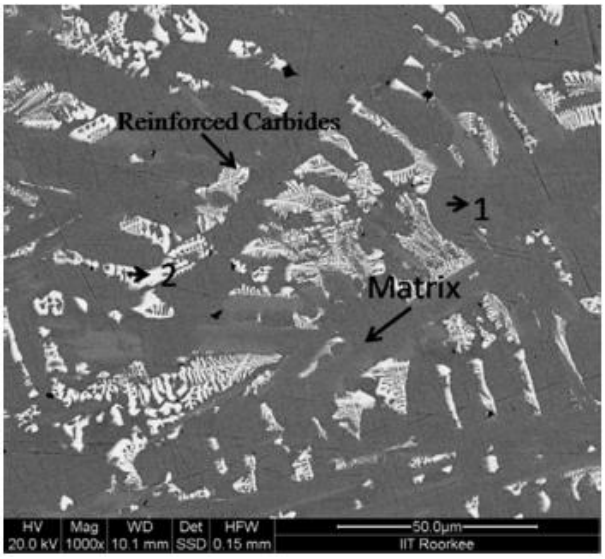

Fig. 2.18: Typical back scattered SEM image showing skeleton like microstructures in microwave processed clad [Gupta and Sharma (2011)]

Sharma and Gupta (2012) investigated the microstructure and flexural strength of metal-ceramic composite cladding developed through domestic microwave energy on austenitic

stainless steel. Clads were developed within 420 seconds of microwave exposure at 2.45 GHz and 900 W power. It was reported that due to intense heat generated through microwaves there was partial dilution of substrate in the clad. The XRD spectrum obtained for the microwave processed cladding is shown in Fig. 2.19, which reports the formation of some intermetallic hard phases.

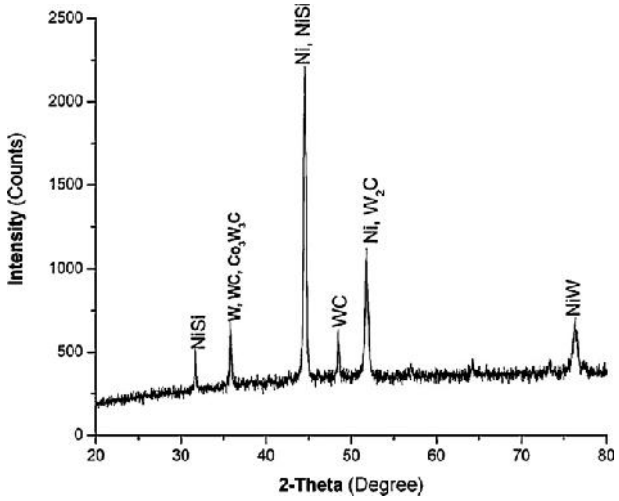

Fig. 2.19: XRD spectrum of metal-ceramic clad developed through MHH [Sharma and Gupta (2012)]

The developed clad revealed that the hardness at the interface is approximately twice that of the substrate. Gupta and Sharma (2014) exhibited microwave cladding as a new approach in surface engineering. The theory of clad formation was explained using suitable illustrations. It was reported that clad formation involves partial dilution of substrate and formation of strong metallurgical bonding between substrate and deposits. Tungsten carbide based WC10Co2Ni powders clads were produced on austenitic steel by microwave hybrid heating at 2.45 GHz frequency at a power rating of 900 watt. The processing time of 120 seconds was recorded to develop defect free clads. Zafar and Sharma (2015) developed WC-12Co based cermet clads on AISI 304 SS steel. Clads were developed by using industrial microwave applicator at 2.45 GHz and 1.4 kW power. The particle size of 45 μm of WC-12Co powders was used and it took only

600 seconds of microwave exposure to form dense cladding. It was reported that developed clads exhibit significant resistance to wear due to the microwave-induced dense microstructure and material properties. Further, Zafar and Sharma (2016) used commercially available WC-12Co nano-structured powder with an average grain size of 100-200 nm was used to develop clads on SS-304 steel substrate using microwave energy. It was reported that excellent metallurgical bonding at the interface was obtained and clads were free from interfacial cracking. The role of localized convective current in the melt pool was reported, that caused partial dilution of the clad layer and the substrate material. The formation of various intermetallic carbides such as WC, W_2C, Co_6W_6C, Co_7W_6 and $Co_3W_9C_4$ due to microwave induced heating was reported. The uniform distribution of nano particles were reported (Fig. 2.20) and further it was found that the intense heating through microwaves caused dilution of some carbide in the clad which led to five time high microhardness of clad (1760±128 HV) than metal substrate.

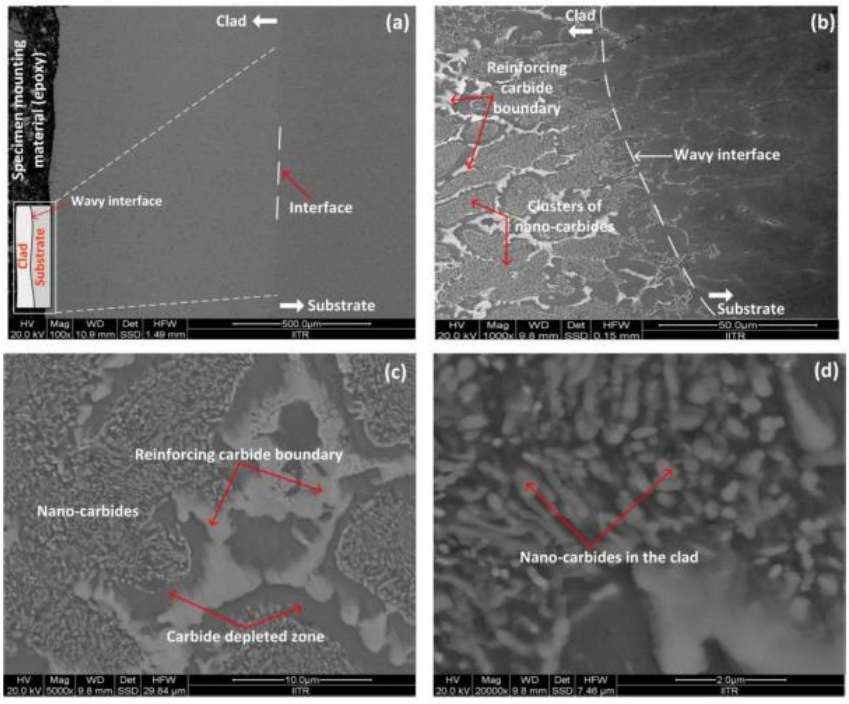

Fig. 2.20: SEM images showing the (a) Microwave processed clad, (b) Microstructure of the clad, (c-d) Magnified images showing the detailed structure [Zafar and Sharma (2016)]

Kaushal et al. (2017b) reported microwave cladding approach for the development of functionally graded clads on the austenitic stainless steel substrate. Functionally graded claddings with four layers of pure Ni, Ni+10%SiC, Ni+20%SiC and Ni+30%SiC were obtained by microwave heating at 2.45 GHz and 900 watt power. The processing time for each of the clad was ~300 seconds. The developed FGC and layer wise deposition is shown in Fig. 2.21.

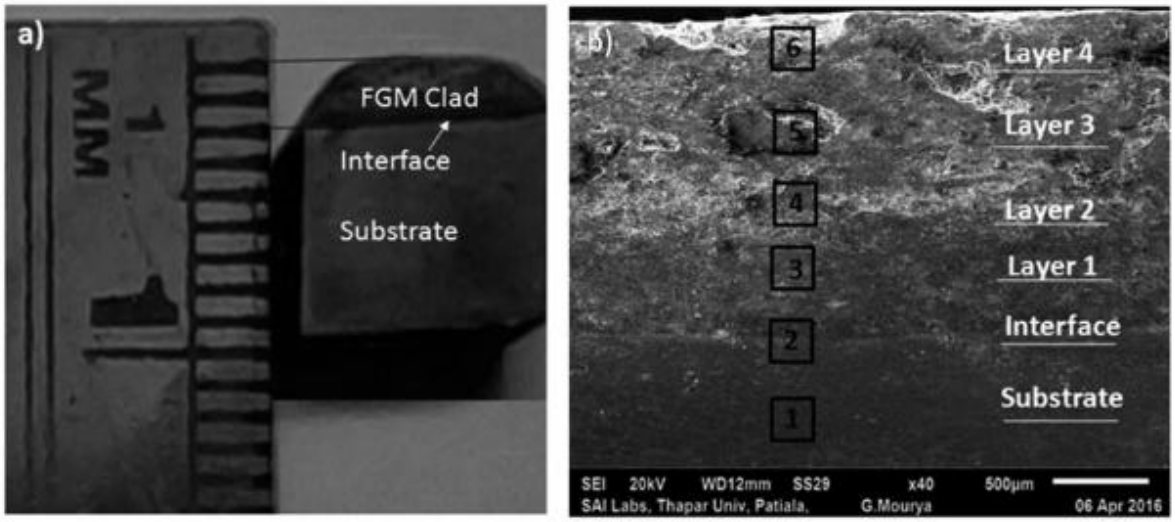

Fig. 2.21: (a) Microwave processed FGC and (b) Layers developed by microwave heating [Kaushal et al. (2017b)].

It was reported that the developed clads were free from cracking and SiC was uniformly distributed in the Ni melted matrix. The maximum Vickers microhardness was 1020 HV. It was reported that he microwave hybrid heating technology offers possibilities to develop FGM clad layers of various compositions.

The literature reviewed revealed that microwaves were efficiently used in the processing of metal based powdered clads on various metallic substrates. The characterization results revealed the partial melting of powdered particles and even dilution of substrates by microwave heating. Microwave processed clads were free from the defects such as extensive porosity and

cracking's. Further, the processing time for development of cladding was comparatively lower than the other available processing methods.

2.3.4 Microwave Synthesis of Metallic based Powders

The favorable characteristic of microwave heating has attracted many researchers in the field of materials synthesis. Komarneni et al. (1995) used novel microwave-hydrothermal process to synthesize various nano metallic powders such as copper, nickel, cobalt and silver. Metallic powders were obtained by reducing their salts or hydroxides with ethylene glycol. It was reported that the microwave hydrothermal process was rapid and within minutes the metallic powders were synthesized. The powders synthesized were uniform in size and were spherical in shape as shown in Fig. 2.22 (a-d).

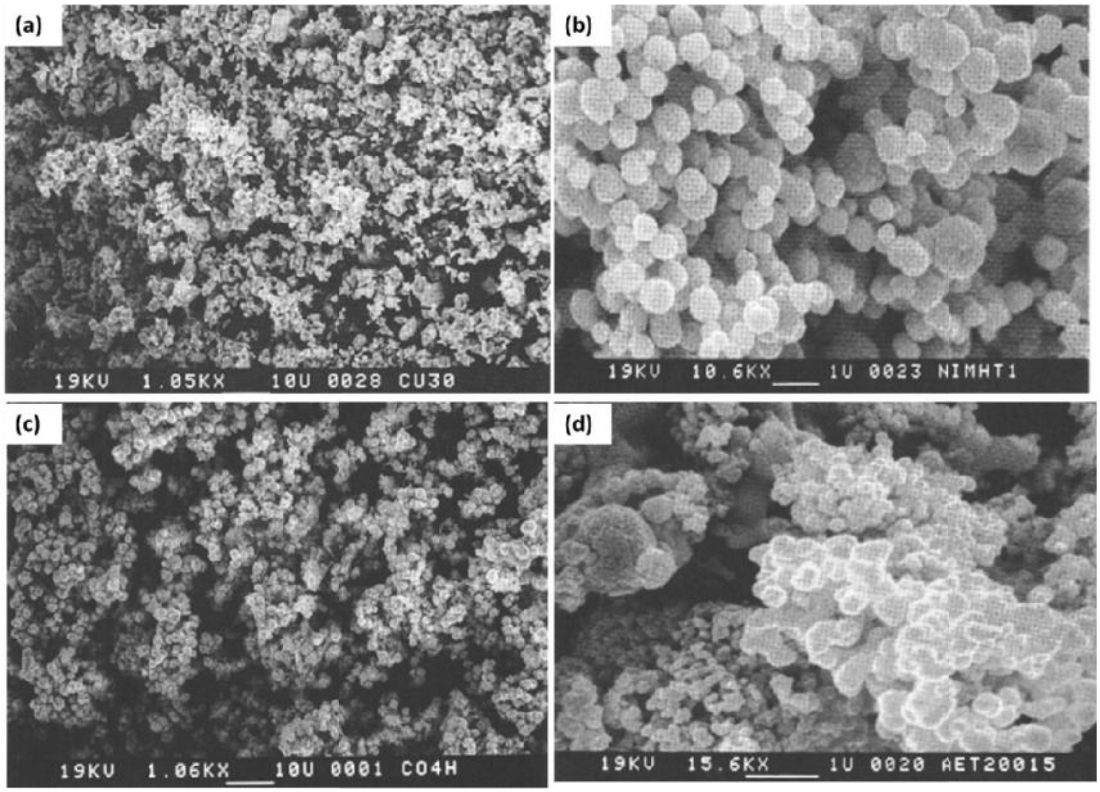

Fig. 2.22: Microwave- hydrothermal synthesis of (a) Copper powder, (b) Nickel powder, (c) Cobalt powder and (d) Silver powder from respective salts [Komarneni et al. (1995)]

Harpeness and Gedanken (2004) used microwave assisted polyol reduction for the synthesis of core-shell gold/palladium bimetallic nano particles. It was reported that the process was simple, with short reaction time and was cheap to prepare the nano structures.

In a patent filed by Krupashankara et al. (2002) method of producing ultrafine powders was reported using microwave plasma apparatus and chemical synthesis technique. Zhu et al. (2004) reported the rapid synthesis of copper nano particles under microwave radiations. The synthesis was carried out using microwave oven for 5 minutes with medium power and continuous stirring. It was reported that well dispersed copper nano particles of diameter 10 nm were obtained rapidly.

Zhao et al. (2004) reported the microwave-induced polyol process for synthesis of copper and copper oxide nano crystals with controlled morphologies. It was stressed that microwave irradiations play a critical role in the synthesis of particles. Zhu and Zhu (2006) reported the single step synthesis of polyacrylamide-metal nano composites using microwaves. It was stated that microwave heating was a convenient and efficient method for in-situ single step synthesis of metal nanoparticles and simultaneous polymerization of acrylamide monomer. It was reported microwave heating with the use of ethylene glycol does not require any additional initiator, surfactant or stabilizers for synthesis and contributes to the lost cost production method.

Klinowski et al. (2011) reviewed the microwave applications in the synthesis of Metal-Organic Framework (MOF). It was reported that microwave heating allowed shorter reaction times, fast kinetics of crystal nucleation and growth, and high yields of desirable products. It was stressed that over the time microwave heating has an extensive effect on the MOF's synthesis in an economical way. Nadagouda et al. (2011) investigated the green synthesis of silver nano structures. It was reported that over the period of time microwave chemistry has been established

as a well defined route for the synthesis and production technique in many academic and industrial labs. The production of silver nano-rods within 2 minutes of microwave exposure was reported as compared to the conventional oil bath synthesis for 1 hour. The synthesized silver nano rods are shown in Fig. 2.23.

Galletti et al. (2013) reported the novel microwave synthesis of copper nano particles without using any stabilizing agents and studied the anti bacterial response of synthesized particles. It was again emphasized that MW radiations can increase the reaction rates up to one to two orders of magnitude and lead to energy savings. The average particle size of nano copper was in the range of 7-15 nm ascertained through TEM microscopy.

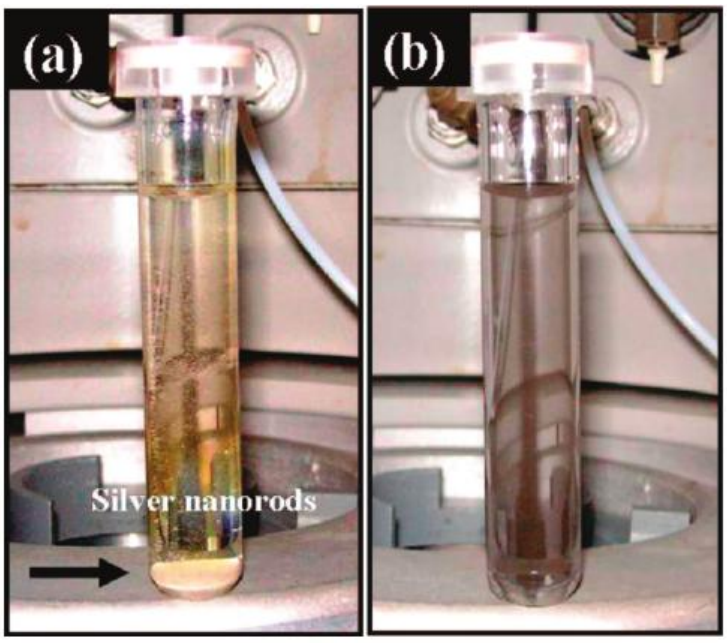

Fig. 2.23: Synthesis of silver nano-rods by (a) Microwave heating reaction within 2 minutes and (b) Reaction carried out by oil bath in 1 hour [Nadagouda et al. (2011)]

Similar research on synthesis of various materials involving microwaves revealed the potential applications of this microwave heating technology in various commercial

manufacturing applications. Reviewed literature revealed that by using microwaves, the reaction rate becomes ultrafast thus producing better products with lower energy consumptions.

2.3.5 Microwave Melting of Metals/Metallic Powders

Limited literature is available on melting of metallic based materials through microwave energy due to the incompatibility of microwave absorption in bulk metals/metallic powders. The literature review on microwave processing of claddings has already revealed the partial melting of metallic powders. These results indicated the bright future in the field of microwave melting of metals.

Moore at al. (2006) filed a US patent and claimed the method and apparatus for melting of metals using microwave energy as the primary heating source. It was reported that metal was melted in a ceramic crucible which was encased in a ceramic casket for insulation. The metal was heated in a controlled oxygen free environment and molten metal was either poured in a mold outside or a mold placed just below the crucible by dripping or running.

Takayama et al. (2008) have reported the production of pig iron by microwave processing of mixed magnetite and carbon powder at the frequencies 2.45 GHz and 30 GHz. Cho and Lee (2008) have reported a carbothermic reduction of the mill scale using microwave heating. The experiment was conducted in a microwave furnace of 1.2 kW power and operating at 2.45 GHz. The mixture of the mill scale and graphite particles was heated at a very rapid heating rate (100 °C/min) via microwave heating. As a result of this process, self-assembled metallic droplets of 1 mm to 5 mm in diameter were produced in less than 15 min as shown in Fig. 2.24.

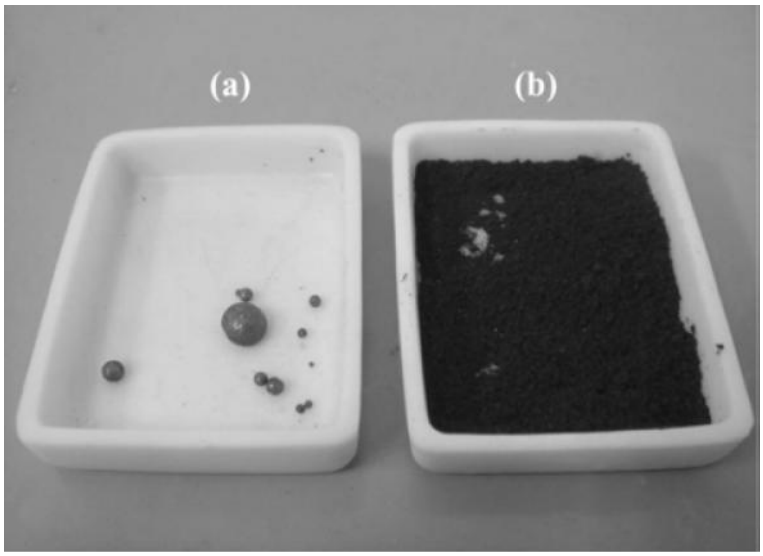

Fig. 2.24: View of the reaction products: (a) metallic droplets and (b) unreacted remaining powders [Cho and Lee (2008)]

Chandrasekaran et al. (2011) reported successful results on melting of metallic materials using microwave hybrid heating. Melting of lead, tin, aluminium and copper was experimentally investigated by varying microwave power level and the load using MHH. Microwave melting of metals was carried out at three different power levels 100% (1300 W), 70% (910 W) and 40% (520 W) and at various loads (50 g to 150 g). The operating frequency of microwaves was 2.45 GHz. Tin and lead granules of average diameter 3 mm were used for melting. Experimental results indicate, melting of tin was achieved in 5 minutes for 100% and 70% power, whereas melting was achieved within 7 minutes at 40 % power. The time required for melting tin was the same for all loads up to 150 g at a given power level. It was seen that melting of lead was achieved in 5.5 minutes for 100% power, 6 minutes for 70% power and 9 minutes at 40% power Bulk aluminum metal of diameter 14 mm and thickness 12 mm were used for the investigation. The experiments were carried out in the presence of argon in order to minimize aluminum oxidation. The time required for melting were 9 minutes at 70 – 100% power and 14 minutes at 40% power level. Copper turnings of average thickness 2 mm were used for melting studies.

Copper has a tendency to oxidize at high temperatures in ambient air and hence argon atmosphere was maintained to minimize oxidation. The time required for melting was 20 minutes at 70 – 100% power and 29 minutes at 40% power level. On comparing with a conventional furnace, microwave melting was found to be twice faster and safer to handle.

Opportunities in the field of microwave casting were reported and in-situ microwave casting using domestic oven at 900 W and 2.45 GH was carried out by Mishra and Sharma (2016a). In situ casting of copper was successfully carried out by using split mold having cope and drag with microwave oven and setup is shown in Fig. 2.25. Another work reported by Mishra and Sharma (2016c) investigated the in-situ casting of aluminium alloy AA 7039. Casting was carried out in a water cooled industrial multi-mode microwave applicator at 1400 W and 2.45 GHz. Microwave was equipped with built in infrared (IR) pyrometer (range: 350°C–1800°C and least count: 1^0C) for measuring the in-situ temperatures. The schematic of microwave in-situ casting set up is shown in Fig. 2.26.

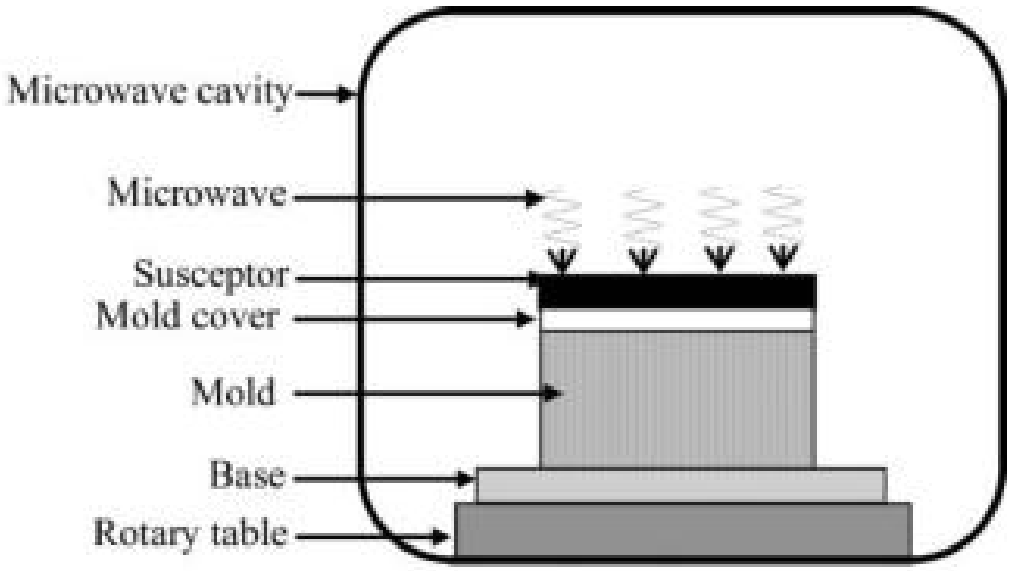

Fig. 2.25: Microwave in-situ casting setup used for copper [Mishra and Sharma (2016b)]

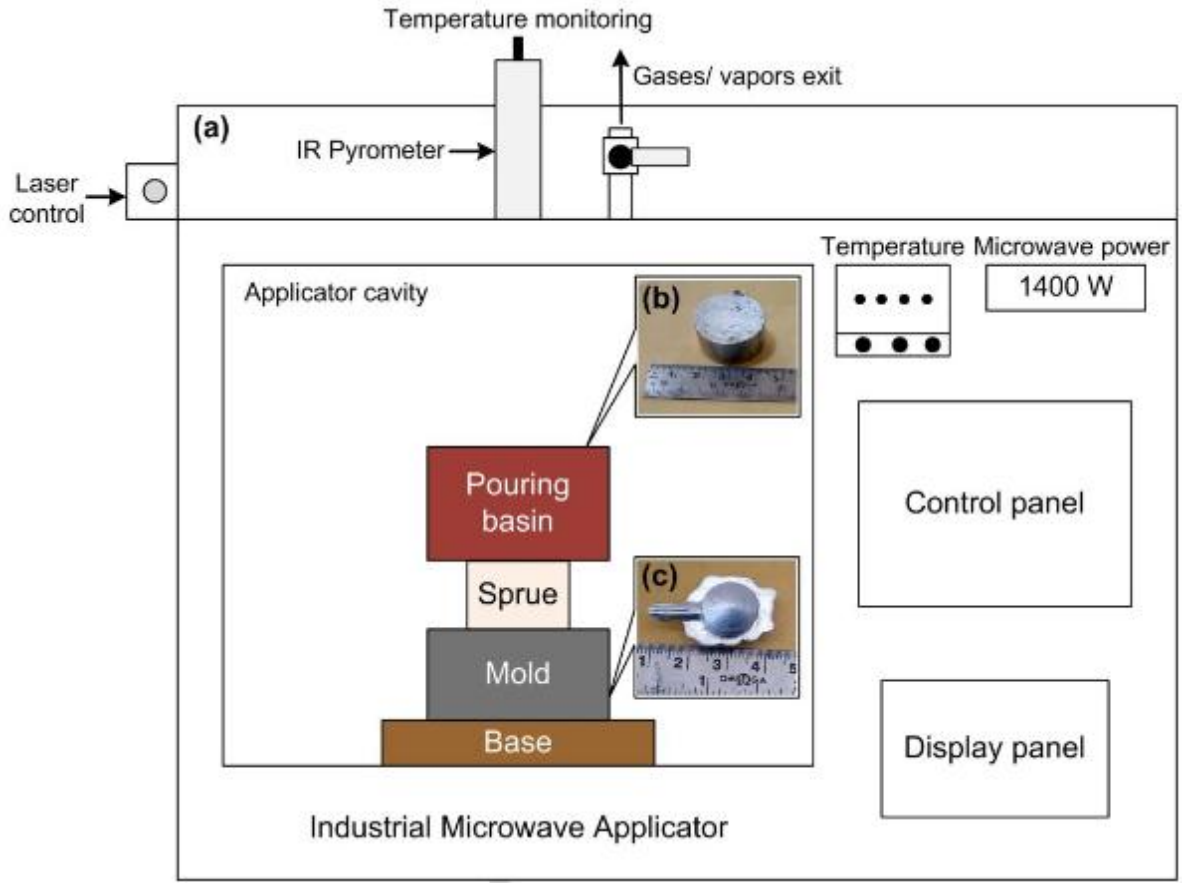

Fig. 2.26: Schematic representation of in-situ microwave casting process [Mishra and Sharma (2016c)]

The effect of critical temperature was reported beyond which aluminium alloy started absorbing microwaves. The oxide layer grown during the heating process acts as a susceptor and helped in achieving the melting temperatures. Low level of porosity (2%) in the developed cast was due to the lowering of thermal gradients between mold wall and liquid melt during solidification.

This limited literature microwave melting and casting provides an ample opportunity to carry out research in this novel field, where microwave energy can be utilized with reduced energy consumptions.

2.4 OBJECTIVES AND SCOPE OF THE WORK

In the present scenario of cut throat engineering, the sustainability of any industry mainly depends on the energy consumptions in manufacturing. Melting and casting of materials is one of the prime areas where huge amount of energy is required. Further, melting of materials involves pollution of the environment; which is a major concern globally. The researchers are continuously working to develop new materials processing methods which require lower energy, consumes less time and are environment friendly. Such developed technologies will help in the sustainability of the manufacturing sector for any nation.

The developments in the microwave materials processing have shown tremendous results in achieving the economic processing. The sintering of materials through microwave energy is now well established route in industries. Microwaves as a heating source can be a substitute for the existing/conventional sources and can overcome limitations associated with these processes. The main characteristics of microwave heating include: (1) volumetric heating due to direct absorption of microwaves, (2) rapid heating of materials, (3) controllable field distributions, (4) selective heating of materials, and (5) high processing rates. These inherent characteristics of microwave processing can provide more rapid and uniform heating in a clean environment, offering improvements in product quality, production of better microstructures and properties, and reductions in manufacturing costs and processing times. A lot of literature is available where property-structure correlations have been studied extensively for microwave processed materials. However, heating of metals/metallic powders and subsequently melting and casting of metallic based materials using microwave is a challenging task due to poor penetration depth (in micron) of microwaves at common frequency 2.45 GHz at room temperature. Thus, the main aims of the present work have been formulated as:

1. Investigation and feasibility study on the development of metal-ceramic composites casting by using a domestic microwave oven of frequency 2.45 GHz.
2. To develop and study the effect of process parameters like exposure time, power level and preheating of powders on output responses.
3. Metallurgical and mechanical characterizations of the developed metal-ceramic composites casting on optimized process parameters.
4. To study the tribological wear behavior of developed metal-ceramic composite castings.
5. Fractographic study of worn samples for analysis of wear mechanism of the developed metal-ceramic composite castings.

2.4.1 Scope of the Work

The major scope of the present work is;

a) Exploring the possibilities for melting and development of powdered metal-ceramic composite castings through microwave heating.

b) Investigation of the mechanism of metallic particles melting and casting of metal-ceramic composite powders using the domestic microwave oven.

c) Development of metal-ceramic castings of Ni-based (EWAC) powder premixed with various ceramic reinforcements (Silicon carbide, alumina and tungsten carbide) at varying volume fraction; using microwave heating.

d) Metallurgical characterization of microwave melted and cast composites in terms of phase analysis, growth of structure, assessment of porosity, cracks etc.. The techniques used for this characterization would be X-ray diffraction (XRD), field emission scanning electron microscope (FE-SEM), energy dispersive spectroscopy (EDS).

e) Mechanical characterization of castings in terms of tensile strength, percentage elongation and microhardness (using Vicker's microhardness tester).

f) Functional characterization (dry sliding wear behavior) of EWAC and composite castings at varying parameters.

g) Mechanism of wear by studying the fractured surface using SEM and EDS.

2.5 PLAN OF THE PRRESENT WORK

The proposed plan of the present work is illustrated in the flow chart as shown in Fig. 2.27.

2.6 SUMMARY

The metal-ceramic composites belong to the advanced materials category and are widely used in many aerospace, automobile and structural applications. However, processing of such materials requires high temperatures are difficult to process. Conventional sintering of such materials involves higher energy consumptions and processing time. Though microwave sintering is effectively used as a processing technology, but it is very difficult to eliminate the defects such as porosities and to control the diffusion rate. Further, casting of materials can enhance the strength of such materials due to homogeneity achieved. But, melting and casting of such materials by conventional route is not an economical way. A comprehensive review of relevant literatures on microwave processing of metallic materials has been presented. The gaps observed in the available literature on microwave processing of metallic materials have been explored.

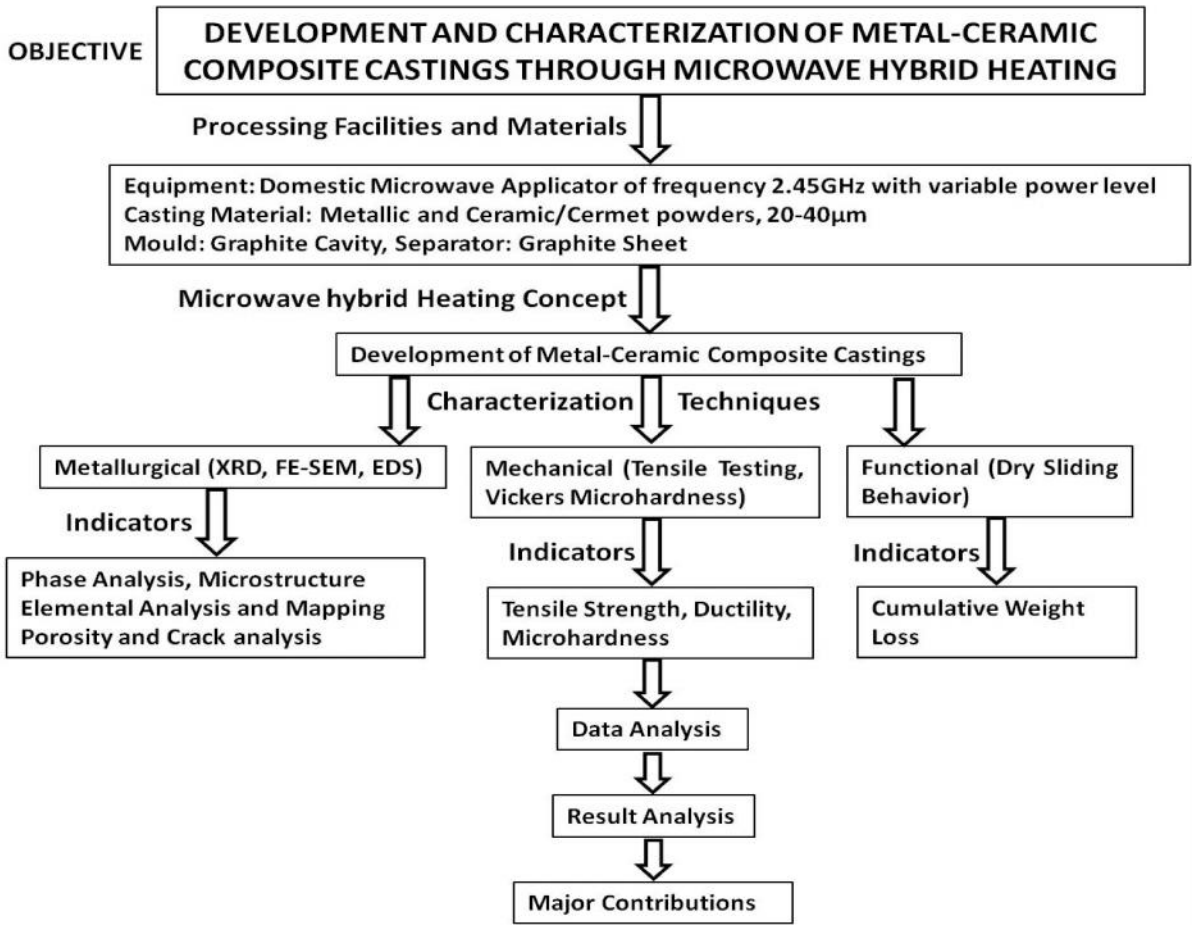

Fig. 2.27: Flow diagram showing the plan of the present work

The available literatures show that heating and sintering of metallic particulates and joining of bulk metallic materials through microwave have been carried out-in the last decade. But, it was observed that limited literature on melting and casting of metallic based materials using microwave as a heating source is available. Accordingly, the objectives and scope of the present study have been formulated. The detailed research methodology adopted in the present work has been presented in the form of a flow chart.

CHAPTER 3

MECHANISM OF MICROWAVE CASTING PROCESS

The progress in the field of processing various types of materials through microwave energy has been reported for the past few decades. The journey from the processing of foodstuffs to the processing of non microwave absorbing materials such as metals; is due to the continuous efforts of scientists, researchers and academicians working in this novel field. The advantageous characteristics of microwave heating have been known since the development of domestic ovens; which require lesser energy and processing times to heat foodstuffs. These characteristics of microwave heating were well utilized in the processing of many materials and eventually lead to the well established route for sintering of various ceramics/ metallic powders/ composites. A lot of work is carried out in the development of high frequency and high power magnetrons which can be utilized in many thermonuclear experimental reactors [Kalaria et al. (2014)]. However, limited research is carried out in the melting and casting of metallic based powders. This is the thrust area where researchers are focusing to minimize the cost of melting and casting in industries. The developed theory of microwave melting and casting of metallic powders is presented in this chapter.

3.1 DIFICULTIES IN MICROWAVE HEATING OF METALS

It is well known fact that metallic powders tend to reflect microwaves radiations at 2.45 GHz at room temperatures due to the significantly lower skin depth of metals. The skin depth of any material with respect to microwave processing is defined as ‘the distance into the material at which the incident power drops to 1/e (36.8%) of the surface value’ [Gupta and Sharma (2011)]. Thus, by altering the skin depths of materials or increasing the penetration depths of microwave

radiations, the microwave-materials interactions can be enhanced by sufficient factor that can cause the intense heat generation. It has been reported [Gupta and Sharma (2011)] that the skin depth (δ) associated with materials can be increased by altering the temperature dependent properties such as resistivity (ρ) and magnetic permeability (μ); at a particular frequency (f = constant). The '*microwave effects*' has been reported by many authors [Clark et al. (2000); Aravindan and Krishnamurthy (1999)] while processing materials through microwave energy and these effects are due to variability of such temperature dependent properties. It was reported that there exists a critical temperature value at which ceramic undergoes phase changes that transited properties into a higher loss tangent. Even, skin depths are altered at critical temperatures, which enhances the heating rates. If the material skin depths are comparable to particle size, only then the effective heating through microwave absorption will take place. However, it is not always possible that bulk/macro size powder materials skin depth is of the same magnitude of their dimension. It becomes practically unfeasible to process such metallic materials through microwave radiations at room temperatures. The phenomenon of microwave effects was reported at some critical temperatures, depending upon the materials properties. The possibility to determine the critical temperatures for all the metallic materials is a very cumbersome process due to the complexity involves in microwave heating of metallic materials. The straightforward solution to this problem is to raise the initial temperatures to the critical temperature, by applying the concept of hybrid heating, such that direct microwave interactions can cause a sufficient rise in temperatures which can lead to melting. This microwave hybrid heating technique utilizes an additional material (susceptor) that readily absorbs electromagnetic energy even at room temperatures. This heated susceptor develops heat that propagates and elevates the initial temperature of the metallic materials via conventional modes of heat transfer. This allows the temperature dependent properties to vary, such that increase in skin depths of

metallic materials causes interactions with the microwave radiations. This elevated temperature is called, critical temperature (Tc) at which the skin depth of the particles increases as illustrated by Gupta and Sharma (2011). Further, after the coalescence is achieved (say in metallic materials) during microwave processing, the skin depths can again reduce and stops the effective coupling of microwaves. In microwave hybrid heating process, the absorbed electromagnetic energy is shared by various materials such as susceptor, cavity material, separator, etc.; and it becomes practically impossible to calculate the energy share for individual materials. But, the electromagnetic energy injected into the fixed mass of material can be estimated by equation 3.1 [Sharma and Gupta (2012)].

$$E = \int_0^T p\, dt \tag{3.1}$$

Where, E (J) is the total energy injected in the work load, p (W) is the applied microwave power which can vary with time and T (s) is total microwave exposure time.

In present work nickel based powder (EWAC 1004EN) containing 97% nickel is used as the matrix material for the development of metal-ceramic composite castings. The skin depths associated with nickel particles can be calculated by using equation 3.2.

$$\delta = \sqrt{\frac{\rho}{\pi f \mu_r \mu_o}} \tag{3.2}$$

Where, δ = skin depth in μm, ρ = resistivity (μΩ-cm), f = frequency of microwaves (2.45 GHz), μ_r = relative permeability and μ_o = absolute permeability (H/m), where $\mu = \mu_r \mu_o$ (Magnetic permeability).

For calculation of skin depth for nickel the numerical values were taken from reference *"http://www.microwaves101.com/encyclopedia/conducting.cfm"* which reports ρ = 8.707 μΩ-

cm, f = 2.45 GHz, μ_o = 4π×10^{-7} H/m and μ_r = 600 at room temperature of 25°C. The calculated value of $\boldsymbol{\delta}$ was approximately 0.12 µm at 2.45 GHz frequency, which is comparatively very less than the average particle size of the EWAC powder (40 µm) particles used in the present work. Hence, due to low skin depths the microwave radiations will not be absorbed within the nickel particles and will be reflected back as shown in Fig. 3.1 (a). This problem can be overcome by applying microwave hybrid heating which will help in increasing the skin depths such that microwaves can penetrate within the material particles as shown in Fig. 3.1 (b) [Gupta and Sharma (2011)].

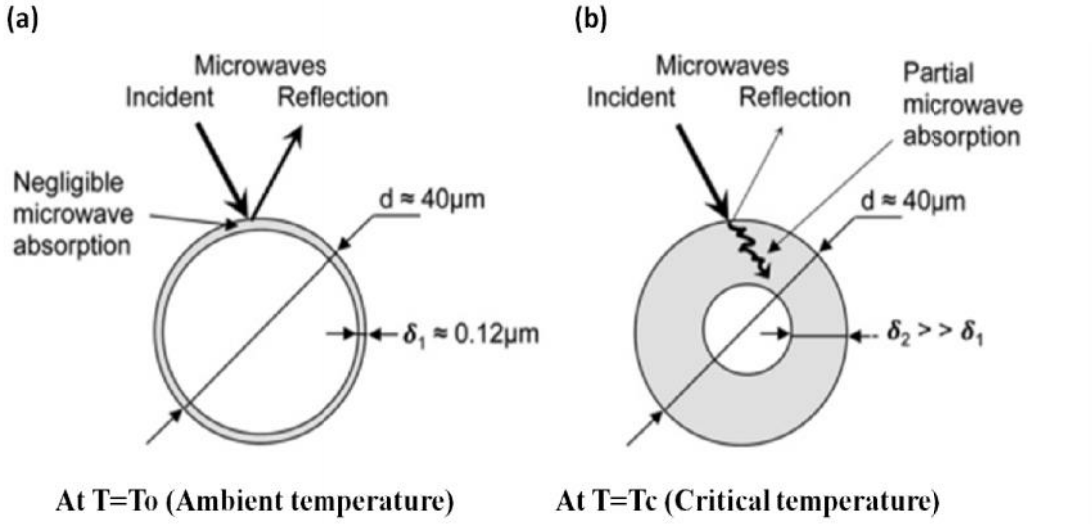

Fig. 3.1: Interaction of microwaves with Nickel powder at (a) Ambient temperatures, which lead to negligible microwave absorption, (b) Critical temperatures, which lead to increase in skin depth and absorption of microwaves [Gupta and Sharma (2011)]

Thus, microwave hybrid heating may be employed to overcome the difficulties in heating of low microwave absorbing materials such as metals.

3.2 PROPOSED MECHANISM OF MICROWAVE CASTING PROCESS

The microwave hybrid heating of metallic based powders involves complex phenomenon and hence the proposed mechanism has been discussed with suitable illustrations; for processing

(melting and casting) of metallic based particles in this section. The schematic representation of microwave casting process is shown in Fig. 3.2.

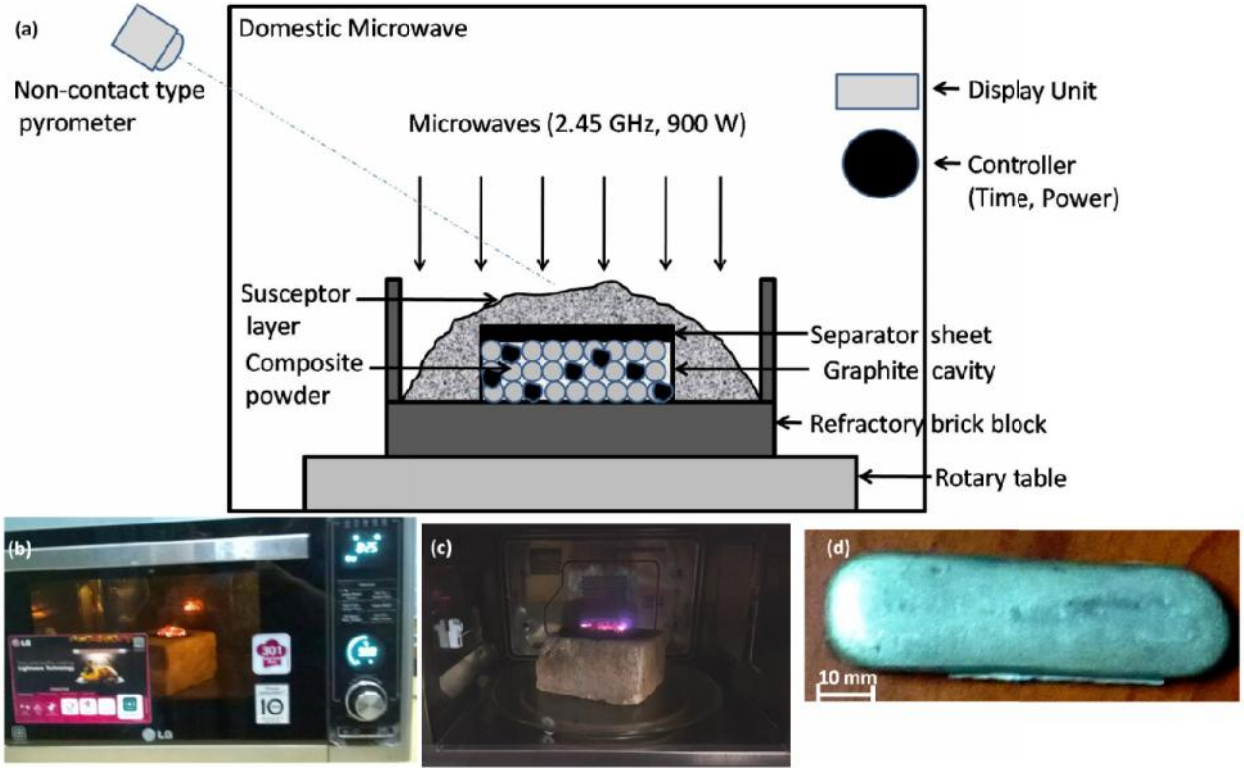

Fig. 3.2: (a) Schematic representation of microwave hybrid heating process (for melting and casting of metal-ceramic composites); (b) Actual domestic microwave oven used for processing; (c) Heating of charcoal and cavity by microwaves and (d) Near shape casting obtained by melting the metallic powder (~60 x 22 x 8 mm).

To understand the mechanisms taking place in the melting and casting of metallic powders through microwaves, the process is divided into four main stages. These stages are explained with the proper illustrations in the following sections.

3.2.1 Initial Susceptor Heating

Let us consider a cross sectional view of the powdered region within the cavity (say cylindrical cavity) and divide it in “n” number of small finite regions (R1, R2… Rn); shown by

dotted lines in Fig. 3.3 (a). The corresponding temperature of the regions during microwave exposure is represented by T_{R1}, T_{R2}…..T_{Rn}.

Let the initial temperature of the whole system is ambient temperature (Ta). The commencement of microwave exposure allows the susceptor powder particles to absorb (being good absorber of microwaves) and convert the radiations into heat. This rapidly developed heat raises the initial temperature of susceptor material and some portion of developed heat is conducted through the thin walls of graphite cavity and propagates towards the metal-ceramic powder particles (Ref. Fig. 3.3 (b)). With the increase in exposure time the complete layers of charcoal powders start burning and provides conventional heating throughout the cavity. The graphite cavity being good microwave absorbing material; interacts directly with radiations and assist in raising the temperature of pre-placed powder particles significantly.

3.2.2 Heat Generation and Propagation

The available/developing heat from the susceptor and cavity is continuously transferred by conventional modes of heating to the powder particles in rapid form. The powder particles, which are in direct contact with cavity walls gets heated up quickly and starts heating the adjacent powder particles. This process of heat propagation is instantaneous and continuously keeps on transferring heat from cavity walls to the core of cavity which is filled with powder. The composite powder placed inside the cavity contains some reinforcement particles (say silicon carbide) which being good absorber of microwaves can also absorb radiations at lower temperatures. But, these ceramic particles are poor conductors of heat; owing to which they slowly heats the adjacent metallic powders via conventional modes of heating (Ref. Fig. 3.3 (c)).

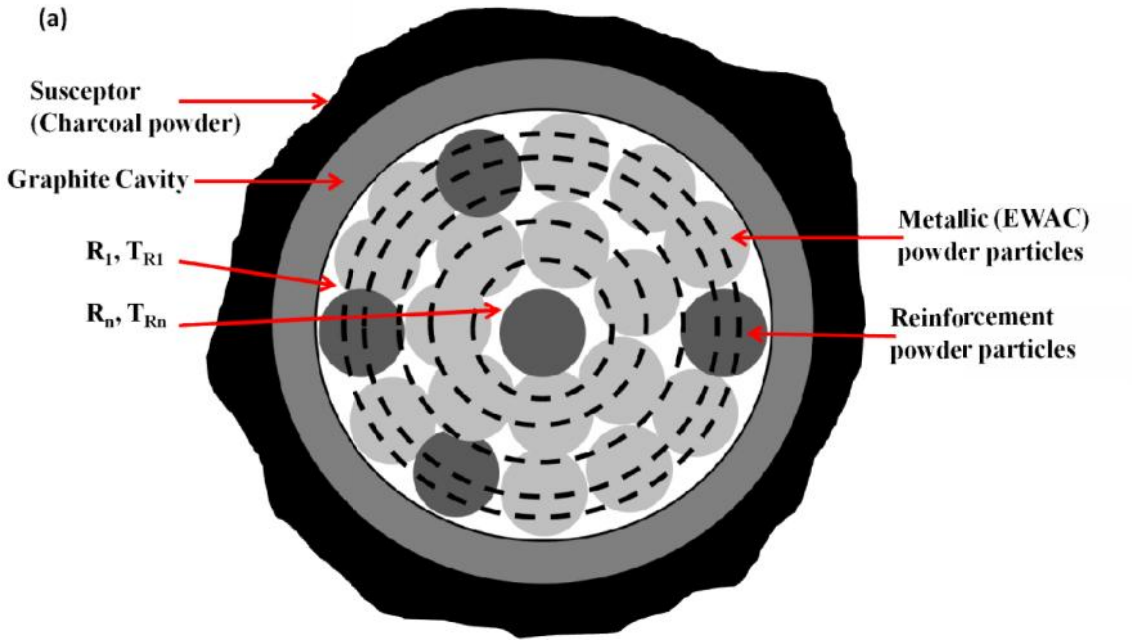
(a)
Susceptor
(Charcoal powder)
Graphite Cavity
R_1, T_{R1}
R_n, T_{Rn}
Metallic (EWAC)
powder particles
Reinforcement
powder particles

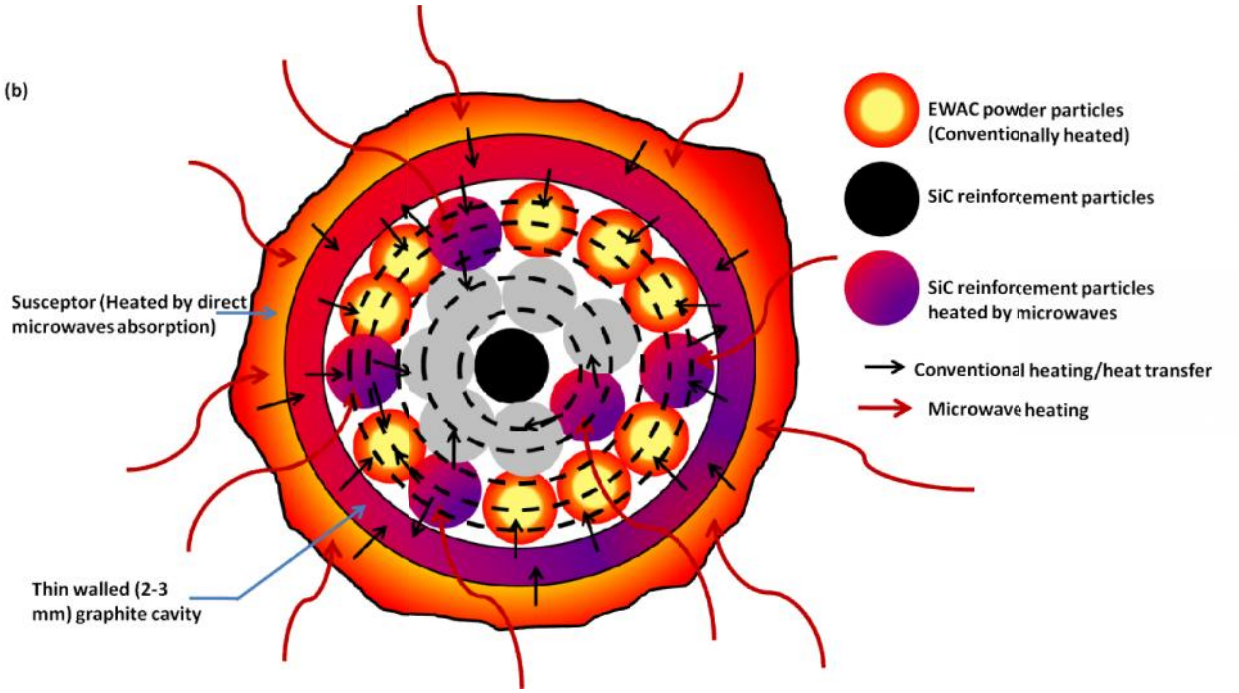
(b)
Susceptor (Heated by direct microwaves absorption)
Thin walled (2-3 mm) graphite cavity
EWAC powder particles (Conventionally heated)
SiC reinforcement particles
SiC reinforcement particles heated by microwaves
Conventional heating/heat transfer
Microwave heating

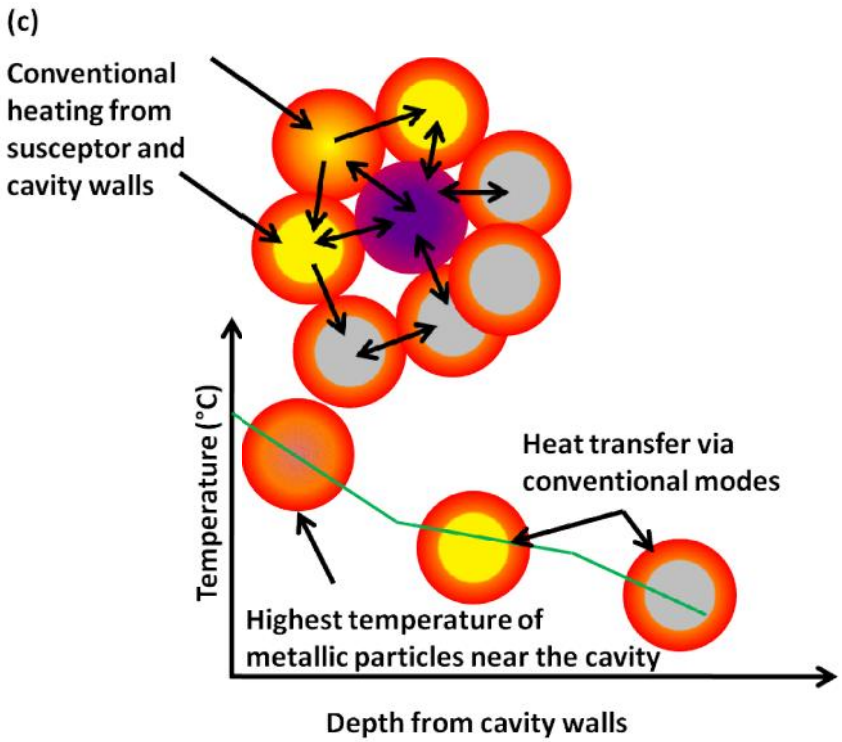
(c)
Conventional heating from susceptor and cavity walls
Temperature (°C)
Heat transfer via conventional modes
Highest temperature of metallic particles near the cavity
Depth from cavity walls

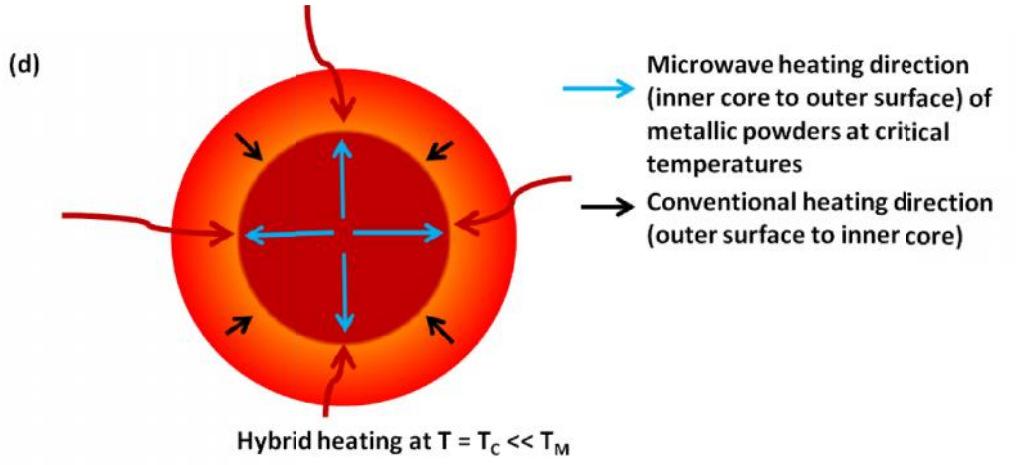
(d)
Microwave heating direction (inner core to outer surface) of metallic powders at critical temperatures
Conventional heating direction (outer surface to inner core)
Hybrid heating at T = T_C << T_M

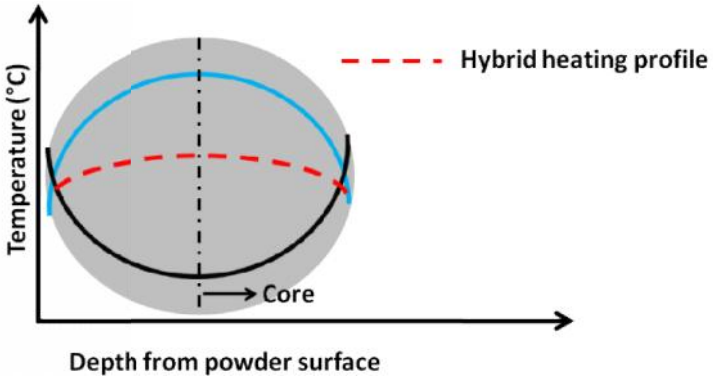
Hybrid heating profile
Temperature (°C)
Core
Depth from powder surface

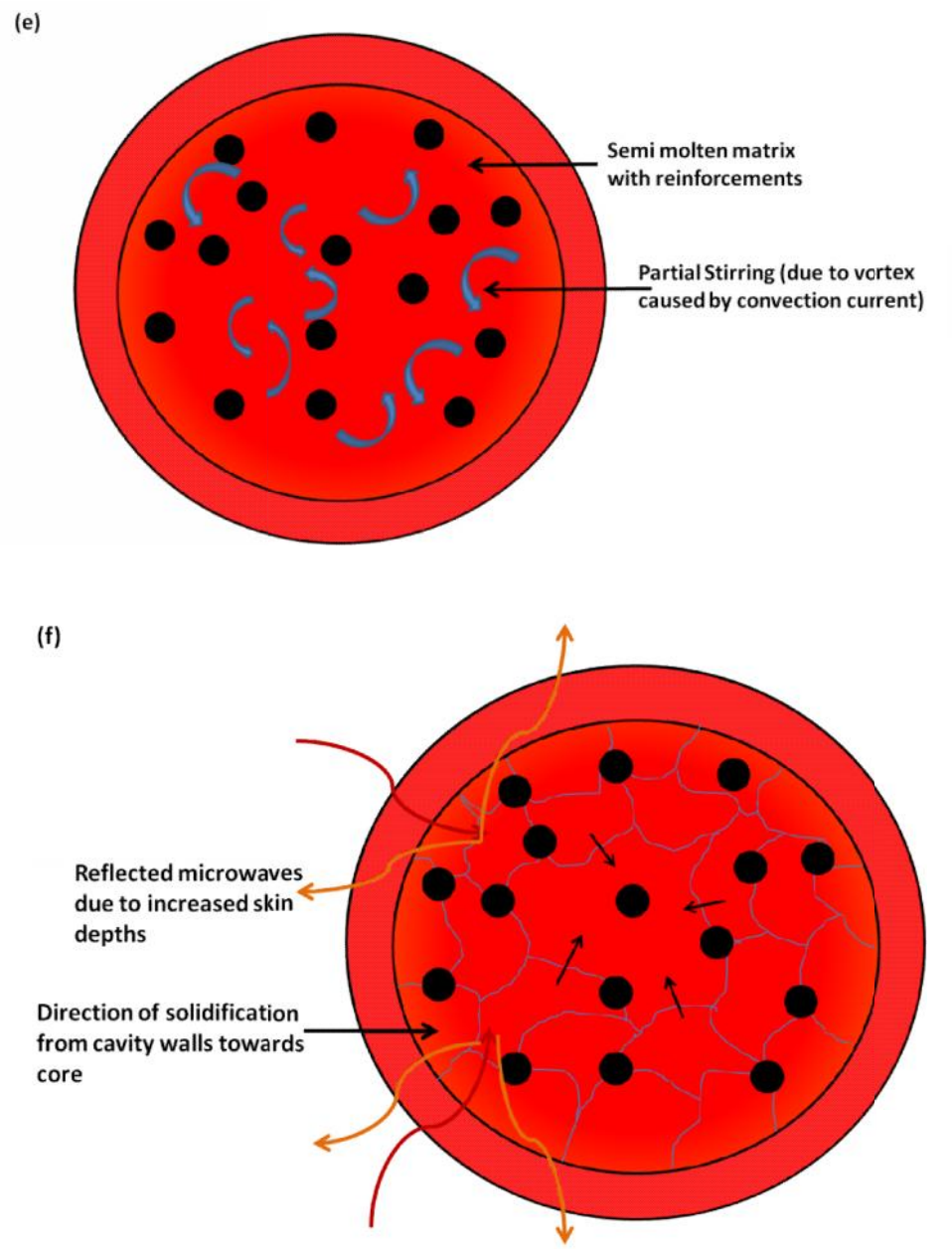

Fig. 3.3: (a) Cross sectional view of cylindrical powder filled cavity with distributed regions, (b) Initial microwave heating of cavity and conventional heat transfer from cavity walls to the powder particles, (c) progressive heat transfer within the metallic powders via conventional routes, (d) bi-directional heating (hybrid heating) of metallic powders at critical temperatures T_C (microwaves starts interacting due to increased skin depths in metallic particles), (e) Melt formation due to intense heating by microwave hybrid heating process and partial stirring due to developed convection current in semi molten pool, and (f) Solidification and coalescence increases skin depth (which causes reflection of microwaves from melt surface)

3.2.3 Attainment of Critical Temperatures and Bi-Directional Heating

The initial microwave exposure allowed temperature rise (T_{R1}) in R_1 region, which is adjacent to the cavity walls. Further, heat from R_1 region transfers to the adjacent regions (R_2…Rn) via conventional modes of heating, which increases their respective region temperatures (such that $T_{R1} > T_{R2} > \ldots > T_{Rn}$) as shown in Fig. 3.3 (b-c). As temperature rises rapidly, the powder particles attain an elevated temperature, which is enough for causing microwave absorption and hence known as critical temperature (T_C); which is much less than the melting temperature ($T_M >> T_C$). At this temperature the powder particles of the various regions start to couple directly with microwaves as shown in Fig. 3 (d). The direct absorption of microwaves by the metallic powder particles and conventional heating from outside cause rapid temperature rise, which results in diffusion of particles (say at temperature $T_D < T_M$). This phenomenon continues at a rapid pace for all powder regions ($R_1 \ldots R_n$) till all the particles melt and the temperature equalizes at melting temperature (say T_M).

3.2.4 Casting and Solidification

During the melting of metallic powder particles, the magnetic field associated with the microwaves causes the generation of convention currents. The presence of convention current [Gupta and Sharma (2011)] in the semi molten state acts as a partial stirrer mechanism which helps in reducing the agglomeration of reinforcements in the semi molten matrix phase as shown in Fig. 3.3 (e). After melting and coalescence of particles, the skin depth of molten material is again reduced as semi molten fused particles act as bulk metal with dimensions in mm. This will lead to the decrease in penetration depth which will clog the microwave interactions with bulk molten metal and hence reflection of radiations will again start. This stops the heating process

automatically [Gupta and Sharma (2011); Sharma and Gupta (2012)] as indicated in Fig. 3 (f) and further exposure of microwaves will only add to the total power consumption.

Further, on stopping the microwave radiation exposure; the temperature starts falling down, which allows cooling and solidification of semi-molten metal to produce the desired metal matrix composite casting. Since, the semi molten metal is in direct contact with the cavity walls and cavity is exposed to the atmosphere, which allows outer walls to become the favorable sites for heat dissipation. The maximum temperature gradient occurs at wall/melt interface and the temperature gradient decreases in the molten metal region.

Hence, it can be assumed that the temperature remains constant across the semi molten metal inside the cavity. However, the heat from the semi molten metal is transferred through the walls of the cavity. This starts the solidification of molten metal from cavity walls; towards the center of the molten pool with reduced temperature gradients (under atmospheric conditions).

3.3 SUMMARY

This chapter presented the theory behind melting and casting of metal-ceramic powdered composites by microwave energy. Mechanisms involved in the microwave hybrid heating process employed for melting of powders have been explained with suitable illustrations. The effect of critical temperature on the skin depth has been explained and bi-directional heating involved in the process has been presented. The heat generation during the process and its propagation in the powdered layers were represented with illustrations. It has been explained that after coalescence is achieved, the skin depth reduces and microwave heating stops automatically.

CHAPTER 4

EXPERIMENTAL PROCEDURE

The development of a new energy efficient process for the processing of a variety of materials is itself a challenging task. Any process development requires validation and optimization of the process parameters and their cause-effect matrix, which is even more challenging. The process development requires well planned experimentation and results to prove its scientific relevance. Further, the process capabilities are to be explored for the utmost performance of the developed process, which can be replicated and universally accepted. The theory and science behind the process is to be cemented as a well scientific concept. This section of thesis, reports the systematic approach for different experimental results, which were carried out to develop a process for in-situ melting and casting of metal-ceramic composites via microwave hybrid heating route.

4.1 SELECTION OF MATERIALS FOR CASTINGS

The selection of materials is one of the most important phases and challenging work for any research. It is always desirable to have materials which can be easily transformed into the desired shapes and yet exhibit excellent strength and desirable properties. Researchers always put efforts to develop new methods for efficient processing of advanced materials which are required for high end engineering applications. Development of such materials for practical applications requires great effort from scientists, engineers and materials professionals. This process involves a lot of time and resources for the commercialization of such materials in applicable engineering fields, which can yield better results than the already used conventional

materials. Proper selection of materials is the first step in the development of advanced tailor made materials which are expected to perform better then the available materials.

4.1.1 Selection of Matrix Material

Nickel and nickel based alloys/composites find extensive applications in wear and corrosion resistance materials category [Omrani et al. (2015); Borkar et al. (2014)]. The significant work has been reported on the development of self lubricating nickel matrix composites in the area of tribology [Scharf et al. (2009); Hwang et al. (2008)]. Further, nickel based alloys are widely used in marine, aviation, power generation applications. To prevent the severe damages caused by wear and corrosion phenomena; nickel and chromium based coatings are commercially carried out on various engineering components to improve the service life. The superior properties of high strength, toughness and corrosion resistance at elevated temperatures allows nickel based super alloys to be widely utilized in aerospace and turbine applications [Hrutkay and Kaoumi (2014)].

The nickel based powder (EWAC 1004EN, a product of Larson & Toubro, containing more than 97% Ni) is selected as a matrix material due to the excellent properties offered by nickel. This powder is extensively used in repairing of turbines, welding of high strength structures and claddings of turbine blades. As per the manufacturers (*http://www.ewacalloys.com/products-services/maintenance-repair-products/ewac-thermalspray-powders)* EWAC 1004 EN is used on cast iron and provides good machinability coupled with high impact strength and ductility. It is used in thermal spray applications for engine blocks, exhaust manifolds, gears, etc.; and can produce high hardness (80-100 HRB at 3 mm thickness). It has been reported [Gupta and Sharma, (2011)] that cladding of EWAC powder yield higher hardness (304 ± 48 HV) in comparison to the austenitic stainless steel. Tensile strength of ~82%

of base metal Hastelloy was reported [Singh et al. (2017)] when joining was carried out by using EWAC powder. Bulk metallic nickel composites reinforced with nano silicon carbide particle were developed by using spark plasma sintering [Huang et al. (2015)]. It was reported that the tensile strength of Ni-SiC composite was approximately twice that of the pure nickel sintered specimens. Nickel is also used for the processing of various steels which imparts the combined properties of strength, toughness and ductility. However, limited work has been reported on the bulk material design of nickel powder based metal matrix composites through melting and casting. This provides an opportunity to work on the development of nickel powder based MMC's by melting nickel powders through microwave energy.

4.1.2 Selection of Reinforcement Materials

The main role of reinforcements added in the metal matrix is to provide better properties than the matrix material and to impart the characteristics of increased hardness, toughness and strength to composite system. Reinforcement selection depends upon the desired properties to be achieved and development of various MMC's offers tailored properties for various hi-tech applications. The metal matrix being week is reinforced suitability with desired amount of reinforcements such that processed metal matrix composites are expected to yield the combined properties of matrix materials and reinforcements. The role of matrix is to provide the support for reinforcement particles, overall shape, surface appearance, environmental tolerances and durability, while reinforcements increase the load bearing capacity thus providing macroscopic strength and stiffness. The metal matrix composites provide the unique and superior mechanical properties than the matrix phase, because it combines the most desirable properties of their parent constituents while suppressing their least preferred properties. The effect of adding reinforcements on the properties of the matrix has been shown in Fig. 4.1.

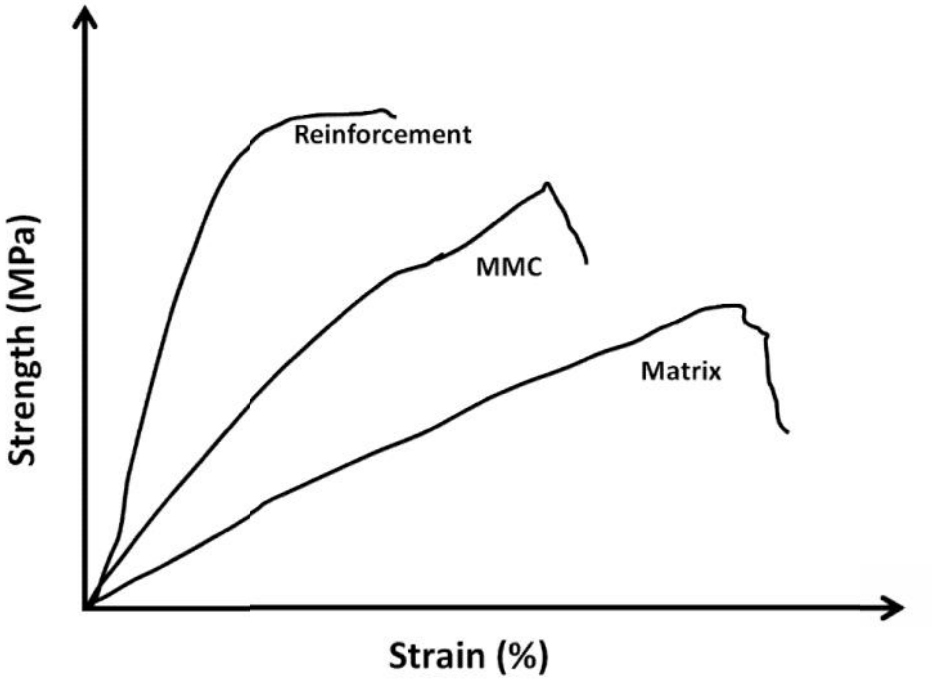

Fig. 4.1: Effect of reinforcement on strength and ductility of metal matrix composites

Addition of reinforcements though increases the strength of the matrix, but some negative effects can be incorporated in the composites such as loss in ductility. By proper selection of materials, i.e. matrix and reinforcements; tailor made properties can be obtained for various engineering applications. In the present work, hard and tough reinforcements in the form of silicon carbide powder (SiC), alumina powder (Al_2O_3) and tungsten carbide powder (WC-8Co) are selected. Silicon carbide is extensively used as a reinforcement material for aluminium alloys, for development of aluminium based MMC's. These composites are widely used in aerospace, automotive, anti wear, anti corrosion and many structural applications [Sadagopan et al. (2017); Suryanarayanan et al. (2013); Adebisi et al. (2011); Prasad and Asthana (2004)]. Similar applications of alumina as reinforcements are reported in the literature [Fathy et al. (2012), Bijwe et al. (2012); Etemadi et al. (2014)] and are extensively used in the development of many MMC's and PMC's. Addition of alumina improves the strength, anti wear and anti corrosion properties of metals. Tungsten carbide as a reinforcement is widely used in cutting tool

inserts and in development of coatings and claddings [Pathania et al. (2015); Gupta and Sharma (2011)], for imparting high wear resistance and corrosion resistance. Addition of WC particles significantly improves the strength of metal matrix and also improves the hardness at elevated temperatures [Durlu (1999); Liu et al. (2013); Ghasali et al. (2015)]. Majority of the cutting tools are prepared by sintering of WC particles, which provides the enough strength and red hardness to machine various difficult to machine materials.

In the present work metal-ceramic composites are obtained by first mixing the powders in mechanical mixtures to obtain the desired volume fraction of reinforcement and then processing of composite powder to obtain bulk composites. The volume fraction is obtained by using the equation 4.1 [Seo and Kang (1995)].

$$V_{fr} = \frac{\frac{M_r}{\rho_r}}{\frac{M_m}{\rho_m} + \frac{M_r}{\rho_r}} \times 100 \qquad (4.1)$$

Where; V_{fr} = volume fraction of reinforcement (%), M = mass (g), ρ = density (g/cm^3), and subscripts r and m refers to reinforcement and matrix respectively.

4.2 CHRACTERIZATION OF MATERIALS

4.2.1 Characterization of Matrix Material

The characterization of raw materials is an essential part prior to its processing. There are various techniques available for materials characterizations, but for the selected matrix powder (EWAC 1004 EN), the available characterization techniques of Scanning Electron Microscopy (SEM, Make and Model: JEOL, JSM6510LV) equipped with Energy Dispersive X-ray Spectroscopy (EDS) and X-ray Diffraction (XRD, Make and Model: PAN analytical, XPert PRO), were used for studying physical, chemical, and mechanical properties.

4.2.1.1 Physical and Mechanical Properties of Nickel Based Powder (EWAC 1004 EN)

The nickel based powder EWAC 1004EN is commercially available in the market under the brand of Larson & Toubro; India in the packing of 500 grams and is gray colored powder as shown in Fig. 4.2 (a-b).

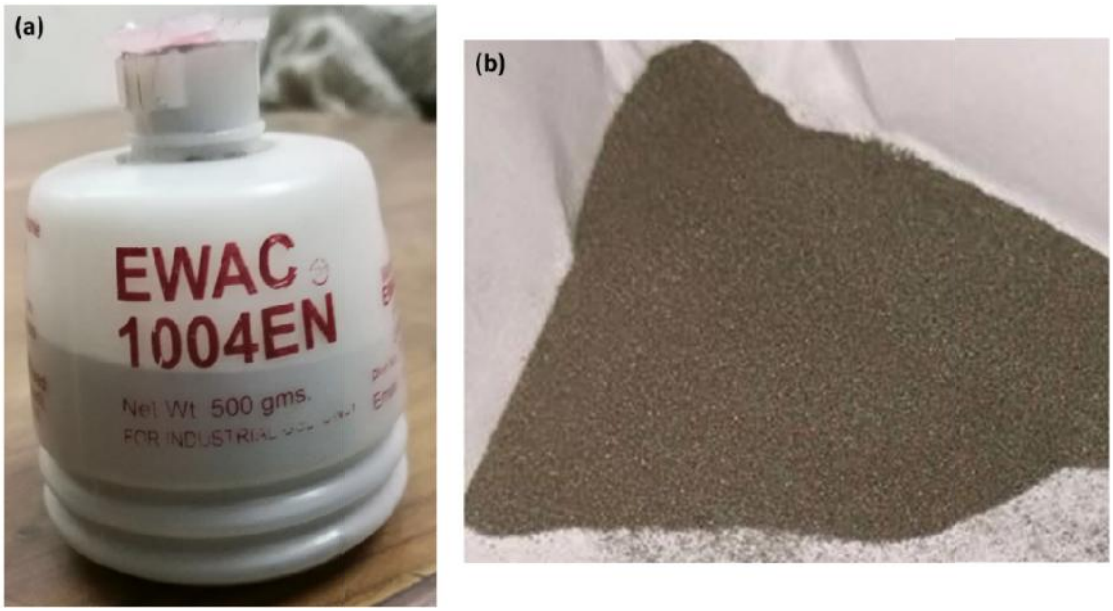

Fig. 4.2: (a) Commercially available EWAC powder and (b) Gray color EWAC powder particles

The characterization of as received powder was carried out for its physical and chemical properties using scanning electron microscope equipped with energy dispersive X-ray spectroscopy. The results are presented in Fig. 4.3 (a-b), which revealed the spherical morphology of EWAC powder, having an average particle size of ~40 μm. The EDS analysis revealed the predominance of nickel (>97%) with some minor amount of elements, like, chromium, silicon, carbon and iron.

The weight percentage elemental composition of EWAC powder is presented in Table 4.1, which shows that ~97% of powder consists of nickel.

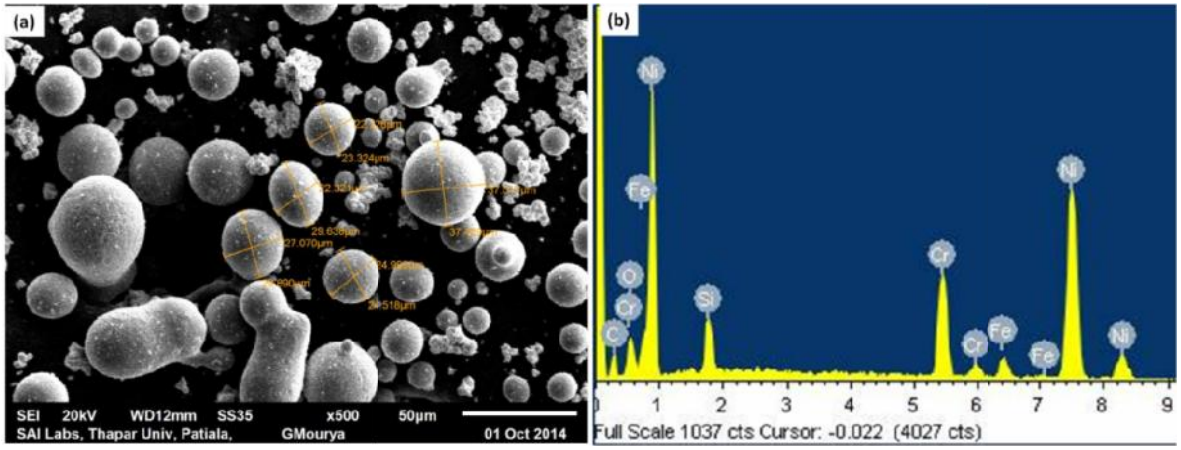

Fig. 4.3: (a) SEM image showing spherical morphology of EWAC powder, and (b) EDS analysis of EWAC powder

Table 4.1: Elemental composition of matrix (EWAC) powder

Element	Cr	C	Si	Fe	Ni
Weight (%)	0.1-0.5	0.25	0.8-1.5	0.5 Max.	Bal.

Typical XRD spectrum of EWAC powder is presented in Fig. 4.4, which shows the dominant presence of nickel element peaks.

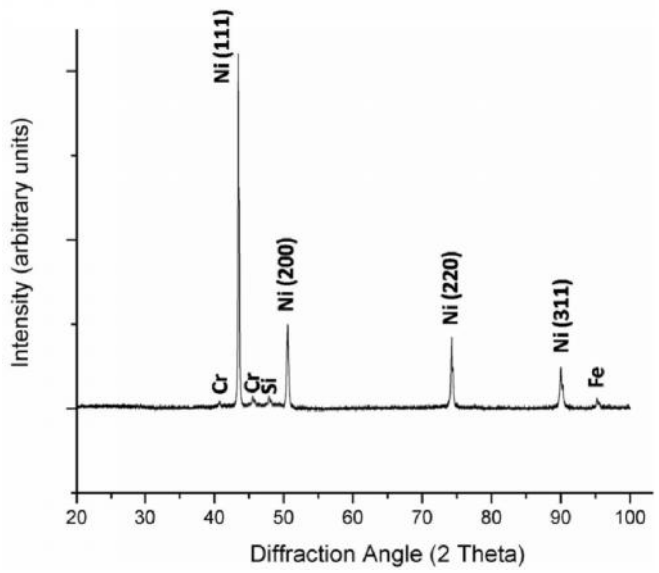

Fig. 4.4: Typical XRD pattern of as received EWAC powder

Nickel peaks were observed corresponding to the diffraction angles (2θ) of 44.508°, 51.85°, 76.37° and 92.95. Some peaks of chromium (42.10° and 45.78°), silicon (48.93°) and iron (97.8°) were also observed.

Some of the important physical and mechanical properties of major constituents of EWAC powder i.e. nickel are reported in Table 4.2 and Table 4.3.

Table 4.2: Physical properties of EWAC 1004EN powder [Gupta et al. (2012)]

S. No.	Property	Value
1	Density (g/cm^3)	8.9-9.1
2	Melting point (°C)	1453
3	Skin Depth (μm, at room temperature, 2.45 GHz)	0.12

Table 4.3: Mechanical properties of EWAC 1004EN powder [Gupta et al. (2012)]

S. No.	Property	Value
1	Vickers Microhardness (HV)	75
2	Fracture Toughness K_{IC} (MPa $m^{1/2}$)	100
3	Elastic Modulus (GPa)	334

4.2.2 Characterization of Reinforcement Materials

The reinforcement powders were also characterized for their chemical and physical properties by using relevant characterization techniques as discussed earlier.

4.2.2.1 Physical and Mechanical Properties of Silicon Carbide Powder (SiC)

Silicon carbide powder is commercially available in bulk in a variety of mesh sizes and under various brands. It is one of the most commonly used reinforcements used in metal matrix composites (mainly for aluminium and magnesium metals) to improve the strength and wear

resistance properties. In the present work, SiC of mesh size 400 (~38 μm) is purchased from a local vendor, Shankar Pvt. Ltd. New Delhi; and was available in 500 g air tight containers packing. As received powder was analyzed by using scanning electron microscopy and energy dispersive X-ray spectroscopy and results are presented in Fig. 4.5 (a-b). The SEM image reveals that the morphology of SiC powder was irregular shaped particles with sharp edges. The average particle size of the particles measured through SEM was 40 ± 5μm. The EDS analysis of powder particles confirms the presence of silicon and carbon elements only. Table 4.4 shows the percentage elemental composition of the powder with 98% purity index with some traces of oxygen.

Table 4.4: Elemental composition of silicon carbide powder

Element	**C**	**Si**	**O**
Weight (%)	50.7	47.38	1.92

The typical XRD spectrum of as received SiC powder was obtained at room temperature in XPert PRO PAN analytical diffractometer using Cu *K*α X-rays; at a scan rate of 1° min^{-1}; in the range of 20°-100°. The obtained XRD spectrum is shown in Fig. 4.6.

XRD pattern revealed the predominance peaks of silicon carbide corresponding to the diffraction angle of 34.06°, 35.598°, 38.10°, 43.47°, 60.026°, 65.70°, 72.03°, 73.33° and 95.57°. Some peaks of silicon oxide were also observed and this may be due to the impurities present in the powder.

Some of the important physical and mechanical properties of SiC powder are reported in Table 4.5 and Table 4.6 [*http://www.syalons.com/advanced-ceramic-materials/silicon-carbide-ceramics*].

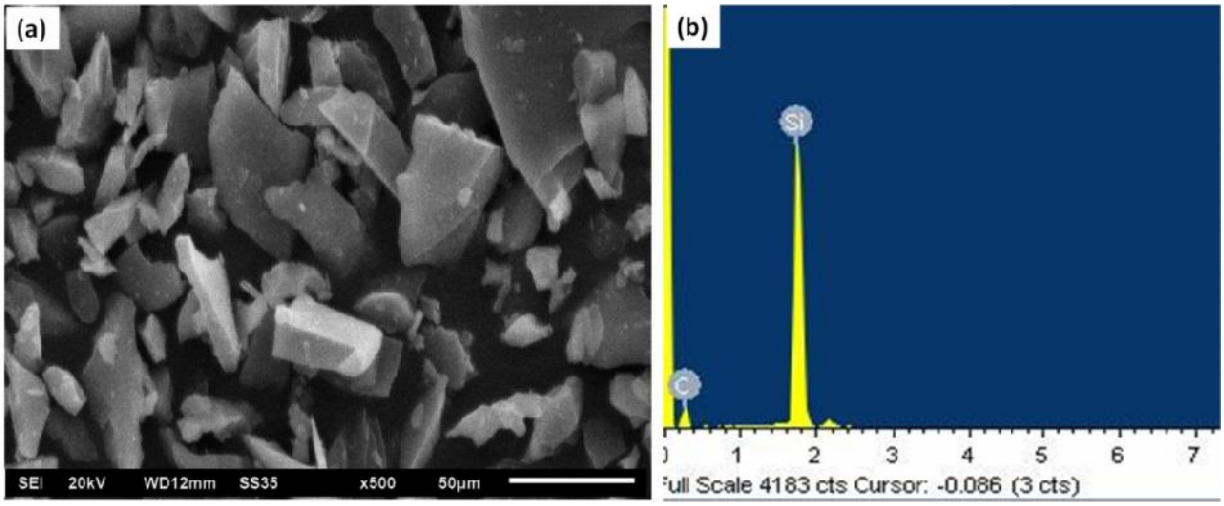

Fig. 4.5: (a) SEM image of SiC particles showing the morphology and (b) EDS of SiC particle

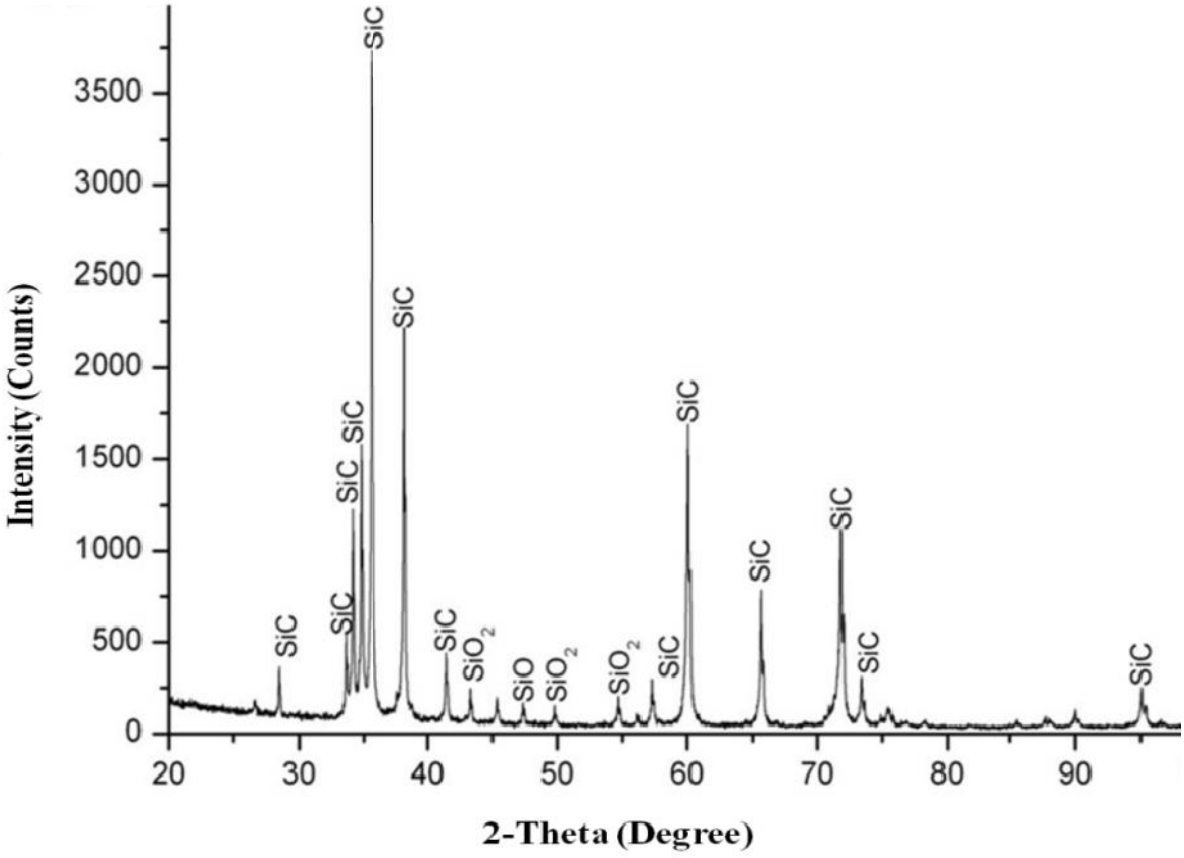

Fig. 4.6: Typical XRD spectrum of as received SiC particle

Table 4.5: Physical properties of silicon carbide (SiC) powder [Kaushal et al. (2017)]

S. No.	Property	Value
1	Density (g/cm^3)	3.2
2	Melting point (°C)	2700
3	Skin Depth (mm, at room 20 °C)	40

Table 4.6: Mechanical properties of silicon carbide (SiC) powder

S. No.	Property	Value
1	Vickers Microhardness (HV_{50})	2000-2500
2	Fracture Toughness K_{IC} ($MPa\ m^{1/2}$)	4.0
3	Elastic Modulus (GPa)	410

4.2.2.2 Physical and Mechanical Properties of Alumina Powder (Al_2O_3)

Alumina is also known as aluminium oxide and is used in many engineering applications. It is widely as reinforcement materials for many metal matrix composites. Alumina is widely used as a coating material due to high hardness, anti-wear and anti-corrosion resistance. It is mainly processed by sintering process and sintered alumina composites are used in many heat resistant applications [Kumari et al. (2008)]. Due to the very high skin depth of alumina particles, it acts as transparent to microwaves, but authors have successfully sintered alumina using 2.45 GHz microwaves [Cheng et al. (2000); Cheng et al. (2002); Mizuno et al. (2004)]. The alumina powder was procured from Shankar Pvt. Ltd. New Delhi. The mesh size of alumina powder was 400. Typical SEM image with EDS analysis of alumina powder is shown in Fig. 4.7 (a-b).

The SEM image results revealed that the average particle size of particles is 40 μm and morphology of particles shows irregular shape.

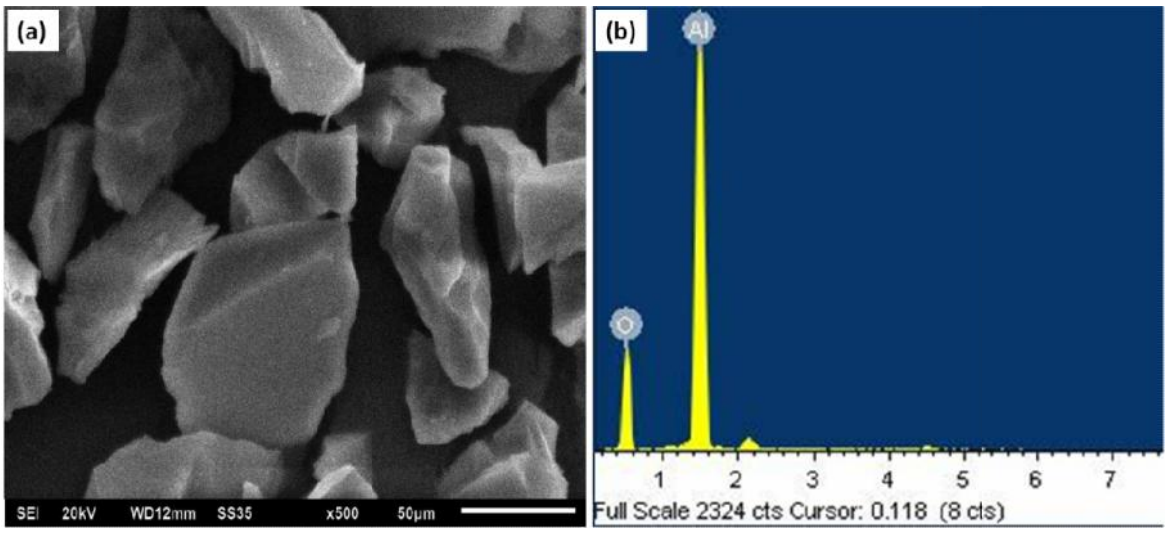

Fig. 4.7: SEM image (a) and EDS analysis of as received alumina powder

The percentage elemental composition of the alumina powder with 97% purity index is presented in Table 4.7, which show that majority content is aluminum and oxygen, but some traces of silicon, iron, chromium and carbon as impurity is also present. The typical XRD spectrum of as received alumina powder was obtained at room temperature at a scan rate of 1° min^{-1}; in the diffraction range of 20°-100°. The obtained XRD spectrum is shown in Fig. 4.8.

Table 4.7: Elemental composition of alumina powder

Element	Al	O	Si	Fe	Cr	C
Weight (%)	Bal.	46.85	0.8 max	0.5	0.9	0.6

The majority of the peaks in XRD pattern is of alumina with some peaks of iron and chromium carbide. Dominant peaks of alumina can be seen at diffraction angle of 31.02°, 35.02°, 36.9°, 37.12°, 39.49°, 67.76° and 73.3°. Peaks of silicon can be seen corresponding to the diffraction angle of 26.7° and 54.23°. Some phases of iron and chromium carbide were also present in the diffraction pattern.

Some of the important physical and mechanical properties of alumina powder are reported in Table 4.8 and Table 4.9 [*http://www.syalons.com/advanced-ceramic-materials/alumina-ceramics*].

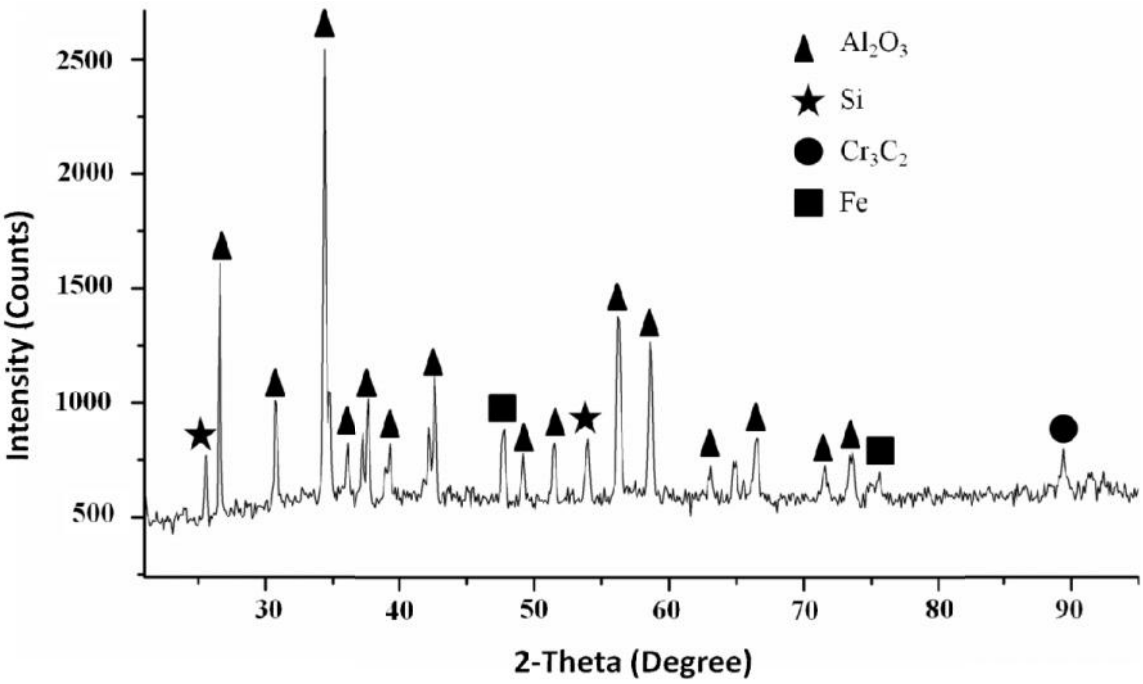

Fig. 4.8: Typical XRD spectrum of as received alumina powder

Table 4.8: Physical properties of alumina (Al_2O_3) powder [Kaushal et al. (2017)]

S. No.	Property	Value
1	Density (g/cm^3)	3.7-3.95
2	Melting point (°C)	2072
3	Skin Depth (mm, at room 25 °C)	12563

Table 4.9: Mechanical properties of alumina (Al_2O_3) powder

S. No.	Property	Value
1	Vickers Microhardness (HV_{50})	1250-1600
2	Fracture Toughness K_{IC} (MPa $m^{1/2}$)	4.5
3	Elastic Modulus (GPa)	400

4.2.2.3 Physical and Mechanical Properties of Tungsten Carbide Powder (WC-8Co)

Tungsten carbide powder is readily available commercially in the market in premixed quantity with cobalt binder. This powder is mainly used in making tool inserts, coating various

components, cladding and manufacturing of various mechanical components with higher strength, hardness and wear resistance properties. In the present work, commercially available (WC-8Co) powder was procured from local vendor from New Delhi, with purity index of 97%. The powder was characterized by using relevant techniques to study the particle size, morphology and elemental compositions. Typical SEM image with EDS analysis of (WC-8Co) powder is shown in Fig. 4.9 (a-b).

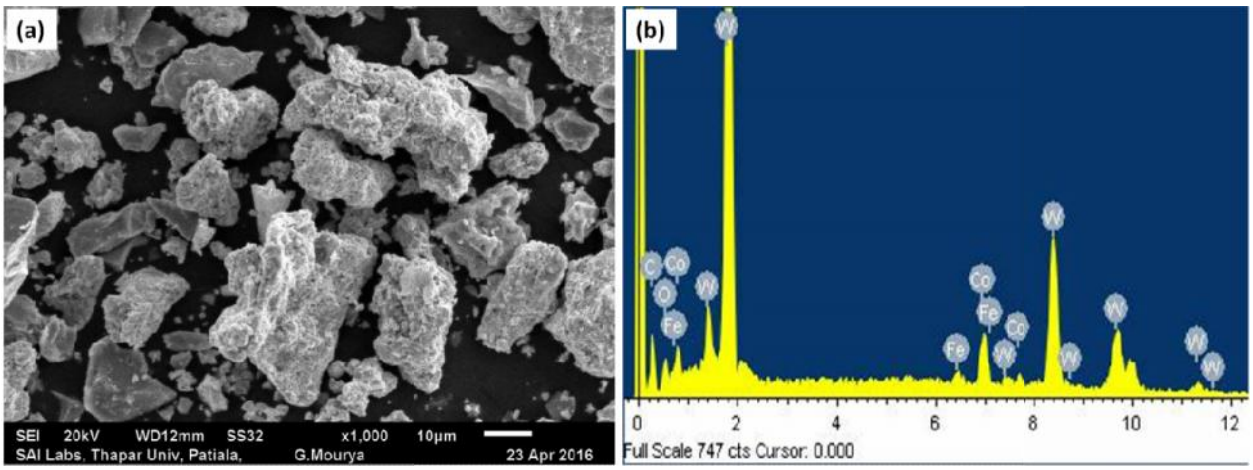

Fig. 4.9: (a) SEM image and (b) EDS analysis of as received (WC-8Co) powder

The SEM image results revealed that the average particle size of particles is 30 µm and morphology of particles shows irregular shape. The EDS analysis revealed the predominance presence of tungsten and carbon peaks. The peaks of cobalt with some peaks of impurity such as iron and oxygen are present in the EDS analysis. The percentage elemental composition of the as received powder is presented in Table 4.10, which show that majority content is tungsten and carbon; but some traces of iron, cobalt and oxygen is present.

Table 4.10: Elemental composition of (WC-8Co) powder

Element	W	C	Co	Fe	O
Weight (%)	Bal.	14.2	7.8	1.5	5.12

The XRD spectrum of as received tungsten carbide powder was obtained at room temperature and is shown in Fig. 4.10.

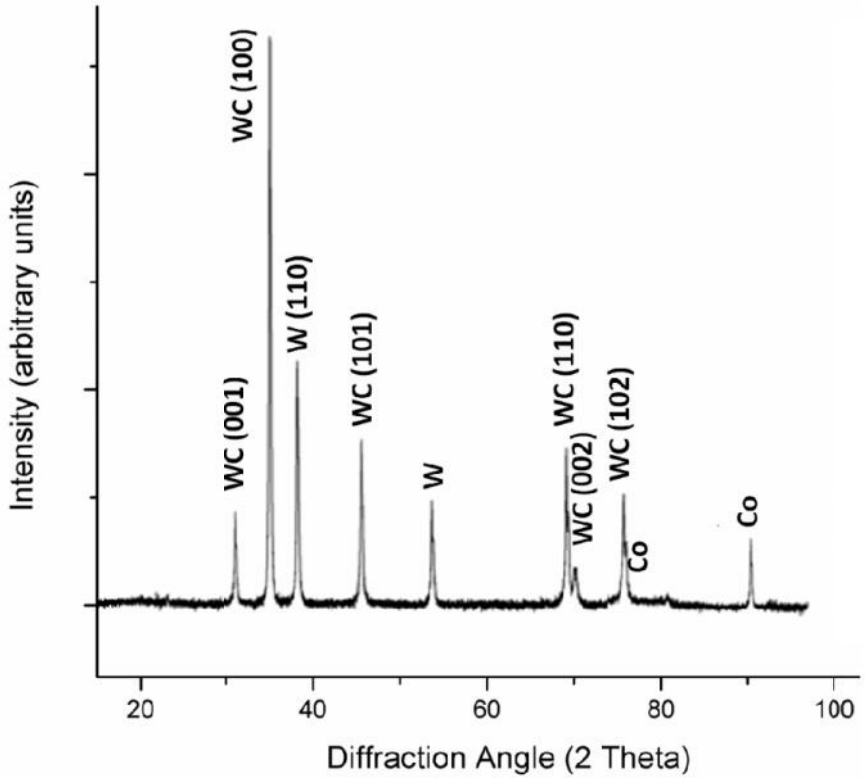

Fig. 4.10: Typical XRD spectrum of (WC-8Co) as received powder

The spectrum of WC-8Co powder shows predominant peaks of WC at diffraction angles of 31.7 º, 35.89 º, 48.65º, 73.66º and 75.4º. Peaks of cobalt can be clearly seen at diffraction angles of 75.8º and 92.2º. The important physical and mechanical properties of tungsten carbide powder are reported in Table 4.11 and Table 4.12.

Table 4.11: Physical properties of (WC-8Co) powder

S. No.	Property	Value
1	Density (g/cm^3)	15.6
2	Melting point (°C)	2870
3	Skin Depth (μm, 20°C, 2.45 GHz)	4.7 [Rodiger et al. (2001)]

Table 4.12: Mechanical properties of (WC-8Co) powder

S. No.	Property	Value
1	Vickers Microhardness (HV_{50})	1500-1800
2	Fracture Toughness K_{IC} (MPa $m^{1/2}$)	10-14
3	Elastic Modulus (GPa)	630-650

4.3 EXPERIMENTAL METHOD

The processing of metal based materials through microwave energy is quite challenging task and requires knowledge of materials properties, heat transfer mechanisms and interaction of materials with microwaves. Different materials, respond differently to the microwave exposure. Before the casting and melting of the required metallic based powder, it is always required to carry out some feasibility tests and further, to optimize the process parameters. It is very difficult to optimize the parameters by repetitive experimentation and further very less literature is available on melting of metallic based powders through microwaves at 2.45 GHz. The following sections will describe the effects of various parameters on microwave powdered MMC castings and their optimization.

4.3.1 Composite Powder Preparations

In the present work, metal matrix composites are prepared by exposing the premixed metal-ceramic powder in definite proportions to the microwave radiations. The metallic powder of EWAC was premixed with 5% and 10% of ceramic reinforcement by using equation 4.1. The powders in definite proportions were measured and premixed in mechanical mixture for 2 hours. Homogeneity in mixing of powders was obtained by taking random samples out of the mixed powder and by examining the mixed powders using optical microscope. If reinforcement lumps

were present in the premixed powder; it was again mixed using the mixer, till uniform dispersion was achieved.

4.3.2 Microwave Casting Setup

The heating through microwave radiations is due to the interactions between the targeted materials and microwaves. Materials which can easily absorb the radiations can efficiently convert them into heat by various phenomena as discussed in chapter 2. However, all the materials cannot absorb microwaves and hence cannot be processed in the similar way as microwave absorbing materials. The microwaves at a particular temperature and frequency can be transmitted (transparent materials such as glass), reflected (opaque materials such as metals) or absorbed either fully or partially (absorber materials such as carbide ceramics) by various categories of available materials. Metallic materials cannot be processed directly as microwaves will be reflected back by metals owing to lower skin depths at 2.45 GHz and at room temperatures. This causes radiations to reflect from the surfaces and becomes a critical issue in the processing of metallic based materials.

However, the skin depths (δ) associated with such materials can be altered and increased for a particular material at a particular frequency; by changing the temperature dependent parameters such as resistivity (ρ) and magnetic permeability (μ) (Ref. equation 3.2).

The skin depth of matrix material, i.e. EWAC which consist of ~97% nickel is ~0.12 μm [Gupta et al. (2011], which is about 330 times less than the average particle size, i.e. 40 μm of nickel particles. Due to the lower skin depth associated with nickel particles, it is not possible to directly process the powder using microwaves and if radiated with microwaves, particles will reflect back the radiations as shown in Fig. 2.3 and Fig. 3.1. To overcome this problem

microwave hybrid heating is employed as discussed in chapter 3. The schematic representation of microwave hybrid heating is shown in Fig. 4.11.

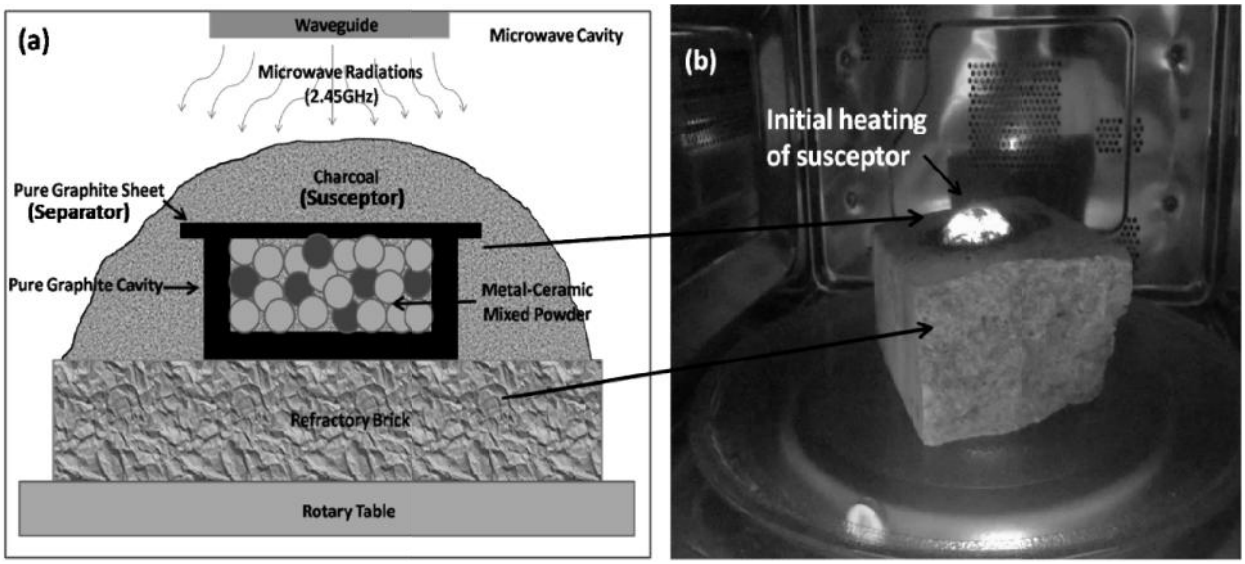

Fig. 4.11: (a) Schematic representation of microwave hybrid heating and (b) Actual processing of metallic powders using microwave hybrid heating in domestic microwave applicator

In the present work, a suitable susceptor (in the form of amorphous charcoal powder) was used for hybrid heating. The composite powder placed in the cavity was prevented from susceptor contamination by using a thin 1mm, 99% pure graphite sheet as a separator. The cavity was machined out from the block of pure graphite block and was placed on the refractory brick so that heat developed can be restrained to the casting setup only. Brick also prevents the heat transfer to the base glass plate present in the microwave oven.

The development of metal-ceramic MMC's castings through microwave energy is mainly dependent on properties of powders selected, powder particle size and processing parameters such as microwave power and exposure time. The parameters affecting the microwave casting process are presented in Fig. 4.12.

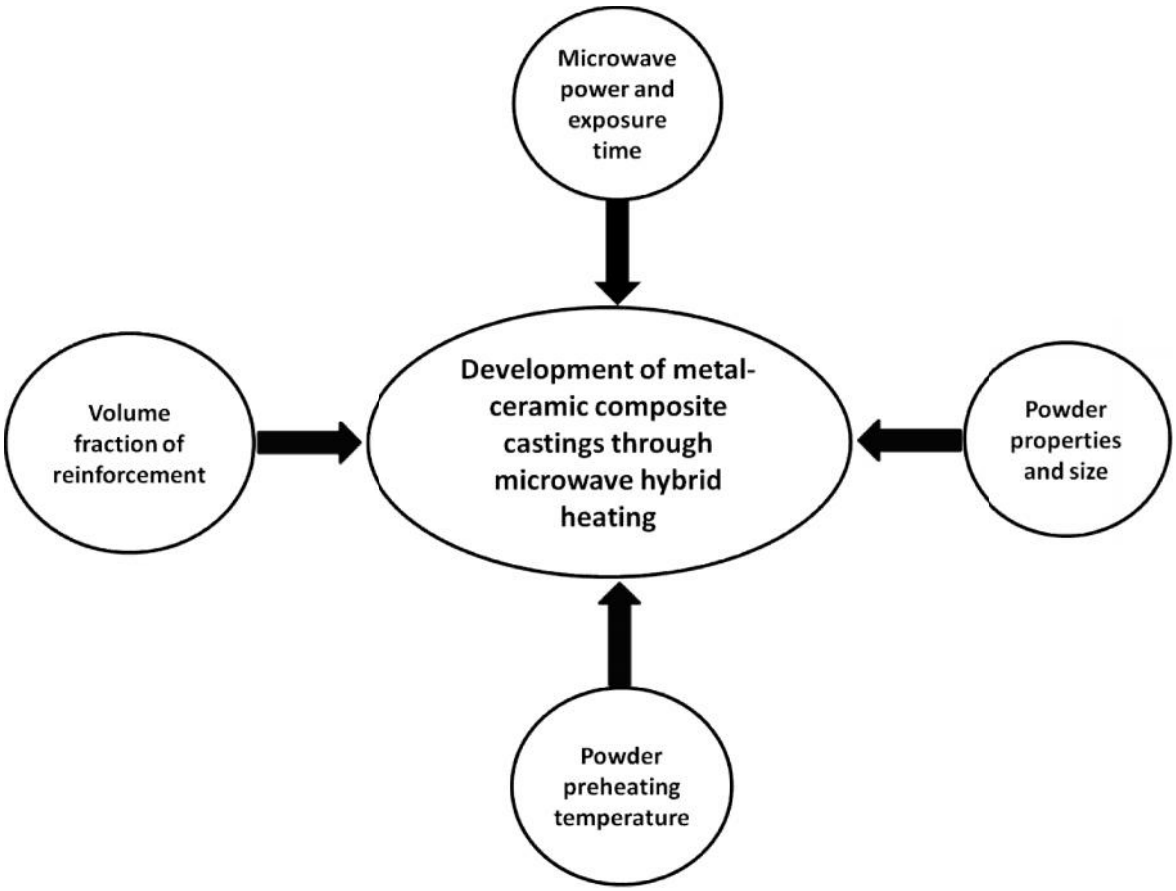

Fig. 4.12: Main parameters affecting the microwave casting process

However, some of the parameters such as powder particle size are already fixed and cannot be varied. In the present work, trial and final experiments were carried out in a multimode domestic microwave applicator having variable power levels. The details of the processing unit are shown in Table 4.13. Initial experiments were carried out repeatedly to find the optimum ranges of processing parameters, which are discussed in the next sections.

4.3.3 Some Feasibility Tests on Melting and Casting of Metal Matrix Composites

The experiments on microwave melting and casting of metal-ceramic powders were started on the basis of the results reported on partial melting of powders during microwave cladding [Gupta and Sharma (2014)]. Feasibility tests were carried out on 10 grams of pure EWAC powder at various power levels.

Table 4.13: Details of processing unit used for the microwave casting process

S. No.	Description
Microwave Applicator	Domestic Multimode Microwave Oven (LG made, Model: Light wave convection)
Operating Frequency	2.45 GHz (fixed)
Power Levels	540, 720 and 900 Watt
Preset Temperature Range	200°C maximum
Timer	Available with 5 second step mode

But at lower power level of 540 W the heat generated was not significant to cause melting and casting even after 15 minutes of exposure time. The experiments revealed that with 720 W of power, some melting and bonding of layers was observed within 10 minutes of microwave exposure. However, after 12 minutes of exposure, the castings were produced, but some layers lacks melting and sintering was observed in the middle and lower sides. To further reduce the processing time, experiments were carried out at 900 W (maximum); with an exposure interval of 1 minute. In repeated trials, it was observed that after 6 minutes of microwave exposure, the partial melting and bonding was started. The experiments were repeated to optimize the processing time and it was observed that 8 minutes of microwave exposure was sufficient to melt and cast 10 grams of metallic powder. Further, metal-ceramic composite castings were tried with 10% volume fraction of ceramic reinforcement and it was observed that within 6-7 minutes of exposure level, sound castings were observed as shown in Fig. 4.13.

Some of the feasibility results revealed that due to overheating of the castings, changes in the shape was observed. This was due to the presence of dominating convection current inside the melt pool (Ref. Fig. 4.13 (a & c)).

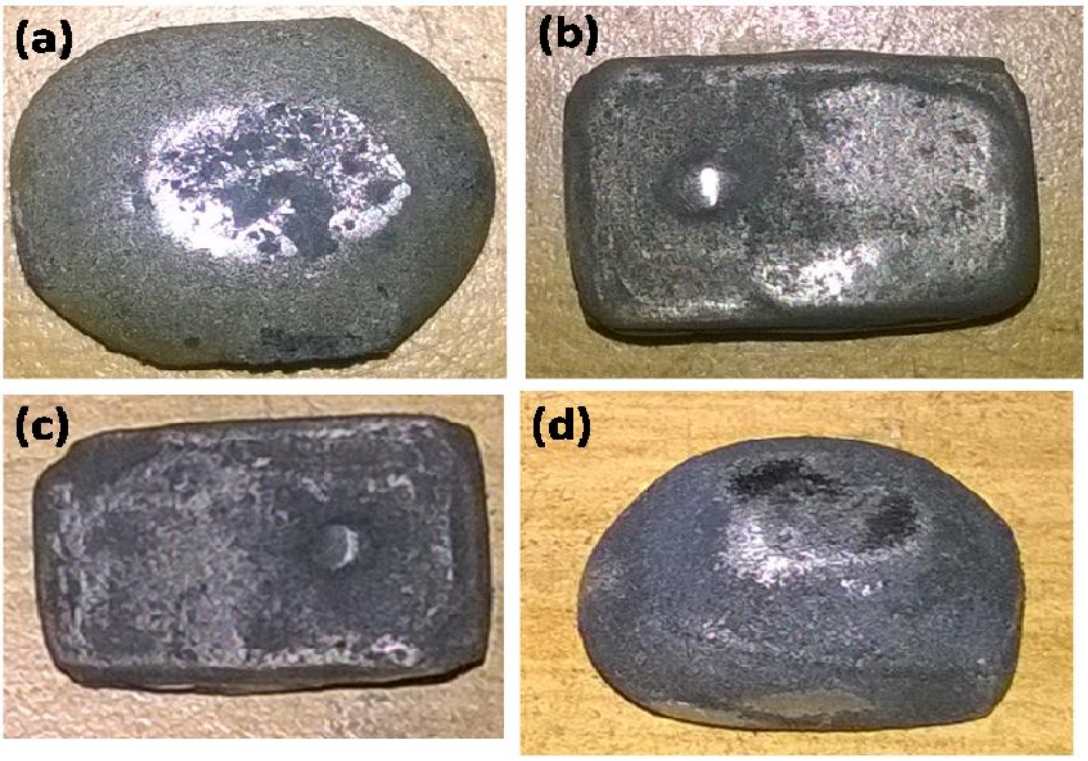

Fig. 4.13: Feasibility results on microwave melting and casting (a) EWAC powder, (b) EWAC+10%SiC powder, (c) EWAC+10%Al_2O_3 powder and (d) EWAC+10%(WC-8Co) powder

The results obtained were encouraging, but the next challenge was to perfectly melt and cast specimens of bigger size (60 x 25 x 7 mm), which can be subjected to proper mechanical testing. From the feasibility studies microwave power level of 900 W was fixed for further experimentations.

4.3.4 Effect of Microwave Exposure on MMC Powder Castings

The load (EWAC powder) was increased from 10 grams to 40 grams to obtain bigger specimens. The optimization of exposure time was again carried out at 720 W and 900 W to melt and cast the powders. The processing time graph for both the power levels and for varying load of EWAC powder is shown in Fig. 4.14.

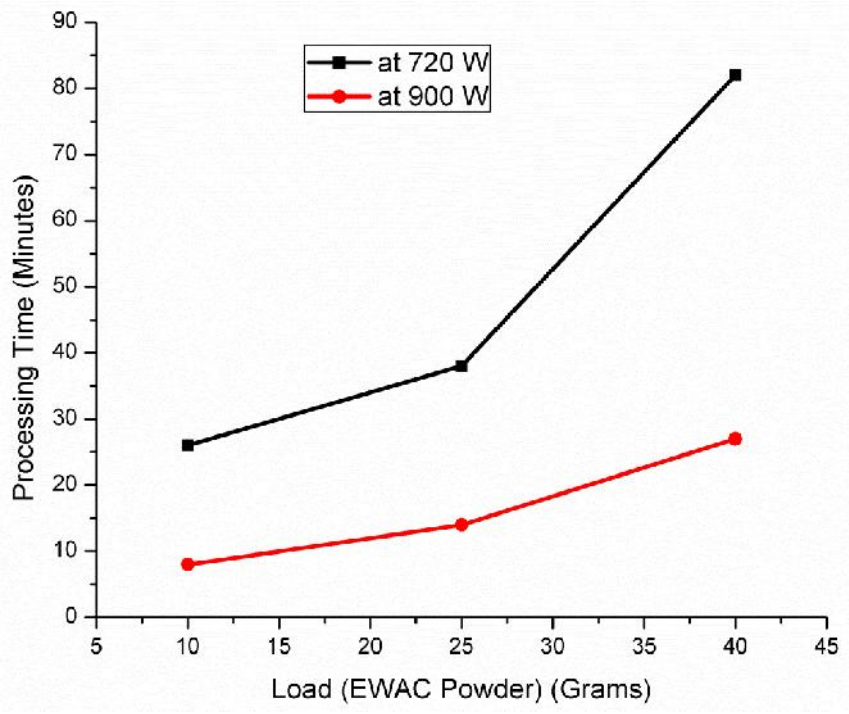

Fig. 4.14: Effect of power level and load on processing time

The detailed results on the microwave exposure time observations for EWAC casting are reported in Table 4.14, which shows that the after 10 minutes of microwave exposure the powder compaction starts but no melting was reported.

Table 4.14: Effect of microwave exposure time on the development of EWAC casting (40 gram) at 900 W and 2.45 GHz

Exposure Time (Min)	Observations and possible inference
10	Adherence of powder particles without melting
15	Localized sintering of upper layers with some melting
20	Formation of partial melting and diffusion, causing densification of powder
22	Melting of matrix powder was observed with some semi melted layers in the centre of cast
24	Observed some un-melted powder particles in the core of casting
26	Complete melting and casting leading to dense MMC castings

After 15 minutes of microwave exposure, some localized sintering of layers with partial melting was observed. With further increase in the time (above 26 minutes), the castings were obtained with complete melting of powders. The experimental results revealed that the optimum time for the development of pure EWAC casting was 26 minutes.

4.3.5 Effect of Reinforcement on Microwave Exposure Time

The microwave exposure time was optimized for the EWAC casting, but it is necessary to study the effect of reinforcement material on the processing times. Experiments were again carried out to study the effect of reinforcement on processing time. The effect of various reinforcements (with 10% volume fraction) on the microwave processing time at 900 W and 2.45 GHz frequency has been shown in Fig. 4.15.

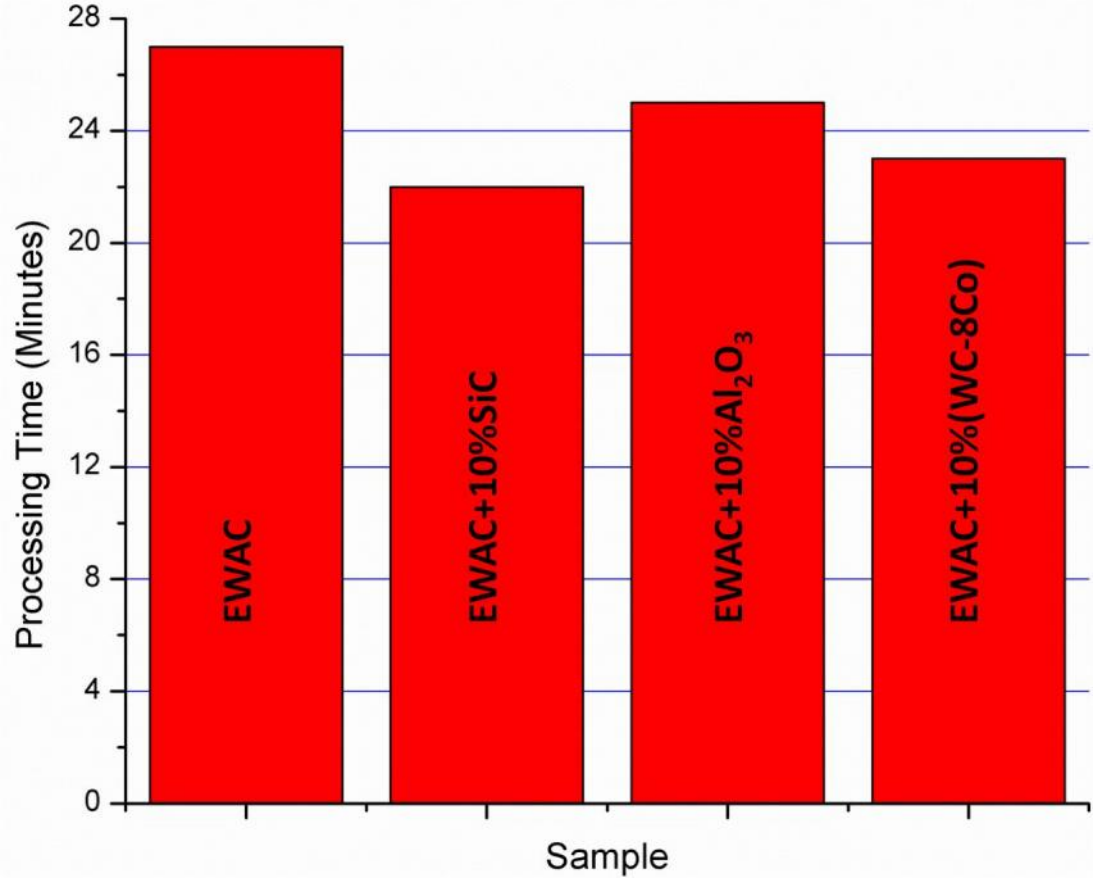

Fig. 4.15: Effect of reinforcements on microwave processing time for 40 grams of powder load

The results revealed that by adding the reinforcements, the processing time was lowered up to some extent. In case of carbide reinforcements such as silicon carbide and tungsten carbide, the processing time was lowered by 18%, i.e., from 27 minutes for pure EWAC to 22 minutes for EWAC+10%SiC MMC. This was due to the better absorption of microwaves by carbide reinforcements which helped in raising the initial temperature of matrix powder particles (Ref. Chapter 3). In case of alumina reinforcement, which acts as transparent to microwaves; the processing time was lowered and this was due to the fact that by adding ceramic reinforcement the total matrix load to be melted is reduced. Overall results revealed that on adding the ceramic reinforcements in pure metallic based matrix, the processing time decreases.

4.3.6 Effect of Preheating Temperatures on Microwave Exposure Time

It is well known fact that microwaves are reflected by the metallic powders at room temperatures due to lower skin depth. However, as the initial temperature of material increases, the temperature dependent properties updates and this can cause an increase in skin depth and further, metallic powders can start interacting with microwaves directly. Sometimes this phenomenon is also known as '*microwave effects*' where it has been reported that there exists a critical temperature value at which ceramic materials undergoes phase changes and properties gets transited into higher loss tangent [Aravindan and Krishnamurthy (1999)]. At this temperature, the microwaves directly couple with ceramics to enhance the heating rates, where the heating profile suddenly becomes sharp. This effect has already been discussed in chapter 3 with proper illustrations.

In the present work, the effect of preheating temperature on processing time has been carried out. The powders were preheated to various temperatures in microwaves conventional

mode before processing. But this temperature is reduced while placing the powder in the cavity and then completing the setup for microwave casting.

The effect of preheating temperature on EWAC casting are shown in Fig. 4.16, which reveals that on increasing the preheating temperatures, the processing time reduces. This is due to the fact that with an increase in the initial temperature of metallic powder particles, critical temperatures can be easily attained within a short period of microwave exposure. On achieving the critical temperatures; two directional heating occurs and it allows achievement of high temperatures, which are sufficient for melting powder particles.

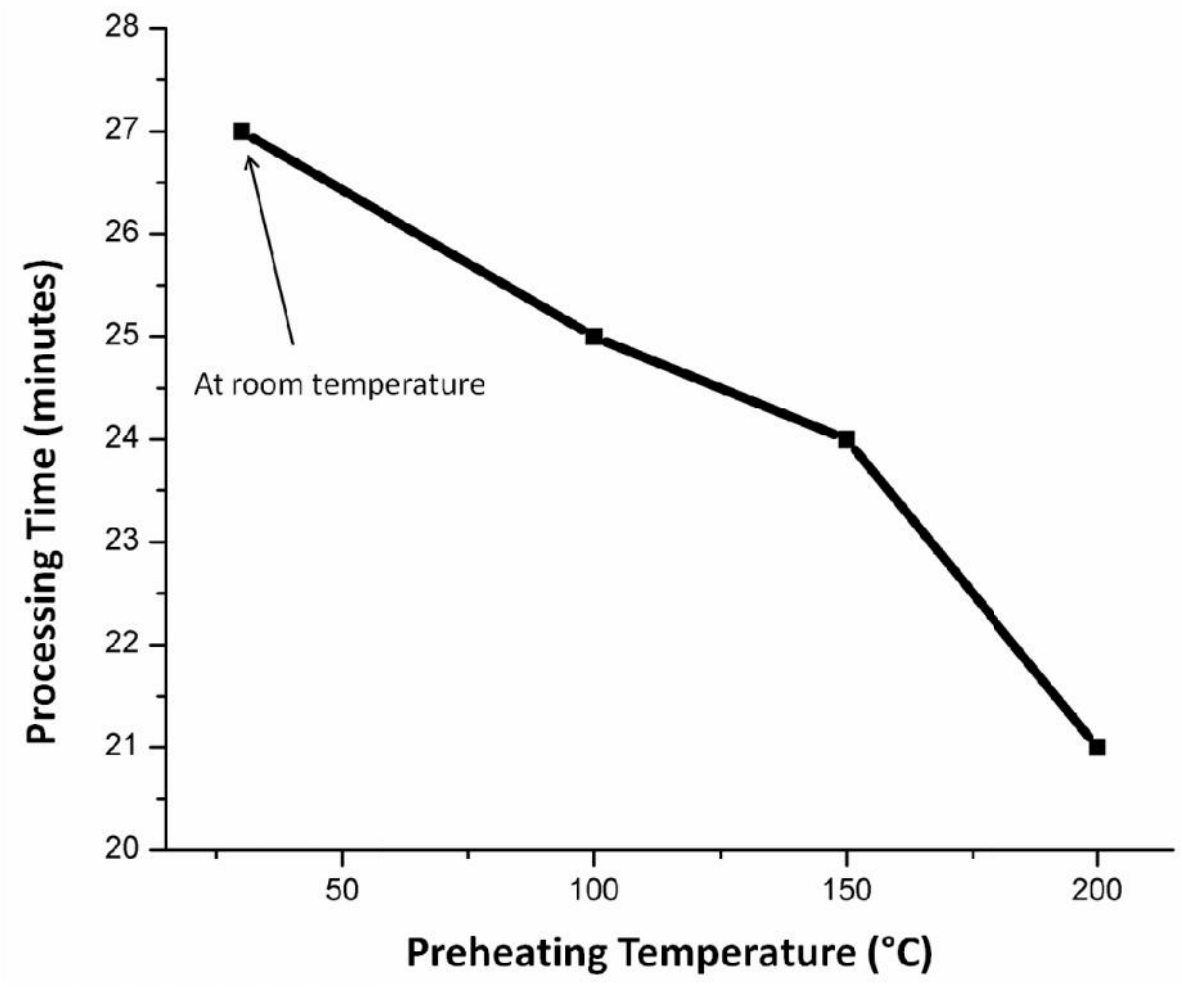

Fig. 4.16: Effect of preheating temperatures on processing time for EWAC casting

Similar results were observed in the other microwave processed MMC castings. For the final development of MMC's, premixed powders were first heated up to 200 °C and then processed at 900 W for the optimized time.

The ranges of operating variables on different powder systems and optimized conditions for the processing of these powders are presented in the Table 4.15. The same conditions were also used for the development of bulk powdered metal matrix composite castings through microwave energy by using the domestic microwave oven.

Table 4.15: Optimized microwave processing conditions used in the experimentations

Particulars	**Ni-based (EWAC) casting**	**EWAC+10%SiC MMC casting**	**EWAC+10% Al_2O_3 MMC casting**	**EWAC+10% (WC-8Co) MMC casting**
Powder	EWAC	EWAC + SiC	EWAC + Al_2O_3	EWAC + WC-8Co
Average particle sizes	40µm	40µm + 38µm	40µm + 40µm	40µm + 30µm
Optimized exposure time	23-28 min	18-22 min	21-26 min	19-24 min
Cavity material	Pure Graphite Machined Mold			
Microwave frequency	2.45 GHz (fixed)			
Microwave power	900 Watt			
Atmosphere	Air			

Though, there are fair chances of oxidation of castings due to the presence of oxygen in the environment, but it has been reported [Gupta et al. (2011)] that during susceptor heating all the oxygen is consumed and the environment becomes reducing in nature.

4.4 CHARACTERIZATION METHODS FOR MICROWAVE PROCESSED MMC CASTINGS

The metal matrix composite castings and EWAC castings developed through microwave energy were washed thoroughly using acetone prior to the various characterizations. The developed castings were cut cross-sectional using low-speed diamond saw (model: MS-10; make: DUCOM, India, Ref. Fig. A-1 in the Appendix-A) and were polished in a cloth wheel machine using emery papers of grades 600, 800, 1X, 2X, 3X and finally using 5 μm diamond paste. Specimens were again cleaned using water to remove any sticking particles, dried in hot air and were stored in air tight containers for further characterizations.

4.4.1 Metallurgical Characterizations

The metallurgical characterizations of developed castings were carried out through XRD, Optical Microscopy, SEM and EDS. The details of the technique and equipments used in the present study are briefly described in the following sections.

4.4.1.1 X-Ray Diffraction (XRD) Study

The X-ray diffraction technique was used in the present work to characterize and study the different phases evolved in the various castings due to the microwave hybrid heating. The various intermetallic compounds formed during the process were studied using XRD study. The X-ray diffraction measurements for all the developed castings were carried out at room temperature in the XPert PRO PANanalytical diffractometer using Cu *K*α radiations. A view of the facility present in SAI Labs of Thapar Institute of Engineering & Technology is presented in Fig. A-2 in the Appendix-A. In the present work the scan rate for XRD was maintained at 1° min^{-1} in the scan range of 10° to 100°.

4.4.1.2 Microstructure Study

The microstructure analysis and chemical composition of the castings were carried out using a metallurgical microscope (Make: Carl Zeiss, Ref. Fig. A-3) and scanning electron microscope (SEM, Make and Model: JEOL, JSM6510LV) equipped with Energy Dispersive X-ray Spectroscopy (EDS). This facility of SEM is available in SAI Labs of Thapar Institute of Engineering & Technology, Patiala and is presented in Fig. A-4.

4.4.1.3 Porosity Measurement

Defects in terms of porosity in the microwave processed castings of different powder systems were measured using a linear count method using optical microscope. The final polished sample without etching was used to measure the porosity at various locations. The selected location was divided into a number of small square regions by using graduation scale lens. The pores in the sample at different locations were counted using optical microscope and were converted into percentages. The averages of at least ten readings were considered as the final value of porosity percentage. The percentage porosity was calculated using the equations 4.2 [Gupta et al (2012)].

$$\% \, Porosity = \frac{\sum x}{121} \times 100 \tag{4.2}$$

Where, x = number of square grids with pores.

4.4.2 Mechanical Characterizations

The mechanical characterizations on the microwave processed castings were carried out in terms of Vickers microhardness, tensile strength and percentage elongation. Test details are provided in the following sections.

4.4.2.1 Measurement of Microhardness

The microwave processed castings were cut cross sectional and Vickers microhardness tests were performed on the castings to evaluate their structure property correlation. Vickers microhardness measurements were carried out at 100 g load with a dwell period of 20 s (Make: Meca Tech; Load Range: 5g to 1Kg). The complete details of the facility are presented in Appendix-A Fig. A-5 and is available in the mechanical engineering department of Thapar Institute of Engineering & Technology. To study the effect of reinforcements and, five indentations were carried out at various locations on the MMC castings. The average value is considered as the final microhardness of the selected casting sample.

4.4.2.2 Measurement of Tensile Strength and Percentage Elongation

The tensile strength of the various castings was studied by using Tinius Olsen (Model H50KS) tensile testing machine, which is available in the mechanical department of the IIT Ropar. A view of the facility is presented in Fig A-6. Tensile testing was carried out at room temperature as per ASTM standards and at a strain rate of 0.083 mm/s [Srinath et al. (2012)]. The percent elongation during the tensile tests were also recorded to study the effect of adding the ceramic reinforcement in nickel based matrix on ductility of microwave processed castings.

4.4.3 Functional Characterizations

The nickel based powders and their composite claddings were recently developed and studied for anti wear applications [Hebbale and Srinath (2015, 2016); Gupta and Sharma (2011); Pathania et al. (2015); Kaushal et al. (2017a, 2017b, 2015)]. In the present work an attempt is made to study the wear resistance properties of the bulk MMC castings developed through microwave energy and to compare the results with microwave claddings.

4.4.3.1 Dry Sliding Wear

To study the sliding wear performance of bulk casting processed through domestic microwave oven at 2.45 GHz, a pin on disc rotating type tribometer (Make: Ducom India; Model: TR20LE) (Fig. A-7) was used. Castings were cut to produce the wear pin with dimensions of (8 mm × 8 mm × 6 mm), and were held against a rotating counter disc made of alumina. The pins were fixed and tightly hold in V groove holder without any play. The hardness of the ceramic counter disc was ~1400 HV, which is widely used as a counter surface for hard materials. The cut samples were initially cleaned and polished to an initial surface roughness of R_a = 0.2 µm prior to the sliding wear tests. The standard test parameters used for the dry sliding wear tests are presented in the Table 4.16.

Table 4.16: Parameters for dry sliding wear experiments

Parameters	Description
Wear test rig	Wear and Friction Monitor (Tribometer), Model: TR-201LE, DUCOM
Test samples	Nickel based MMC's castings: 1. Pure EWAC casting 2. EWAC+5% and 10% SiC composite casting 3. EWAC+5% and 10%Al_2O_3 composite castings 4. EWAC+5% and 10% (WC-8Co) composite casting
Counter Disc	Alumina plate, Hardness ~ 1400 HV
Sliding Distances (m)	500, 1000 and 1500
Sliding velocities (m/s)	0.5, 1.0 and 1.5
Normal load (N)	10, 15 and 20
Lubrication condition	Dry
Temperature (°C)	Room temperature

To evaluate the dry sliding wear performance of bulk castings and to compare the results; the various parameters were selected from the literature [Gupta and Sharma (2011)]; which were used for the wear testing of EWAC based microwave cladding.

4.5 SUMMARY

The bulk metal-ceramic composite castings were developed by adding reinforcement powders of silicon carbide, alumina and tungsten carbide (WC-8Co) in metal matrix nickel based powder (EWAC 1004EN). The characterization of raw powders has been presented in detail. The microwave hybrid heating setup used in the present work has been explained and all the processing parameters and their effect on the processing of castings have been discussed. Optimized ranges of parameters were selected based upon extensive experimental results. The detailed characterization methods used for the microwave processed castings have been explained in detail. The need of functional characterization, i.e. dry sliding wear was stated and parameters were selected based upon the previous work such that the usefulness of developed MMC's can be proved in anti wear applications.

CHAPTER 5

METALLURGICAL AND MECHANICAL CHARACTERIZATIONS: RESULTS AND DISCUSSION

This chapter presents the results of various metallurgical and mechanical characterizations of microwave processed castings. Metallurgical characterizations of so developed castings have been carried in different capacities to investigate various phases, compounds, elements presents and their distribution by using XRD and EDS techniques. The initial investigation of cast microstructure was carried out by using an optical microscope and further, in detail by using scanning electron microscope (SEM).The optical microscopy was used for the study of porosity measurements. For mechanical characterizations the various castings were subjected to the Vicker's microhardness tests and tensile tests. All the characterization results obtained for various castings were systematically presented in this chapter. The possible phenomena for the varying properties achieved by different castings are discussed in the vicinity of the results obtained from characterizations. Fractographic analysis of fractured cast specimens was also carried out to study the possible mechanisms of failure during tensile tests. The following sections describe the stepwise characterization results of all the castings processed through microwave energy.

5.1 MICROWAVE PROCESSED CASTINGS AT OPIMIZED PARAMETERS

All the castings were obtained at the optimized process parameters which are presented in chapter 4. The powders were preheated in the oven at 200 °C to remove any moisture content and were placed in the graphite cavity. The cavity was placed on the refractory brick as per the experimental setup (Ref. Fig. 4.11) and fine charcoal powder was spread over the cavity as a

susceptor. The microwaves at 2.45 GHz and 900 W were used to process the powders for the optimized times as mentioned in Table 4.15. The castings were allowed to cool down in the ambient atmospheric conditions after processing.

Some of the microwave processed castings obtained through microwave hybrid heating are shown in Fig. 5.1.

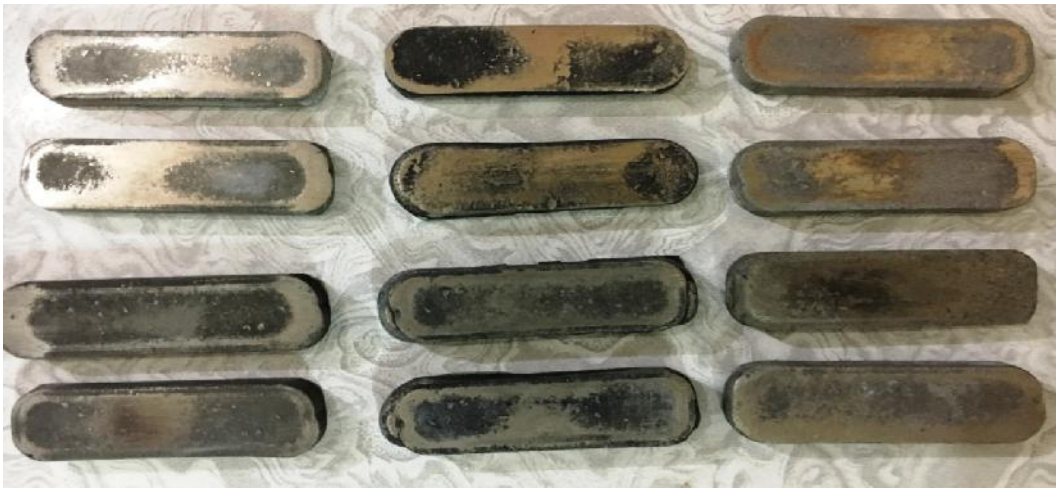

Fig. 5.1: Cavity shaped microwave processed powdered castings at 2.45 GHz and 900 W

It was observed that the obtained microwave processed castings were near shape castings, having cavity shape and some shrinkage was observed. The castings appeared to be dense and free from any visible defects such as porosity and cracks. However, a black layer was observed on the castings and this may be due to the carbon layer deposition from cavity walls on the surface. The developed castings were further subjected to the various characterizations.

5.2 CHARACTERIZATION OF MICROWAVE PROCESSED EWAC CASTINGS

This section represents the results of pure EWAC powder casting obtained at optimized process parameters. The initially obtained casting samples were cleaned using acetone and were polished for studying the microstructure and microhardness.

5.2.1 X-Ray Diffraction Study of EWAC Castings

The microwave processed EWAC casting was characterized by XRD to study the formation of phases or intermetallics due to the intense heating by microwaves. Typical XRD diffraction pattern of EWAC casting is presented in Fig. 5.2.

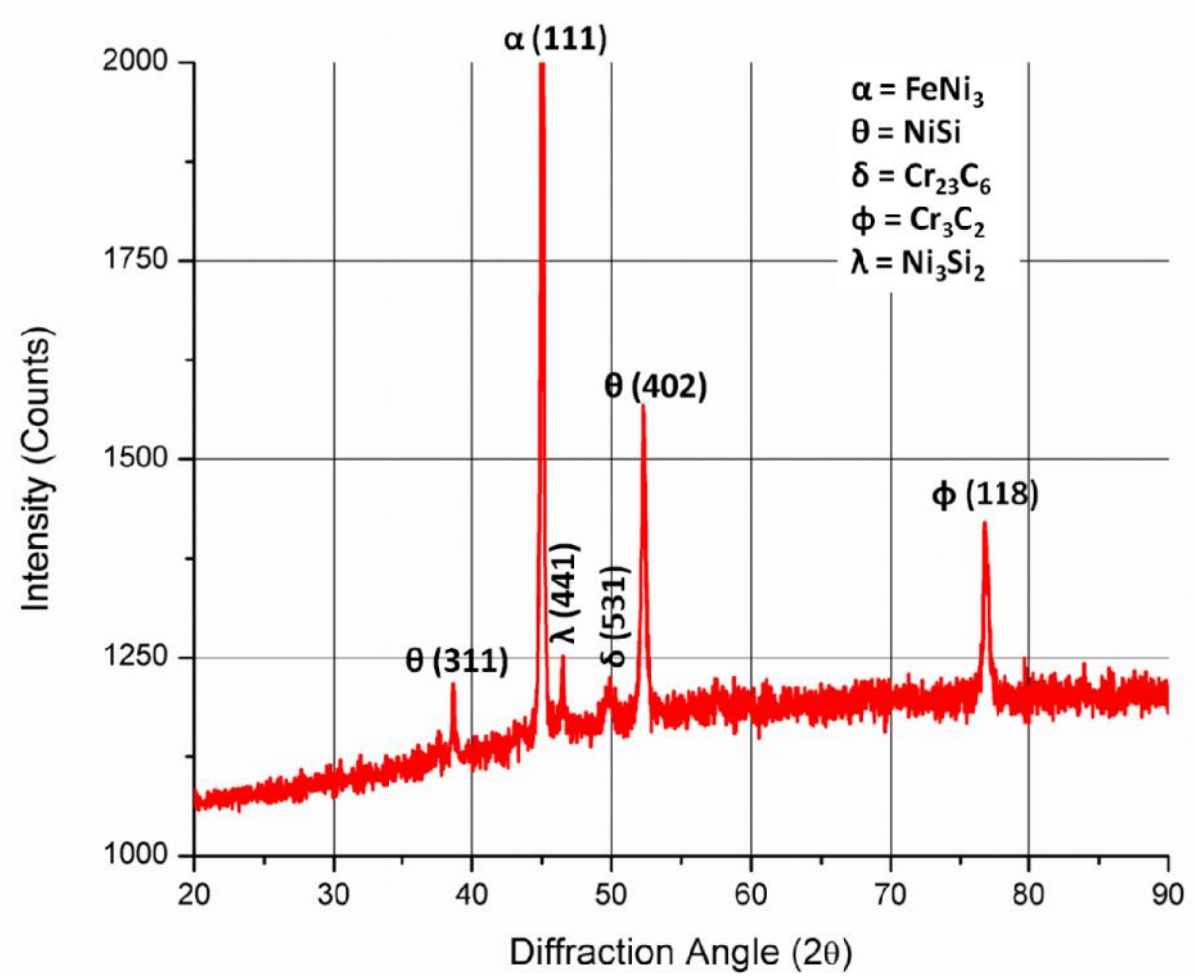

Fig. 5.2: Typical XRD spectrum of microwave processed EWAC casting

The XRD results revealed the formation of some intermetallics of chromium and nickel. Peaks of chromium carbide, nickel silicides and $FeNi_3$ intermetallics are clearly visible. At high temperatures, various possible reactions between the elements might have favored the formation of these intermetallic phases. Formations of such intermetallics have been reported while

processing of nickel based claddings on steels [Gupta and Sharma (2011), Hebbale and Srinath (2016)]. During the microwave processing of EWAC powder, the reactions occurred are given by equations 5.1-5.3.

$$23Cr + 6C \rightarrow Cr_{23}C_6 \text{ and } 3Cr + 2C \rightarrow Cr_3C_2 \quad (5.1)$$

$$Fe + 3Ni \rightarrow FeNi_3 \text{ [Chen et al. (2012)]} \quad (5.2)$$

$$Ni + Si \rightarrow NiSi \text{ [Gupta et al. (2012)] and } 3Ni + 2Si \rightarrow Ni_3Si_2 \quad (5.3)$$

At elevated temperatures, the chromium and carbon present in the EWAC powder (Ref. Table 4.1) react to form chromium carbides; and their peaks are represented in the XRD pattern corresponding to the diffraction angle of 50.62° ($Cr_{23}C_6$) and 76.49° (Cr_3C_2). Similarly, at an elevated temperature nickel reacts with silicon to form intermetallic of $FeNi_3$ corresponding to 2θ of 44.12°; reacts with silicon to form nickel silicides corresponding to 2θ of 46.73 (Ni_3Si_2) and NiSi at 52.23°.

Further, the approximate percentage phases present in the microwave processed EWAC casting was analyzed using peak intensities for the particular phases. A method of Normal Intensity ratio (NIR) was used to approximate the percentage of phase formations and NIR of the first phase is calculated by using equation 5.4 [Peelamedu et al. (2002), Gupta and Sharma (2011)].

$$NIR_1 = \frac{I_1 - I_{back}}{I_1 + I_2 + I_3 + \cdots + I_n - nI_{back}} \quad (5.4)$$

Where, I_1, I_2, I_3…..I_n are the intensities of the 1st , 2nd….nth phase respectively; and I_{back} is the background intensity. Similarly, the NIR can be determined for other phases using equation5.4 and the results of NIR are presented in Table 5.1.

Table 5.1: Relative phase intensities and NIR (%) of microwave processed EWAC casting

S. No.	Phase	I_1	I_2	I_3	I_4	I_5	I_6	I_{back}	NIR (%)
1	NiSi	1223						1120	5.25
2	$FeNi_3$		1996					1120	44.58
3	Ni_3Si_2			1252				1120	6.72
4	$Cr_{23}C_6$				1220			1120	5.08
5	NiSi					1612		1120	25.04
6	Cr_3C_2						1382	1120	13.33

The result of NIR revealed that FeNi3 intermetallic compound accounts for ~44.58% of entire phases. However, this method only represents the rough estimate of phases present in the material system.

5.2.2 Microstructural Characterization of EWAC Castings

The obtained castings were cut along the transverse direction and polished as mentioned in section 4.4. Prior to the detailed microstructure analysis, etching was carried out using swab of acidic solution obtained by mixing equal quantity of nitric acid (HNO_3), hydrochloric acid (HCl) and acetic acid (CH_3COOH). The SEM image of microwave processed EWAC casting along the transverse direction is shown in Fig. 5.3.

The SEM images revealed that the microstructure of EWAC casting consists of nearly equiaxed grains throughout the cross section with some superficial pores on the surface. The average grain size observed in the casting was ~55 μm.

The formation of equiaxed grains is due to the volumetric heating characteristics of the microwaves; that reduces the chances of dendritic transitions from equiaxed or cellular structures [Hebbale and Srinath (2016)].

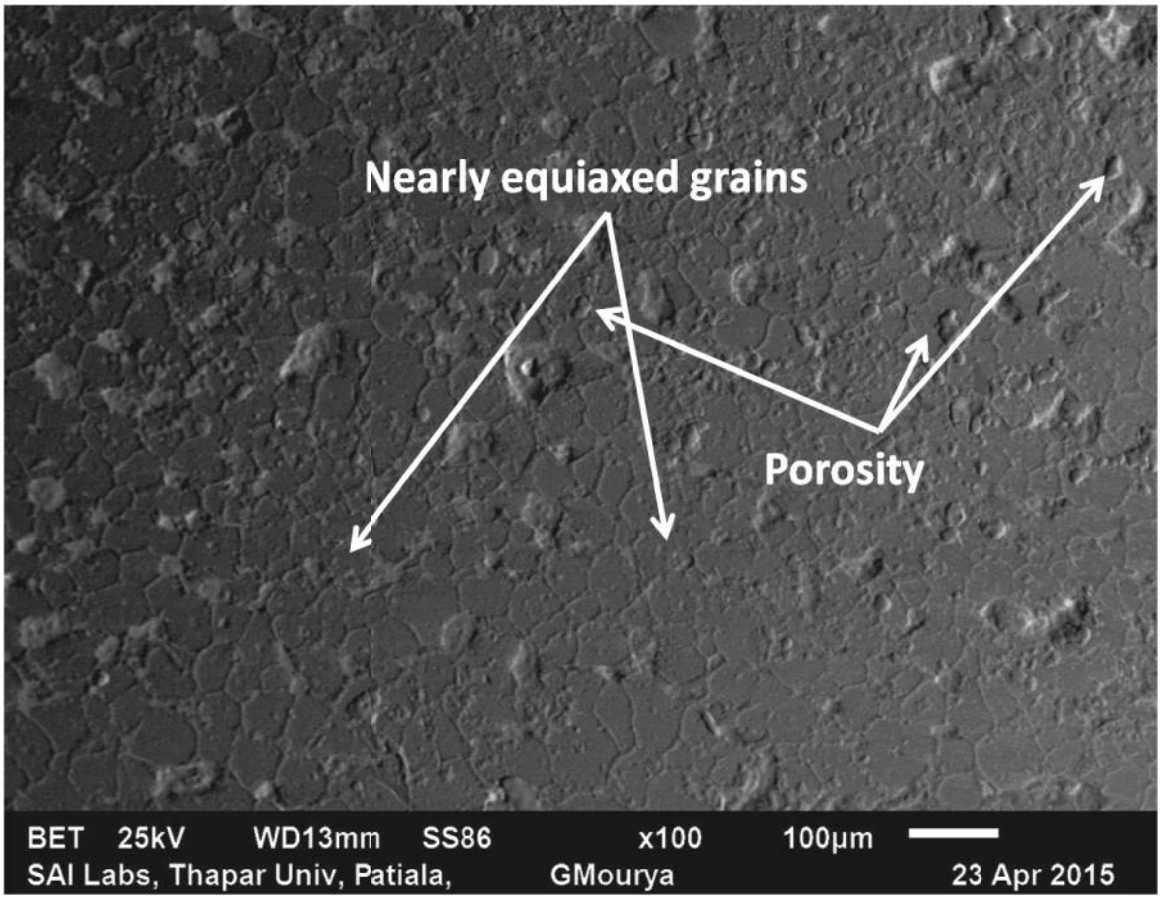

Fig. 5.3: Typical transverse cross-section SEM images of EWAC casting showing the equiaxed microstructure

Further, when the microwave irradiation was stopped, the solidification occurs by transfer of heat from the melt towards the cavity walls. The equiaxed structures are often reported to grow in the direction of heat flow, i.e. from the core to the outer surface. Fig. 5.4 shows the equiaxed grain growth near the end surface of castings where average grain size increases to ~64 µm. The presences of superficial voids on grain surface are due to the over etching.

Further, microstructures were analyzed for porosity content in the castings using optical microscope.

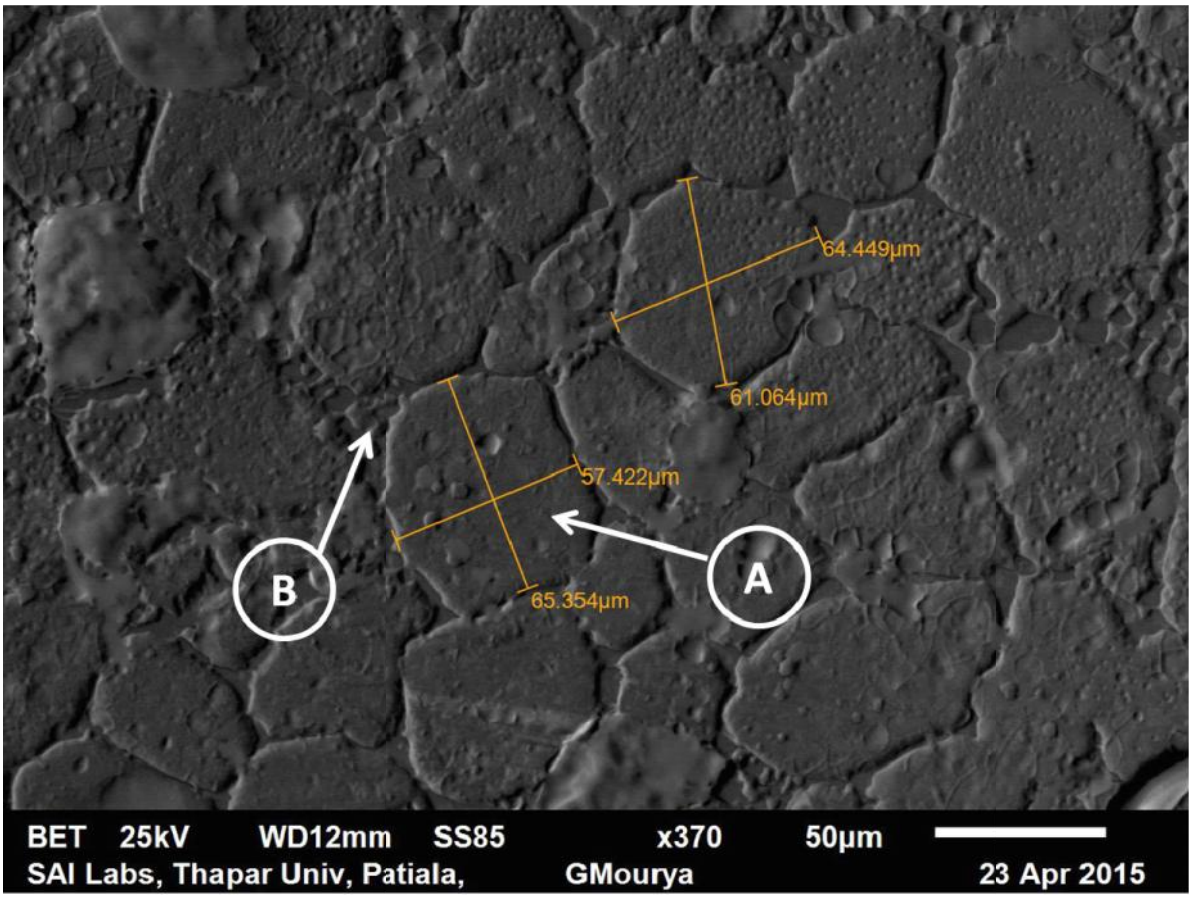

Fig. 5.4: SEM image showing the growth of equiaxed grains near the end surface of the casting

The results of porosity measurement revealed that very few pores were visible throughout the cross section of the microwave processed casting. Volumetric heating during microwave processing may lead to the lower defects (porosity) in the developed castings. In EWAC casting the porosity was present in the range of 0.5-1.2%, which was calculated using a metallurgical microscope at various locations on casting cross section.

5.2.3 EDS Analysis of EWAC Castings

The EWAC casting was subjected to EDS analysis and elemental distribution was carried out at various locations in the casting; namely on the grain surface (A) and on grain boundaries (B) (Ref. Fig. 5.4) and results are presented in Fig. 5.5.

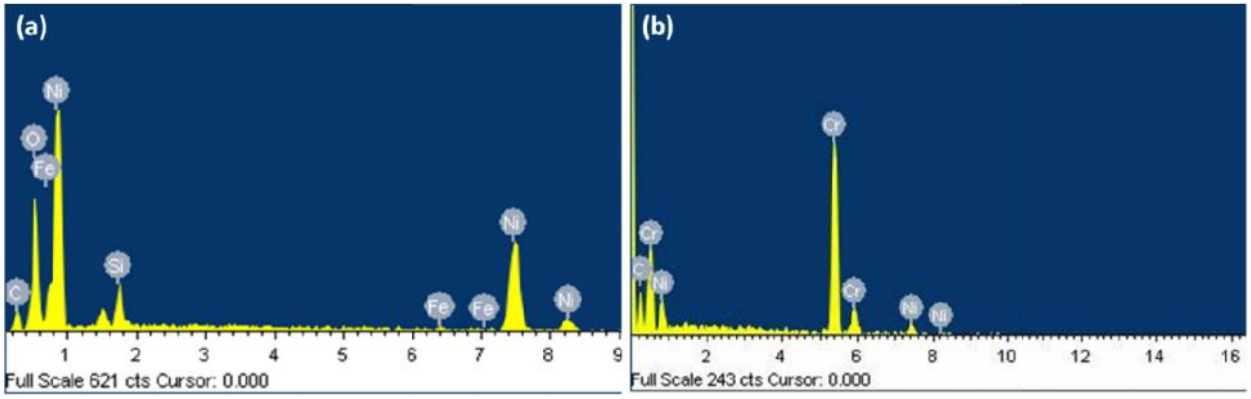

Fig. 5.5: EDS analysis on (a) Grain surface and (b) grain boundary

The results revealed the higher presence of carbon and chromium content of the grain boundaries and the predominant presence of nickel, silicon and iron on the grain surfaces. The presence of higher chromium and carbon at grain boundaries is due to the precipitation of chromium carbides along the grain boundaries during microwave processing. The grains are mainly composed of nickel and intermetallics of nickel, silicon and iron. The formation of these intermetallics has already discussed in XRD analysis.

5.2.4 Microhardness Study of EWAC Castings

The Vicker's microhardness of microwave processed EWAC casting was carried out at five different locations along the cross section. The tests were carried out at 100 g load with 20 s of dwell time. The typical indentations obtained on EAWC castings are shown in Fig. 5.6.

The results of microhardness test revealed that there were some variations in the microhardness values recorded at various locations. This is due to the fact that when indentation falls on the grain surface, the value recorded is lower due to the plastic deformation of the material, but, the value increases when indentation falls on the grain boundaries due to precipitation of of hard phases like intermetallic and carbides.

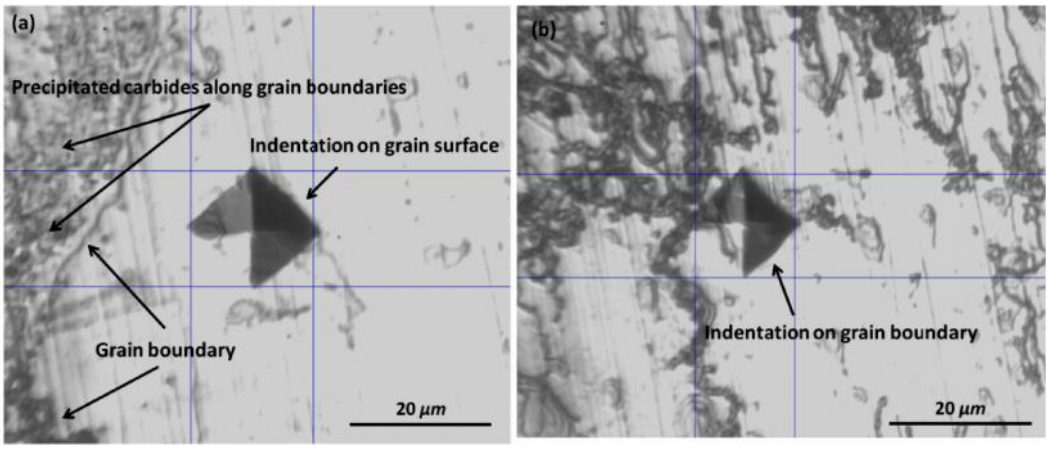

Fig. 5.6: Optical micrographs of indentations on EWAC casting (a) grain surface and (b) grain boundary

The formation and precipitation of carbides along the grain boundaries caused the variations in the microhardness. The average microhardness of the microwave processed casting was 410 ± 55 HV. The results of microhardness tests are presented in Fig. 5.7.

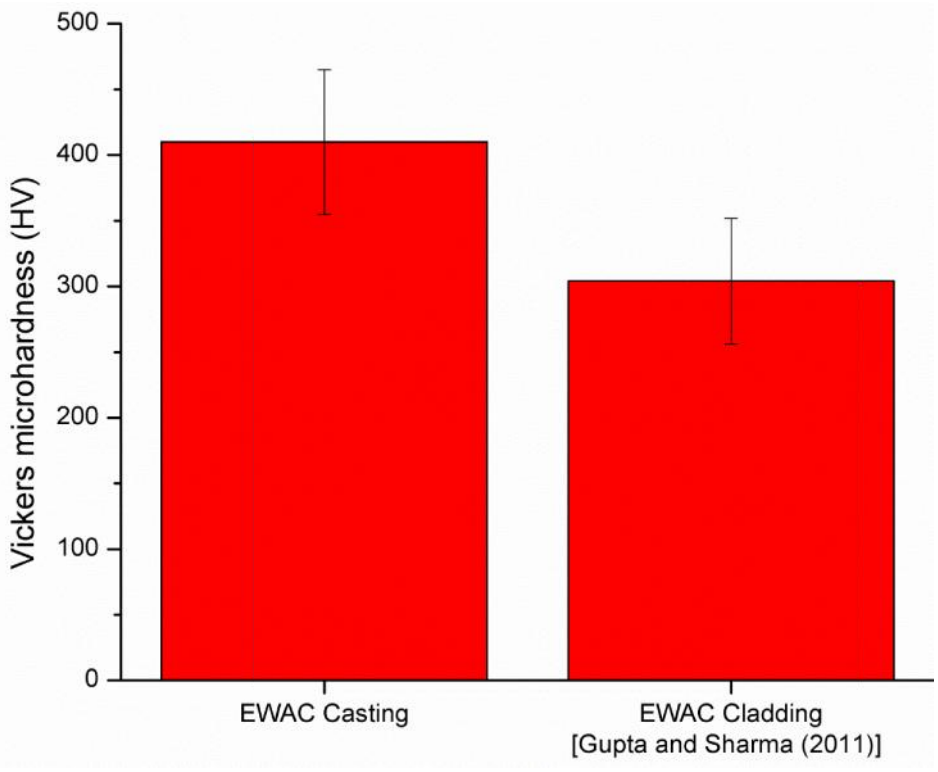

Fig. 5.7: Comparison of average Vicker's microhardness of microwave processed EWAC powder casting and EWAC cladding

The average Vicker's microhardness of microwave processed EWAC casting was comparable to the microhardness obtained in EWAC cladding. But higher processing time in the casting of EWAC powder in comparison to the cladding process may lead to the formation of higher silicides and carbides which eventually led to higher microhardness.

5.2.5 Tensile Strength and Percent Elongation Study of EWAC Castings

The bulk castings obtained through microwave energy were further machined to obtain standard tensile strength specimens of dog bone shape; as per ASTM (E8M) standards with 18 mm gauge length and 3.5 mm width [Srinath et al. (2011)]. Tensile test specimens are shown in Fig. 5.8.

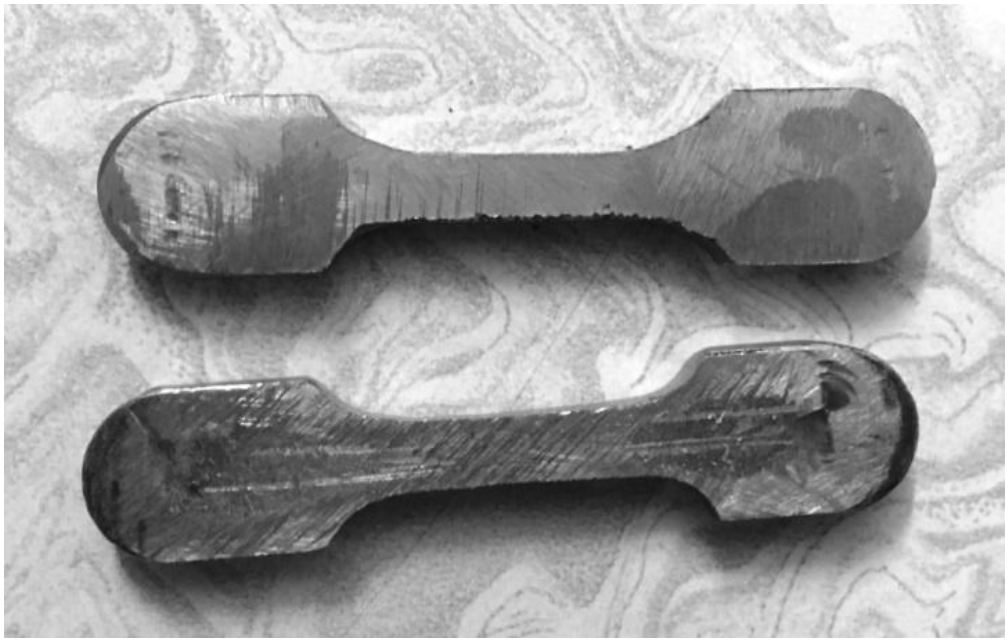

Fig. 5.8: Dog bone shape tensile test specimens as per ASTM (E8M) standards

Tensile tests were performed by applying uniaxial tension at a strain rate of 8.3×10^{-3} mm/s. The typical stress-strain cure for pure EWAC casting is shown in Fig. 5.9.

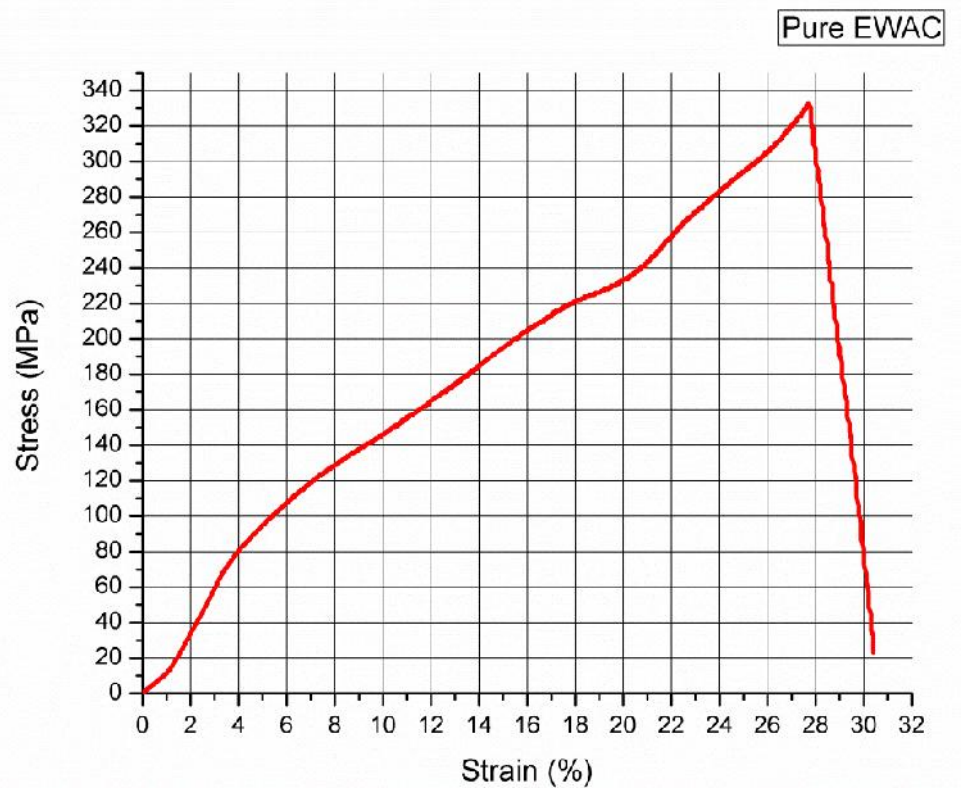

Fig. 5.9: Typical stress-strain curve for microwave processed EWAC casting

The average ultimate tensile strength of the EWAC casting was 330 ± 15 MPa with percentage elongation of 33 ± 2. Results revealed that strength of EWAC casting was ~ 76.6% of the pure nickel strength of 450 MPa at 20° C (Nickel 200, commercially pure grade with 99.6% Ni) [Source internet: *http://www.nickel-alloys.net/commercially_pure_nickel.html*]. Similarly the percentage elongation recorded was ~ 71% in comparison to the 47% elongation of nickel 200. The decrease in the elongation was due to the formation of carbides along the grain boundaries, which restricts the plastic deformation during a tensile test. The fractured surface of EWAC casting is shown in Fig 5.10, which reveals cup-cone type ductile fracture. This formation of cone surface also shows that nickel powder was completely melted to form the casting. The formation of dimples all over the area represents the typical ductile fracture of the sample. However, the formation of some carbide along the grains caused a reduction in elongation.

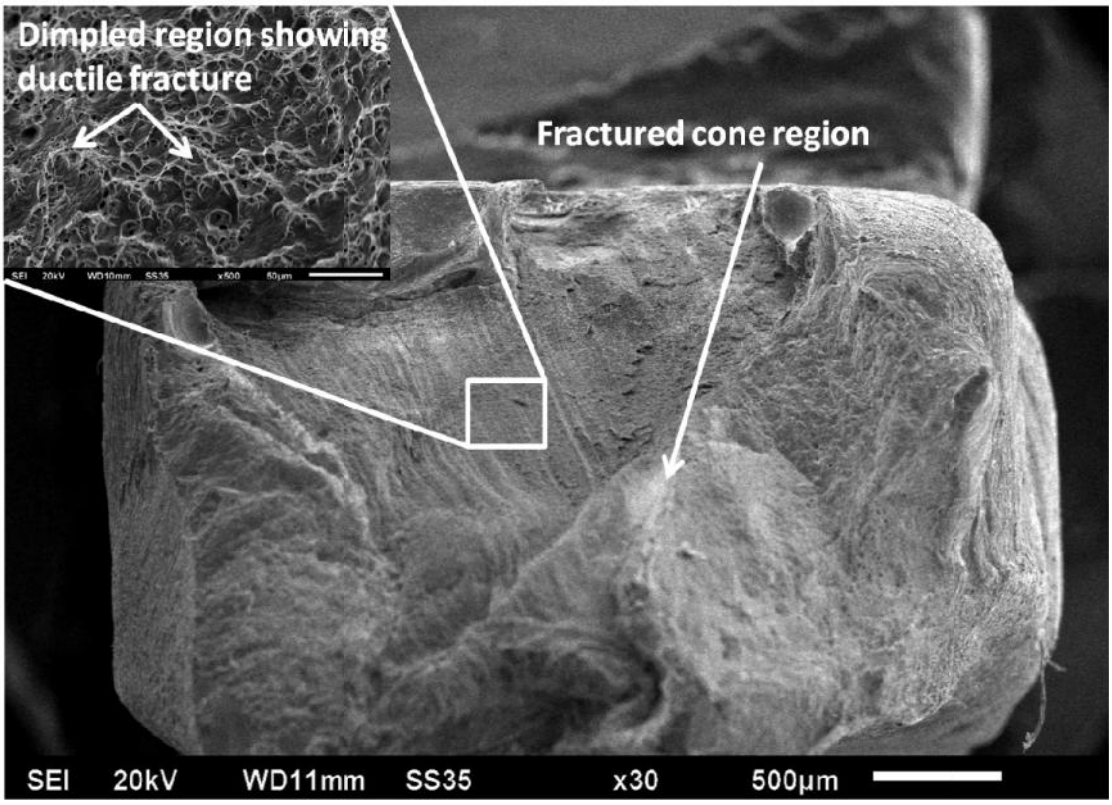

Fig. 5.10: Fractured surface of microwave processed EWAC casting showing cup-cone type ductile fracture and inset shows the magnified dimpled surface for ductile fracture

These dimples are the result of high plastic deformations induced in the ductile material during rupturing.

5.3 CHARACTERIZATION OF MICROWAVE PROCESSED EWAC+SiC COMPOSITE CASTINGS

The addition of silicon carbide reinforcement in EWAC matrix helped in lowering the processing time (Ref. Fig. 4.15) due to better microwave (2.45 GHz) absorption characteristics of SiC particles. The premixed powder containing 5% and 10% volume fraction of SiC reinforcement in EWAC powder was processed using MHH as discussed in chapter 4. The developed EWAC+5%SiC and EWAC+10%SiC MMC's were subjected to various characterizations and the results are discussed in the following sections.

5.3.1 X-Ray Diffraction Study of EWAC+SiC Composite Castings

The microwave processed metal-ceramic composite castings containing silicon carbide as reinforcement in EWAC matrix were subjected to XRD characterization. This study is carried out to find the effect of reinforcement particles on the formation of new phases or intermetallics. The typical XRD patterns of SiC reinforced EWAC matrix composites are shown in Fig. 5.11.

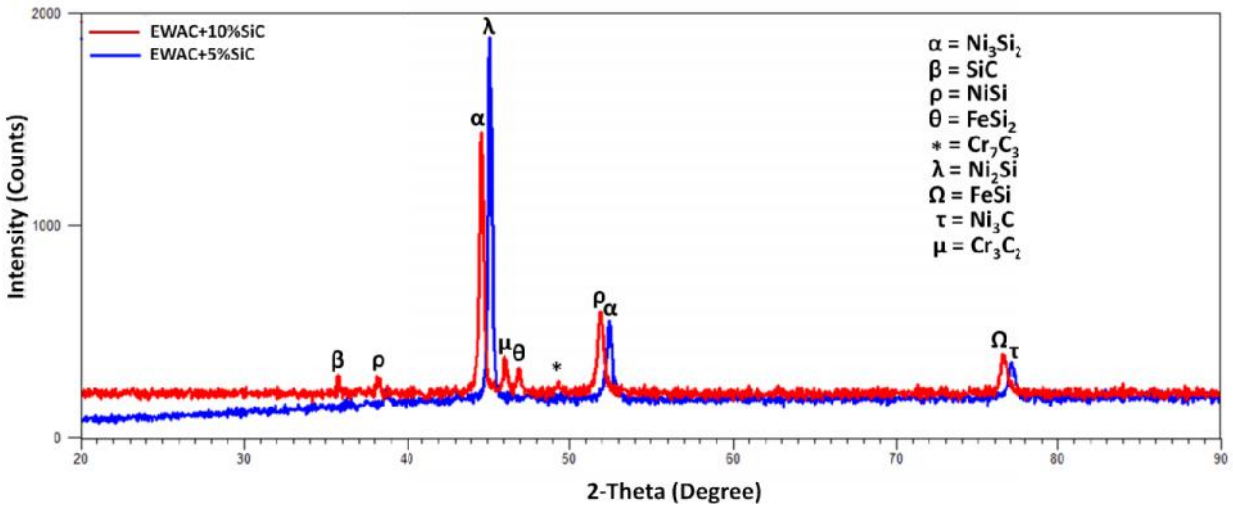

Fig. 5.11: Typical XRD spectrum of EWAC+5% SiC and EWAC+10% SiC microwave processed castings

The XRD results revealed that on adding silicon carbide as reinforcements, the major peaks obtained were of nickel silicides (Ni_3Si_2 and Ni_2Si) in comparison to the $FeNi_3$ phase obtained in EWAC casting (Ref. 5.2). This may be due to the of decomposition of silicon carbide into free silicon and carbon at high temperatures. It has been reported [Kang and Kang (2006)] that at high temperatures, the thermal decomposition of silicon carbide into silicon and carbon takes place during the plasma spraying process. Following reaction might have taken place during the intense microwave heating and are presented by equations 5.5 - 5.8 [Liu et al. (2001); Kang and Kang (2006) and Kaushal et al. (2017)].

$$SiC \rightarrow Si + C \tag{5.5}$$

$$3Ni + 2Si \rightarrow Ni_3Si_2 \text{ Or } 2Ni + Si \rightarrow Ni_2Si \text{ Or } Ni + Si \rightarrow NiSi \tag{5.6}$$

$$Fe + 2\,Si \rightarrow FeSi_2 \tag{5.7}$$

$$3Ni + C \rightarrow Ni_3C \text{ Or } 3Cr + 2C \rightarrow Cr_3C_2 \text{ Or } 7Cr + 3C \rightarrow Cr_7C_3 \tag{5.8}$$

During the microwave processing, the various elements have reacted with one another to form the intermetallics, but the presence of silicon based intermetallics were basically due to the addition of silicon carbide reinforcement. In EWAC+5% SiC composite, the highest peak of Ni_2Si was observed at a corresponding diffraction angle of 45.49°, peak of Ni_3Si_2 was observed at an angle of 52.32° and Ni_3C at an angle of 78.2°. With further increase in the volume fraction of silicon carbide to 10%, the peak of SiC was observed corresponding to 2θ of 35.67°. The decomposed SiC again reacted with nickel and iron to form silicides and reacted with chromium to form carbides. The formation of NiSi was confirmed by a peak at diffraction angle of 38.61° and 52.23°, and $FeSi_2$ at an angle of 48.05°. Peaks of chromium carbides were observed at diffraction angles of 46.55° (Cr_3C_2) and 49.28° (Cr_7C_3) respectively. The effect of SiC reinforcement on the formation of these silicides and carbides was favorable at high temperature microwave processing. These intermetallics may lead to the high hardness and strength of the developed MMC.

Further, the phases present in the microwave processed EWAC +10% SiC casting was analyzed using normalized intensity ratio (NIR) and results are presented in Table 5.2.

Table 5.2: Relative phase intensities and NIR (%) of microwave processed EWAC+10%SiC MMC casting

S. No.	Phase	I_1	I_2	I_3	I_4	I_5	I_6	I_7	I_{back}	NIR (%)
1	SiC	200							120	9.75
2	NiSi		152						120	3.90
3	Ni_3Si_2			504					120	46.83
4	Cr_3C_2				202				120	10.0
5	$FeSi_2$					192			120	8.78
6	Cr_7C_3						186		120	8.05
7	FeSi							224	120	12.68

The NIR of silicide phase of nickel (Ni_3Si_2) was highest with 46.83%, followed by iron silicide (FeSi) with 12.68% and chromium carbide (Cr_3C_2) with 10%.

5.3.2 Microstructural Characterization of EWAC+SiC Composite Castings

The microwave developed MMC casting shows complete melting, densification and coalescence of powder particles to form near shape casting. There were no visible cracks and porosity on the surfaces of as obtained castings. The developed castings were cut cross-sectional and were subjected to microstructural characterizations by using optical microscopy and scanning electron microscopy. The main objectives of the microstructural characterizations are to study the reinforcement distribution behavior and microstructure of the casting. The optical microscopic images of castings without etching are shown in Fig. 5.12 (a-b), which shows the uniform distribution of SiC reinforcement in the matrix. However, on the addition of 10% SiC reinforcement, some agglomeration of particles was observed which may be due to the increased particle-particle interactions. Fig. 5.13 shows the etched sample of EWAC +10% SiC composite which reveals the formation of equiaxed grains.

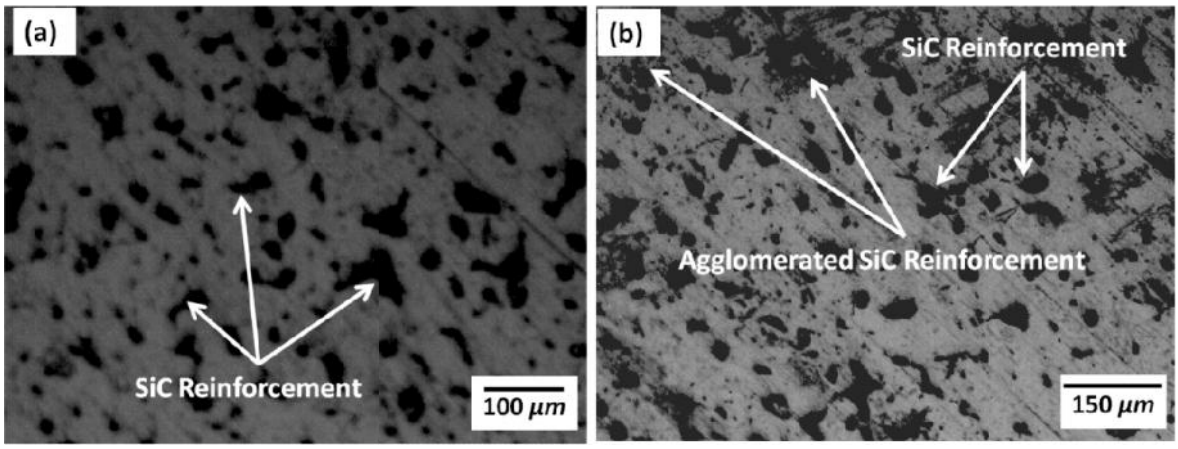

Fig. 5.12: Optical microscopic images of (a) EWAC+5% SiC and (b) EWAC+10% SiC microwave processed composite

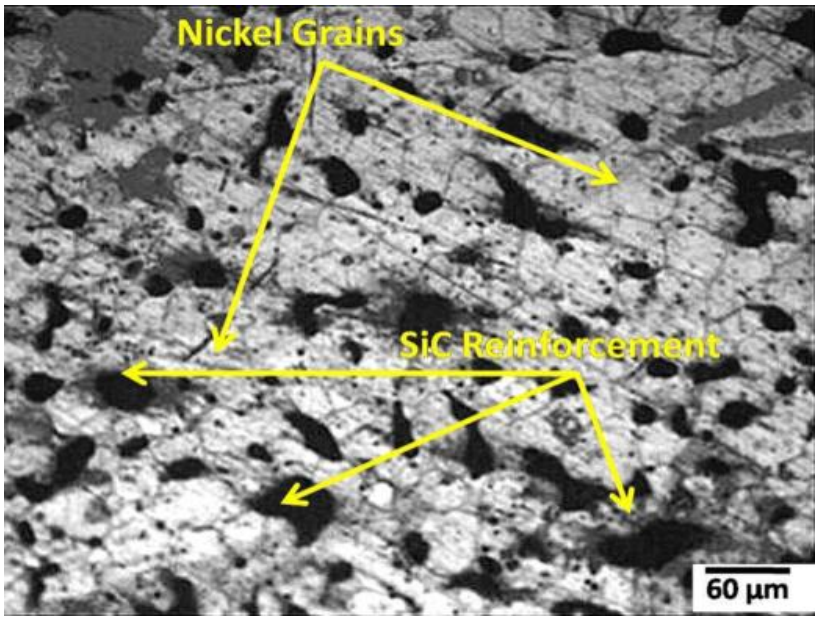

Fig. 5.13: Optical microscopic images of etched EWAC +10% SiC casting

The backscattered SEM image of EWAC+10% SiC composite casting is shown in Fig. 5.14., which reveals the formation of equiaxed structures throughout the casting and SiC reinforcement is uniformly distributed. The average grain size measured at various locations was ~58 μm. Colors are inverted for better understanding the distribution behavior of reinforcement.

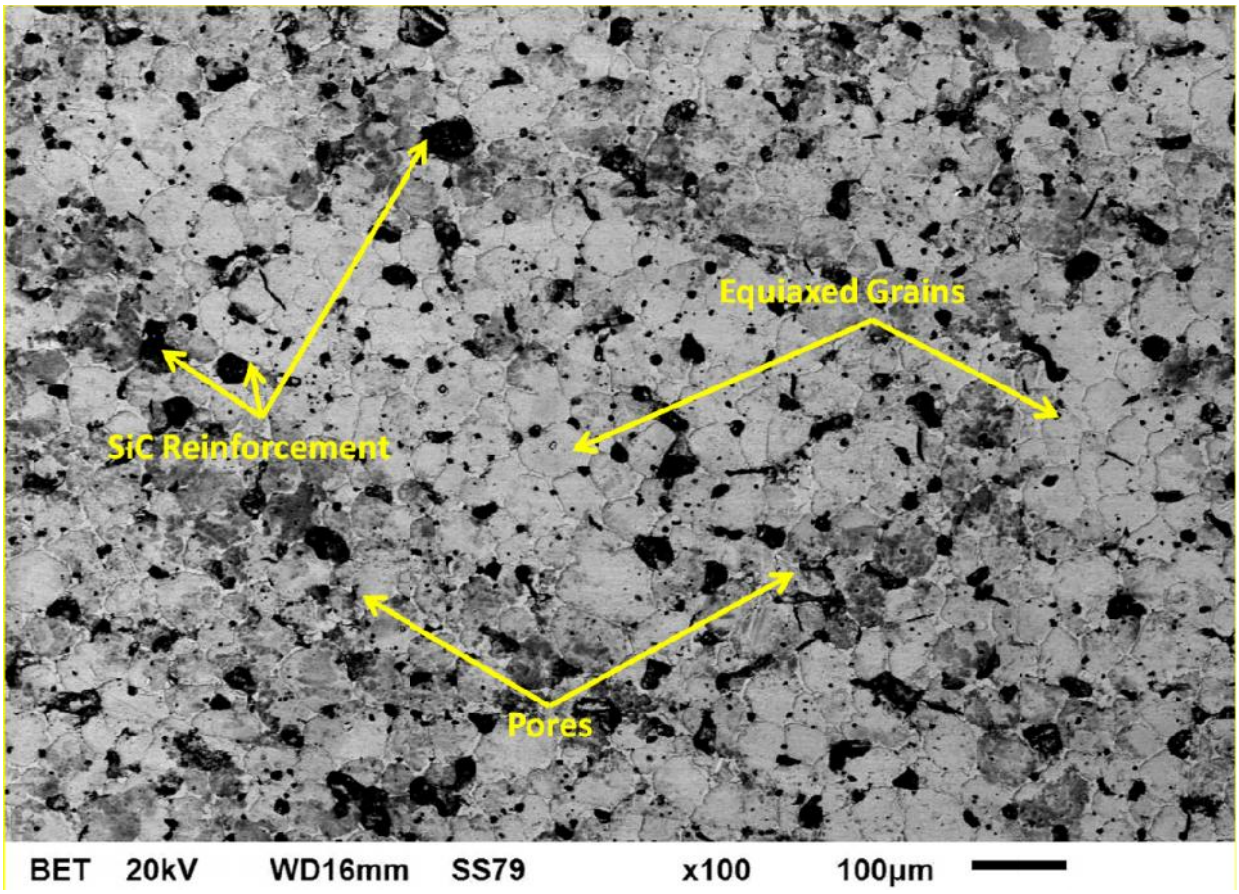

Fig. 5.14: SEM image showing the equiaxed grains in EWAC+10% SiC reinforced composite

The microstructure of microwave processed casting did not show any dendritic transitions from equiaxed structures and the main reason behind this was volumetric heating obtained through microwaves. Volumetric heating reduces the thermal gradients within the casting and prevents the transition of structures into dendrites. Further, it was observed that some of SiC particles were decomposed into smaller sizes due to the intense microwave heating and better microwave absorption behavior of SiC particles. The convection current associated with the microwaves helped in the dispersion of reinforcement throughout the matrix. The magnified SEM image of reinforcement particle embedded in the matrix is shown in Fig. 5.15 (a). It can be clearly seen that the SiC reinforcement particle is strongly embedded in the matrix

grains and interfaces are free from defects and fractures. The line scanning EDS analysis of SiC particle is also performed and results are shown in Fig.5.15 (b).

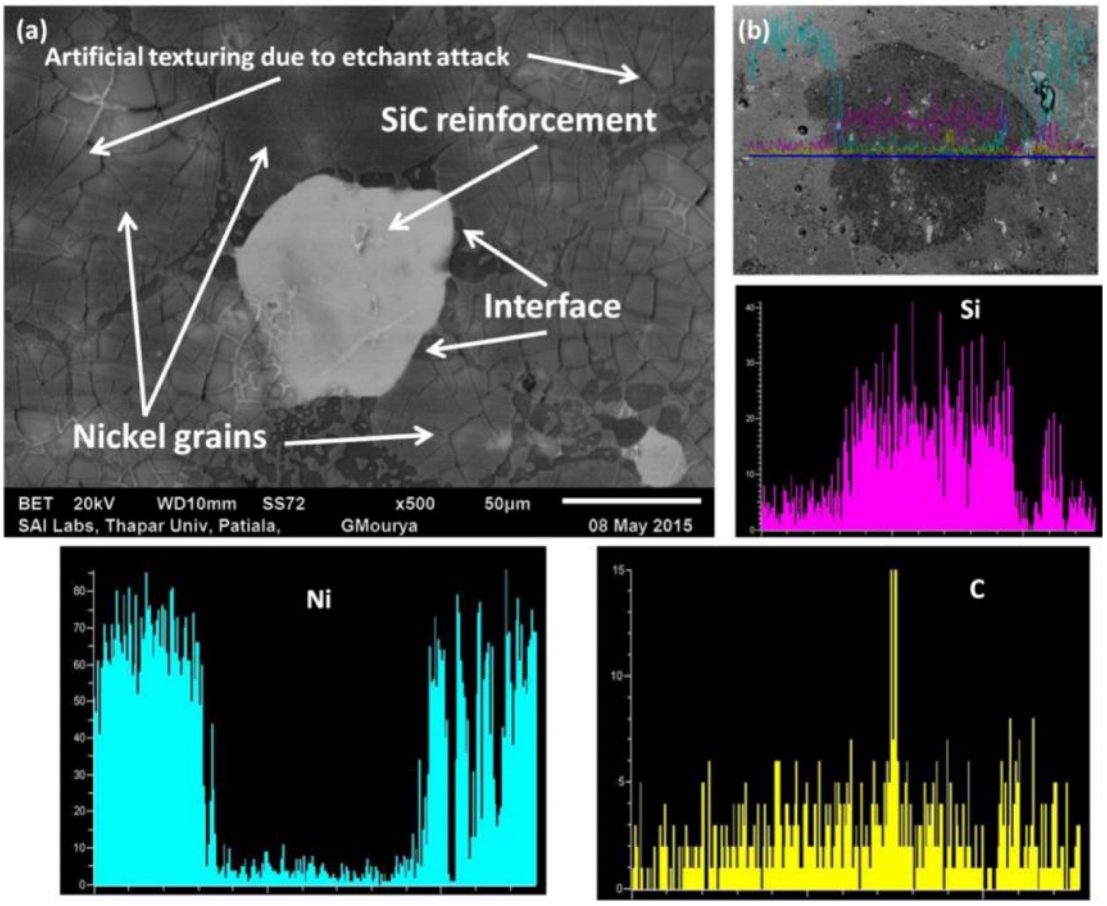

Fig. 5.15: (a) Magnified backscattered SEM image showing SiC particle and nickel matrix interface, and (b) EDS line mapping of SiC particle

The porosity measurement was carried out by using an optical microscope and ImageJ software along the cross section of developed composite and was found to be in the range of 1.68%–1.75%. The presence of significantly lower porosity defects may be attributed to the bulk heating of sample through microwave heating which reduces the chances of differential heating. The reported results of some authors are compared with the present results of porosity and microhardness which are shown in Table 5.3.

Table 5.3: Comparison of porosity levels for present work and previously published data

S. No.	Material System	Processing Method	Porosity	Ref.
1	EWAC+10% SiC Composite Casting	Microwave Casting	1.68-1.75%	Present work
2	Al-Al_2O_3 Composite Castings (Micro/Nano)	Stir Casting Compo Casting	1.1-5.6% 1.1- 5%	[Sajjadi et al. (2012)]
3	Al-SiC Composite Castings	Conventional Stir Casting	3-12%	[Ahmad et al. (2007)]
4	Ni-SiC MMC	Electrodeposition	NA	[Gul et al. (2012)]
5	Ni+30%WC Composite Coating	Plasma Spray	4.7%	[Guo et al. (2013)]
6	Ni-C-B-Si-W alloy	Laser Cladding	4%	[Balu et al. (2015)]
7	Ni based powder	Laser Cladding	4.97-7.62 % at 2.5 kW	[Zeng et al. (2016]

The present results revealed that the microwave casting process produced significant lower porosities in comparison to the available data. The microwave heating caused reduced thermal gradients throughout the casting which supported the formation of uniform equiaxed grains, restricted the transitions to dendrites and lowered the defect formation in the castings.

5.3.3 EDS Analysis of EWAC+SiC Composite Castings

The results of XRD study revealed the formation of various intermetallics during microwave heating and to confirm the same EDS analysis was carried out at various locations of casting. Fig. 5.16 (a) shows the various locations where EDS analysis was carried out and results are shown in Fig. 5.16 (b-d).

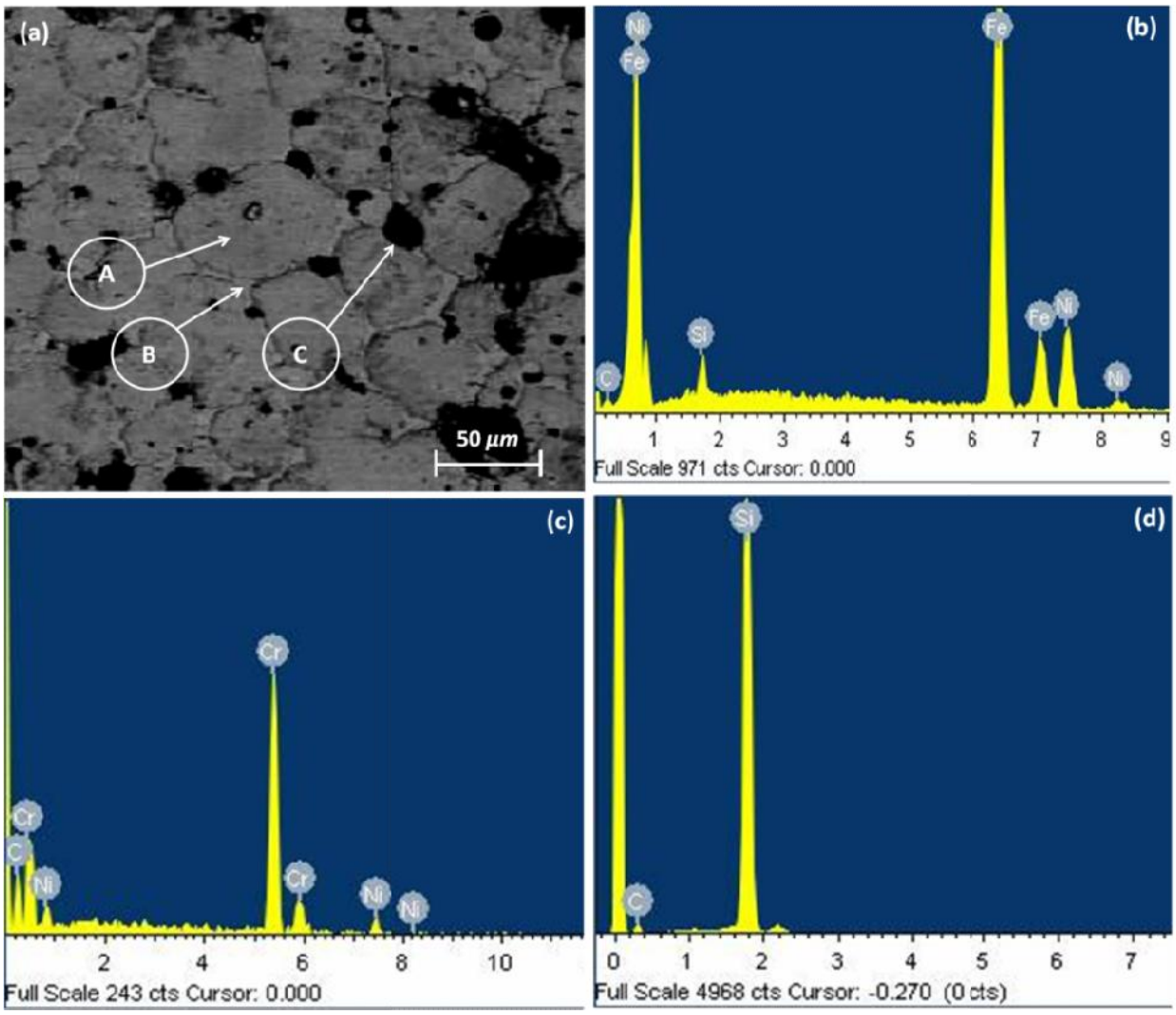

Fig. 5.16: (a) SEM image showing the locations for EDS analysis, (b) EDS analysis result on grain surface, (c) EDS analysis on grain boundary and (d) EDS analysis on SiC particle

The EDS results revealed that on the grain surface, the elements present are nickel, iron and silicon. This is due to the formation of intermetallics of nickel silicides and iron silicides during microwave heating as explained in XRD analysis. On the grain boundary, the presence of chromium, carbon and nickel increases, which is due to the precipitation of chromium carbides and nickel carbides along the grain boundaries. Presence of silicon carbide as reinforcement is clearly visible and EDS analysis confirms the SiC particles in embedded in EWAC matrix.

5.3.4 Microhardness Study of EWAC+SiC Composite Castings

The effect of reinforcement on hardness was studied by carrying out microhardness tests on the cross section of the developed castings. The results of average Vicker's microhardness obtained on various EWAC + SiC samples and their comparison with others results are shown in Fig. 5.17.

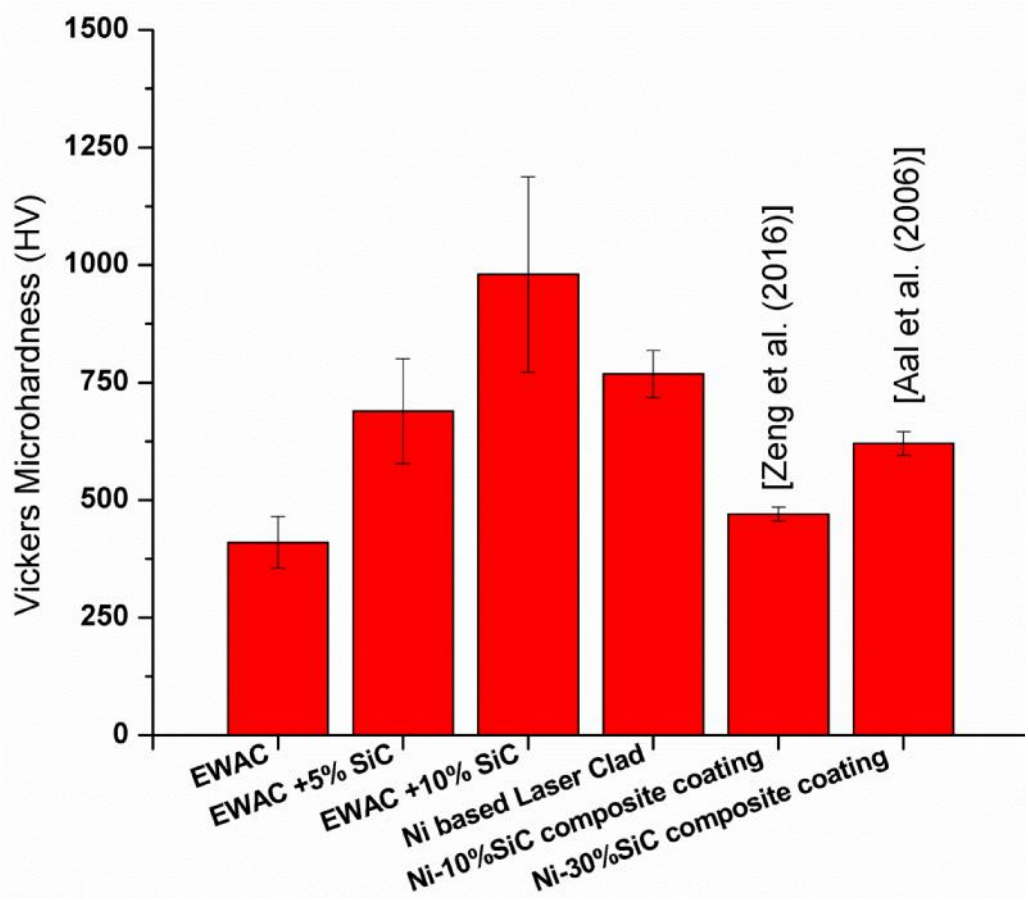

Fig. 5.17: Vicker's microhardness results of microwave processed EWAC+SiC composite castings and comparison with other published data

The microhardness results revealed that microwave processed EWAC +10%SiC composite casting possessed higher average microhardness of 980 ± 208 HV in comparison to the pure EWAC casting microhardness of 410 ± 55 HV, which is 2.4 times higher. The addition of 5% volume fraction of SiC reinforcement resulted in ~685 ±110 HV microhardness which

further increased by adding 10% volume fraction of SiC reinforcement. This may be attributed to the metallurgical changes which occurred during the microwave heating of composite casting. The formation of intermetallics such as hard carbides and silicides (Ref. Fig. 5.11) may have contributed to the higher microhardness. Also, the microstructure analysis (Ref. Fig. 5.14) revealed the formation of uniform equiaxed grains and uniform distribution of reinforcements which contributed to the overall microhardness. It was observed that when indentation falls on reinforcement phases, higher microhardness was recorded in comparison to the indentations on matrix phase. This was due to the inherent hardness possessed by SiC which resists the deformations, but nickel matrix being ductile shows higher order deformations and lower microhardness value. This deviation of microhardness values at various locations led to the higher variations of 208 HV in 10% SiC composite casting. Fig. 5.18 (a-b) shows the morphologies of indentations and revealed higher plastic deformations by indent when falls on the matrix, but reinforcement phase resists the deformations and contributes to higher microhardness.

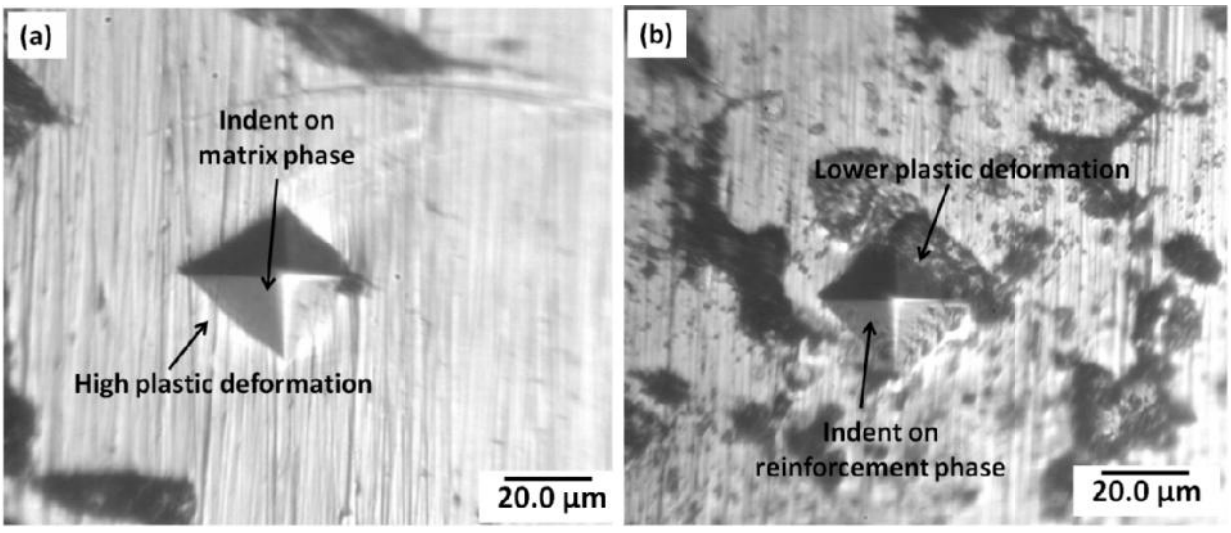

Fig. 5.18: Indentation morphologies on (a) matrix phase and (b) reinforcement phase

5.3.5 Tensile Strength and Percent Elongation Study of EWAC+SiC Castings

The reinforcement material has a significant effect on the various properties of metal matrix composite materials mainly, strength. These effects further depend upon the materials system, i.e. matrix properties and reinforcement properties. In literature [Ozben et al. (2008); Bahrami et al. (2014); and Walczak et al. (2014)], SiC reinforcement is mainly added to increase strength, load bearing capacity and wear resistance of metal matrix. In the present work, study on the effect of SiC reinforcement on tensile properties is carried out by performing tensile tests as per ASTM standards. The results of tensile strength of EWAC and EWAC + SiC composite castings are shown in Fig. 5.19.

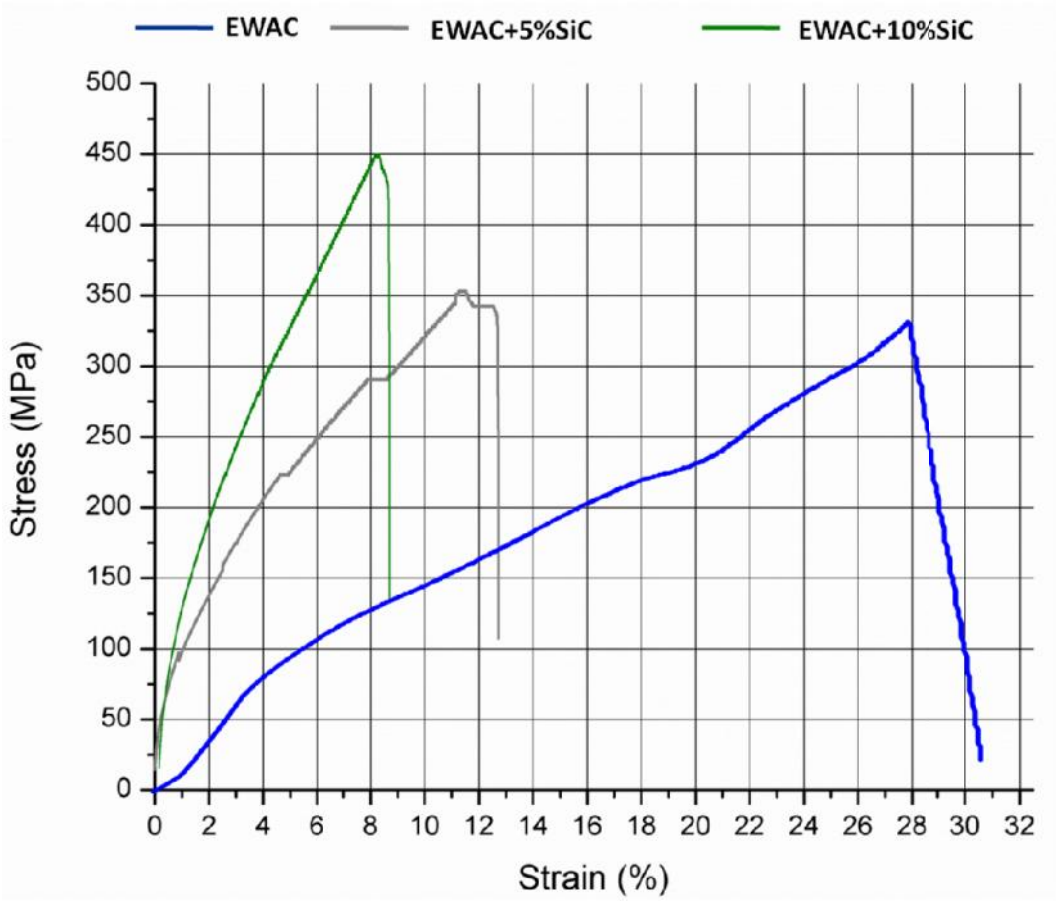

Fig. 5.19: Stress-strain plot for microwave processed EWAC and EWAC+SiC castings

The results revealed that on adding the SiC material as a reinforcement, the strength of the composite system has been increased significantly, but it has been observed that a significant decrease in the percent elongation of composite casting. In comparison to the pure EWAC casting (330 MPa), the strength for 5% SiC reinforced composite increased by 7.04% (355 MPa). By increasing the content of SiC to 10% volume fraction, the strength further increased by 26.67% (450 MPa) in comparison to EWAC casting. This increase in strength in EWAC + SiC composites may have occurred due to smaller grain diameters which help in strengthening of material as per Hall-Petch relationship shown by equation 5.9 [El-kady and Fathy (2014)].

$$\sigma_o = \sigma_i + KD^{-\frac{1}{2}} \tag{5.9}$$

In equation 5.9, σ_o is flow stress, σ_i is stress opposing the movement of dislocations, K is constant and D is average grain size diameter. Also, the presence of intermetallics increased the strength of the casting.

The presence of hard SiC particles and carbides along the grain boundaries, increases the load bearing strength during the tensile loading, but due to constrained deformations (being hard and brittle), these carbides act as stress risers from where crack initiation starts. Developed cracks propagate throughout the cross section and leads to the failure. Due to this constrained deformation, the percentage elongation of EWAC + SiC composites reduces in comparison to the EWAC casting. On adding 5% SiC the average percent elongation observed was 15 ± 3, whereas on adding 10% SiC reinforcement, the percent elongation further reduced to 10.5 ± 2. This can also be related to the overall increased microhardness of the reinforced sample. With the increase in the microhardness, the ductility decreases more than half of the ductility of EWAC casting.

The fractured morphology of EWAC + 10% SiC reinforced composite casting is as shown in Fig. 5.20.

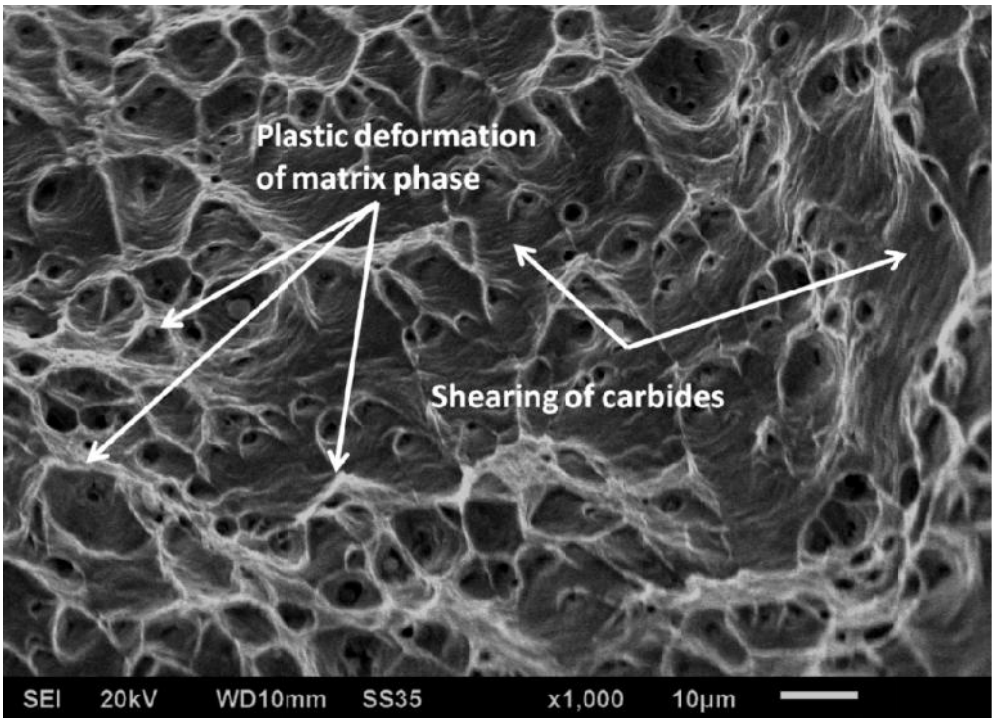

Fig. 5.20: SEM image showing the fractured area of EWAC+10% SiC composite casting

The fractured surface reveals the mixed ductile and brittle modes of failure. The brittle mode can be judged from the shearing of carbide surface, thus forming scales along the shearing planes; whereas the presence of dimples represents the ductile fracture showing higher order deformations. Thus, on adding the SiC particles, the plastic deformations were reduced and shear mode of brittle fracture was observed.

5.4 CHARACTERIZATION OF MICROWAVE PROCESSED EWAC+Al_2O_3 COMPOSITE CASTINGS

Alumina as reinforcement in micron and nano levels plays an important role in increasing the strength, wear and corrosion resistance of MMC's [Lim et al. (2005); Zadeh et al. (2014);

Tazegu et al. (2014). Alumina is used in the development of various anti-wear coatings, claddings and composites. In the present work novel microwave heating is used to melt and develop casting of nickel based EWAC+Al_2O_3 composites. Alumina is added in 5% and 10% volume fraction in the EWAC powder and is mixed using powder mixing machine to obtain a composite powder. This powder is preheated and directly processed using MHH to obtain the castings. The detailed characterization results are reported in the following sections.

5.4.1 X-Ray Diffraction Study of EWAC+Al_2O_3 Composite Castings

The XRD patterns of microwave processed castings were obtained at room temperature using Cu K (alpha) radiations at a scan rate of 1° min^{-1}. Fig. 5.21 shows the typical XRD patterns of EWAC+5% Al_2O_3 and EWAC+10% Al_2O_3 composite castings.

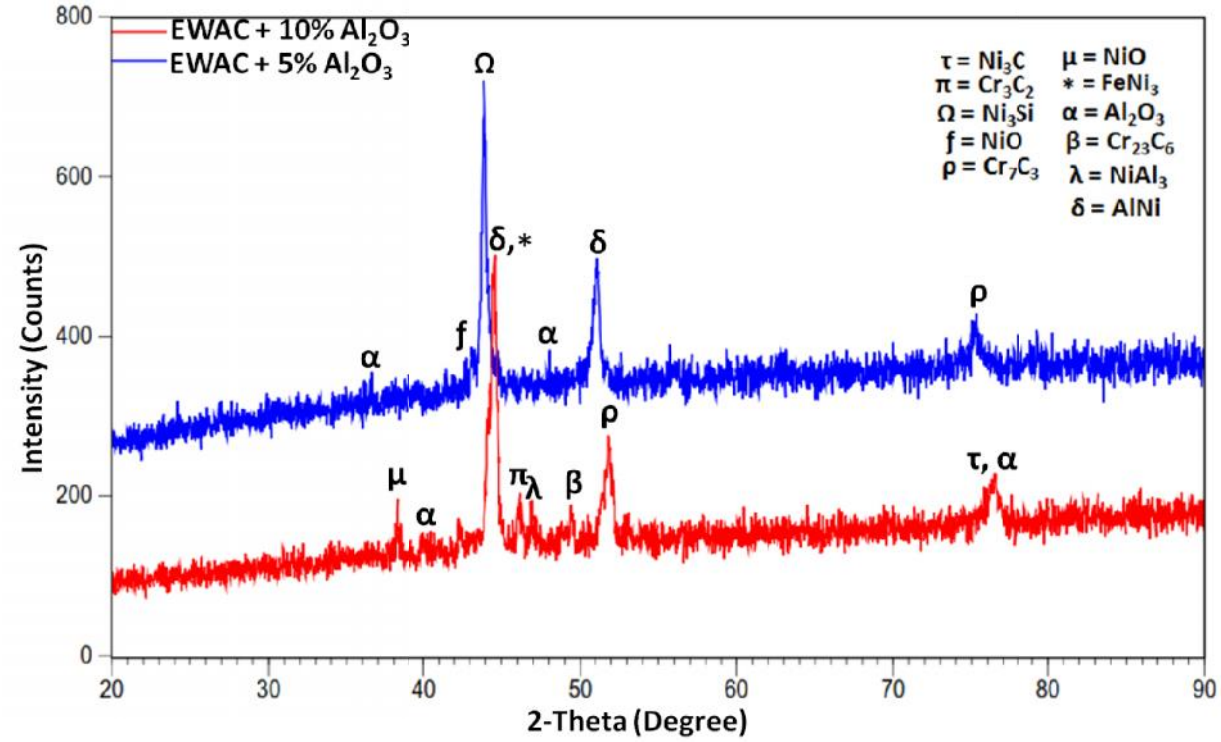

Fig. 5.21: Typical XRD spectrum of alumina reinforced composite castings

Though, alumina acts as transparent to microwaves, but generation of high temperatures may have decomposed some of the alumina particles [Shin and Min (2013)]. This resulted in the formation of some intermetallics of aluminium and nickel. Further, the presence of some aluminum powder particles in the alumina powder might have reacted with nickel to form nickel aluminides (AlNi and $NiAl_3$).

The diffraction pattern of 5% alumina reinforced composite show some peaks of alumina corresponding to diffraction angles of 35.89° and 48.65°. A small peak corresponding to angle 43.24° represents the NiO, which might have occurred due to oxidation during microwave heating. The formation of Ni_3Si is due to the presence of silicon in EWAC powder which might have reacted with nickel to form this intermetallic. The formation of chromium carbide (Cr_7C_3 at $2\theta = 76.80°$) has already been explained in equation 5.8. It was observed that on adding 5% Al_2O_3 reinforcement, the highest peak obtained was of Ni_3Si corresponding to the diffraction angle of 43.58°. However, in composite containing 10% Al_2O_3, the major peak obtained was of intermetallic AlNi corresponding to the diffraction angle of 44.83° and $FeNi_3$ at 44.27°. Another nickel aluminide (in the form $NiAl_3$) peak was observed corresponding to 2θ of 7.046. This may be due to the presence of the high alumina content and more chances of decomposition of alumina into aluminium, which aids the formation of AlNi and $NiAl_3$ intermetallics.

Further, the phases present in the microwave processed EWAC +10% Al_2O_3 composite casting was analyzed using normal intensity ratio (NIR). The results of NIR% for various phases present in the casting are shown in Table 5.4.

The NIR% of intermetallic alloy of nickel and aluminium (AlNi) phase was highest with 39.24% followed by Alumina with 25.64%. Other phases (NiO with 5.6%, Cr_3C_2 with 5.7%,

NiAl3 with 5.8%, $Cr_{23}C_6$ with 5.01% and Ni_3C with 8.58) NIR% were below 10%, which shows that significant phase is of AlNi alloy, which has properties of both ceramic and metal.

Table 5.4: Relative phase intensities and NIR (%) of microwave processed EWAC+10%Al_2O_3 MMC casting

S. No.	Phase	I_1	I_2	I_3	I_4	I_5	I_6	I_7	I_8	I_{back}	NIR (%)
1	NiO	200								150	5.6
2	Al_2O_3		380							150	25.64
3	AlNi			502						150	39.24
4	Cr_3C_2				201					150	5.7
5	$NiAl_3$					202				150	5.80
6	$Cr_{23}C_6$						195			150	5.01
7	Cr_7C_3							190		150	4.45
8	Ni_3C								227	150	8.58

5.4.2 Microstructural Characterization of EWAC+Al_2O_3 Composite Castings

The microwave processed EWAC + Al_2O_3 composite castings containing 5% volume fraction and 10% volume fraction of alumina reinforcement were subjected to microstructural characterizations using optical microscope and scanning electron microscope. Samples were cut along the cross section and were polished using emery papers and diamond paste prior to the characterizations as discussed in chapter 4.

The optical micrographs of non-etched EWAC+5%Al_2O_3 and EWAC+10%Al_2O_3 samples are shown in Fig. 5.22 (a-b). It was observed that alumina reinforcement was uniformly distributed in the EWAC matrix. The optical micrographs revealed crack and porosity free castings and no agglomeration of reinforcements were observed.

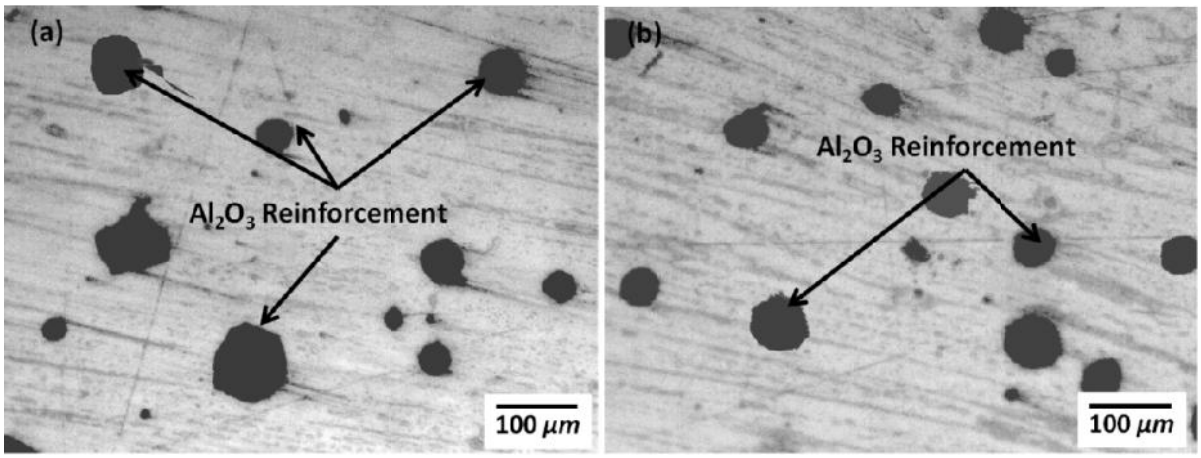

Fig. 5.22: Optical micrographs showing reinforcement dispersion in (a) EWAC+5%Al_2O_3 and (b) EWAC+10%Al_2O_3 composite castings

The detailed microstructure of the castings was studied by carrying out SEM analysis on an etched sample of castings and backscattered electron images are shown in Fig. 5.23 (a-b).

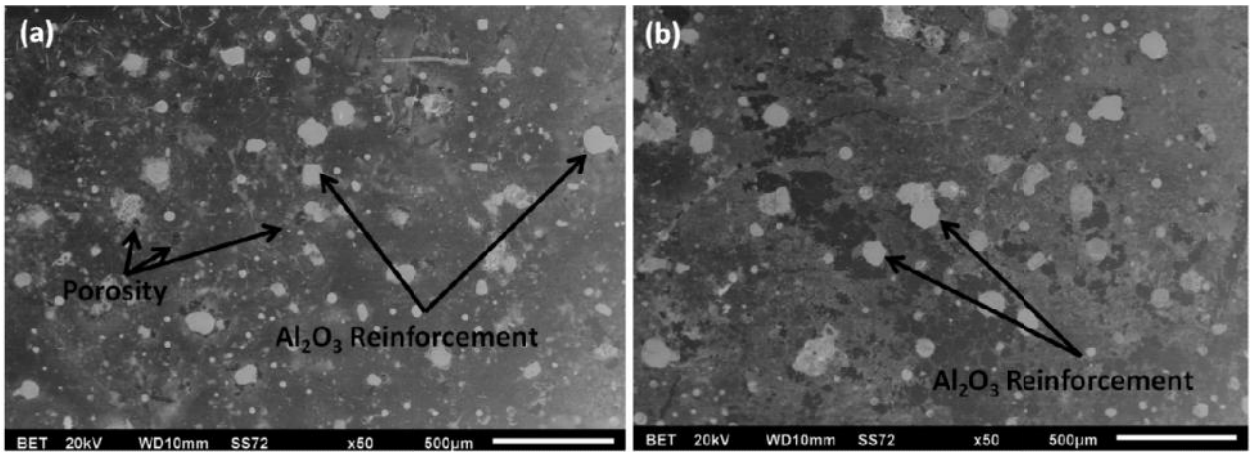

Fig. 5.23: Back scattered electron image showing the microstructure of (a) EWAC+10%Al_2O_3 and EWAC+5%Al_2O_3 composite castings

The back scattered images revealed the uniform dispersion of alumina reinforcement particles in the EWAC matrix, but due to the etchant attack microstructure is not clear. To study the microstructure in a better way, the color of the image was inverted so that proper detailing of

microstructure can be obtained. Fig 5.24 shows the inverted color image of EWAC+5%Al_2O_3 composite casting.

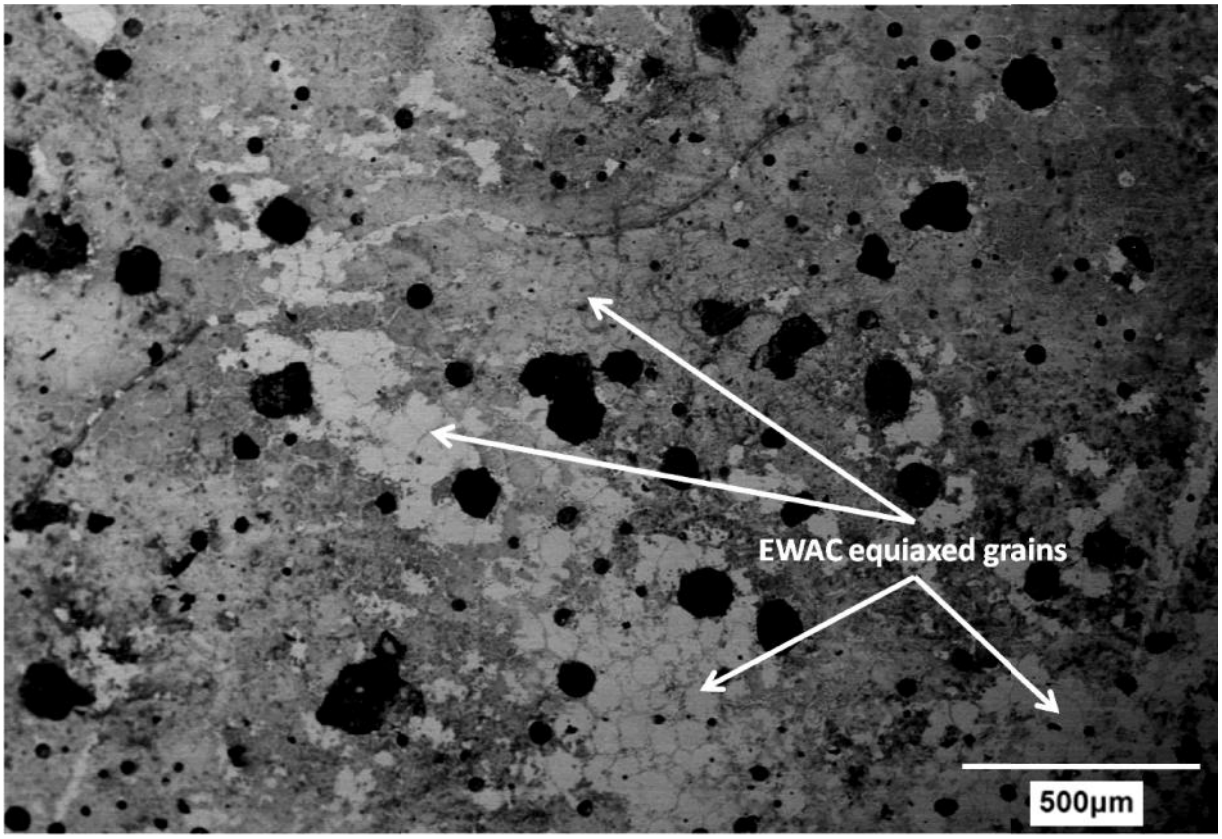

Fig. 5.24: Showing the equiaxed grain formation in EWAC+5%Al_2O_3 composite castings

The formation of equiaxed grains in the microwave processed casting and this is again due to the uniform and volumetric heating imparted through microwave hybrid heating as shown in Fig. 5.24. The reduction in differential heating due to microwaves reduces the chances of cellular structures to dendritic structure transformations. Further, due to corrosion caused by acidic etchant, these grains were not visible throughout the section of castings. The magnified view of microstructure of EWAC+10%Al_2O_3 composite castings is shown in Fig 5.25, which clearly reveals the formation of equiaxed grains.

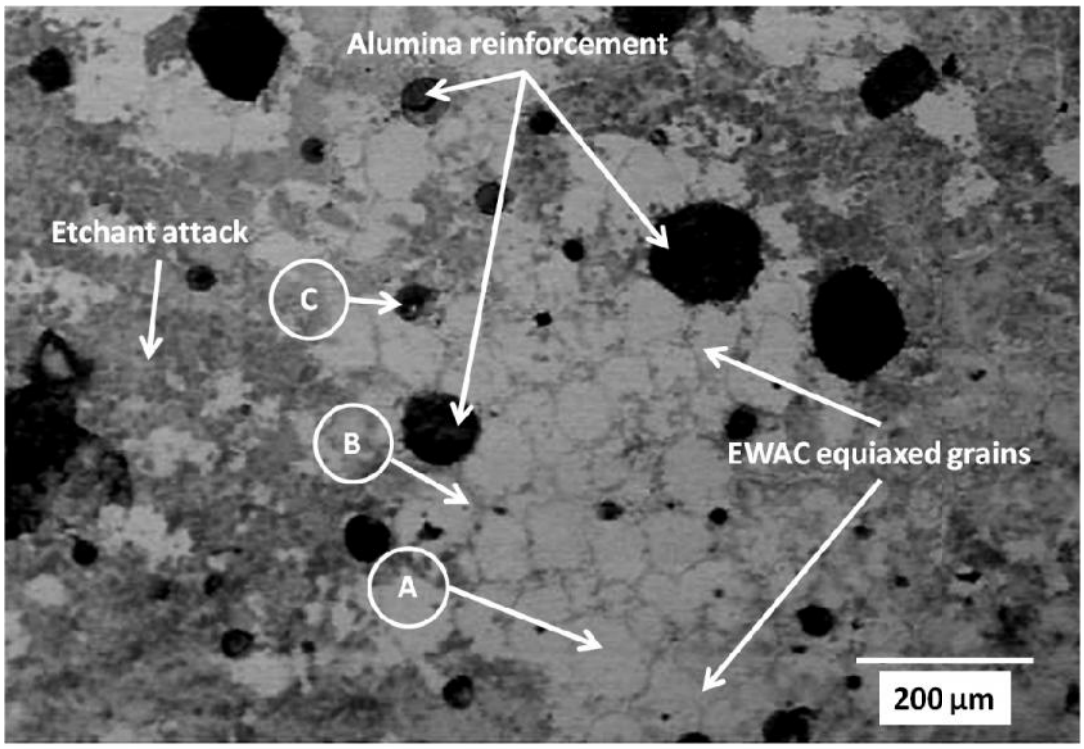

Fig: 5.25: Magnified image showing the microstructure of EWAC+10%Al_2O_3 composite casting

The porosity measurements were carried out at various locations using optical microscope and was found to be in the range of 3.2% - 5.4%. The presence of higher porosity may be due to the release of some oxygen when alumina degrades at higher temperatures and further entrapment of air may have increased the porosity levels.

5.4.3 EDS Analysis of EWAC+Al_2O_3 Composite Castings

To study the elemental composition of casting at various locations, i.e. of grain surface, grain boundary and on reinforcement, EDS analysis was carried out. The various positions where EDS was carried out are shown in Fig. 5.34 and are marked with A, B and C. Results of EDS analyses are shown in Fig. 5.26 (a-c).

The EDS results revealed the predominance presence of nickel, silicon, aluminium, oxygen and iron on the grain surface. The presence of aluminium on grain surface may be due to

the formation of nickel aluminide intermetallic alloy and presence of silicon and iron is due to formation of silicides during microwave heating.

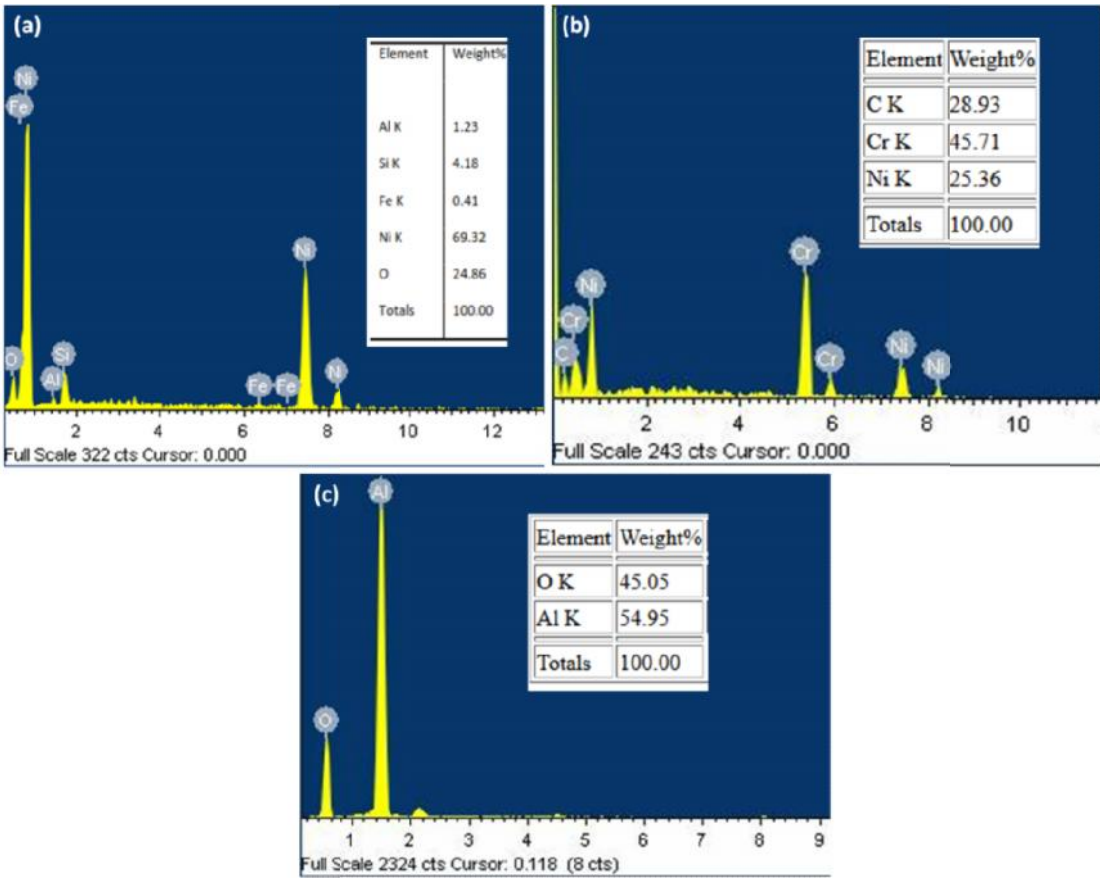

Fig. 5.26: Results of EDS analysis at (a) Grain surface, (b) Grain boundary and (c) Reinforcement particle

Presence of predominance of chromium, carbon and nickel along the grain boundary is due to the precipitation of formed carbides. XRD analysis (Ref. Fig. 5.21) also revealed the formation of these chromium carbides and nickel carbide.

5.4.4 Microhardness Study of EWAC+Al_2O_3 Composite Castings

The microwave processed composite castings were tested for Vicker's microhardness and results are shown in the Fig. 5.27.

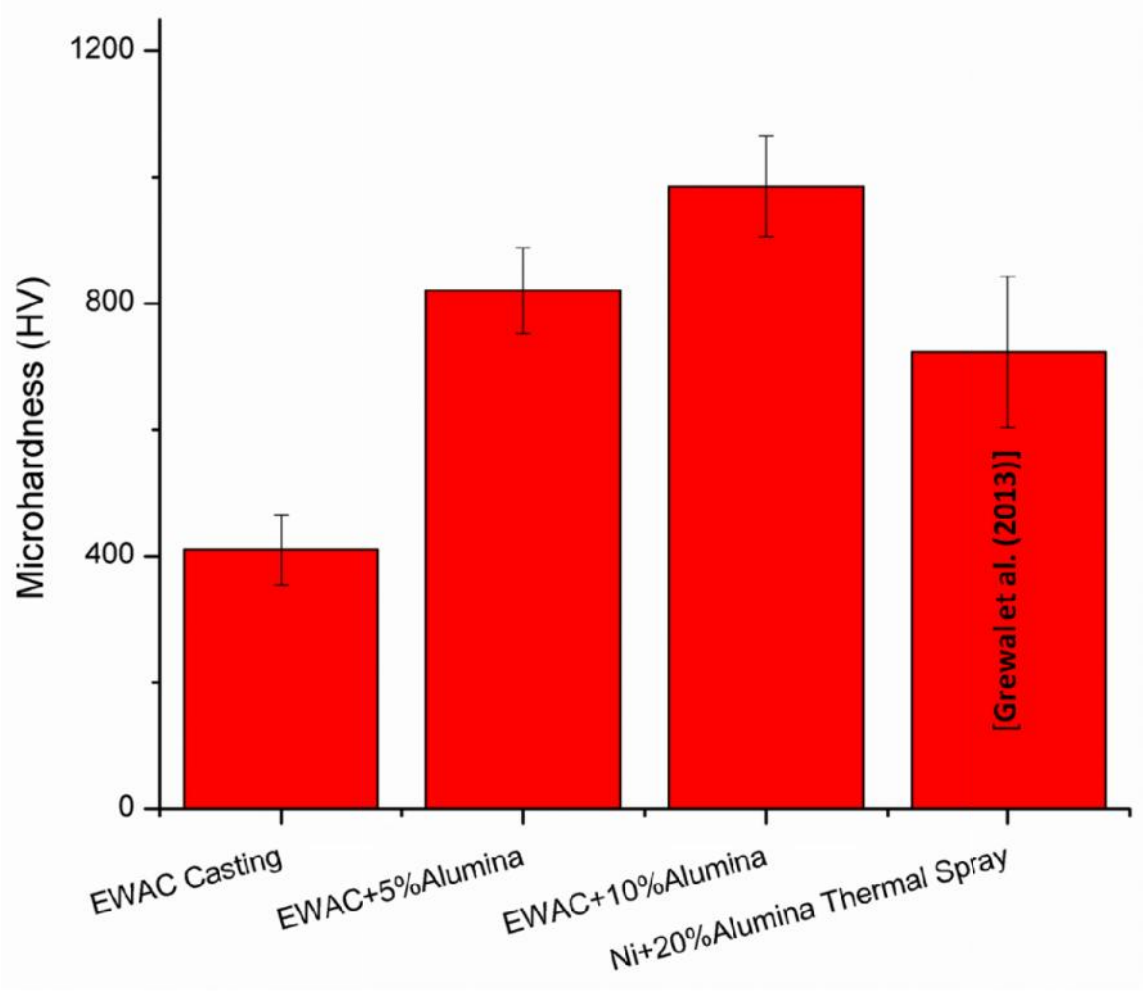

Fig. 5.27: Vicker's microhardness of Microwave processed castings and some published results

The results revealed that on adding alumina reinforcement, the microhardness increased significantly in comparison to EWAC casting. The average microhardness exhibited by EWAC+5%Al_2O_3 composite casting revealed average microhardness of 822 ± 68 HV, which is 2 times the average microhardness of EWAC casting. By increasing the alumina content from 5% v/f to 10% v/f, the microhardness for EWAC+10%Al_2O_3 composite casting increased to 985 ± 80 HV, which is 2.4 times higher than the microhardness of EWAC casting (410 HV). This increase in hardness is due to the formation of hard intermetallic phases such as nickel aluminide and uniformed presence of alumina reinforcements throughout the casting. In comparison to the Ni+20%Alumina thermal sprayed coating [Grewal et al. (2013)], the microhardness of

microwave processed castings are higher and this may be due to the lower defect formation and better structure property correlations observed in microwave processed parts [Bansal et al. (2015)].

5.4.5 Tensile Strength and Percent Elongation Study of EWAC+Al_2O_3 Composite Castings

The microwave melted and processed castings containing alumina reinforcements were subjected to the tensile testing to evaluate the effect of reinforcement on materials strength. The stress-strain% plot for the develop castings are shown in Fig. 5.28.

It was observed that on adding the 5% volume fraction of alumina, the tensile strength was even less than the EWAC casting. The average tensile strength of EWAC+5%Al_2O_3 composite casting was 308 ± 8 MPa with average percent elongation of 20 ± 2. This reduction in strength may be due to the lack of intermetallic alloy formation as degradation of alumina is difficult as it behaves transparent to the microwaves. Also the presence of porosity defects allowed the crack generation and propagation within the casting. Presence of carbides along the grain boundaries restricted the plastic deformation which reduces the overall percent elongation of 5% alumina casting. However, on increasing the alumina content to 10%, the formation of nickel aluminides was favored as shown in XRD study, which slightly increases the strength.

The average ultimate tensile strength of 10% alumina reinforced composite was 355 ± 10 MPa, with percent elongation of 18 ± 3. There was no considerable enhancement in the tensile strength of alumina reinforced composites, but elongation was significantly reduced in comparison to EWAC casting.

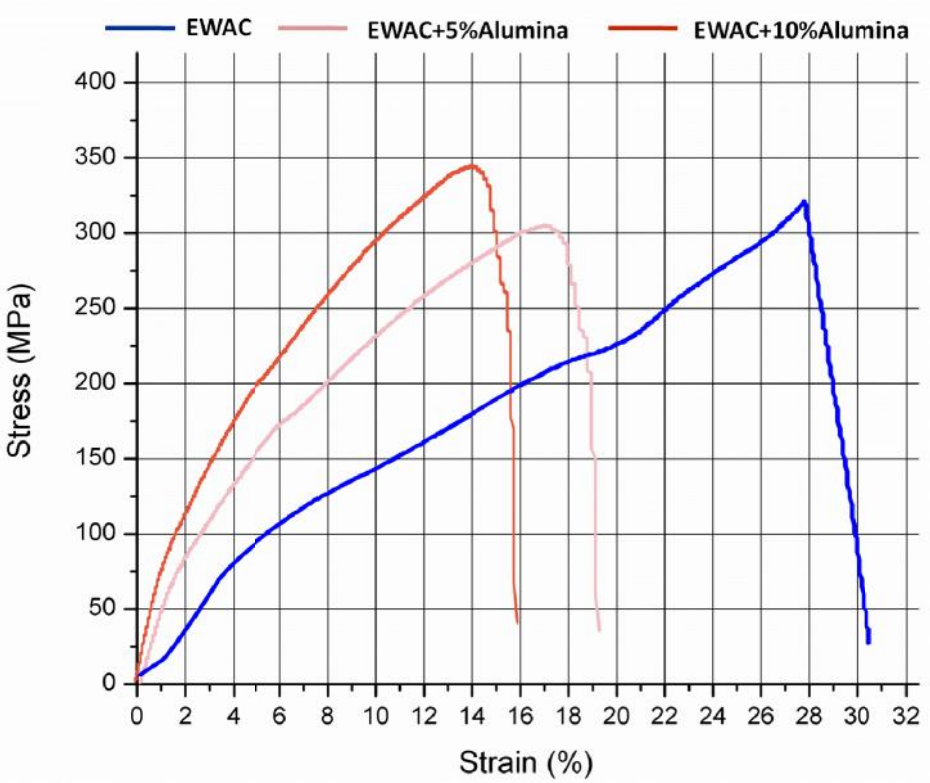

Fig. 5.28: Stress-strain plot for microwave processed EWAC and EWAC+Al_2O_3 castings

The magnified SEM image of EWAC + 10%Al_2O_3 composite casting fractured surface is shown in Fig. 5.29, which revealed the brittle fracture mode.

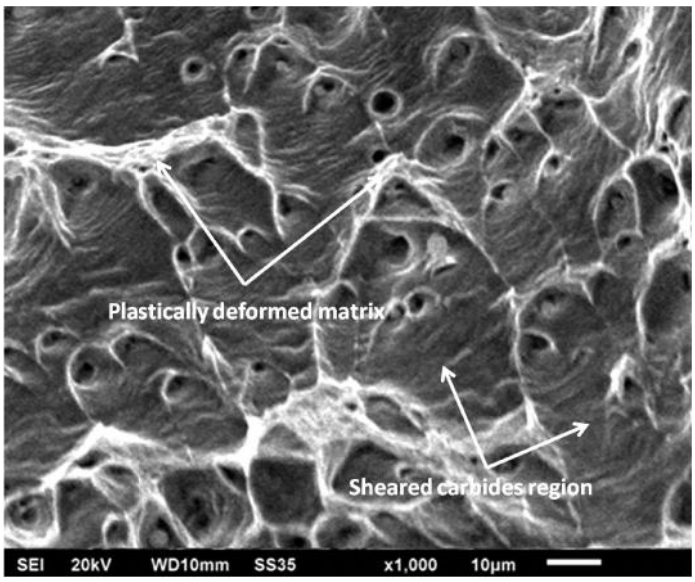

Fig. 5.29: SEM image of EWAC+10%Al_2O_3 composite casting fractured surface

The failure basically occurred by shearing of formed carbides along the grain boundaries and matrix phase shows some plastic deformation during fracture.

5.5 CHARACTERIZATION OF MICROWAVE PROCESSED EWAC+(WC-8Co) COMPOSITE CASTINGS

Tungsten carbide as a reinforcement is used in many engineering applications and is a vital material for manufacturing industries. It is used from the smallest cutting tool to the rocket engines. In the present work EWAC matrix is reinforced with 5% and 10% volume fraction of commercially available WC-8Co particles. Where, cobalt present in the WC particles acts as a binder. The powders of EWAC and (WC-8Co) were mixed in the mechanical mixer and were preheated prior to the microwave processing. The detailed characterization results of microwave processed composite castings are presented in the following sections.

5.5.1 X-Ray Diffraction Study of EWAC+(WC-8Co) Composite Castings

The XRD spectrums of EWAC+5%(WC-8Co) and EWAC+10%(WC-8Co) composite castings are shown in Fig. 5.30 (a-b). In 5%(WC-8Co) reinforced casting; major peak obtained was of an intermetallic FeNi corresponding to 2θ of 44.60°. Presence of WC peaks corresponding to 2θ of 31.57° and 35.72° can be seen in the XRD pattern. The formations of intermetallic phases in the casting are due to the results of transformations which might have occurred during intense microwave heating. At a certain temperature the WC may break down into free tungsten and W_2C as explained by equation 5.10-5.11 [Sharma and Gupta (2012)].

$$WC \rightarrow W + C \tag{5.10}$$

$$2WC \leftrightarrow W_2C + C \tag{5.11}$$

The available free carbon and tungsten might further react with the Cobalt and nickel to form complex phases such as Co_3W_3C and Fe_6W_6C.

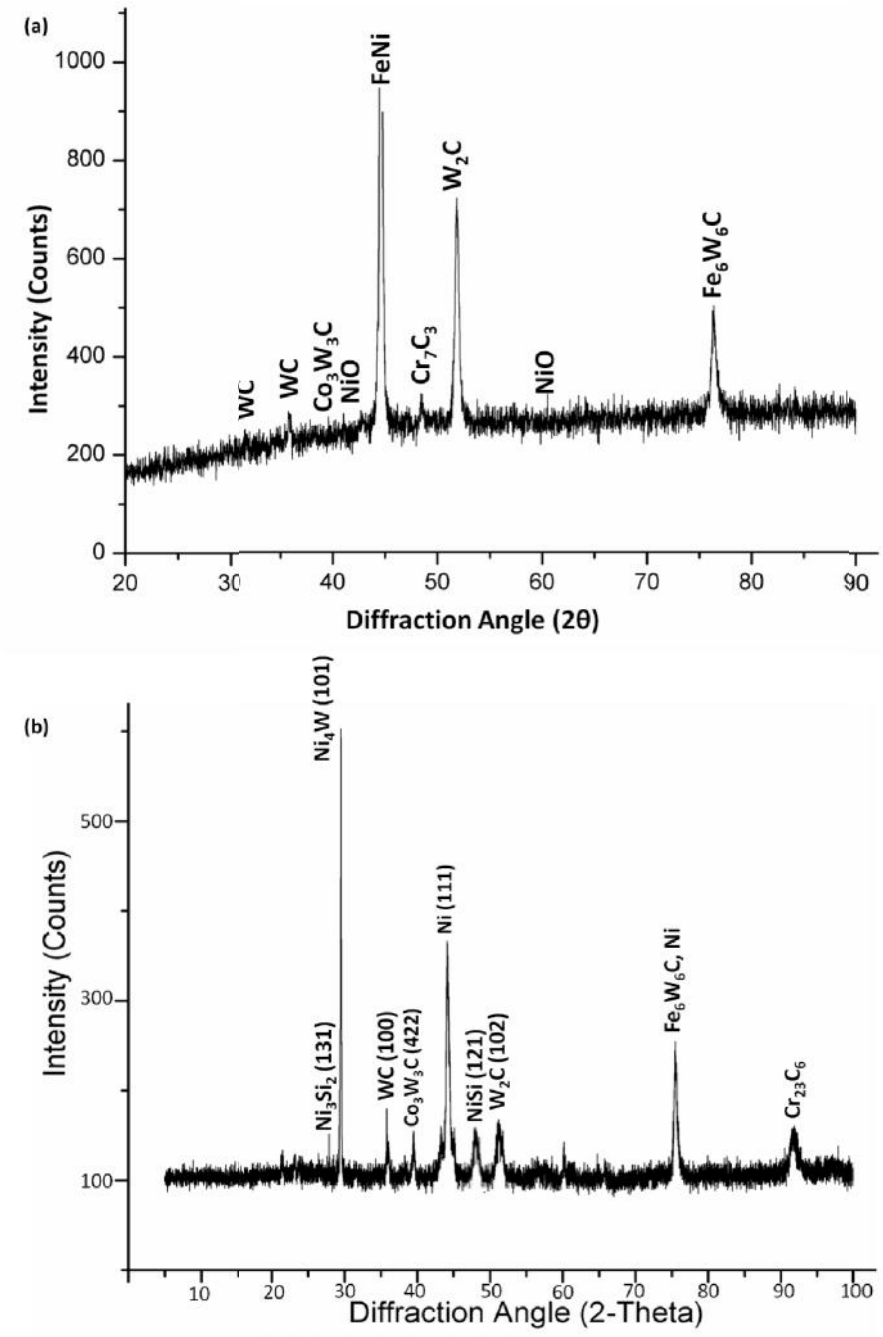

Fig. 5.30: Typical XRD patterns of (a) EWAC+5%(WC-8Co) and (b) EWAC+10%(WC-8Co) composite castings

Some of the nickel reacted with the oxygen present in the atmosphere to form nickel oxide (NiO) corresponding to 2θ of 43.47° and 61.28°.

The XRD spectrum of EWAC+10%(WC-8Co) shows the formation of some intermetallics of tungsten and nickel. The phases of Ni_3Si_2 (28.87°), Ni_4W (29.56°), WC (35.64°), Co_3W_3C (39.78°), NiSi (47.22), W_2C (52.3°), Fe_6W_6C (75.29°) and $Cr_{23}C_6$ (91.99°) are present. Some peaks of nickel can be seen at diffraction angle of 44.51° and 75.29°. The available free carbon and tungsten (Ref. equation 5.10-5.11) might further react with the cobalt and nickel to form complex phases and are represented by equations 5.12-5.14 [Sharma and Gupta (2012)].

$$3W + 3Co + C \rightarrow Co_3W_3C \quad (5.12)$$

$$W + 4Ni \rightarrow Ni_4W \quad (5.13)$$

$$23Cr + 6C \rightarrow Cr_{23}C_6 \quad (5.14)$$

Further, some of the nickel reacted to the silicon present in the EWAC powder to form nickel silicides (Ni_3Si_2). The particles of WC remain suspended in the nickel matrix whereas other carbides and silicides precipitate out at the grain boundaries. The presence of these carbides and silicides in the casting may attribute to the higher hardness. The formations of such intermetallics during microwave heating of materials have been reported in earlier work [Pathania et al. (2015)].

Further, the phase presents in the casting were analyzed using peak intensities of the respective phases. The phases present in the XRD spectrum of microwave processed castings is analyzed and their values are shown in Table 5.5. The result of NIR shows that an intermetallic compound of Ni_4W accounts for ~ 41.68%.

Table 5.5: Relative phase intensities and NIR(%) in microwave processed EWAC+10%(WC-8Co) composite casting

S.No.	Phase	I_1	I_2	I_3	I_4	I_5	I_6	I_7	I_8	I_9	I_{back}	NIR (%)
1	Ni_3Si_2	149									110	3.29
2	Ni_4W		604								110	41.68
3	WC			177							110	5.65
4	Co_3W_3C				152						110	3.54
5	Ni					363					110	21.35
6	NiSi						156				110	3.88
7	W_2C							165			110	4.64
8	Fe_6W_6C								250		110	11.81
9	$Cr_{23}C_6$									159	110	4.13

5.5.2 Microstructural Characterization of EWAC+(WC-8Co) Composite Castings

The optical micrographs showing the distribution of (WC-8Co) reinforcement in the EWAC matrix is shown in Fig. 5.31 (a-b). Optical micrographs revealed that the reinforcement was uniformly dispersed in the form of agglomerated patterns. The typical backscattered electron micrographs of EWAC+5%(WC-8Co) and EWAC+10%(WC-10Co) casting are shown in Fig. 5.32 (a-b) which shows the formation of nearly equiaxed grains throughout the casting microstructure.

The reinforcement of sub micron WC particles is dispersed in random order throughout the casting. The WC particles are partially agglomerated at the different locations, forming dispersed pattern like structures. The magnified image showing the matrix microstructure is presented in Fig. 5.32 (b), which reveals the equiaxed grains of nickel matrix.

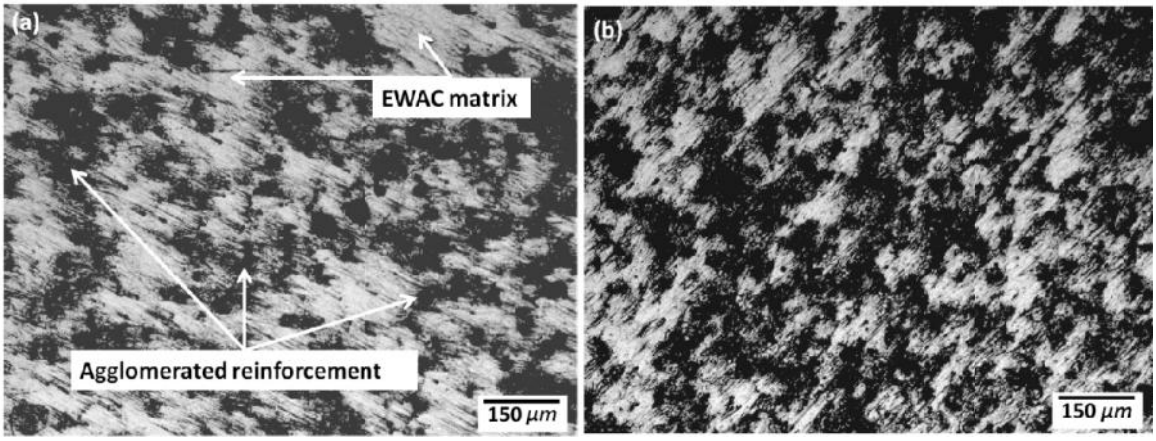

Fig. 5.31: Optical micrographs of (a) EWAC+5%(WC-8Co) and (b) EWAC+10%(WC-8Co) composite casting

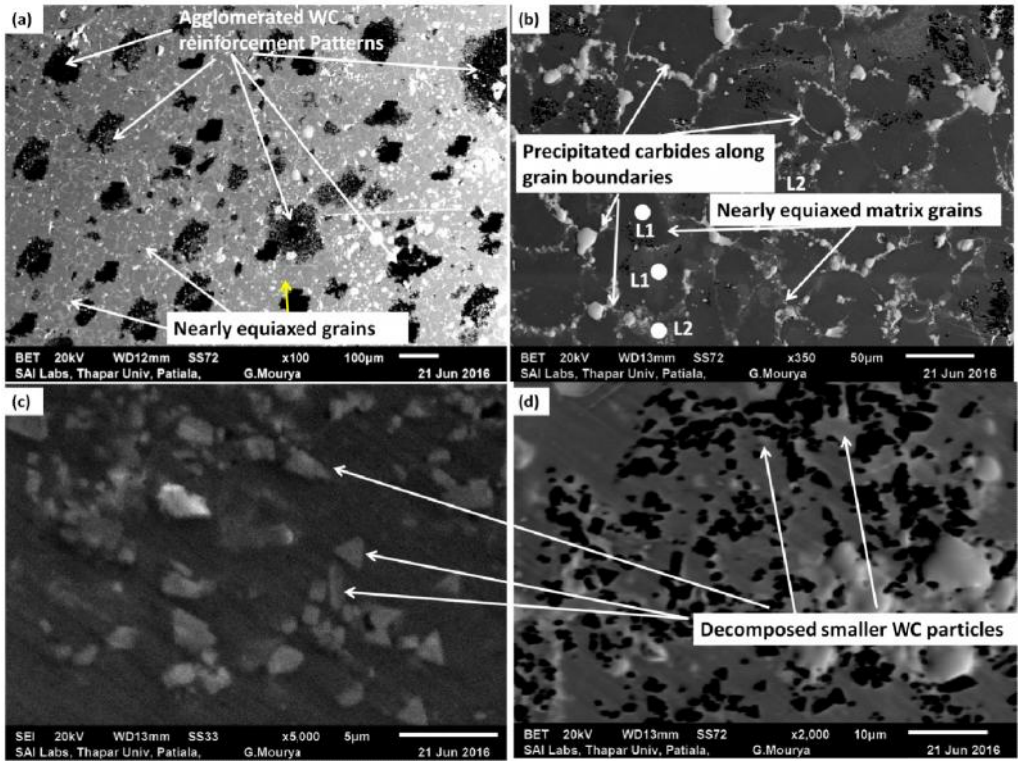

Fig. 5.32: (a) Typical backscattered electron image showing matrix grains and reinforcement pattern, (b) Magnified BET image showing nearly equiaxed grains of matrix, (c) SEM image showing the partially agglomerated decomposed WC particles and (d) BET image showing the dispersed WC particles

These grains formations may be attributed due to the volumetric heating provided by microwaves, which restricts the transitions of structures in dendrites. It was observed that due to

intense and rapid heating by microwaves, the particles of reinforcements were decomposed and sub micron sizes were further reduced to nano-metric particle sizes as shown by SEM and BET images in Fig. 5.33 (c-d).

These distributed nano sized carbides in the matrix would provide localized strength and will affect the overall strength of composite casting. The volumetric heating coupled with lower thermal gradients within the cast melt and slow solidification rate of the melt pool resulted in the lower defects within the composite; and resulted in the nearly equiaxed grains. The uniform thermal gradients did not allow the cell to dendritic transition and such formation of dendrites were not seen in the microstructures. However, some artificial pores were present in the microstructures which may be formed due to the etchant attack on the surface of composite.

5.5.3 EDS Analysis of EWAC+(WC-8Co) Composite Castings

In order to determine and verify the elements of different phases present in the microstructures of the casting, energy dispersive X-ray spectroscopy (EDS) was carried out at various locations. The EDS on the matrix grains and grain boundary were carried out to study the elemental composition at locations L1 and L2 (Ref Fig. 5.32 (b)) and results are reported in Table 5.6. The EDS plots obtained at various locations of casting are shown in the Fig. 5.33.

The presence of higher amount of carbon along the grain boundaries shows the precipitation of intermetallics carbides such as chromium carbides during solidification of composite. Also, some of the WC particles are present along the grain boundaries of EWAC matrix, which increased the percentage of W and C.

Table 5.6: Elemental analysis of developed microwave casting

Average element composition (%)	On grain surface	On grain boundaries
Ni	Bal.	Bal.
C	12.76	26.84
Cr	0.16	5.4
W	10.8	14.86
Si	1.2	2.5
Fe	1.93	2.35
Co	0.82	7.6
Others	0.5	0.2

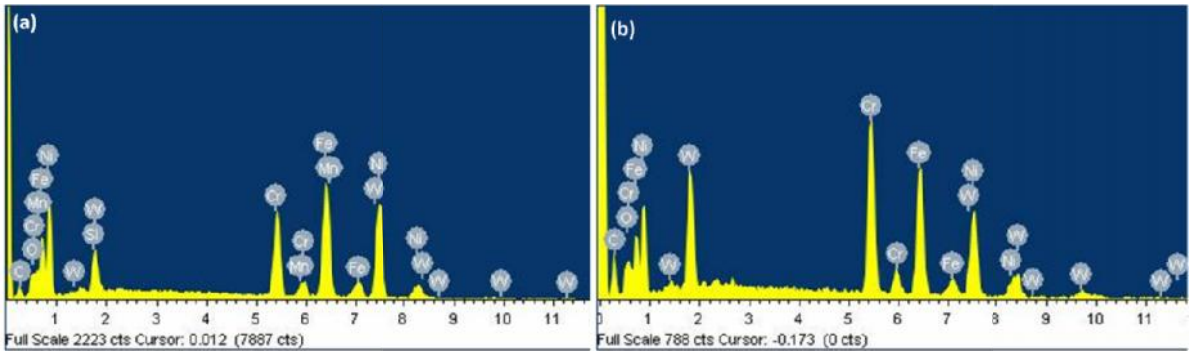

Fig. 5.33: Results of EDS analysis on (a) grain surface and (b) grain boundary of EWAC+10%(WC-8Co) composite casting

The EDS line mapping across the WC particle embedded in the nickel matrix is shown in Fig. 5.34. The line mapping across the particle confirms the WC particle as the presence of carbon and tungsten in is an abundance and presence of nickel in the matrix phase.

5.5.4 Microhardness Study of EWAC+(WC-8Co) Composite Castings

The Vicker's microhardness tests were carried out along the cross section of the developed composites as per the method described in chapter 4.

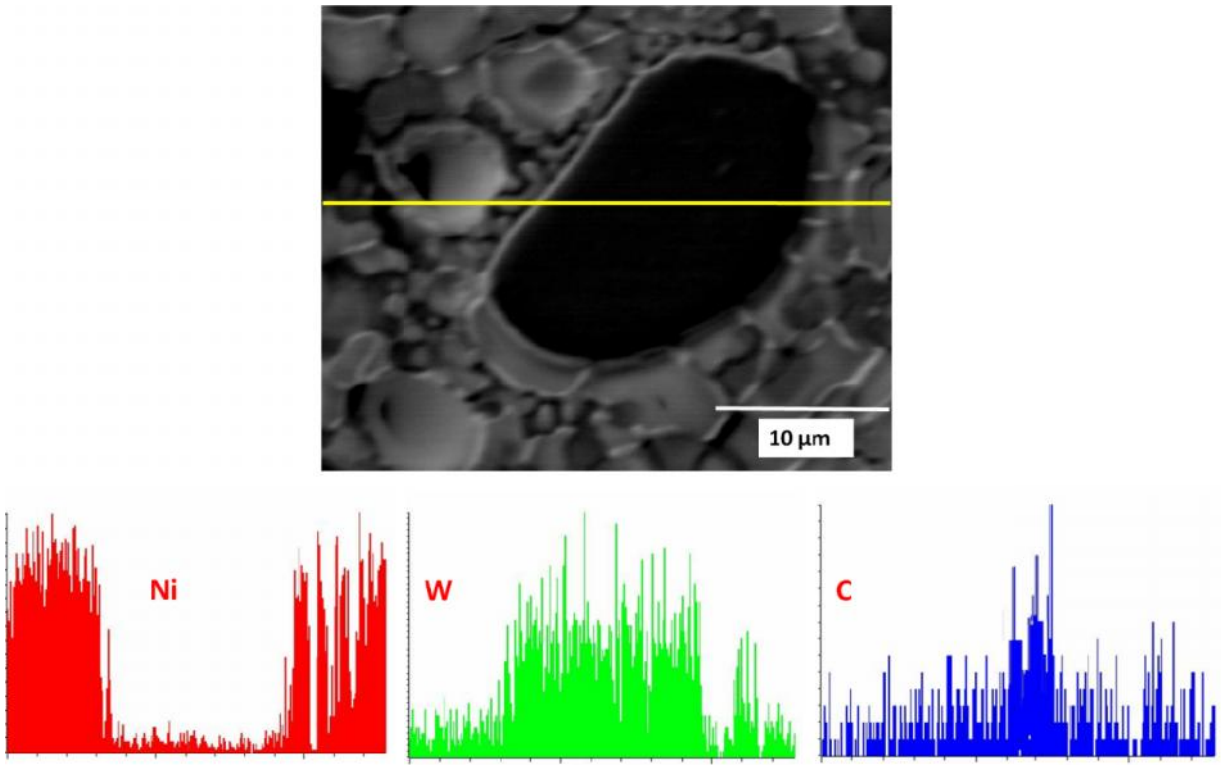

Fig: 5.34: EDS line mapping of WC particle embedded in the EWAC matrix

The results of Vicker's microhardness are shown in Fig. 5.35 and results revealed that with the addition of WC-8Co reinforcement in the EWAC matrix, the microhardness increases significantly. The addition of 5% of reinforcement in the EWAC matrix, the microhardness increased to 825±58 HV, which was ~2.01 times the EWAC casting microhardness 410±55 HV.

With increasing the WC-8Co content to 10%, the average microhardness recorded was 1012±108 HV, which was 2.46 times higher than EWAC. Besides, the pure clad of EWAC exhibit only 304±48HV of hardness and Ni+WC clad produced microhardness of 1028±90HV. Degradation of micro sized WC particles into nano sized particles and uniform dispersion in the EWAC matrix allowed higher micro-hardness values of castings.

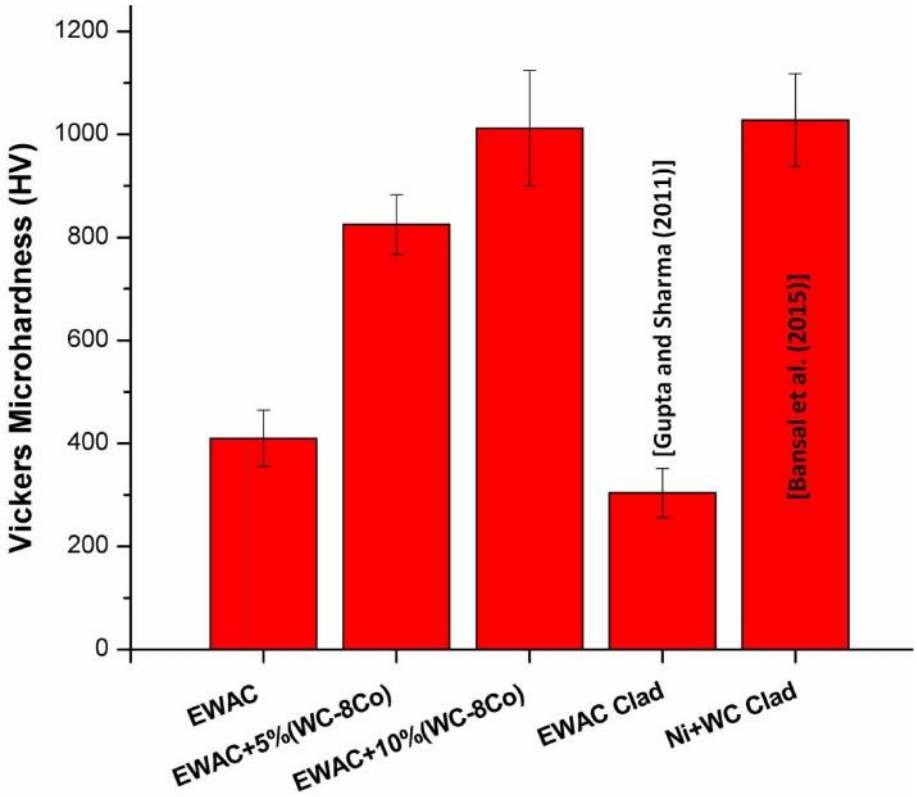

Fig. 5.35: Vicker's microhardness of developed castings and comparison with available data

The indentation morphologies on EWAC matrix and degraded nano sized dispersed WC particles is shown in Fig. 5.36 (a-b).

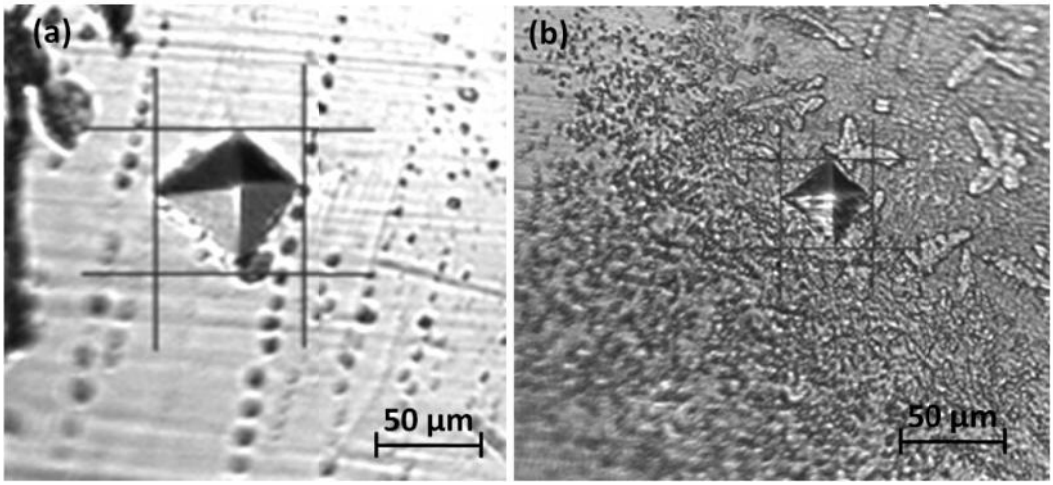

Fig. 5.36: Optical micrographs showing the indents on (a) EWAC matrix and (b) decomposed WC nano dispersed particles

Indentation morphology shows that when indent falls on matrix phase, then due to ductile phase plastic deformation takes place and indent flows plastically. However, the presence of hard phases of WC particles restricted the deformation and plastic flow is constrained which resulted in small indentation.

5.5.5 Tensile Strength and Percent Elongation Study of EWAC+(WC-8Co) Composite Castings

The effect of WC-8Co reinforcement on the strength of EWAC matrix was studied by performing tensile tests as per ASTM standards explained in chapter 4. The stress-strain plots for the EWAC+5%(WC-8Co) and EWAC+10%(WC-8Co) composite castings in comparison to the EWAC casting are shown in Fig. 5.37.

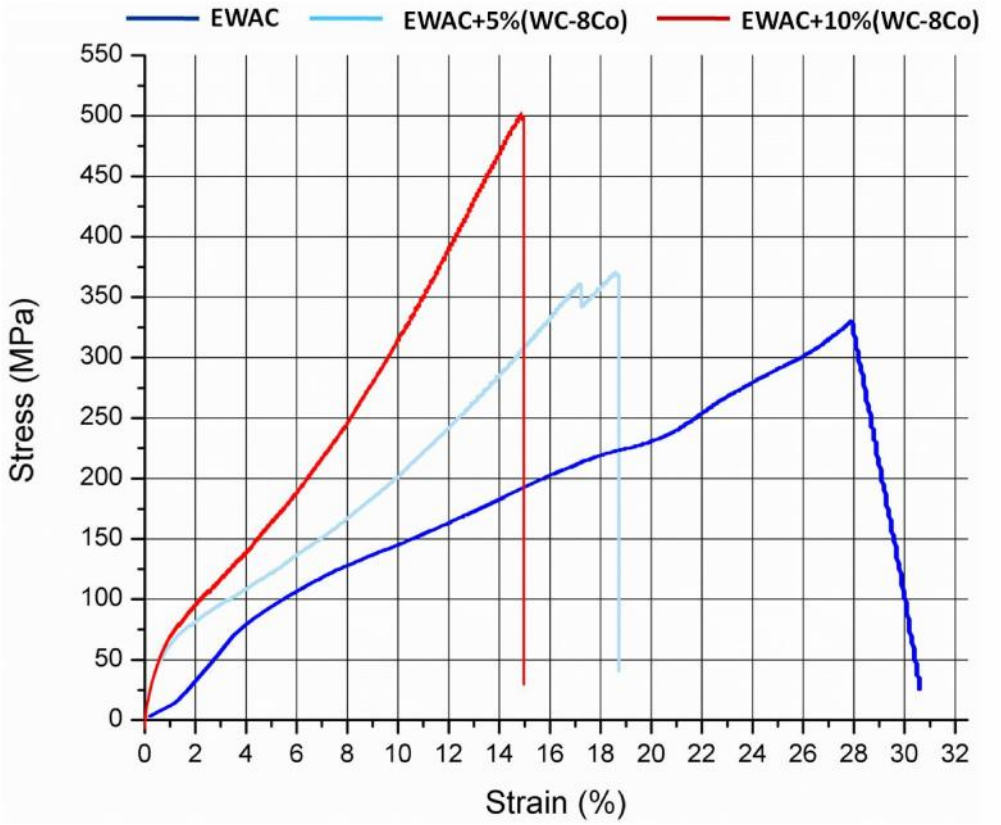

Fig. 5.37: Typical stress-strain plots for microwave processed EWAC and EWAC+(WC-8Co) castings

Results revealed that by adding the (WC-8Co) reinforcements, the strength of castings increased and this may be due to the strengthening effect of reinforcement. Moreover, the degradation of WC particles in nano sized particles and uniform spread helped in achieving the structure-property correlations in the composite. The addition of 5% reinforcement increased the ultimate tensile strength to 385±8 MPa with percent elongation of 20±3. With increase in the volume fraction of reinforcement, the ultimate tensile strength of EWAC+10%(WC-8Co) composite increases to 508±6 MPa with percent elongation of 18±4. In comparison to the EWAC casting, 10% WC-8Co reinforced composite revealed 1.54 times higher strength. The presence of the cobalt binder allowed higher deformations in comparison to the other composite castings.

The fractured surface of EWAC+10%(WC-8Co) composite casting is shown in Fig. 5.38, which revealed the shearing of carbide plane.

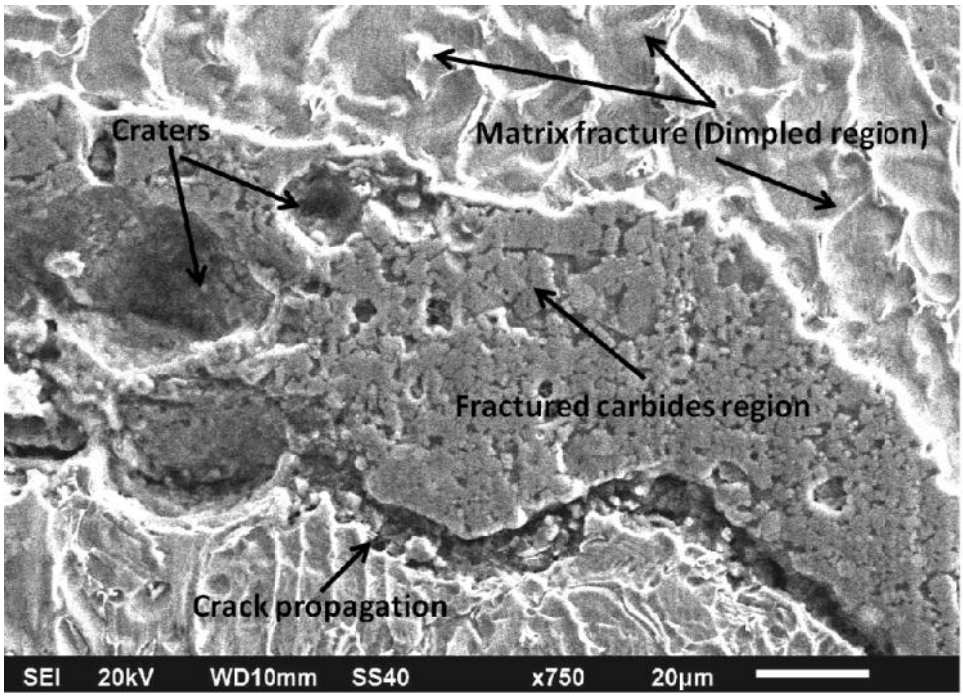

Fig. 5.38: SEM image showing the fractured surface of EWAC+10%(WC-8Co) composite casting

Presence of WC agglomerated particle patterns across the casting led to the predominant brittle mode of failure along the fractured surface. The presence of cracks revealed that during the loading of the specimen, the hard phases of carbides restricted the deformations, which eventually led to the initiation of cracks. These cracks further propagated and led to the failure with the shearing of carbide regions. Along the matrix phase some plastic deformation was observed, which reveals the ductile fracture with the formation of dimples.

5.6 COMPARISON OF MECHANICAL PROPERTIES OF DEVELOPED CASTINGS

This section compares the various mechanical properties of the microwave processed castings. This will provide a clear view of the effect of various reinforcements on the properties of developed castings. Fig. 5.39 shows the effect of various reinforcements on microhardness of various developed castings.

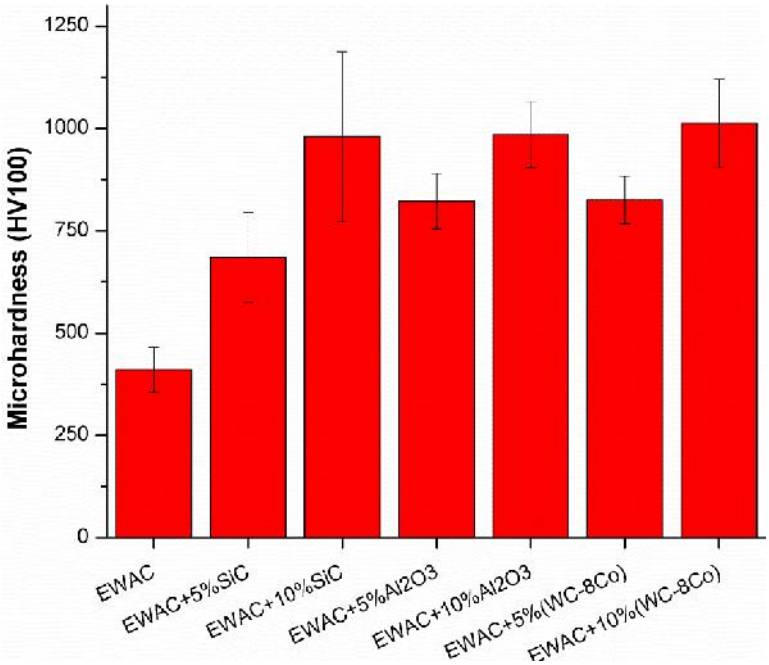

Fig. 5.39: Comparison of microhardness values of various microwave processed castings

The comparison results revealed that the presence of 10%(WC-8Co) reinforcement produced maximum microhardness and is comparable with the 10%SiC reinforced EWAC composite casting. It is clearly visible that the addition of various reinforcements altered and increased the microhardness of processed MMC castings.

Fig. 5.40 and Fig. 5.41 presents the effect of reinforcements on the tensile strength and percent elongation of microwave processed castings.

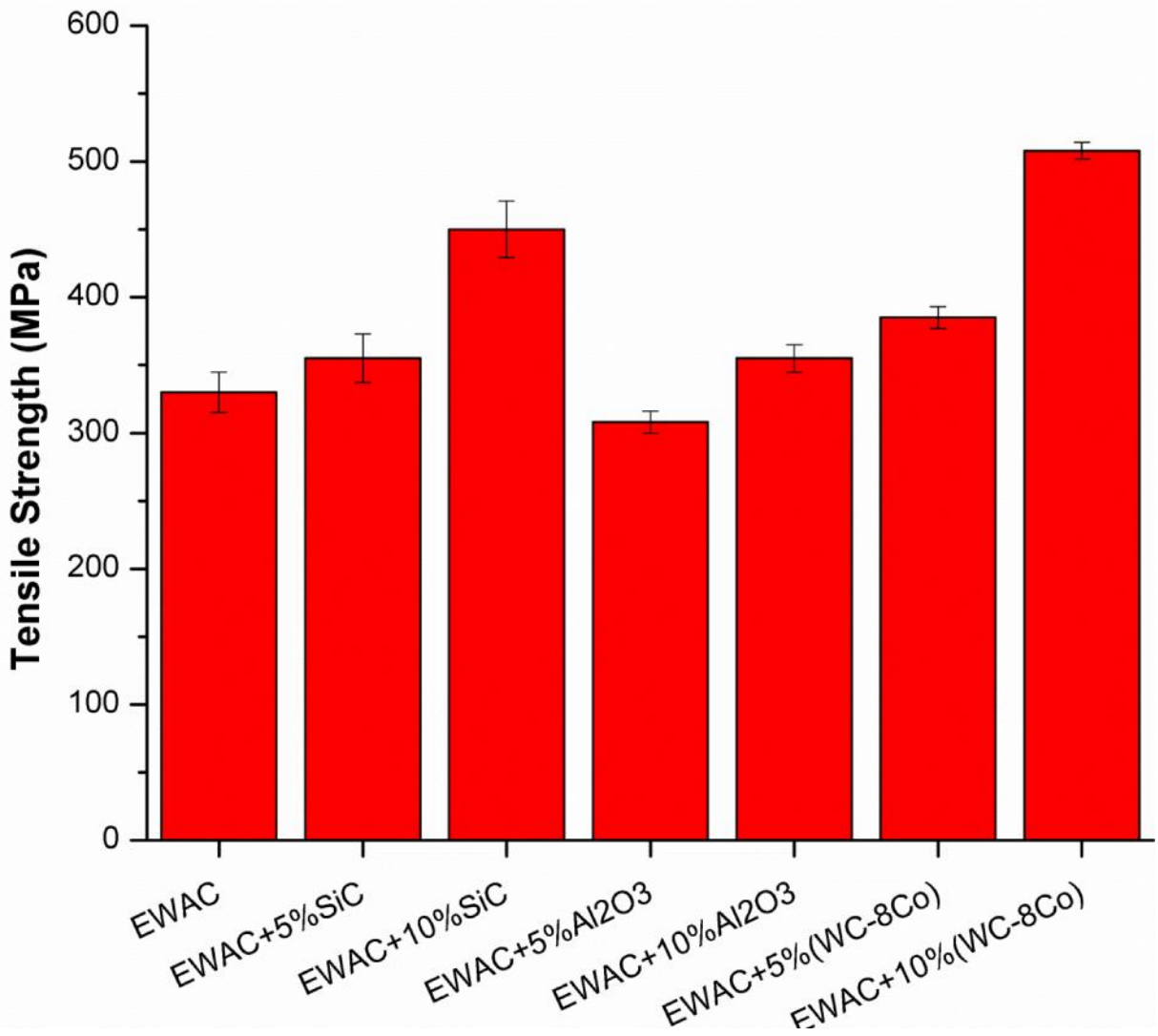

Fig. 5.40: Comparison of tensile strength of various microwave processed castings

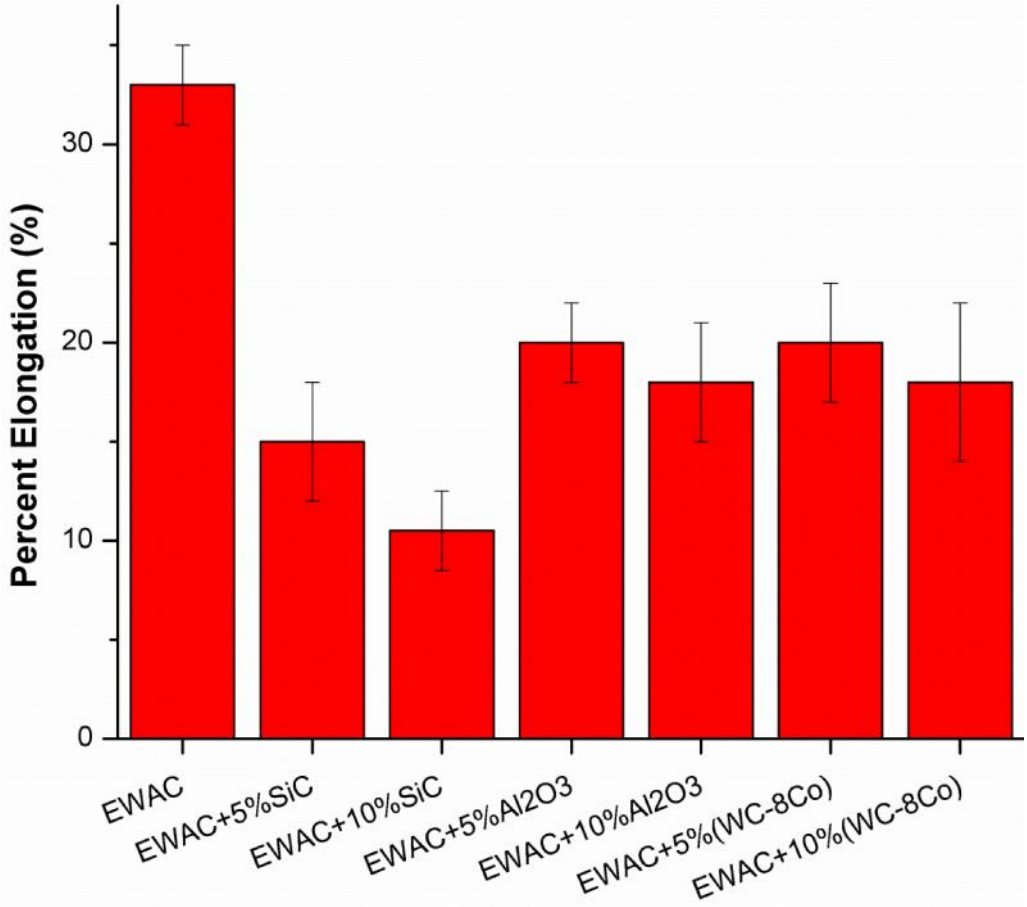

Fig. 5.41: Comparison of percent elongation of various microwave processed castings

The comparison of tensile strength results revealed that on adding the ceramic reinforcements, the strength improves significantly. The maximum strength was obtained for 10%(WC-8Co) reinforced MMC casting, followed by 10% SiC reinforced casting. The reasons for increase in the strength have already been explained in the above sections corresponding to the mechanical characterization results. The addition of reinforcements reduced the ductility and due to this pure EWAC casting revealed highest percent elongation. Presence of cobalt binder phases in the WC-8Co powder helped in achieving some ductility but other reinforcements significantly lowered the percent elongation. Further, addition of reinforcements caused the

transition from ductile-mixed mode fracture of EWAC to brittle and shear mode fracture for the various MMC's.

5.7 SUMMARY

The detailed microstructural and mechanical characterization results are presented with illustrations. The effect of various reinforcements on the microstructure, XRD phases, microhardness, tensile strength and percent elongation of various microwave processed casting has been reported with proper discussion. Results are compared with the pure EWAC casting to evaluate the performance of different reinforced composites. The fractured surfaces analysis and study is presented; and details of failure modes for various castings are presented in this chapter.

CHAPTER 6

FUNCTIONAL CHARACTERIZATION: RESULTS AND DISCUSSION

This chapter presents the results of functional characterizations of so developed microwave cast specimens. The tribological performance of cast speciemes has been evaluated by dry sliding wear tests. The dry sliding wear tests were carried out on a pin on disc apparatus, at varying parameters which are presented in chapter 4. All the results obtained for various castings were analyzed and systematically presented in this chapter. The various modes of wear taking place and the effect of reinforcements on wear mechanisms are discussed in details. The effect of parameters on wear mechanisms has been discussed in the vicinity of the results obtained from the characterization. The interactions between the mating surfaces were analyzed by using SEM and EDS. Fractographic analysis of worn out samples was carried out to study the possible mechanisms which occurred while sliding. The following sections describe the weight loss results of all the castings processed through microwave energy.

6.1 DRY SLIDING WEAR STUDY OF EWAC CASTING

The samples of microwave processed EWAC castings were subjected to the dry sliding wear tests to evaluate their performance as anti-wear material. The testing parameters used in the experiments are presented in the Table 4.16. The average cumulative weigh loss graphs of EWAC casting at various parameters are shown in Fig. 6.1 (a-c). The results revealed that on varying the parameters such as normal load, sliding speed and sliding distances, there was a significant change in the weight loss. The effects of various parameters on weight loss mechanisms are as discussed below.

6.1.1 Effect of Normal Load on Weight Loss of EWAC Casting

It is clear from the Fig. 6.1 (a-c) that by increasing the normal load from 10 N to 20 N, there is a linear increase in the weight loss. At 10 N of normal load and 0.5 m/s of sliding velocity the recorded value of cumulative weight loss is 14.84 mg at the end of 2000 m of sliding distance, which increases to 22.45 mg at 15 N of normal load and reaches maximum of 28.68 mg at 20 N of load.

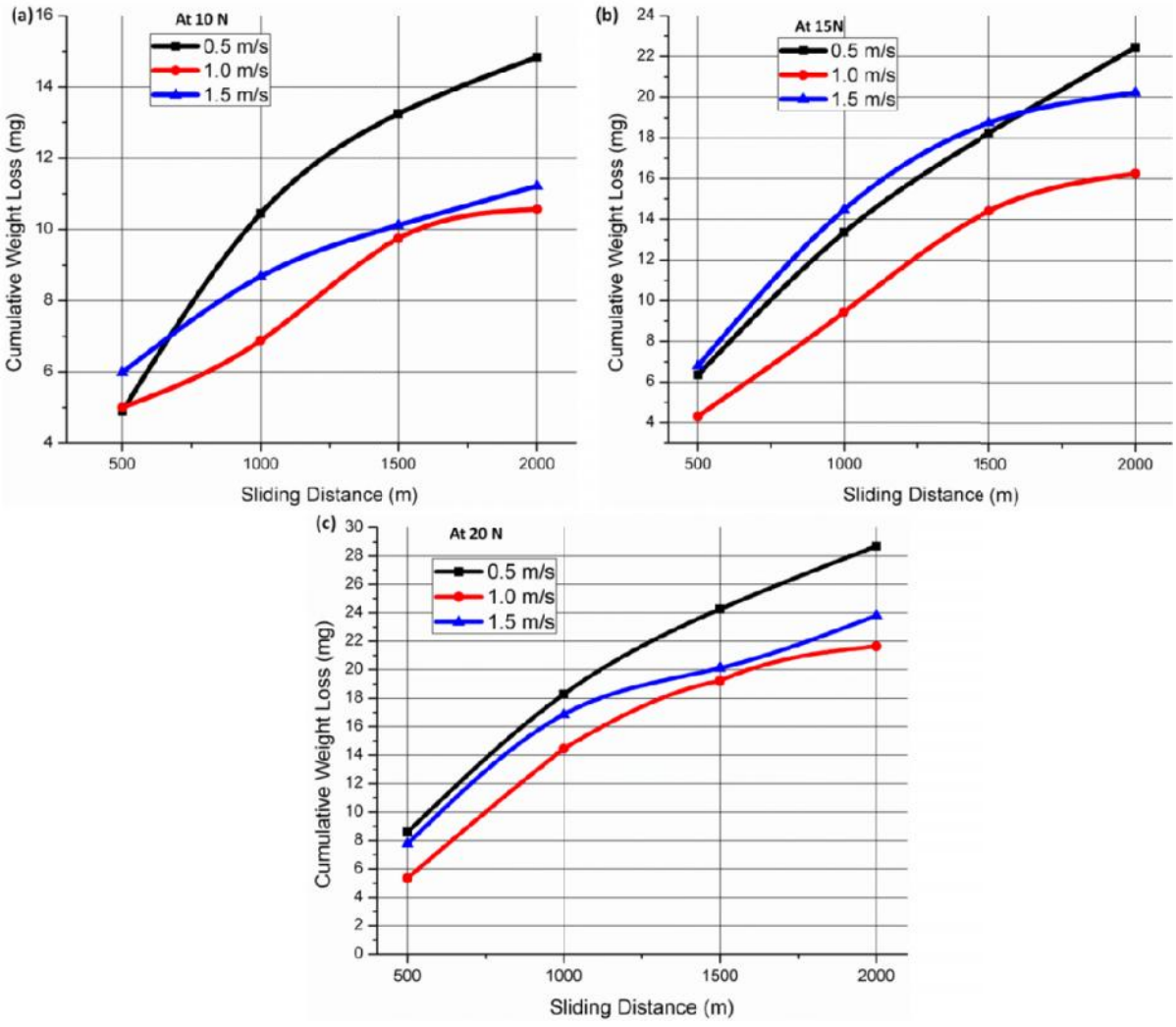

Fig 6.1: Cumulative weight loss graphs of microwave processed EWAC castings at varying sliding velocities, sliding distances and under varying normal loads

This increase in weight loss was may be due to the fact that by increasing the normal load, the contact surface increases and causes more ploughing of surfaces during sliding. Increase in load also favors the formation of localized welds due to increased friction between the mating surfaces. It can be seen from the weight loss graph that at lower load the difference between the weight loss at 0.5 m/s and 1.5 m/s sliding velocity is high but this gap reduces with increasing the load. This may be due to the fact that on increasing the load, the formations of tribo oxide layers were favored to minimize the direct contact of two bodies.

Initially, at 10 N of normal load and at the end of 500 m of sliding the weight loss at 0.5 m/s and 1.0 m/s of sliding velocity is almost identical which is ~4.9 mg, however at 1.5 m/s of sliding velocity the weight loss recorded was 6 mg. The weight loss during the first 500 m of sliding under varying normal loads show some variation, but weight loss was recorded a minimum for 1.0 m/s sliding velocities. This may be due to the fact that at moderate velocity, there might exist a balance between heat generation and dissipation, which lowers the localized welding and hence a lower weight loss in terms of adhesion and ploughing wear. Also at this sliding velocity of 1.0 m/s, the formation of hard oxide tribo layers were favored due to the surface interactions taking place at the high temperatures at mating surfaces.

The SEM images of worn out surfaces of the EWAC casting at 10 N and 20 N of normal load with sliding velocity of 1.0 m/s at the end of 2000 m of sliding is shown in Fig. 6.2 (a-b). At 20 N of load, the wear tracks appear to be more intense and wear is mainly due to the surface adhesion, pull out and micro ploughing of surface. However, at 10 N of load the wear is mainly due to the abrasion of surfaces.

The images clearly show that on increasing the load, the wear mechanism changes from surface abrasion to the surface adhesion, pull out and micro ploughing.

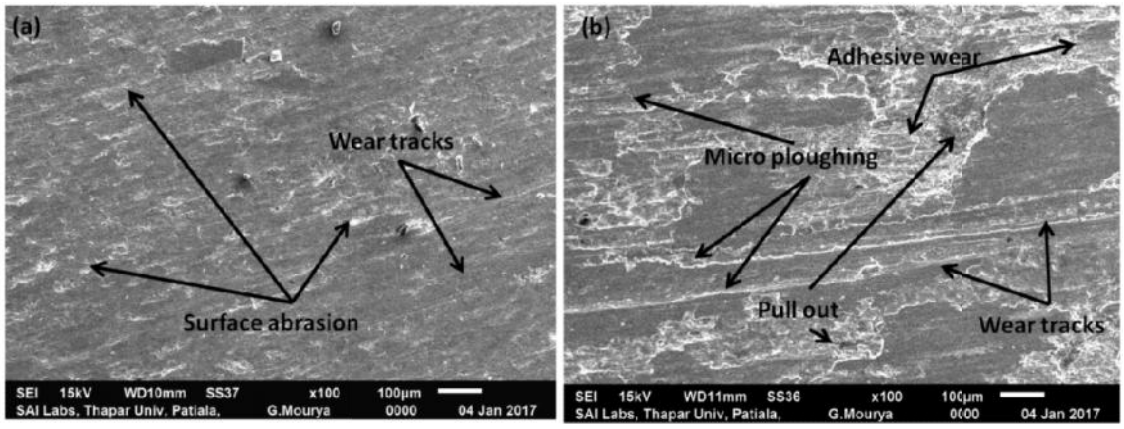

Fig.6.2: SEM images showing the worn out samples at the end of 2000 m of sliding at 1.0 m/s velocity under (a) 10 N and (b) 20 N of normal load

6.1.2 Effect of Sliding Distance on Weight Loss of EWAC Casting

It is clear from the weight loss graphs that, with increase in sliding distance, the wear (weight loss) increases for every 500 m of sliding. However, for 1000 m of sliding there is a linear increase in the weight loss and after 1000 m of sliding the curve starts flattening. This linear increase in weight loss till 1000 m of sliding distance is may be due to the initial run in wear of samples; but after 1000 m, the surface interactions such as formation of tribo-layers come into play and affected the weight loss mechanisms.

Fig. 6.3 (a) shows the formation of tribo layer after 1000 m of sliding at 1.0 m/s sliding velocity under 15 N of normal load. The EDS analysis of tribo layer revealed the formation of nickel oxide and iron oxide layers on the surface as shown in Fig. 6.3 (b). This formation of oxides is further affected by the moisture present in the atmosphere; as tests were performed under ambient conditions.

At 20 N of normal load and 1.0 m/s of sliding velocity, the weight loss at the end of 2000 m of sliding distance was 21.65 mg. In the first 500 m of sliding the weight loss recorded was 5.35 mg which is approximately 24.67% of total weight loss.

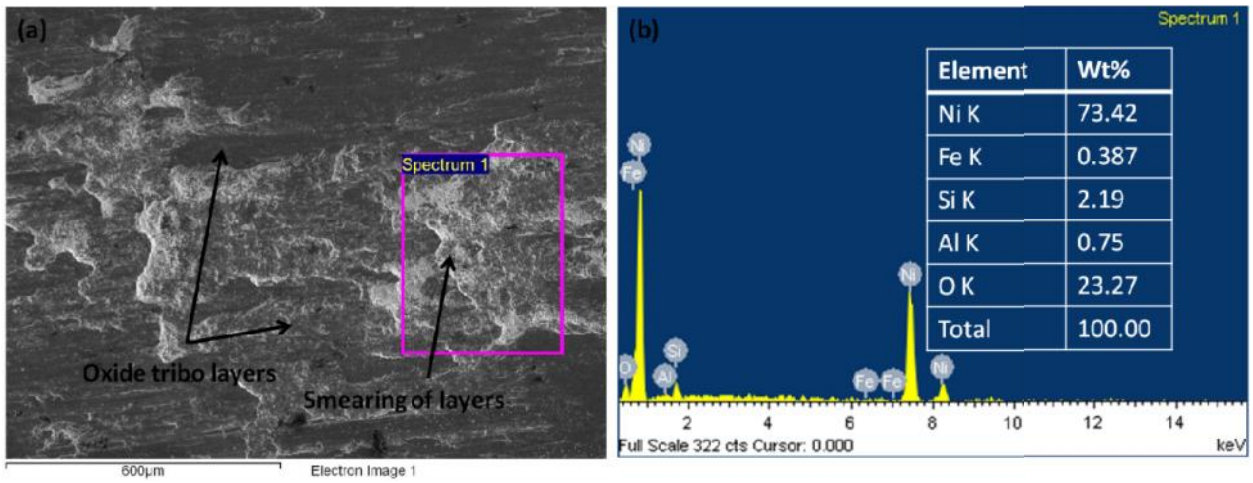

Fig. 6.3: (a) SEM image showing the formation of an oxide tribo layer at 1.0m/s sliding velocity and (b) EDS analysis of formed tribo layer

In 1000 m of sliding the total cumulative weight loss recorded was 14.45 mg which is 66.74% of total weight loss. Thus, a maximum of the wear occurred during the first 1000 m of sliding and after this the curve starts flattening. This may be due to the formation of some unstable oxide layers on the mating surfaces after 1000 m of sliding as there is enough temperature rise which leads to the formation of possible stable oxide layers. But, normal load and sliding velocities further affect the formation and smearing of tribo layers which directly affects the weight loss of castings.

6.1.3 Effect of Sliding Velocity on Weight Loss of EWAC Casting

The sliding velocities have great influence on weight loss and mechanisms involved in wear; and the effects of sliding velocities are clearly visible from Fig. 6.1 (a-c). At lower velocities i.e. 0.5 m/s, the contact time between the mating area increases, which causes higher friction and abrasion between the mating surfaces. This leads to the higher stick slip phenomenon; where localized welding and breaking of bonds occurs simultaneously. Further, due to the lower velocities, the heat generation is less and no oxide layer formation was

observed. The weight loss at 0.5 m/s sliding velocity continues to increase almost in a linear trend at all the normal load conditions. Weight loss at 20 N of load and 0.5 m/s of sliding velocity reaches maximum of 28.68 mg; whereas on increasing the sliding velocity the weight loss reduces to 21.65 mg at 1.0 m/s sliding velocity. On further increasing the velocity to 1.5m/s, the weight loss increases to 23.8 mg at the end of 2000 m of sliding. Similar results were obtained at 10 N and 15 N of normal load.

But lower weight loss at 1.0 m/s of sliding velocity is again due to the formation of a stable oxide film on the mating surfaces. However, at 1.5 m/s the heat generation is too high which causes the smearing of the formed oxide films and increases the weight loss. Lower sliding velocity, i.e. 0.5 m/s fails to generate required heat for the formation of oxide layers. Thus, under moderate sliding velocities, the formation of oxide layers were favored and lower weight loss was observed under all the loading conditions.

6.2 DRY SLIDING WEAR STUDY OF EWAC+SiC COMPOSITE CASTINGS

The presence of various reinforcements in the metal matrix behaves differently to the sliding wear tests. Some reinforcements can reduce the wear by forming lubricating tribo layers, whereas some gets abraded while testing. Further, complex phenomena can take place during sliding of mating surfaces and hard particles can cause three body wear mechanisms. Also, the parameters selected for the wear test can significantly affect the wear modes and mechanisms. Authors [Mazahery and Shabani (2013); Zhan and Zhang (2004) and Srivastava et al. (2007)] have reported that the addition of SiC can significantly improve the wear resistance of various metal matrix composites. In the present work, the effect of three parameters, namely sliding distance, sliding velocity and normal load; was studied on the dry sliding wear behavior of EWAC + SiC reinforced composites castings. The Fig. 6.4 (a-c) shows the cumulative weight

loss graphs at intervals of 500 m sliding distance for EWAC +5% SiC composite casting at varying sliding velocities and normal loads.

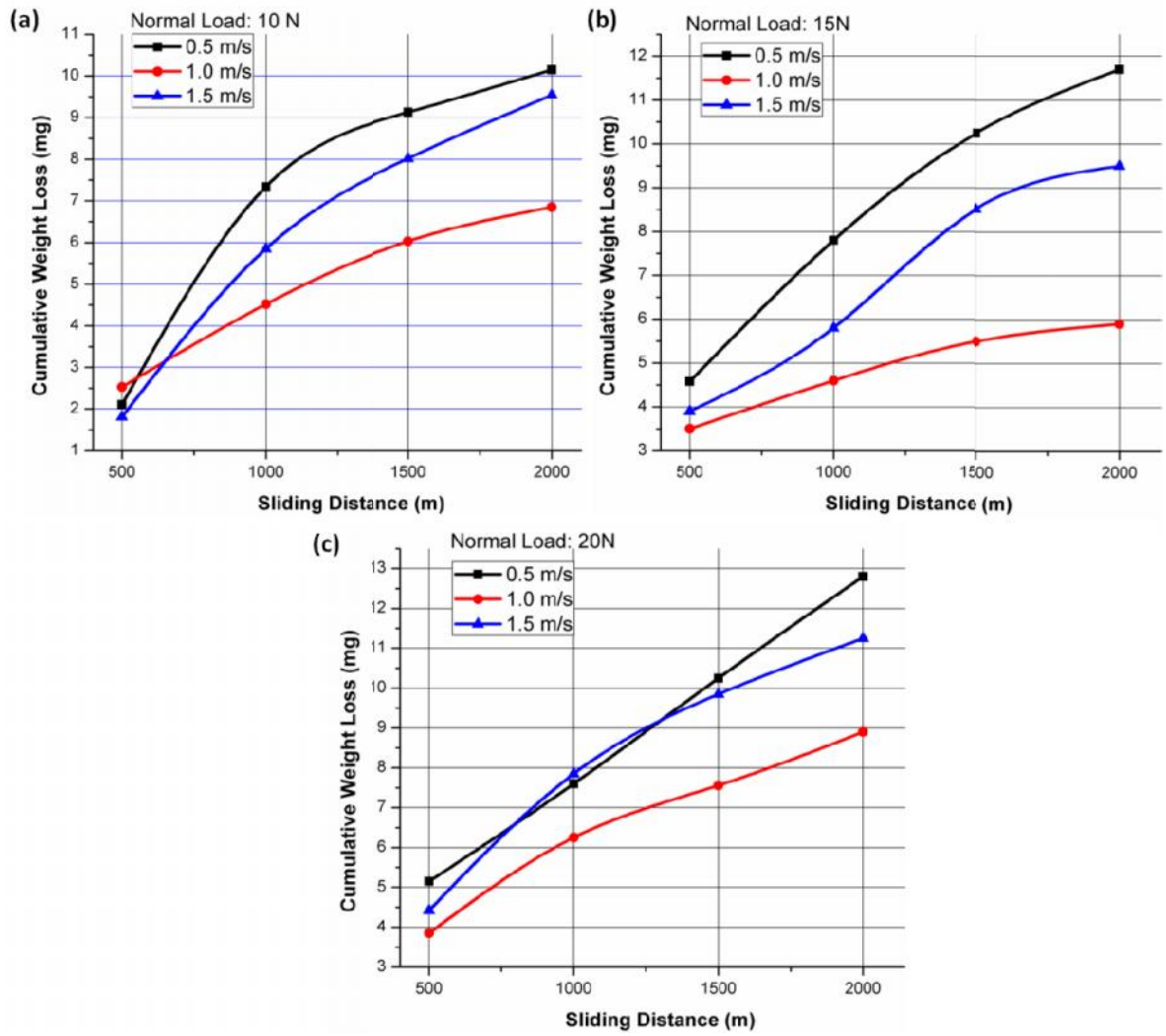

Fig. 6.4: Cumulative weight loss graphs of EWAC+5% SiC composite casting under (a) 10 N, (b) 15 N and (c) 20 N of normal load; with varying sliding distances and sliding velocities

Weight loss graph at 10 N and 15 N clearly show that by increasing the sliding distances, the weight loss first increases linearly and then tend to get stable at all the sliding velocities. But at 20 N normal load the weight loss at 0.5 m/s sliding speed keeps on increasing linearly however, at other velocities graph tends to get stable after 1000 m of sliding. Similar trends of

weight loss were observed in the EWAC + 10% SiC composite casting at varying parameters and results are shown in Fig. 6.5 (a-c).

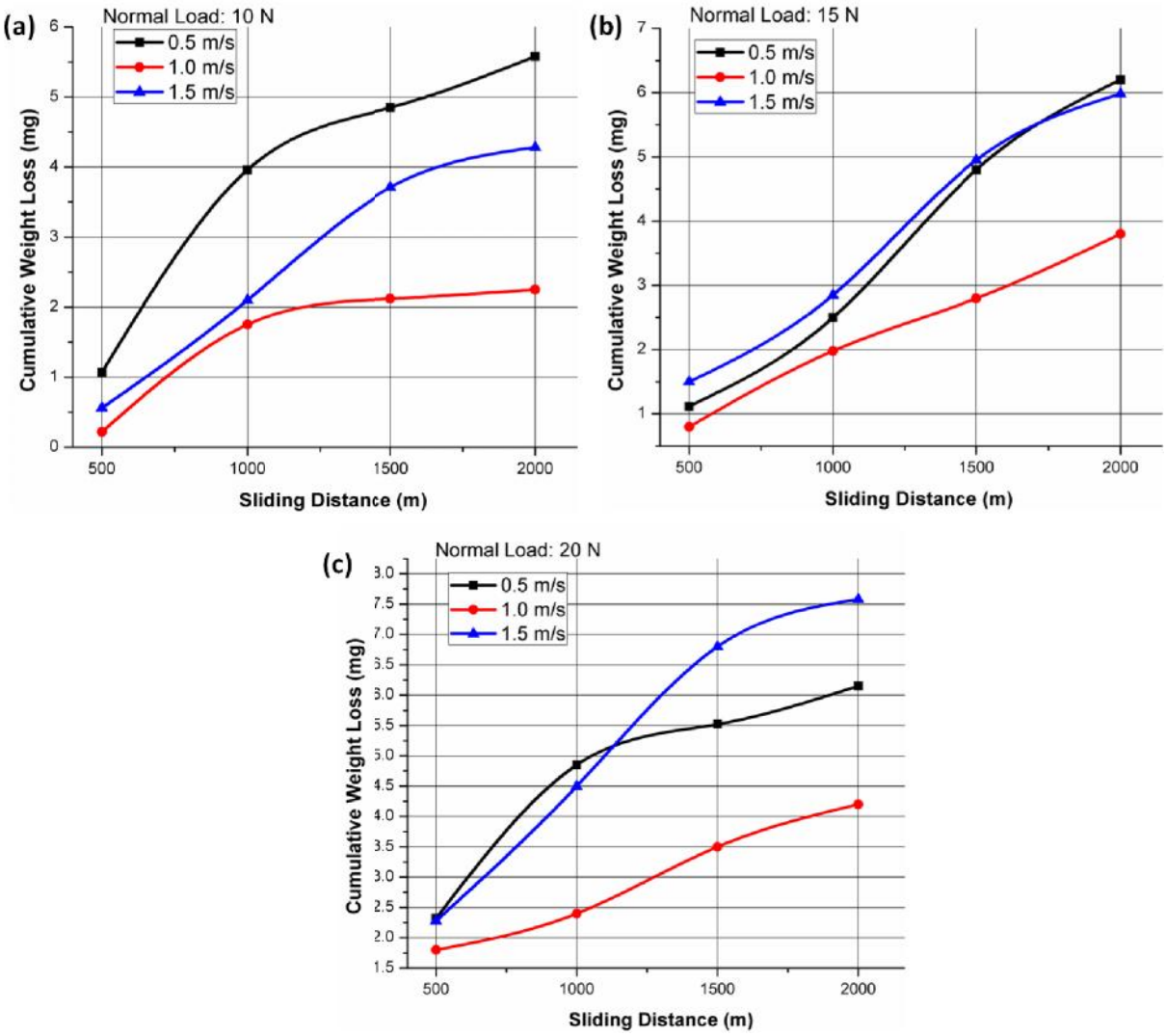

Fig. 6.5: Cumulative weight loss graphs of EWAC+10% SiC composite casting under (a) 10 N, (b) 15 N and (c) 20 N of normal load; with varying sliding distances and sliding velocities

The effect of various parameters on weight loss and mechanisms involved are discussed below.

6.2.1 Effect of Normal Load on Weight Loss on EWAC+SiC Composite Castings

The weight loss graphs for 5% SiC and 10% SiC reinforced composite castings revealed that with increasing the normal load during dry sliding wear tests, the cumulative weight loss increases linearly for the first 1000 m of sliding. This linear increase in weight loss is may be due to the initial run in wear conditions where mating surfaces get abraded till they become smooth. However, after 1000 m of sliding the curve starts to become flat due to steady wear condition. For 5% SiC reinforced composite and under 10 N of normal load, the weight loss was maximized (2.52 mg) for 1.0 m/s sliding velocity in the initial 500 m of sliding and this may be due to increased interaction between surfaces at this velocity. But at the end of 2000 m of sliding the weight loss for 0.5 m/s sliding velocity was highest with 10.25 mg at 10 N load, which further increases to 11.62 mg under 15 N load and reaches 12.78 mg under 20 N normal load. It was also observed that under 20 N normal load, the wear trend again starts to rise after 1500 m of sliding. This may be due to the excessive heat generation between the mating surfaces that causes smearing of formed tribo layers. At 0.5 m/s of sliding speed the weight loss show linear increase till 1000 m of sliding and afterwards stability was observed in the weight loss.

For 10% SiC reinforced casting, the weight loss trend was almost similar to 5% SiC reinforced casting. But an increase in the SiC content the hardness of composite casting was increased which lowered the weight loss. The weight loss was even under 1 mg for 10 N of normal load and this may be due to high hardness of cast samples. But some increasing trends were observed in 10% SiC weight loss after 1500 m of sliding and this may be due to the increased surface interactions, which may lead to particle pullout, enhanced adhesion and abrasion of surfaces. The worn out surfaces of 5% and 10% SiC reinforced casting are shown in Fig. 6.6 (a-f).

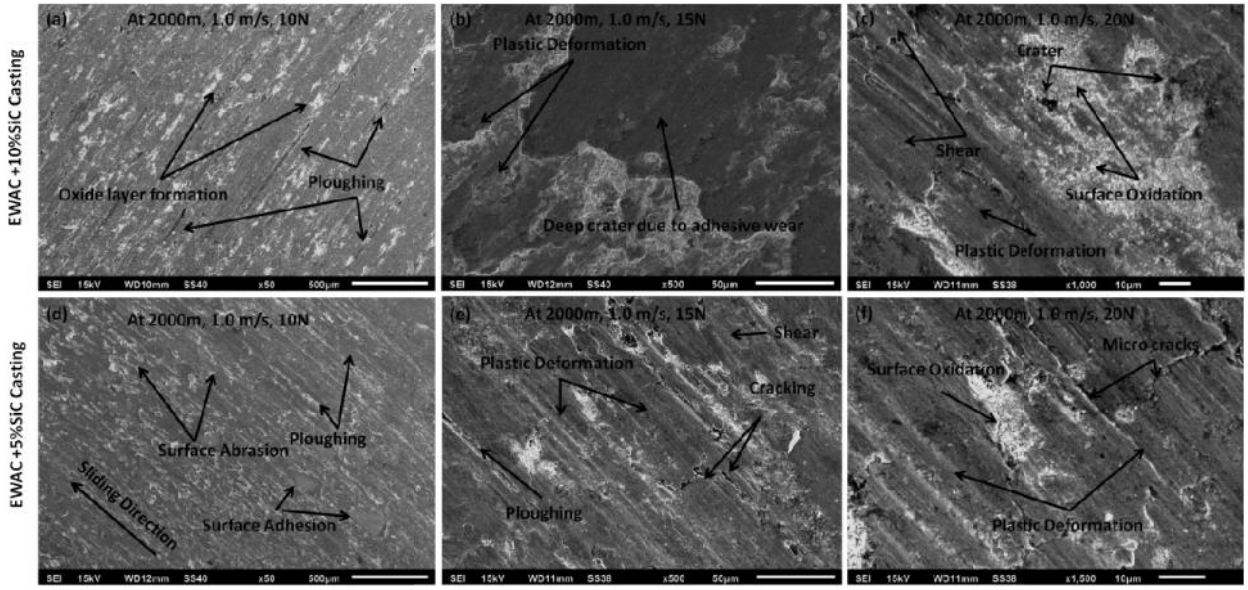

Fig. 6.6: SEM images showing worn out surfaces of EWAC+5%Sic and EWAC+10%SiC castings at (a, d) 2000 m sliding distance, 1.0m/s sliding velocity and 10 N load; (b, e) 2000 m sliding distance, 1.0m/s sliding velocity and 15 N load; and (c, f) 2000 m sliding distance, 1.0 m/s sliding velocity and 20 N load

After 2000 m of sliding under 1.0 m/s velocity and 10 N of normal load, it was clearly observed that EWAC + 10%SiC composite casting show lower abrasion due to higher hardness and wear mechanisms were mainly due to micro ploughing and surface abrasion (Ref Fig. 6.6 (a)). The formations of some oxide layers were observed (white colored patches) throughout the surface. However, for 5% SiC casting wear was intense due to lower hardness and was mainly due to surface abrasion and adhesion with some ploughing of the surface (Ref Fig. 6.6 (d)). On increasing the load from 10 N to 15 N, the wear was higher and wear mechanisms involved were intense surface adhesion causing craters and high plastic deformations for 10% SiC casting (Ref Fig. 6.6 (b)). On the other hand 5% SiC reinforced casting revealed micro cracking, shearing and enhanced plastic deformations (Ref Fig. 6.6 (e)). On further increasing the normal load to 20N, the wear enhanced considerably with the shearing of surfaces due to adhesion, plastic deformations and crater formation for 10% SiC casting (Ref Fig. 6.6 (c)). But 5%SiC casting revealed micro cracks and enhanced plastic deformation due to lower hardness. It was observed

that oxidation of the surfaces was higher in 10%SiC reinforced composite castings and this may be due to the presence of high content of SiC, which in turn helped in exposing the surfaces to the atmosphere for oxidation. It was also observed that under higher load conditions the oxidation of the surfaces was higher, but at the same time smearing was also enhanced which exposes new surface to atmosphere. This smearing and formation of oxides led to higher wear at 20 N of load. In comparison to the EWAC casting, 10% SiC composite casting revealed 3.76 times lower weight loss under 20 N load, 0.5 m/s sliding velocity and 2000 m of sliding distance.

6.2.2 Effect of Sliding Velocity on Weight Loss of EWAC+SiC Composite Castings

It was observed that sliding velocity has a significant effect on the cumulative weight loss of castings as shown in Fig. 6.4 and Fig. 6.5. At lower velocities and under low load the initial wear is lower due to lower initial contact area. But as the load increases, more abrasion of samples occurs and weight loss increases. At high velocity, i.e. 1.5 m/s, the friction was overcome quickly and lower weight loss was recorded under 10 N load in comparison to 0.5 m/s velocity. However, for 10% SiC composite castings with an increase in sliding distance the weight loss mechanisms changes and it was observed that at 1.0 m/s sliding velocity a stable oxide tribo layer was formed, but at the lower sliding velocity of 0.5 m/s there was not enough temperature rise which can cause the formation of oxide layers and this resulted in the formation of some oxide patches. At high velocity of 1.5 m/s the heat dissipation rate was lowered that causes higher heat generations and this might have caused smearing of formed oxide layers. The formation of oxide layers and their EDS analysis is shown in Fig. 6.7 (a-f).

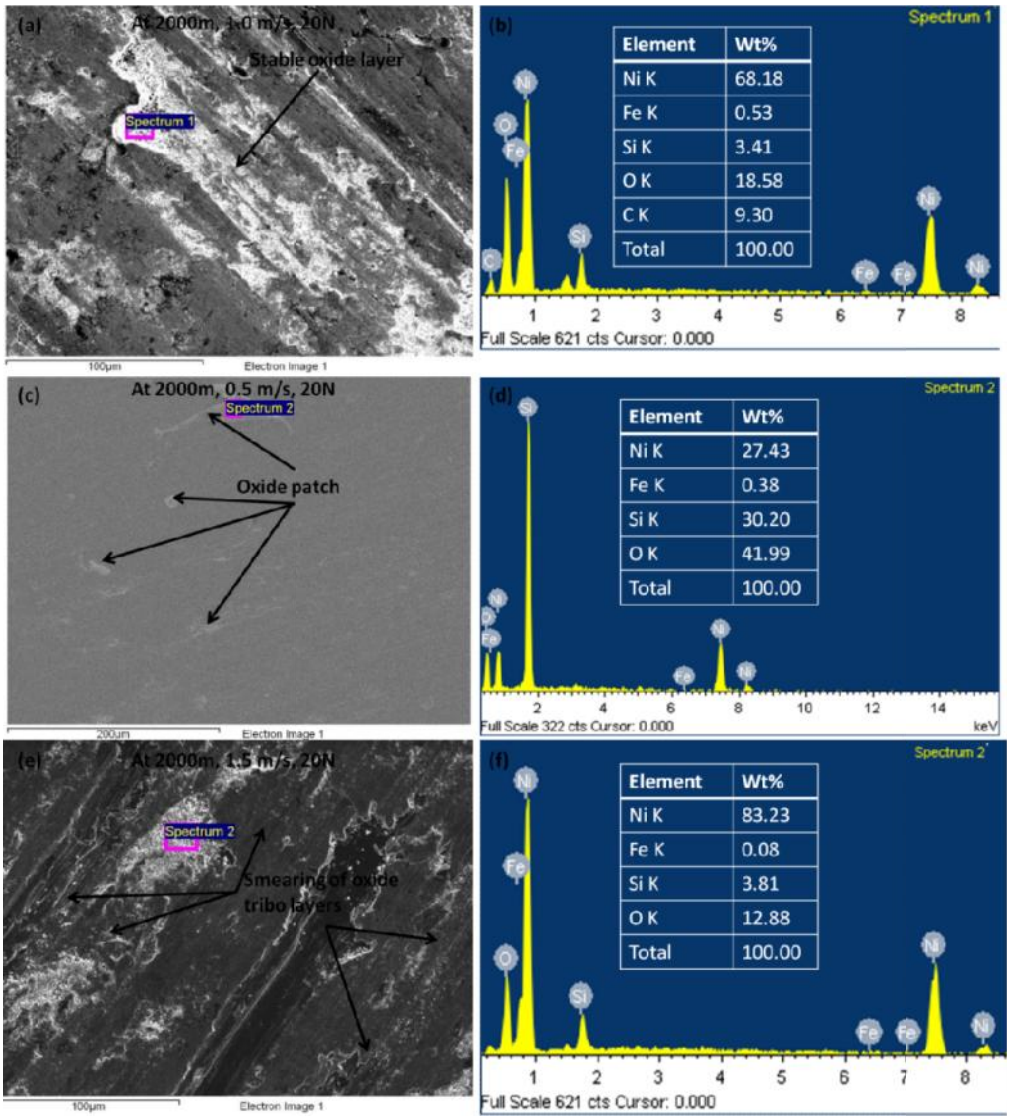

Fig. 6.7: (a, b) Formation of stable oxide layers at 1.0 m/s velocity and EDS analysis; (c, d) Formation of oxide patches at 0.5 m/s velocity and EDS analysis of patch; and (e, f) Smearing of the oxide tribo layer at 1.5 m/s with EDS analysis

The white layer was observed in SEM images (Fig. 6.6) which represents the oxidation layer and further, EDS analysis revealed the formation of oxides of Ni, Si and Fe. The majority of the oxide was formed from nickel element followed by silicon and iron; carbon was present in some EDS analysis and this may be due to the abrasion of surface by SiC particle which led to oxide formation on abraded surface. It is clear from the results that moderate velocity favors the formation of oxide tribo layers which results in lower weight loss.

6.2.3 Effect of Sliding Distance on Weight Loss of EWAC+SiC Composite Castings

The weight loss graphs for EWAC + SiC castings show that weight loss increases on increasing the sliding distance, but the amount of loss varies for every 500 m of sliding. This variation is due to the various surface interactions under varying conditions. As load increases the weight loss increases and tends to increase linearly due to stick slip wear phenomenon occurred at lower velocity of 0.5 m/s. Higher velocity of 1.5 m/s led to a higher strain on the embedded SiC particles and it was observed that at the end of 2000 m of sliding three body abrasive wear occurred under 20 N load. Fig. 6.8 (a-b) shows the three body abrasive wear due to SiC particle pullout from the matrix and deep ploughing groove caused by it.

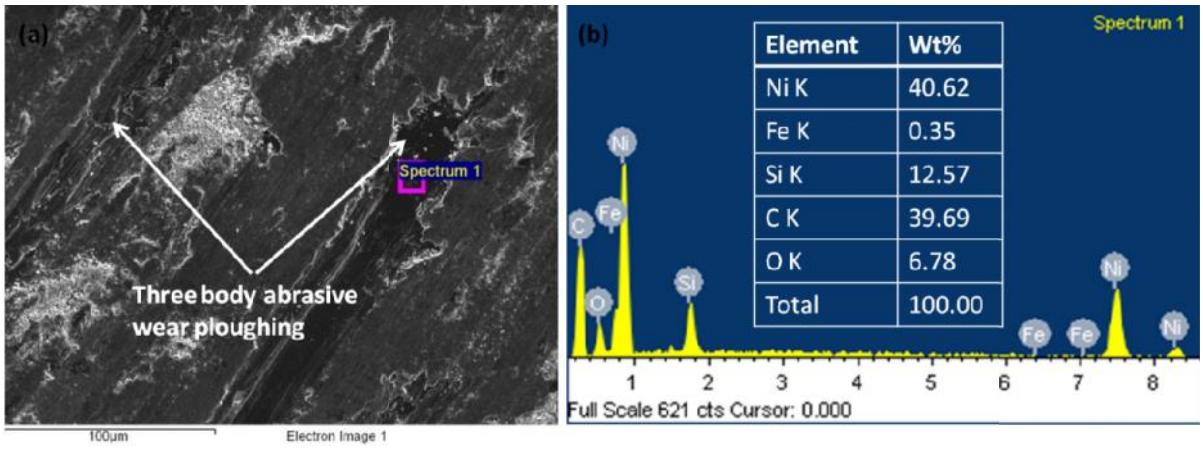

Fig. 6.8: (a) Electron image showing the three body abrasive wear mechanism and (b) EDS analysis of groove

The EDS analysis revealed the presence of higher silicon and carbon content in the grove, which proves that it is caused by SiC particle indentation. With the increase in sliding distance the surface conditions may resist wear due to formation of tribo layers at particular parameters. Also, continuous sliding can cause smearing of formed tribo layers under the high load and high velocity conditions which can result in surface degradation with higher weight loss. Fig. 6.9 (a-b)

show the worn out samples of EWAC + 10% SiC composite after 1000 m and 2000 m of sliding under 15 N of normal load and at 1.0 m/s sliding velocity.

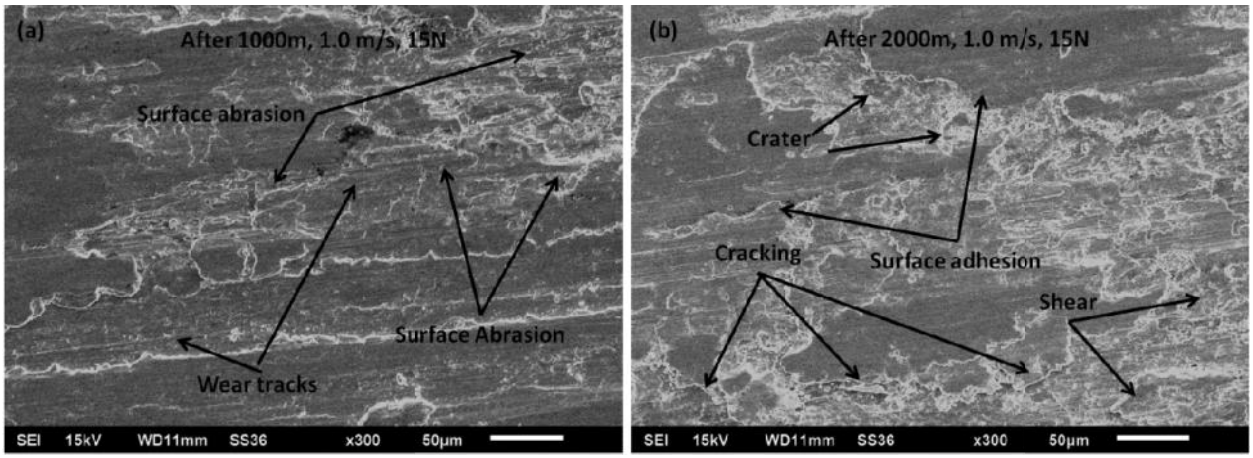

Fig. 6.9: SEM image of worn out surfaces after (a) 1000m and (b) 2000 m of sliding

It was observed that after continuous sliding for 2000 m the wear mechanism changes due to various surface interactions occurring during sliding. The surface degraded and cracking appears due to stick slip phenomena which further lead to adhesive wear by forming and breaking of localized welds.

The wear debris from the samples were collected and analyzed by using SEM-EDS to study the morphology and elemental study of wear particles. Fig. 6.10 shows the image of collected debris at 20N load, 1.5 m/s sliding velocity and after 2000 m of sliding distance of EWAC+10%SiC composite casting.

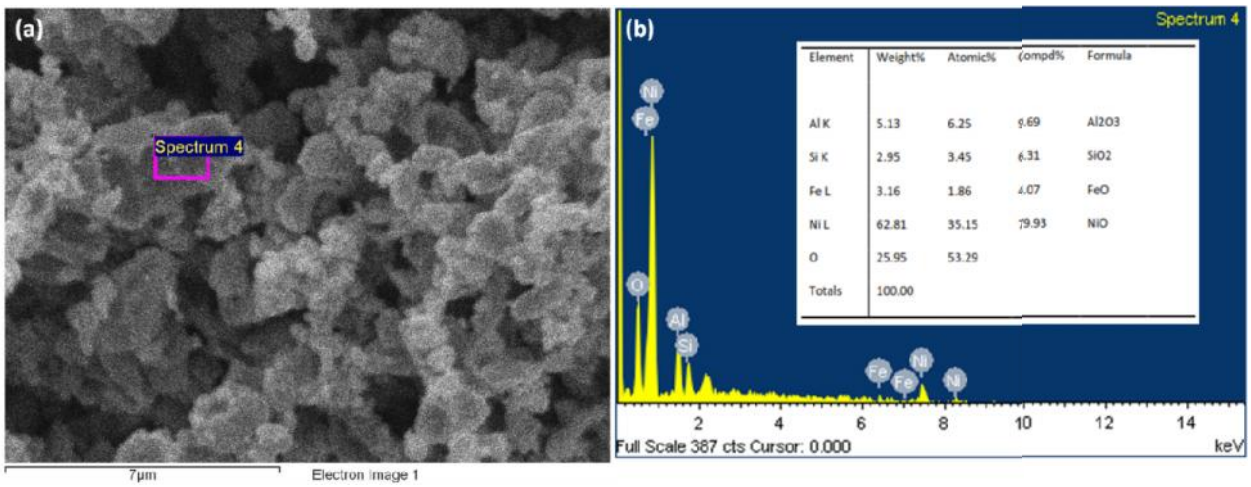

Fig. 6.10: (a) SEM image of collected debris and (b) EDS analysis of debris

The morphology of collected debris is in the form of micro sized agglomerated particles and EDS analysis of these debris revealed that various oxides which were formed during sliding. The debris, mainly consists of NiO, Al_2O_3, SiO_2 and FeO oxides. The presence of alumina was may be due to the abrasion of counter disc, which get transferred to the mating surface. The formed oxide tribo layers were smeared during sliding and contributed to the weight loss in all the castings. However, in some cases, SiC particles were also found which got pulled out of the matrix.

6.3 DRY SLIDING WEAR STUDY OF EWAC+Al_2O_3 COMPOSITE CASTINGS

The developed alumina reinforced composite castings through MHH process were subjected to the dry sliding wear tests to evaluate their performance against the hard ceramic counter plate (alumina). The weight loss plots for the EWAC+5%Al_2O_3 composite and EWAC+10%Al_2O_3 composite; at varying parameters are shown in Fig. 6.11 (a-c) and 6.12 (a-c).

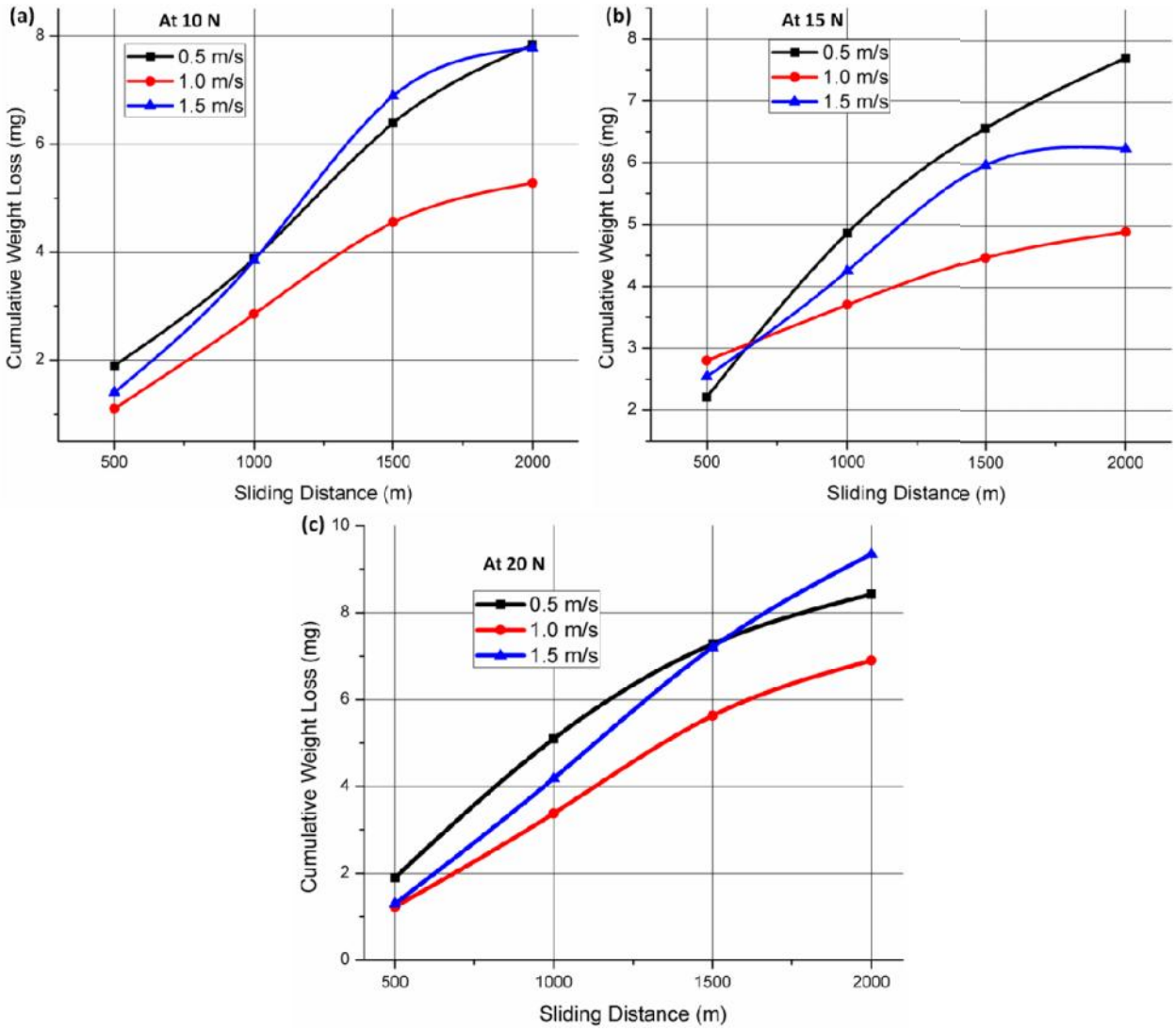

Fig. 6.11: Cumulative weight loss plots under varying sliding velocities, sliding distances and under (a) 10 N, (b) 15 N and (c) 20 N of normal load; for EWAC+5%Al_2O_3 composite castings

The cumulative weight loss graphs revealed that by increasing the sliding distances, the wear increases linearly up to 1000 m of sliding. After 1000 m of sliding the weight loss graph tends to achieve stability after initial wear condition. Also, with the increase in a normal load, the weight loss tends to increase, but some variations were observed at 15 N load where weight loss was similar to the 10 N load condition.

The sliding velocities have varying effect on weight loss mechanisms and weight loss was lower at 1.0 m/s velocity. The formation of some unstable oxide layers during sliding may have affected the weight loss mechanisms.

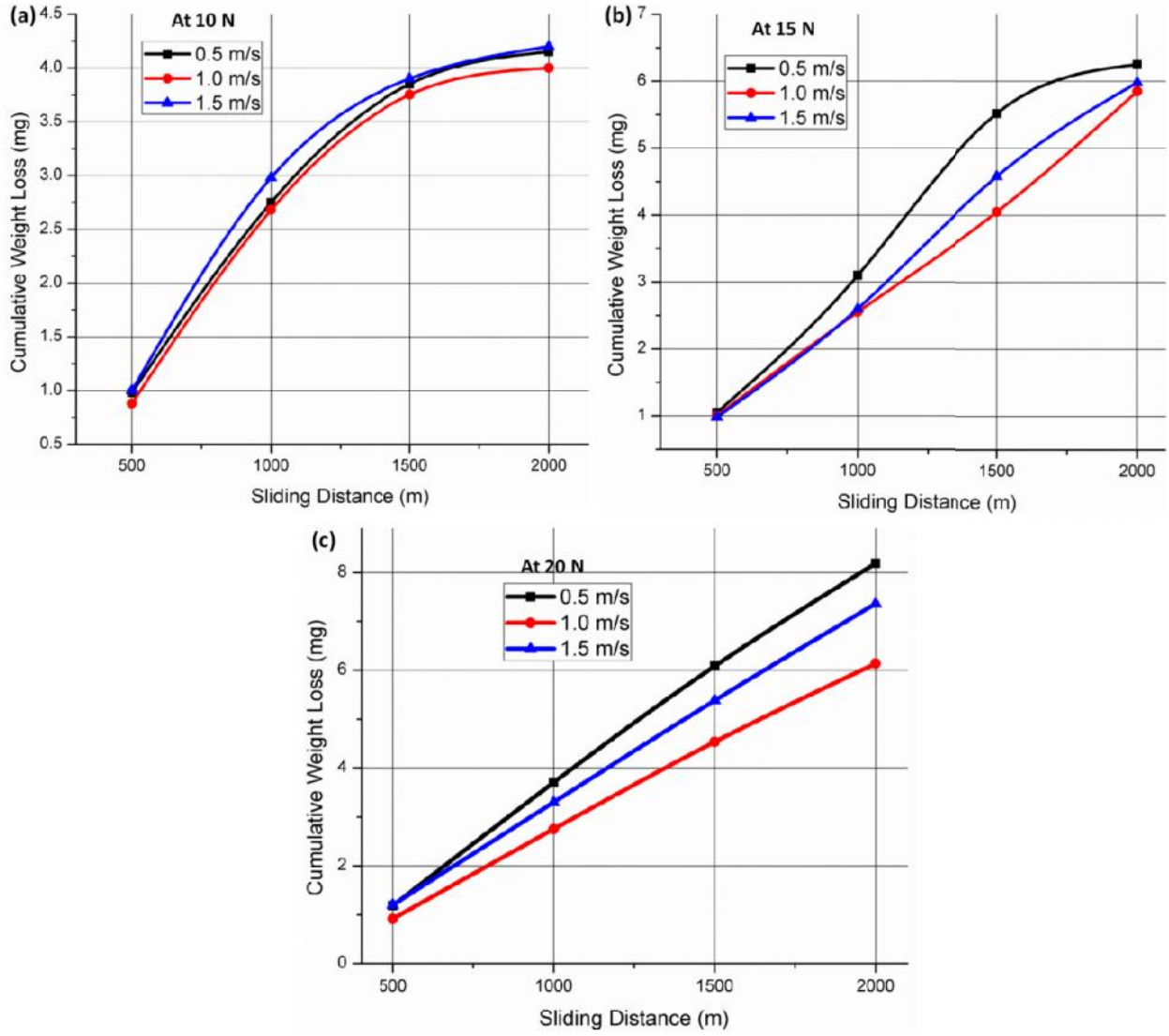

Fig. 6.12: Cumulative weight loss plots under varying sliding velocities, sliding distances and under (a) 10 N, (b) 15 N and (c) 20 N of normal load; for EWAC+10%Al_2O_3 composite castings

It can be observed that on increasing the content of alumina reinforcement to 10%, the weight loss was less in comparison to 5% alumina (Al_2O_3) reinforced composite. This may be

due to the higher hardness of 10% Al_2O_3 reinforced composite casting. The effects of various parameters on the weight loss mechanisms are discussed in the following sections.

6.3.1 Effect of Normal Load on Weight Loss of EWAC+Al_2O_3 Composite Castings

The effects of varying normal loads on cumulative weight loss are clearly presented in the weight loss plots (Ref. Fig. 6.11 and Fig. 6.12). With 10 N of load and 0.5 m/s of sliding velocity, the weight loss of 5% Al_2O_3 reinforced casting increases from 2.21 mg at 500 m of sliding to 7.72 mg at the end of 2000 m of sliding. Wear recorded was higher for initial sliding distance and this was due to the initial run in wear conditions; after which the wear becomes stable as shown by the weight loss curves. For 15 N of normal load the initial wear was observed to be less i.e. 1.89 mg after 500 of sliding, but it increased proportionally to 7.84 mg after 2000 m of sliding. This may have occurred due to the formation of some oxide layers at 15 N of load. But on further increasing the load to 20 N, the weight loss, increased up to 8.42 mg at the end of 2000 m of sliding. Similar trends were observed for other sliding velocities; however, for 15 N of load and 1.0 m/s of sliding velocity the weight loss was higher as compared to other velocities. This may be due to the fact that increases in the load and sliding at moderate velocity initiated the initial stick slip phenomenon by localized welding of asperity interfaces. However, high loads leads to the generation of high temperatures which allowed the formation of oxides and prevent further interlocking of surfaces.

For 10% Al_2O_3 reinforced casting the wear under 10 N of normal load represented the typical weight loss graph which tends to become stable after 1000 m of sliding for all the velocities. This was due to the higher hardness of composite which restricted the enhanced weight loss due to abrasion of surfaces and gains stability. But, for 15 N of normal load, some surface interactions were observed in terms of formation and the smearing of oxide tribo layers

which caused variations in weight loss trends at various velocities. However, with further increase in normal load, i.e. at 20 N, the weight loss graphs show linear trend and this may be due to the excessive smearing of the formed layers due to the high temperature generated on the mating surfaces. The worn out samples of EWAC+Al_2O_3 composites at various parameters are shown in Fig. 6.13 (a-f).

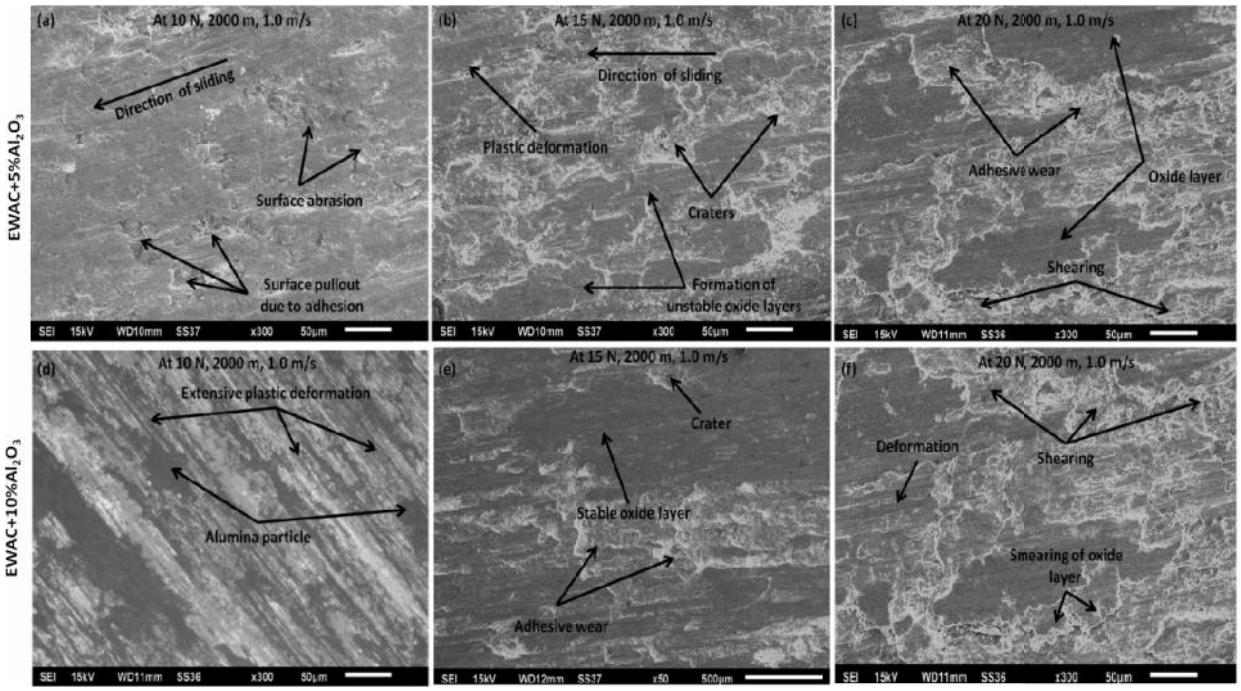

Fig. 6.13: SEM images showing the worn out samples of (a-c) EWAC+5% Al_2O_3 and (d-e) EWAC+10% Al_2O_3 composite castings under varying normal load

It was observed that for 5% alumina reinforced castings the surface abrasion was more dominant at 10 N load. On increasing load, surface adhesion, plastic deformation and shearing of surfaces were observed. This was due to the higher heat generation at mating surfaces. But for 10% alumina reinforced casting the wear mainly occurred due to extensive plastic deformation at 10 N of load and this was due to higher microhardness of the composites. On increasing load the adhesive wear increased and this further led to the formation of oxide tribo layers on the surface.

At 20 N of load the smearing of the formed layers was observed and this led to the shearing of the surface coupled with surface pull out.

6.3.2 Effect of Sliding Velocity on Weight Loss of EWAC+Al_2O_3 Composite Castings

The weight loss plots revealed that at a moderate sliding velocity, i.e. 1.0 m/s the weight loss was less as compared to other velocities. At 0.5 m/s of sliding velocity, the mating surfaces stay in contact with each other for higher time which eventually led to the higher friction due to asperity interlocking and leads to the higher surface abrasion.

At 1.5 m/s it was observed that weight loss increases sharply under 20 N of normal load and this was due to the smearing of the formed oxide tribo layers and more over at higher velocities the temperature kept on increasing due to repetitive sliding on ceramic counter face with shorter intervals. The material of counter disc is alumina which does not allow heat to transfer and led to extensive adhesive wear at higher velocities. On the other hand, sliding velocity of 1.0 m/s allowed balance between the heat generation and dissipation at the counter disc, which favored the formation of oxide layers.

The formed oxide tribo layer on the surface of 10% alumina reinforced composite under the 15 N of sliding and at 1.0 m/s of sliding velocity is shown in Fig. 6.13 (a-b).

The EDS analysis of the layer shows the formation of oxides of nickel, silicon, aluminium and iron. The formed hard oxide layers on the surfaces further prevented the abrasion wear of the material during sliding. But with increase in normal load these layers get degraded and expose new surfaces to the counter disc and this increase the chances of further wear.

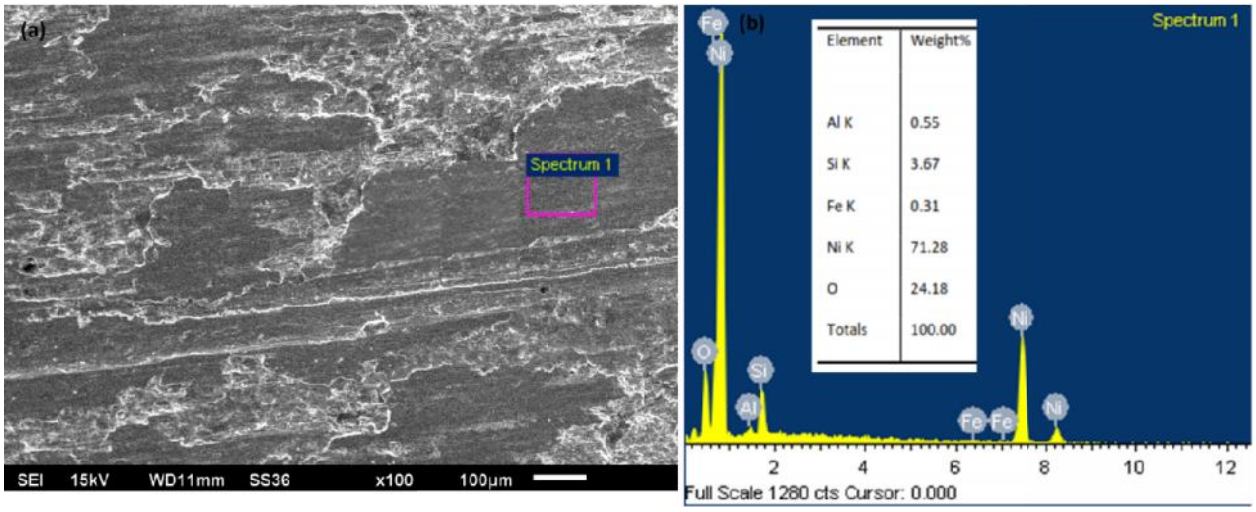

Fig. 6.14: (a) SEM image of 10% alumina reinforced composite showing the formation of tribo layers and (b) EDS analysis of tribo layer

6.3.3 Effect of Sliding Distance on Weight Loss of EWAC+Al_2O_3 Composite Castings

The effects of sliding distances on the weight loss of alumina reinforced composite castings are shown in Fig. 6.11 and Fig. 6.12. For 10% alumina reinforced casting the weight loss graph revealed that for all the sliding velocities the wear increases in a linear trend for initial 1000 m, when sliding under 10 N and 15 N of normal load. After 1000 m, the graph tends to straighten up thus showing some stability in the wear. But under the 20 N normal load, the weight loss trends show a linear increase even at 2000 m of sliding. This was again due to the generation of high temperatures, which softens the matrix material and supported the adhesive wear and shearing of sample surfaces. A comparison of worn out surfaces after 500 m, 1000m and 2000 m of sliding is shown in Fig. 6.15 (a-b), which shown the optical micrographs of samples. As the sliding distance increases; the surface becomes rougher due to abrasion against hard counter face. In some cases the friction causes enough heat generation which supported the formation of tribo layers at moderate velocities. The tribo layer formation shows some resistance

which lowers the weight loss after 1000 m of sliding, but on continuous sliding the smearing of layers occurred under 20 N of load which again causes rise in weight loss weight loss.

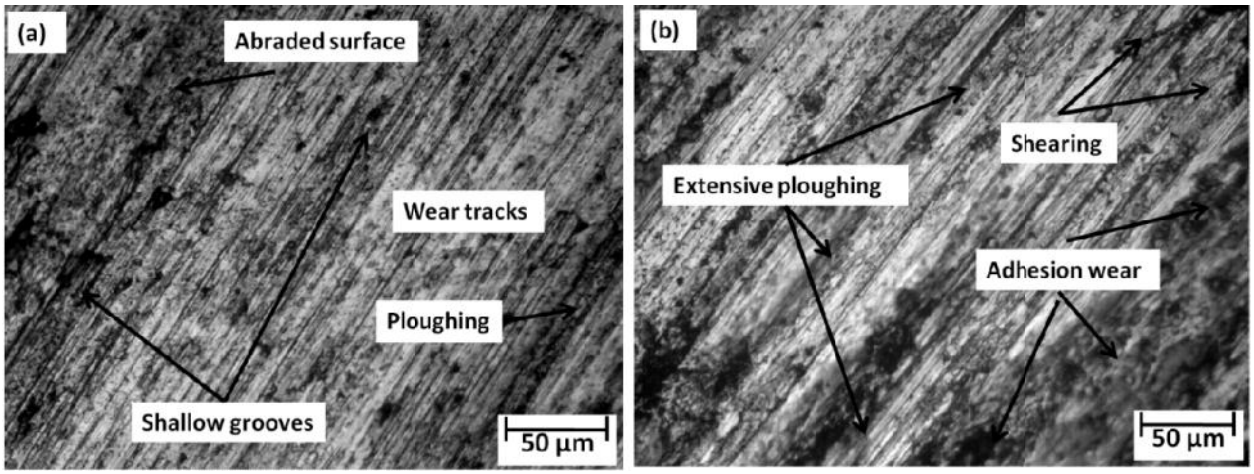

Fig. 6.15: Optical micrographs of 10% alumina reinforced composite after (a) 1000 m and (b) 2000 m of sliding; under 20 N load, 1.0 m/s sliding velocity

In case of 0.5 m/s sliding velocity and 20 N load, the wear was mainly due to the extensive peeling of the surface because of surface adhesion. This adhesion results in surface cracks, craters and extensive deformation after the 2000 m of sliding as shown in Fig. 6.16.

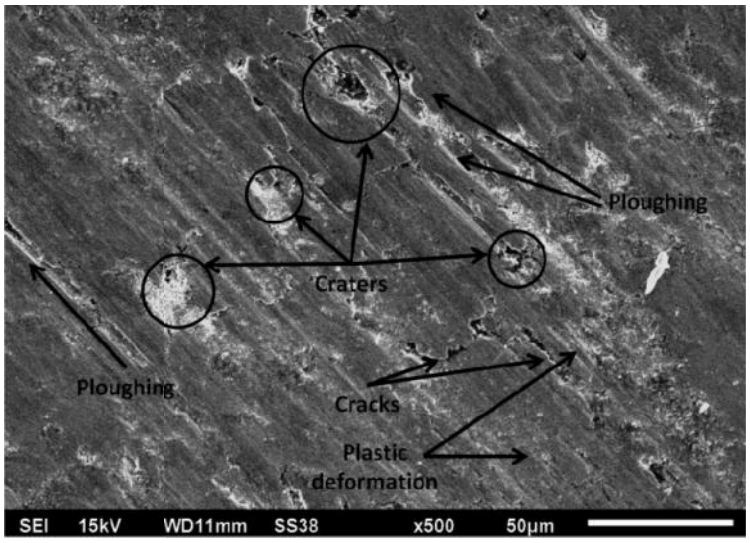

Fig. 6.16: SEM image showing worn out surface after 2000 m of sliding at 0.5 m/s velocity

The weight loss for 5% alumina reinforced casting after 500 m of sliding at 1.0 m/s velocity and 10 N of load was 1.22 mg. For the next 500 m of sliding there was 2.15 mg of weight loss and total weight loss of 1000 m was 3.37 mg. For the next 500 m of sliding, 2.25 mg of weight loss was recorded and for the last 500 m the weight loss recorded was 1.27 mg. This clearly show that for the first 1000 m of sliding higher weight loss was observed and this may be due to the initial run in wear, which occurs due to the presence of irregularities on the surface. Similar trends were observed for the 10% alumina reinforced castings. The presence of alumina reinforcement in the EWAC matrix has improved the microhardness and lowered the weight loss in comparison to pure EWAC casting. It was observed that by adding 5% alumina reinforcement, the weight loss was reduced by 68.13%, whereas on adding 10% volume fraction of alumina the weight loss was reduced by 71.67% under the same conditions of 20 N load, 1.0 m/s sliding velocity and 2000 m of sliding distance.

6.4 DRY SLIDING WEAR STUDY OF EWAC+(WC-8Co) COMPOSITE CASTINGS

The EWAC+(WC-8Co) reinforced composite castings with 5% and 10% volume fraction were developed through MHH and were subjected to dry sliding wear tests. It has been observed that by adding (WC-8Co) reinforcement in the EWAC matrix; the microhardness has improved significantly. This increase in microhardness may have direct influence the dry sliding wear behavior of developed composite castings.

The wear tests for EWAC+5%(WC-8Co) composites and EWAC+10%(WC-8Co) composites were carried out on the selected parameters and cumulative weight loss graphs are plotted which are as shown in Fig. 6.17 (a-c) and Fig. 6.18 (a-c). The results of weight loss revealed that the presence of (WC-8Co) reinforcement lowered the weight loss during test as in comparison to other reinforced composite castings. This may be due to the presence of dispersed

decomposed nano-metric WC particles throughout the casting. However, the weight loss trend appears to be similar to the other castings.

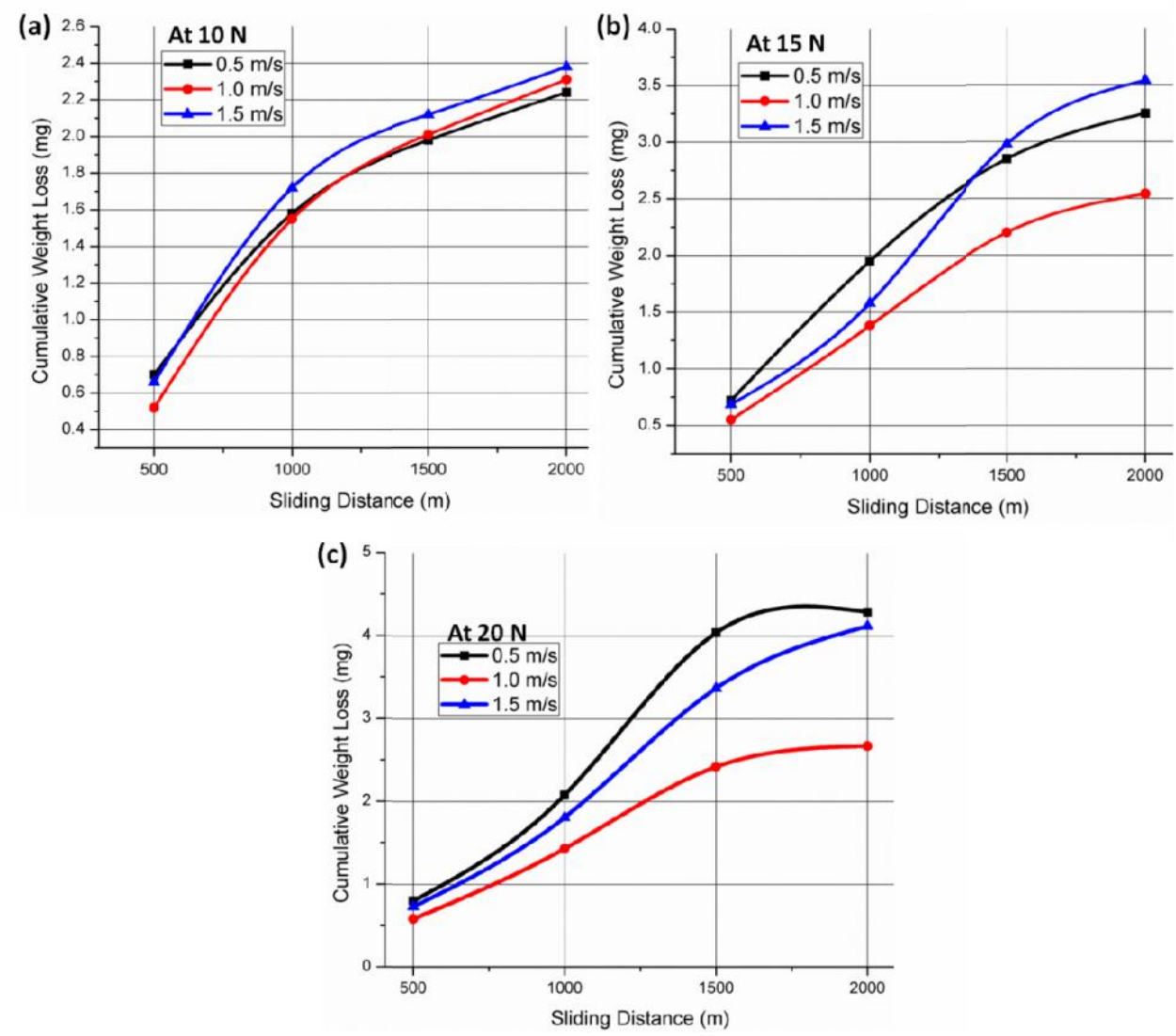

Fig. 6.17: Weight loss plots for EWAC+5%(WC-8Co) composite castings at varying sliding velocities, sliding distances and under (a) 10 N, (b) 15 N and (c) 20 N of normal load

Again, the graph trends show that the cumulative weight loss increases linearly for the initial 1000 m of sliding and then trend tends to deviate from linearity. This may be due to the initial run in wear conditions; where mating surfaces get abraded due to the presence of asperities on the surfaces.

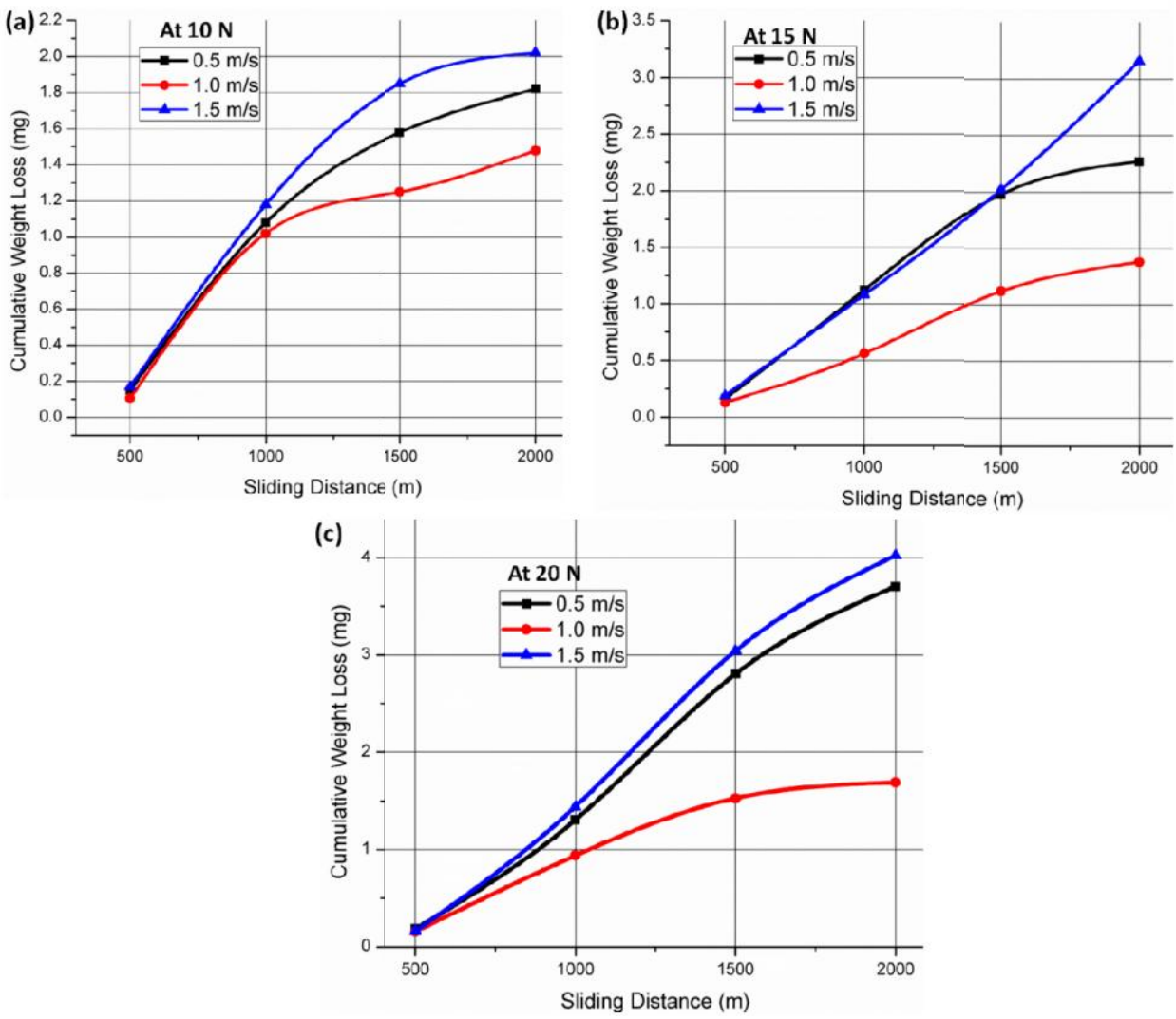

Fig. 6.18: Weight loss plots for EWAC+10%(WC-8Co) composite castings at varying sliding velocities, sliding distances and under (a) 10 N, (b) 15 N and (c) 20 N of normal load

Further, it was observed that for all the samples of EWAC+(WC-8Co) castings, the weight loss is below 1 mg and this may be due to the fact of enhanced hardness of the samples and presence of nano sized degraded particles dispersed all over the surface. This restricted the abrasion of surfaces initially. The Fig. 6.19 shows the SEM image of EWAC+10%(WC-8Co) abraded surface after 500 m of sliding with 1.5 m/s of sliding velocity and under 20 N of load. The topography of the surface reveals that there were no plastic deformations and no wear tracks

were observed. However, surface shows some abrasion marks distributed all over which caused the wear at initial stages of sliding.

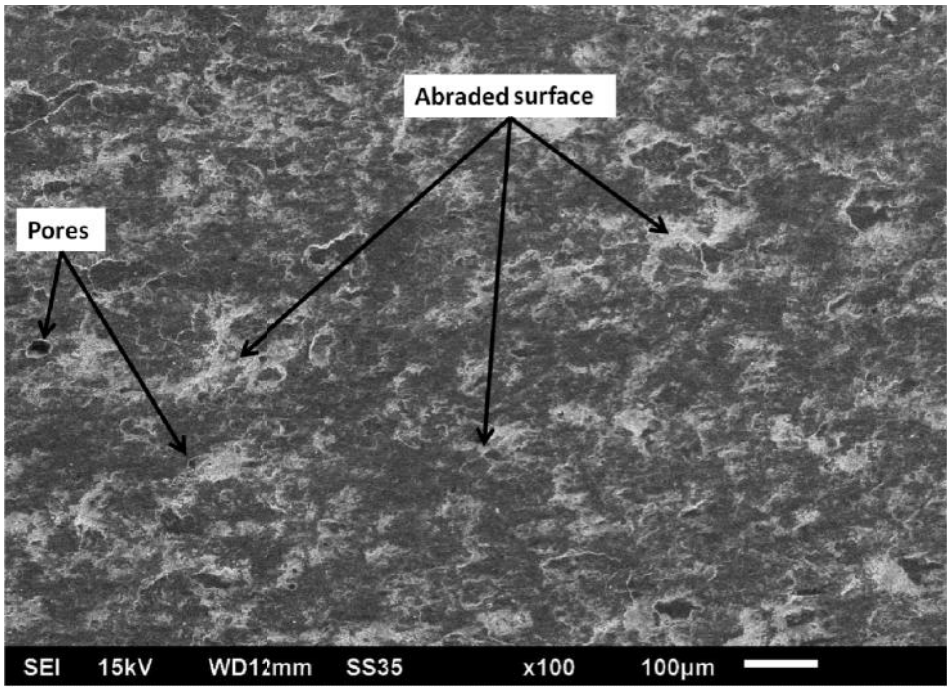

Fig. 6.19: SEM image showing the worn out surface of EWAC+10%(WC-8Co) composite casting under 20 N load, sliding at 1.5 m/s and after 500 m of sliding

6.4.1 Effect of Normal Load on Weight Loss of EWAC+(WC-8Co) Composite Castings

The effect of normal load on weight loss of EWAC+(WC-8Co) composite castings is clearly visible from the weight loss plots shown in Figs. 6.17 (a-c) - 6.18 (a-c). Results revealed that for 5% (WC-8Co) reinforced casting, by increasing the load from 10 N to 15 N the weight loss increases from 2.38 mg to 3.54 mg, for 1.5 m/s of sliding velocity and at the end of 2000 m of sliding. Similarly for 20 N of normal load, the value of weight loss increases to 4.12 mg, which is 1.73 times of the weight loss at 10 N of load. Similarly for 10% (WC-8Co) casting the weight loss increased by 1.27 times when load increases from 10 N to 20 N at sliding velocity of 1.5 m/s and after 2000 m of sliding. This increase in weight loss due to increase in the normal

load was mainly due to the increased abrasion between the mating surfaces at a specified velocity. The optical micrographs of EWAC+10%(WC-8Co) casting under 10 N and 20 N of normal load, after 2000m of sliding and at 1.0 m/s of sliding velocity are shown in Fig. 6.20 (a-b).

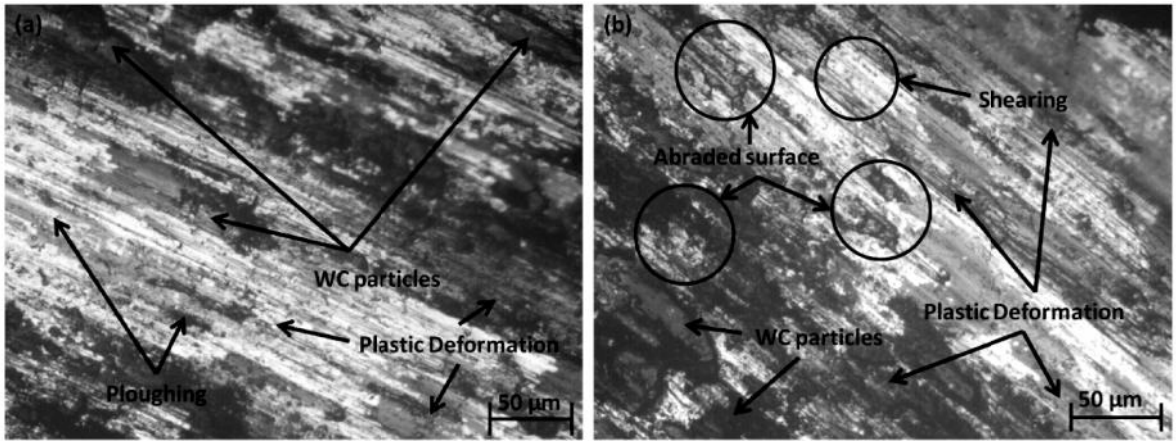

Fig. 6.20: Optical micrographs of worn out EWAC+10%(WC-8Co) casting sample after sliding 2000 m, under the normal load of (a) 10 N and (b) 20 N

The worn out samples study revealed that on increasing the normal load from 10 N to 20 N, the abrasion of surface increases and this may lead to the reinforced material pull out in the form of small fragments from the surface. The plastic deformation is also increased with increase in load and this may be due to the increased temperature which softens the composite matrix. It was also observed from the SEM image (Fig. 6.19) that no stable layers of oxides were formed during the sliding of WC reinforced samples. However, at moderate velocity of 1.0 m/s, some tribo-layers formation was observed and EDS analysis revealed the formation of oxides as shown in Fig. 6.21.

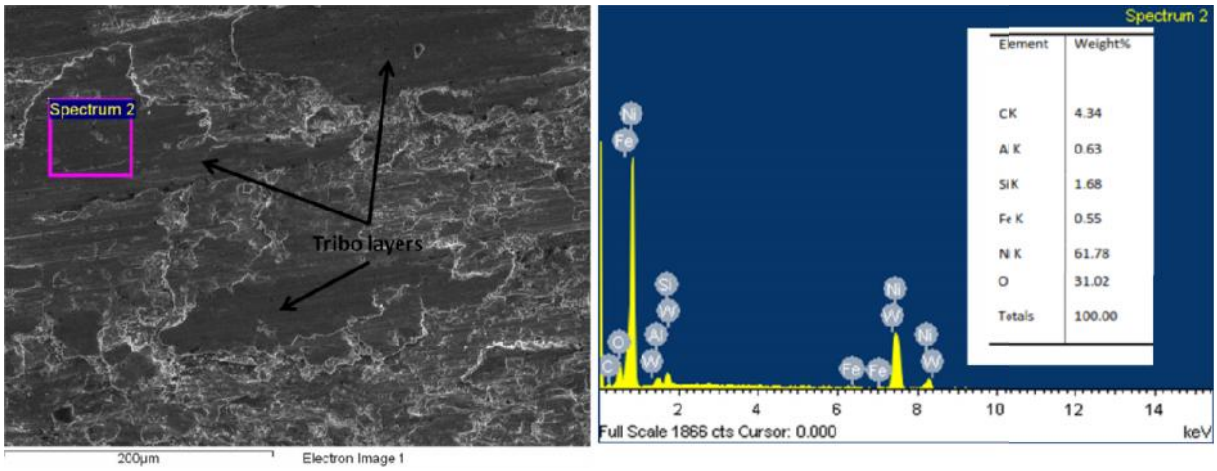

Fig. 6.21: EDS analysis of oxide tribo layer formed at 1.0 m/s sliding velocity and under 15 N load

The EDS analysis revealed that NiO was predominantly present in the tribo layer which was followed by SiO_2 and Al_2O_3. The generation of high temperatures on the mating surfaces and atmospheric test conditions favored the formation of oxide layers. Load also affect the formation of these layers. At l0 N of load, sufficient heat was not generated and this resulted in unfavorable conditions for tribo layer formation, whereas at higher load of 20 N, significant amount of heat was generated during sliding the formed layer gets smeared due to hard carbides. At moderate loading condition i.e 15 N, some tribo layers were observed and this was favored due to the appropriate heat generations and lower abrasion of surfaces which sustains the formation of layers.

6.4.2 Effect of Sliding Velocity on Weight Loss of EWAC+(WC-8Co) Composite Castings

The cumulative weight loss graphs revealed that sliding velocities have a significant role in the wear behavior of the composites. In case of EWAC+5% (WC-8Co) composite, at low loads of 10 N and 15 N, the maximum weight loss was recorded at 1.5 m/s which is different from the other castings weight loss results. The increase in weight loss at higher velocities was due to the insufficient heat dissipation from ceramic counter plate and led to very high

temperature generations. Generation of higher temperatures lowers the strength of the matrix and causes high abrasion and material pull out from the sample surfaces. But, as load increases, the abrasion further increases at low sliding velocity of 0.5 m/s due to the higher contact period for particular area which causes adhesion and separation of fragments from the surface. In the case of EWAC+10%(WC-8Co) composites, the abrasion resistance increases due to high hardness and due to this the maximum weight loss occurred at high sliding velocity of 1.5 m/s. This is again due to the fact that matrix material softens at high temperatures which causes deformations, stick-slip, and adhesion of surfaces. The SEM images shown in Fig. 6.22 reveals the enhanced deformations of the sample surface of 10% (WC-8Co) reinforced composite at 1.5 m/s velocity in comparison to 0.5 and 1.0 m/s sliding velocities.

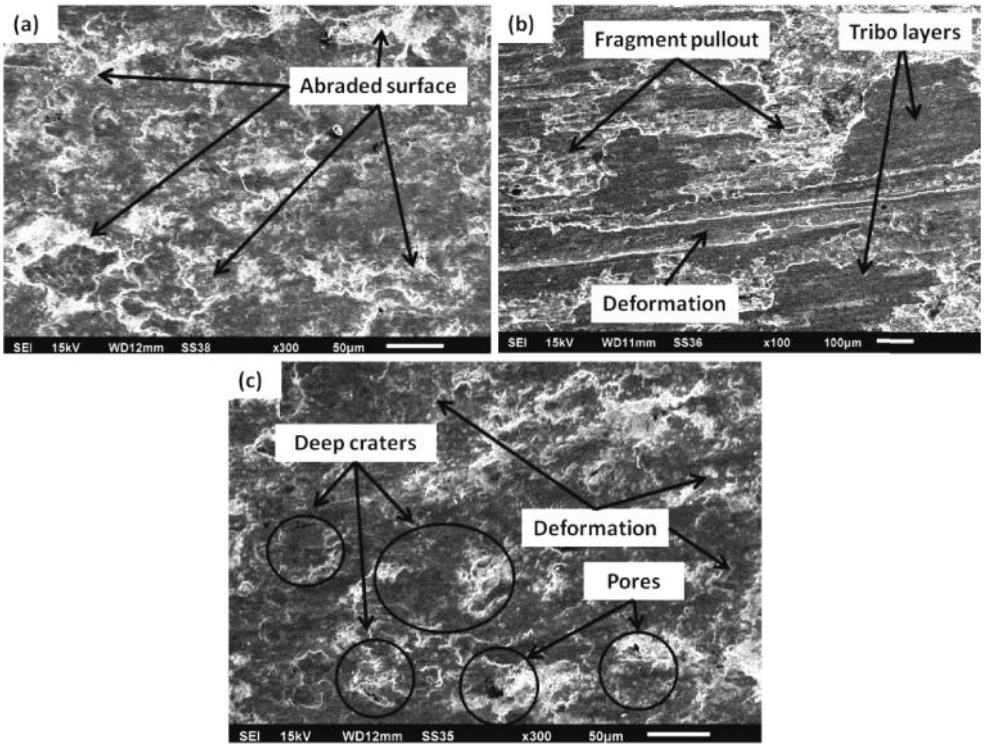

Fig. 6.22: SEM images showing the worn out surfaces at (a) 0.5 m/s (b) 1.0 m/s and (c) 1.5 m/s sliding velocity

Surface topography revealed the formation of some tribo layers at 1.0 m/s sliding velocity and at extreme velocities of 0.5 m/s and 1.0 m/s, the extensive surface abrasion was observed as discussed earlier.

6.4.3 Effect of Sliding Distance on Weight Loss of EWAC+(WC-8Co) Composite Castings

The sliding distance during the wear tests also affects the wear as during the initial rubbing of surfaces there are more chances of weight loss due to initial asperities interlocking and lack of tribo oxide layer formation. After sliding certain distance the surface interactions come into play and formation of tribo layers may affect the weight loss mechanisms. The cumulative weight loss graphs reveal that for the initial 1000 m of sliding there is a linear increase in the weight loss but, after this the wear stablizies and weigh loss trend flattens. For EWAC+5% (WC-8Co) composite, under the low load condition of 10 N, the weight loss curves for all sliding velocities starts achieving stability after 1000 m of sliding as after the initial wear, there was only limited abrasion of surfaces. But as the load increases from 10 N the weight loss continues linearly up to 1500 m of sliding due to enhanced abrasion but as the tribo layers start forming, the weight loss reduces and the curve starts flattening. Similar trends were observed for EWAC+10% (WC-8Co) composite where at 1.0 m/s velocity the formation of tribo layers stabilizes the weight loss after 1000 m of sliding. But it was observed that under 10 N load, the curve again starts to rise after 1500 m of sliding and this may be due to the degradation of protective oxide tribo layers.

The optical microscopic images presented in Fig. 6.23 (a-c) shows the worn out surfaces after 1000 m, 1500 m and 2000 m of sliding distance for EWAC+10% (WC-8Co) composites. During the initial wear, surface abrasion was dominated and as the sliding distance increases, the temperature at the interfaces rise and causes adhesion wear. The rise of temperature also favored

the formation of oxide tribo layers over 1500m of sliding which can be seen from the Fig. 6.23 (b) but, increase in the sliding distance caused ploughing of surface. With further increase in sliding distance, the surface reveals the fragment pullout from the surface and some craters due to excessive ploughing, adhesion and stick slip sliding. The surface degradation after 2000 m of sliding can be judged from the Fig. 6.23 (c).

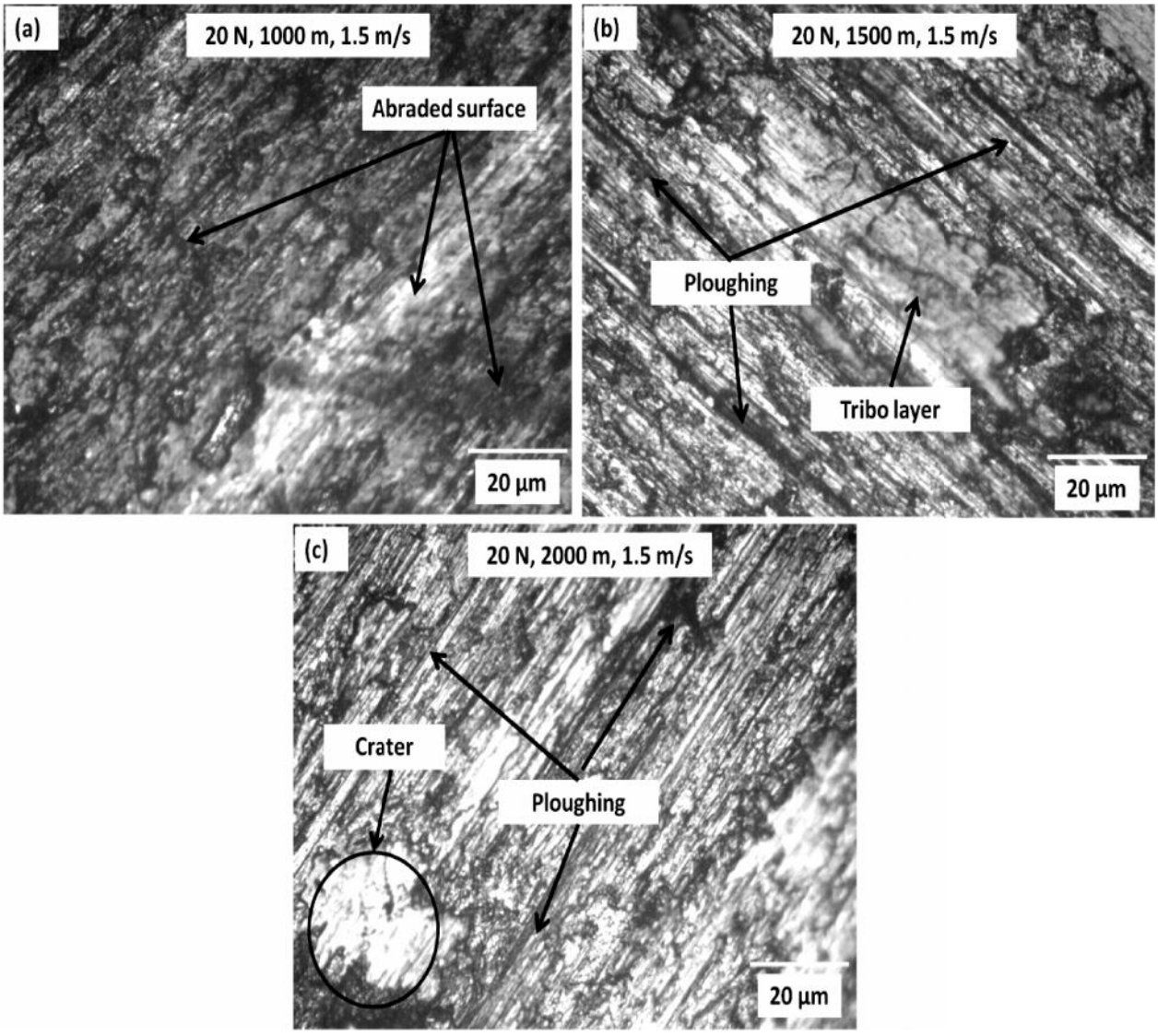

Fig. 6.23: Optical microscopic images of worn out samples after (a) 1000 m, (b) 1500 m and 2000 m of sliding

The wear debris was collected at 20 N load, at 1.0 m/s velocity and after 2000 m of sliding; and analyzed using EDS and results are shown in Fig. 6.24.

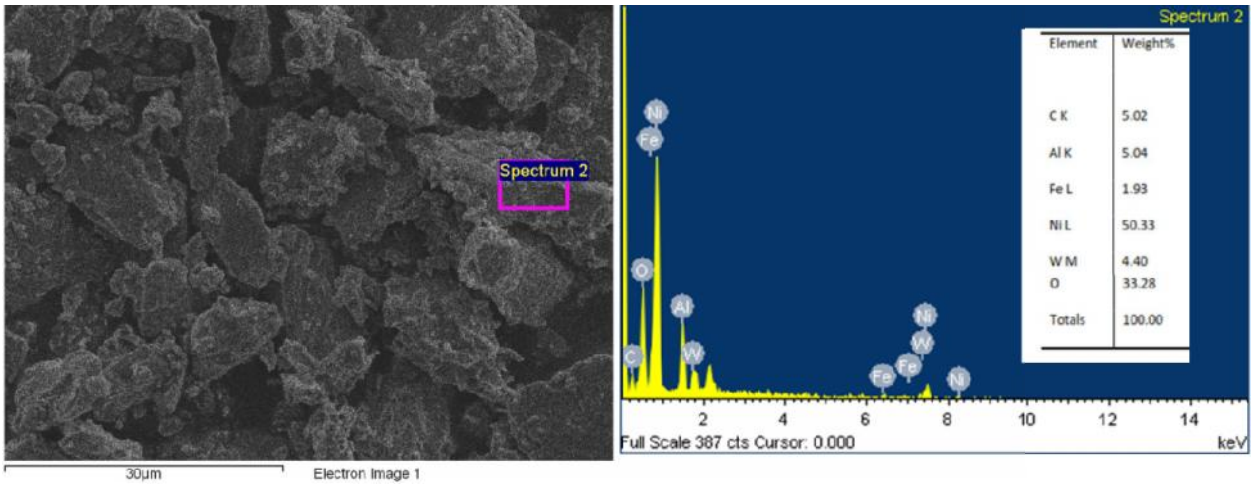

Fig. 6.24: EDS analysis of wear debris collected from EWAC+10%(WC-8Co) composite

The electron image of the debris revealed that the wear occurred mainly in the form of small fragments which were pulled out of the surface and from the smearing of layers. EDS analysis revealed that maximum of the elements were present in their oxide states which was due to the generation of heat which enhanced the oxidation process.

6.5 WEAR RATE COMPARISON OF MICROWAVE PROCESSED CASTINGS

The wear rate of all the microwave composite castings was calculated for the selected test parameters of 20 N load, 1.0 m/s of sliding velocity and 2000 m of sliding. The results are reported in Table 6.1 and are presented in Fig. 6.25. The results revealed that EWAC casting wear rate was highest and presence of various reinforcements lowered the wear rate of castings.

Table 6.1: Wear rate of microwave processed castings at 20 N load, 1.0 m/s of sliding velocity and 2000m of sliding

S. No.	Casting	Wear Rate (10^{-3} mg/s)	Percentage change (in comparison to EWAC casting)
1	Pure EWAC	10.82	0.0%
2	EWAC+5%SiC	4.45	-58.89
3	EWAC+10%SiC	2.10	-80.60
4	EWAC+5%Al_2O_3	3.44	-68.17
5	EWAC+10% Al_2O_3	3.06	-71.68
6	EWAC+5% (WC-8Co)	1.33	-87.67
7	EWAC+10% (WC-8Co)	0.84	-92.24

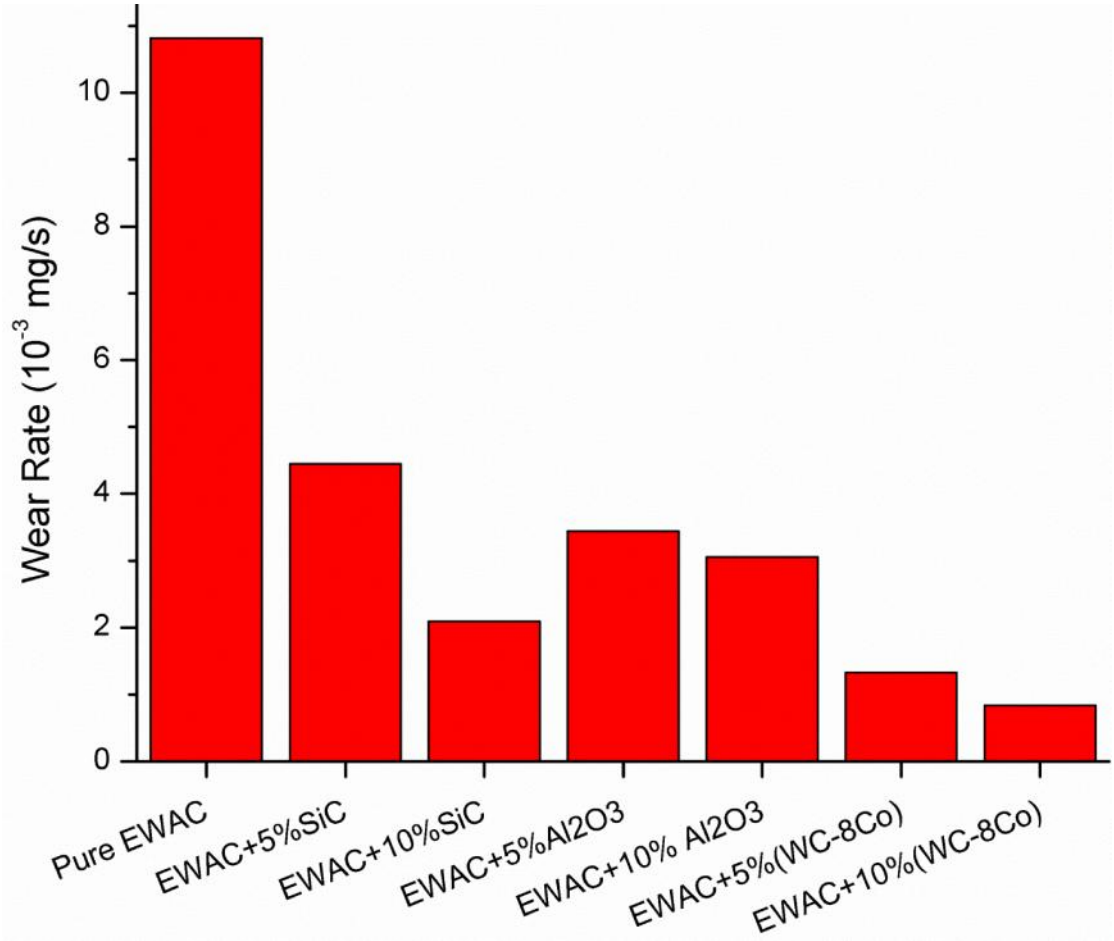

Fig. 6.25: Wear rate comparison of various microwave processed castings

The results revealed that EWAC casting was effective in wear resistance in comparison to EWAC based clads. This resistance is directly linked with development of the intermetallic compounds and enhanced microhardness of EWAC castings.

In the present work, wear rate results revealed that the presence of 10% of reinforcements significantly reduces the wear rate in comparison to 5% reinforced composites. This is again due to the formation of hard intermetallics and enhanced micro hardness on adding 10% reinforcements. In comparison to the pure EWAC casting, 5% SiC reinforced casting produced 58.89% lower wear rate and on increasing the content of SiC reinforcement to 10%, the wear rate was further lowered by 80.60%. The addition of alumina reinforcement lowered the wear rate by 68%-72%, for 5% and 10% volume fraction of reinforcement. This was due to the formation of hard nickel aluminide intermetallic compound which increased the hardness of composites. Presence of WC reinforcements in the EWAC matrix resulted in the lowest wear rate and this was due to the degradation of WC particles in nano metric sizes which were uniformly spread across the composite surface. Presence of WC particles significantly improved the micro hardness, which prevented the abrasion wear up to some extent. The presence of 10% (WC-8Co) reinforcement lowered the wear rate by 92.24% in comparison to the pure EWAC casting.

6.6 SUMMARY

In the present chapter dry sliding wear tests results are presented in term of cumulative weight loss. The effect of selected parameters, i.e. sliding distances, sliding velocities and normal loads; on the weight loss mechanisms are presented with illustrations. The effect of various parameters on the formation and smearing of the oxide layer is as presented and proper justification through SEM and EDS analysis is provided. The effect of presence of varying

volume fraction of reinforcements; on the wear rate is discussed and results are presented with proper illustrations. An overall study revealed that the microwave processed composite castings exhibits the wear resistance properties and can be used in many industrial applications.

CHAPTER 7

CONCLUSIONS AND RECOMMENDATION OF FUTURE WORK

This chapter presents the main conclusions drawn from the present research work, followed by recommendations for the future work in this area.

The major objective of the present work was to utilize the domestic microwave oven working at 2.45 GHz frequency, 900 W max power level; for melting of metallic based powders and to develop metal ceramic composite castings through microwave hybrid heating. Further, the microwave processed MMC's were subjected to the various characterizations. The major conclusions of the present work are summarized below.

7.1 CONCLUSIONS

7.1.1 Development of Metal-Ceramic Composite Castings Through Microwave Energy

The results of feasibility studies on the development of metal-ceramic composite castings revealed that microwave radiations of frequency 2.45 GHz can be successfully employed in the melting of metallic based powders. Following major conclusion are drawn from the experimental results on development of composites:

(a) On increasing the load, i.e. mass of powder to be melted, the processing time increases linearly. Parameters have to be optimized for a given mass of powders for achieving better results.

(b) The microwave power directly affects the processing time required to melt the given mass of powders. Higher the power level, lesser the processing time required for

developments of castings. In the present work maximum power available is 900 W which is optimized for the development of various castings.

(c) The preheating temperature also affects the processing time as preheating of powders causes achievement of critical temperatures quickly and helps in the direct interaction of microwaves of frequency 2.45 GHz with metallic powders. In the present work, the preheating temperature of 200°C lowered the processing time from 27 min to 21 min for EWAC casting. Similar results were obtained for other MMC's.

(d) Presence of reinforcements also lowered the processing time because of better microwave interactions with differenct selected carbide reinforcements. Also, addition of reinforcement lowers the volume of metallic powder to be melted, thus reduces the time required for development of castings.

7.1.2 XRD and Microstructural Characterizations of Microwave Processed Castings

The various castings developed through MHH were subjected to the X-ray diffraction and microstructural analysis by using relevant techniques of XRD, SEM, EDS and optical microscopy. The major conclusions drawn from the results are as follows:

(a) The XRD analysis of various castings revealed the formation of various intermetallics due to the intense microwave heating. In case of EWAC casting the highest peak obtained was of $FeNi_3$. On adding 10% of SiC reinforcement, the intermetallic compound of Ni_2Si, the addition of 10% Al_2O_3 reinforcement produced peak of AlNi and the addition of 10% WC-8Co reinforcement allowed the formation of Ni_4W intermetallic. Formation of chromium carbide was observed in all the castings and this was due to the presence of chromium in the EWAC powder which reacted with free carbon to form carbides.

(b) The microwave processed castings revealed the equiaxed grains throughout the castings and this was due to the fact of volumetric heating associated with microwave heating which restricted the transition of equiaxed structures to dendritic structures. The reinforcements were uniformly distributed within the EWAC matrix.

(c) The EDS analysis of castings revealed that during cooling of the castings, the different carbides were formed and precipitated along the grain boundaries. The results of EDS analysis of microwave processed castings revealed the predominant presence of nickel and silicon on grain surfaces; whereas carbon and chromium is predominantly present along the grain boundaries.

(d) The porosity measurements in various microwave processed castings revealed that maximum porosity of 5.4% was observed in 10 % alumina reinforced composite castings. The main reason behind the presence of lower porosity levels in the casting was the absence of differential heating profile, which allowed uniformity in the cooling and allowed escape of gases before solidification. Porosity in the EWAC casting was in the range of 0.5-1.2%. The SiC reinforced composite casting revealed porosity in the range of 1.68%–1.75%. Similar results were observed for the WC-8Co reinforced castings which revealed porosity content in the range of 1.8-2.6%.

7.1.3 Mechanical Characterizations of Microwave Processed Castings

The mechanical characterizations in terms of Vickers microhardness, tensile strength and percent elongation was evaluated and major conclusions are discussed below.

(a) The results of Vicker's microhardness of microwave processed castings show higher values of microhardness due to the formation of nickel silicides and chromium carbides pahse. EWAC casting revealed the average microhardness of 410±55 HV which is higher

than the EWAC claddings. The addition of various ceramic reinforcements the microhardness further increased. The 10% SiC reinforced composite casting revealed average 980±208 HV of microhardness which is 2.4 times higher than the EWAC casting. By adding 10% of alumina reinforcement the microhardness increased to 985±80 HV and similarly addition of 10%WC-8Co reinforcement produced 1012±108 HV, which is 2.46 times higher than EWAC casting.

(b) Presence of high strength intermetallics in the microwave processed castings led to higher strength. Pure EWAC casting revealed an average tensile strength of 330±15 MPa with average percent elongation of 33±2%. By adding the ceramic reinforcements the load carrying capacity increased, but hard phases of reinforcement restricted the plastic deformations thus producing lower elongations. By increasing the content of SiC to 10% volume fraction, the strength further increased by 26.67% (450±21 MPa) in comparison to EWAC casting with 10.5±2% elongation. The average tensile strength of 10% alumina reinforced composite was 355±10 MPa, with percent elongation of 18±3%. The tensile strength of EWAC+10%(WC-8Co) composite increases to 508±6 MPa, which is 53.93% higher than EWAC casting and average percent elongation of 18±4%.

7.1.4 Functional Characterizations of Microwave Processed Castings

The dry sliding wear tests were performed on the various castings to evaluate their wear resistance and following major conclusions can be drawn from the present work.

(a) For all the microwave processed castings, cumulative weight loss increased with increasing the normal loads from 10 N to 20 N. For pure EWAC casting the weight loss increased from 14.84 mg at the end of 2000 m of sliding at 10 N to 28.68 mg at 20 N of load. This increase in weight loss was due to the increased surface abrasion under high

loads. Similar results were observed for other castings, but weight loss recorded for various microwaves processed MMC's was less in comparison to the EWAC casting. The reduction in weight loss was due to the presence of hard reinforcements which are uniformly distributed over the casting surface and reduces the abrasion of surfaces.

(b) The varying sliding velocities affect the weight loss mechanisms in a significant way. For all the microwave processed castings, the weight loss observed at 1.0 m/s of sliding velocity was low as compared to other velocities. At 1.0 m/s sliding velocity, smooth oxide tribo layer formation was observed and EDS analysis revealed the majority of NiO, SiO_2, and FeO oxides in tribo layer. For 20 N of normal load and after 2000 m of sliding, the EWAC casting revealed weight loss of 21.6 mg at 1.0 m/s of sliding velocity, whereas at 0.5 m/s sliding velocity highest weight loss (28.7 mg) was observed. Similar trends were obtained for most of the castings, which revealed the lower weight loss at 1.0 m/s of sliding velocity.

(c) The effect of sliding distance on the weight loss revealed that at initial sliding distances the weight loss was higher, but after 1000 m of sliding the trend changes and stability was observed for all the castings. This is due to the initial run-in wear which occurs during the initial sliding phase. The asperities present on the surface gets rooted up during initial sliding and this causes smoothness on the surface and stable weight loss trend was observed after 1000 m of sliding.

(d) The wear rate of the microwave processed casting revealed that the most effective anti wear casting is EWAC+10%(WC-8CO). In comparison to the EWAC casting wear rate ($10.82x10^{-3}$ mg/s), the EWAC+10%(WC-8CO) casting revealed 12.8 times lower wear rate ($0.84x10^{-3}$ mg/s) under the 20 N load, 1.0m/s sliding velocity and after 2000 m of sliding. The EWAC+10%SiC casting revealed 5.15 times lower wear ($2.1x10^{-3}$ mg/s) and

EWAC+10%Al_2O_3 casting revealed 3.53 times less wear rate ($3.06x10^{-3}$ mg/s) in comparison to EWAC casting.

7.2 RECOMMENDATION FOR FUTURE WORK

With the present facilities available in the university, the several studies on the development and characterization of microwave processed MMC's was carried out. Some suggestions for the future work are listed below:

(a) In the present work domestic microwave oven working at 900 W maximum power and 2.45 GHz was used. In order to further reduce the processing times industrial microwave applicator with variable frequency and higher power can be used.

(b) Mathematical formulations can be carried out in terms of microwave power, frequency and pre heating time for the processing time required for development of castings.

(c) The effect of processing parameters and type of materials can be studied on the shrinkage of castings. This study can be helpful in the development of near shape and net shape castings.

(d) Effect of inert environment on the properties of castings can be studied in future work.

(e) Optimization of volume fractions of various reinforcements can be carried out for achieving the particular mechanical and functional properties.

LIST OF REFERENCES

[1] Aal A A, Ibrahim K M and Hamid Z A, 2006, Enhancement of Wear Resistance of Ductile Cast Iron by Ni-SiC Composite Coating, Wear, 260, 1070–1075.

[2] Adebisi A A, Maleque M A and Rahman M M, 2011, Metal Matrix Composite Brake Rotor: Historical Development and Product Life Cycle Analysis, International Journal of Automotive and Mechanical Engineering, 4, 471–480.

[3] Agrawal D, 1998, Microwave Processing of Ceramics, Current Opinion in Solid State & Materials Science, 3, 480–485.

[4] Agrawal D, 2006, Microwave Sintering, Brazing and Melting of Metallic Materials, Sohn International Symposium Advanced Processing of Metals and Materials, 4, 183-192.

[5] Agrawal D, 2010, Latest Global Developments in Microwave Materials Processing, Materials Research Innovations, 14, 3–8.

[6] Agrawal D, 2010, Microwave Sintering of Ceramics, Composites and Metal Powders, Ed., Fang, Z Z, Sintering of Advanced Materials. In: Woodhead Publishing Series in Metals and Surface Engineering. Woodhead Publishing, pp 222–248

[7] Agrawal D, Cheng J and Roy R, 2001, Process for Sintering Powder Metal Components, US Patent No. 6183689.

[8] Agrawal, D, Cheng J and Jain Mohit, 2004, Microwave Sintering of Tungsten and Its Alloys, ICHSM 8, 143–145.

[9] Aguilar J, Schievenbusch A and Kättlitz O, 2011, Intermetallics Investment Casting Technology for Production of TiAl Low Pressure Turbine Blades – Process Engineering and Parameter Analysis, Intermetallics, 19, 757–761.

[10] Ahmad S N A S, Hashim J and Ghazali M I, 2007, Effect of Porosity on Tensile Properties of Cast Particle Reinforced MMC, Journal of Composite Materials, 41, 575–589.

[11] Anklekar R M, Agrawal D K and Roy R, 2001, Microwave Sintering and Mechanical Properties of PM Copper Steel, Powder Metallurgy, 44, 355–362.

[12] Apostolos F, Alexios P and Georgios P, 2013, Energy Efficiency of Manufacturing Processes: A Critical Review, Procedia CIRP, 7, 628–633.

[13] Appleton T J, Colder R I, Kingman S W, et al, 2005, Microwave Technology for Energy-Efficient Processing of Waste, Applied Energy, 81, 85–113.

[14] Arasu M and Jeffrey L R, 2009, Energy Consumption Studies in Cast Iron Foundries, Transactions of the 57th IFC, 331–336.

[15] Aravindan S and Krishnamurthy R, 1999, Joining of Ceramic Composites by Microwave Heating. Materials Letters, 38, 245–249.

[16] Ayappa K G, Davis H T, Davis E A, et al., 1991, Analysis of microwave heating of materials with temperature -dependent properties, AIChE Journal, 37 [3], 313-322.

[17] Bahrami M, Helmi N and Dehghani K, 2014, Exploring the Effects of SiC Reinforcement Incorporation on Mechanical Properties of Friction Stir Welded 7075 Aluminum Alloy : Fatigue Life , Impact Energy , Tensile Strength, Materials Science & Engineering A, 595, 173–178.

[18] Balu P, Rea E and Deng J, 2015, Laser Cladding of Nickel-Based Alloy Coatings on Copper Substrates, In: Industrial Laser Applications Symposium 2015, International Society for Optics and Photonics, p 965703

[19] Bansal A, Sharma A K and Das S, 2013, Metallurgical and Mechanical Characterization of Mild Steel-Mild Steel Joint Formed by Microwave Hybrid Heating Process, Sadhana, 38, 679–686.

[20] Bansal A, Sharma A K, Kumar P and Das S, 2014, Characterization of Bulk Stainless Steel Joints Developed through Microwave Hybrid Heating. Materials Characterization, 91, 34–41.

[21] Bansal A, Sharma A, Kumar P, Das S, 2015, Structure–Property Correlations in Microwave Joining of Inconel 718, The Journal of The Minerals, Metals & Materials Society (JOM), 67 [9], 1–12.

[22] Bansal A, Zafar S and Sharma A K, 2015, Microstructure and Abrasive Wear Performance of Ni-WC Composite Microwave Clad, Journal of Materials Engineering and Performance, 24, 3708–3716.

[23] Bao R, Yi J H, Peng Y D, et al., 2015, Skin effect of WC–8 wt% Co Alloy by Microwave Sintering, Rare Metals, 1–5 (published online 23 May 2015).

[24] Bijwe J, Aranganathan N, Sharma S, et al., 2012, Nano-Abrasives in Friction Materials-Influence on Tribological Properties, Wear, 296, 693–701.

[25] Binner J, Wang J, and Vaidhyanathan B, 2007, Evidence for the Microwave Effect During the Annealing of Zinc Oxide, Journal of American Ceramic Society, 90 [9], 2693–2697.

[26] Bist V, Sharma A K and Kumar P, 2014, Development and Microstructural Characterizations of the Lead Casting Using Microwave Technology, i-Manager's Journal on Mechanical Engineering, 4, 6–10.

[27] Borkar T, Sosa J, Hwang J Y, et al., 2014, Laser-Deposited In Situ TiC-Reinforced Nickel Matrix Composites: 3D Microstructure and Tribological Properties, The Journal of The Minerals, Metals & Materials Society (JOM), 66, 935–942.

[28] Borneman K L and Saylor M D, 2008, Microwave Process for Forming a Coating, US Patent No. 0138533A1.

[29] Breval E, Cheng J P, Agrawal D K, et al., 2005, Comparison between Microwave and Conventional Sintering of WC/Co Composites, Materials Science and Engineering: A, 391, 285–295.

[30] Bykov Y V, Egorov S V, Eremeev A G, et al., 2014, Temperature Profile Optimization for Microwave Sintering of Bulk Ni–Al2O3 Functionally Graded Materials, Journal of Materials Processing Technology, 214, 210–216

[31] Bykov Yu V, Rybakov K I and Semenov V E, 2001, High-Temperature Microwave Processing of Materials, Journal of Physics D: Applied Physics, 34, R55–R75.

[32] Cammarota G P, Casagrande A, Poli G and Veronesi P, 2009, Ni–Al–Ti Coatings Obtained by Microwave Assisted SHS: Effect of Annealing on Microstructural and Mechanical Properties, Surface & Coatings Technology, 203, 1429–1437.

[33] Chandrasekaran S, Basak Tanmay and Ramanathan S, 2011, Experimental and Theoretical Investigation on Microwave Melting of Metals, Journal of Material Processing Technology, 211 [3], 482–487.

[34] Cheng J, Agrawal D, Roy R and Jayan P S, 2000, Continuous Microwave Sintering of Alumina Abrasive Grits, Journal of Materials Processing Technology, 108, 26–29.

[35] Cheng J, Agrawal D, Zhang Y and Roy R, 2002, Microwave Sintering of Transparent Alumina, Materials Letters, 56, 587–592.

[36] Cheng J, Agrawal D, Zhang Y, and Roy R, 2001, Microwave Reactive Sintering to Fully Transparent Aluminum Oxynitride (ALON) Ceramic, Journal of Materials Science Letters, 20, 77–79.

[37] Chhillar P, Agrawal D and Adair J H, 2008, Sintering of Molybdenum Metal Powder using Microwave Energy, Powder Metallurgy, 51 [2], 182–187.

[38] Chhillar P, Agrawal D and Adair J H, 2008, Sintering of Molybdenum Metal Powder using Microwave Energy, Powder Metallurgy, 51, 182–187.

[39] Chiu K Y, Cheng F T and Man H C, 2005, A Preliminary Study of Cladding Steel with NiTi by Microwave-Assisted Brazing, Materials Science and Engineering A, 407, 273–281.

[40] Cho Seungyoun and Lee Joonho, 2008, Metal Recovery from Stainless Steel Mill Scale by Microwave Heating, Metals and Materials International, 14 [2], 193–196.

[41] Clark D.E. and Sutton W H, 1996, Microwave Processing of Materials. Annual Review of Materials Science, 26, 299–331.

[42] Clark David E, Folz Diane C and West Jon K, 2000, Processing Materials with Microwave Energy, Materials Science and Engineering A, 287, 153–158.

[43] D Gupta and Sharma A K, 2010, A Method of Cladding/coating of Metallic and Nonmetallic Powders on Metallic Substrate by Microwave Irradiation, Indian Patent No. 527/Del/2010,

[44] Das S, Mukhopadhyay A K, Datta S and Basu D, 2008, Prospects of Microwave Processing: An Overview, Bulletin Material Science, 31 [7], 943–956.

[45] Demirskyi D, Agrawal D and Ragulya A, 2011, Neck Growth Kinetics during Microwave Sintering of Nickel Powder, Journal of Alloys and Compounds, 509, 1790–1795

[46] Demirskyi D, Agrawal D and Ragulya A, 2013, Comparisons of Grain Size-density Trajectory during Microwave and Conventional Sintering of Titanium Nitride. Journal of Alloys and Compounds, 581, 498–501.

[47] Durlu N, 1999, Titanium Carbide Based Composites for High Temperature Applications, Journal of European Ceramic Society, 19, 2415–2419.

[48] El-kady O and Fathy A, 2013, Effect of SiC particle Size on the Physical and Mechanical Properties of Extruded Al matrix Nanocomposites, Materials and Design, 54, 348–353.

[49] Etemadi H, Shojaei A and Jahanmard P, 2014, Effect of Alumina Nanoparticle on The tribological Performance of Automotive Brake Friction Materials, Journal of Reinforced Plastics and Composites, 33 (2), 167–178.

[50] Fang C Y, Randal C A, Lanagan M T and Agrawal D K, 2009, Microwave Processing of Electroceramic Materials and Devices, Journal of Electroceramics, 22, 125–130.

[51] Fathy A, Shehata F, Abdelhameed M, Elmahdy M, 2012, Compressive and Wear Resistance of Nanometric Alumina Reinforced Copper Matrix Composites, Materials and Design, 36, 100–107.

[52] Fisher J G, Woo S K and Bai K, 2003, Microwave Reaction Bonding of Silicon Nitride Using An Inverse Temperature Gradient and ZrO_2 and Al_2O_3 Sintering Additives, Journal of European Ceramic Society, 23, 791–799.

[53] Galletti A M R, Antonetti C, Marracci M, et al., 2013, Novel Microwave-synthesis of Cu Nanoparticles in the Absence of any Stabilizing Agent and their Antibacterial and Antistatic Applications, Applied Surface Science, 80, 610–618.

[54] Gedda H, Kaplan A and Powell J, 2005, Melt-Solid Interactions in Laser Cladding and Laser Casting, Metallurgical and Materials Transactions B, 36, 683–689.

[55] Geedipalli S S R, Rakesh V and Datta A K, 2007, Modeling the Heating Uniformity Contributed by a Rotating Turntable in Microwave Ovens, Journal of Food Engineering, 82, 359–368.

[56] Ghasali E, Pakseresht A H, Agheli M, et al., 2015, WC-Co Particles Reinforced Aluminum Matrix by Conventional and Microwave Sintering, Materials Research 18,1197–1202.

[57] Ghasali E, Pakseresht A, Rahbari A, et al., 2016, Mechanical Properties and Microstructure Characterization of Spark Plasma and Conventional Sintering of Al–SiC–TiC Composites. Journal of Alloys and Compounds, 666, 366–371.

[58] Grewal H S, Singh H and Agrawal A, 2013, Microstructural and Mechanical Characterization of Thermal Sprayed Nickel – Alumina Composite Coatings, Surface and Coatings Technology, 216, 78–92.

[59] Gul H, Kılıc F, Uysal M, et al., 2012, Effect of Particle Concentration on the Structure and Tribological Properties of Submicron Particle SiC Reinforced Ni Metal Matrix Composite (MMC) Coatings Produced by Electrodeposition, Applied Surface Science, 258, 4260–4267.

[60] Guo H-F, Sun T, Li J-L and Yang H-F, 2013, Microstructure and Performance of Ni-based WC Coatings Prepared by Plasma Spraying on TC_4 Titanium Alloy Surface, China Surface Engineering, 2, 1–6.

[61] Guo S, Xu Y, Han Y, et al., 2014, Near Net Shape Casting Process for Producing High Strength 6xxx Aluminum Alloy Automobile Suspension Parts, Transactions of Nonferrous Metals Society of China, 24, 2393–2400.

[62] Gupta D and Sharma A K, 2011, Investigation on Sliding Wear Performance of WC10Co2Ni Cladding Developed Through Microwave Irradiation, Wear, 271, 1642–1650.

[63] Gupta D and Sharma A K, 2012, Microstructural Characterization of Cermet Cladding Developed Through Microwave Irradiation, Journal of Materials Engineering and Performance, 21, 2165–2172.

[64] Gupta D and Sharma A K, 2014, Microwave cladding: A New Approach in Surface Engineering, Journal of Manufacturing Processes, 16, 176–182.

[65] Gupta D, 2012, Microwave Cladding of Metal-based Materials and their Characterisation, PhD Thesis, Indian Institute of Technology Roorkee, Roorkee, India.

[66] Gupta D, Bhovi P M, Sharma A K, et al., 2012, Development and Characterization of Microwave Composite Cladding, Journal of Manufacturing Processes, 14, 243–249.

[67] Gupta M and Wong W L E, 2005, Enhancing Overall Mechanical Performance of Metallic Materials Using Two-Directional Microwave Assisted Rapid Sintering, Scripta Materialia, 52, 479–483.

[68] Harpeness R and Gedanken A, 2004, Microwave Synthesis of Core - Shell Gold / Palladium Bimetallic Nanoparticles, Langmuir, 20 (8), 3431–3434.

[69] Hebbale A M and Srinath M S, 2016, Microstructure and Experimental Design Analysis of Nickel Based Clad Developed Through Microwave Energy, Perspectives in Science, 8, 257–259.

[70] Hossein-zadeh M, Mirzaee O and Saidi P, 2014, Structural and Mechanical Characterization of Al-based Composite Reinforced with Heat Treated Al_2O_3 Particles, Materials and Design, 54, 245–250.

[71] Hrutkay K and Kaoumi D, 2014, Tensile Deformation Behavior of a Nickel Based Superalloy at Different Temperatures, Materials Science and Engineering: A, 599, 196–203.

[72] Huang H, Yang C, Reyes M, et al., 2015, Effect of Milling Time on the Microstructure and Tensile Properties of Ultrafine Grained Ni–SiC Composites at Room Temperature, Journal of Materials Science & Technology, 31, 923–929.

[73] Huang X and Hwang J Y, 2001, Method for direct Metal Making by Microwave Energy, US Patent No. US6277168 B1.

[74] Hwang J Y, Neira A, Scharf T W, et al., 2008, Laser-deposited Carbon Nanotube Reinforced Nickel Matrix Composites, Scripta Materialia, 59, 487–490.

[75] Jerby E, Meir Y, Salzberg A, et al., 2013, Stepwise Consolidation of Metal Powder by Localized Microwaves for Additive Manufacturing of 3D Structures, 14th International Conference on Microwave and High Frequency Heating, AMPERE-2013, UK, 345–348.

[76] Jerby E, Meir Y, Salzberg A, et al., 2015, Incremental Metal-powder Solidification by Localized Microwave-heating and its Potential for Additive Manufacturing, Additive Manufacturing, 6, 53–66.

[77] Kalaria P C, Kartikeyan M V and Thumm M, 2014, Design of 170 GHz, 1.5-MW Conventional Cavity Gyrotron for Plasma Heating, IEEE Transactions on Plasma Science, 42, 1522–1528.

[78] Kang H K and Kang S B, 2006, Thermal Decomposition of Silicon Carbide in a Plasma-Sprayed Cu/SiC Composite Deposit, Materials Science and Engineering: A, 428, 336–345.

[79] Katz J D, 1992, Microwave sintering of ceramics, Annual Reviws in Materials Science, 22, 153–170.

[80] Kaushal S, Gupta D and Bhowmick H, 2017a, Investigation of Dry Sliding Wear Behavior of Ni–SiC Microwave Cladding, Journal of Tribology, 139:41603–41609.

[81] Kaushal S, Gupta D and Bhowmick H, 2017b, An Approach for Functionally Graded Cladding of Composite Material on Austenitic Stainless Steel Substrate Through Microwave Heating, Journal of Composite Materials (published online 20 April 2017).

[82] Kaushal S, Sirohi V, Gupta D, et al, 2015, Processing and Characterization of Composite Cladding Through Microwave Heating on Martensitic Steel, Proceedings of the Institution of Mechanical Engineers, Part L: Journal of Materials Design and Applications (published online 8 Nov 2015).

[83] Kim J, Mun S, Ko H U, et al., 2012, Review of Microwave Assisted Manufacturing Technologies, International Journal of Precision Engineering and Manufacturing, 13, 2263–2272.

[84] Klinowski J and Paz A A, 2011, Microwave-Assisted Synthesis of Metal – Organic Frameworks, Dalton Transactions, 40, 321–330.

[85] Komarneni S, Pidugu R, Li Q H and Roy R, 1995, Microwave-Hydrothermal Processing of Metal Powders, Journal of Materials Research, 10, 1687–1692.

[86] Kriegsmann G A, 1997, Hot Spot Formation In Microwave Heated Ceramic Fibres IMA Journal of Applied Mathematics, 59, 123–148.

[87] Krupashankara S M and Kalyanaraman R, 2002, Microwave Plasma Chemical Synthesis of Ultrafine Powders, US Patent No.US6409851 B1.

[88] Kubel E, 2005, Advancement in Microwave Heating Technology, Industrial Heating, 62, 43-53.

[89] Kumar R, Bhandari S and Goyal A, 2017, Slurry Erosion Performance of High-Velocity Flame-Sprayed Conditions, Journal of Thermal Spray Technology (published online 17 July 2017).

[90] Kumari L, Zhang T, Du G H, et al., 2008, Thermal Properties of CNT-Alumina Nanocomposites, Composites Science and Technology, 68, 2178–2183.

[91] Laurent C, Budinger D E, Vasile Bogdan, N and Holly Sue S, 2008, Process of Microwave Brazing with Powder Materials, U.S. Patent No., 7326892.

[92] Leonelli C, Veronesi P, Denti L, et al., 2008, Microwave Assisted Sintering of Green Metal Parts, J. Mater. Process. Technol., 205, 489–496.

[93] Lim C Y H, Leo D K, Ang J J S and Gupta M, 2005, Wear of Magnesium Composites Reinforced With Nano-Sized Alumina Particulates, Wear, 259, 620–625.

[94] Lingappa S M, Srinath M S, Amarendra H J, 2018, Melting of Bulk Non-Ferrous Metallic Materials by Microwave Hybrid Heating (MHH) and Conventional Heating : A Comparative Study on Energy Consumption, Journal of the Brazilian Society of Mechanical Sciences and Engineering, 7, 1–11.

[95] Link G, Feher L, Thumm M, et al, 1999, Sintering of Advanced Ceramics Using a 30-GHz, 10-kW, CW Industrial Gyrotron, IEEE Transactions on Plasma Science, 27, 547–554.

[96] Liu C Y, Wang Q, Jia Y Z, et al., 2013, Evaluation of Mechanical Properties of 1060-Al Reinforced with WC Particles via Warm Accumulative Roll Bonding Process, Materials and Design, 43, 367–372.

[97] Liu R, Hao T, Wang K, et al., 2012, Microwave Sintering of W/Cu Functionally Graded Materials, Journal of Nuclear Materials, 431, 196–201.

[98] Liu W, Ma Y and Zhang J, 2012, Properties and Microstructural Evolution of W-Ni-Fe Alloy via Microwave Sintering, International Journal of Refractory Metals and Hard Materials, 35, 138–142.

[99] Liu X B, Yu L G, Wang H M, 2001, Synthesis of a nickel Silicide-Base Composite Coating on Austenitic Steel by Laser Cladding, Journal of Materials Science Letters, 20, 1489–1492.

[100] Livshits P, Dikhtyar V, Inberg A, et al., 2011, Local Doping of Silicon by a Point-contact Microwave Applicator, Microelectronic Engineering, 88, 2831–2836.

[101] Luo J, Hunyar C, Feher L, et al, 2004, Potential Advantages for Millimeter-Wave Heating of Powdered Metals, International Journal of Infrared and Millimeter Waves, 25:1271–1283.

[102] Malinauskas M, Albertas Z, Hasegawa S, et al., 2016, Ultrafast Laser Processing of Materials : From Science to Industry, Light: Science & Applications, 5, 1–14.

[103] Manickavasagan A, Jayas D S and White N D G, 2006, Non-uniformity of Surface Temperatures of Grain after Microwave Treatment in an Industrial Microwave Dryer, Drying Technology, 24, 1559–1567.

[104] Mazahery A and Shabani M O, 2013, Microstructural and Abrasive Wear Properties of SiC Reinforced Aluminum-Based Composite Produced by Compocasting, Transactions of Nonferrous Metals Society of China, 23, 1905–1914.

[105] Mincuzzi G, Vesce L, Reale A, et al., 2012, Laser Processing of TiO_2 Films for Dye Solar Cells : A Thermal , Sintering , Throughput and Embodied Energy Investigation, Progress In Photovoltaics: Research And Applications, 2012, 1–10.

[106] Mishra P, Upadhyaya A and Sethi G, 2006, Modeling of Microwave Heating of Particulate Metals, Metallurgical and Materials Transactions B, 37, 839–845.

[107] Mishra R R and Sharma A K, 2016a, Microwave–Material Interaction Phenomena: Heating Mechanisms, Challenges and Opportunities in Material Processing, Composites Part A: Applied Science and Manufacturing, 81, 78–97.

[108] Mishra R R and Sharma A K, 2016b, A Review of Research Trends in Microwave Processing of Metal-Based Materials and Opportunities in Microwave Metal Casting, Critical Reviews in Solid State and Materials Sciences, 41, 217–255.

[109] Mishra R R and Sharma A K, 2016c, On Mechanism of In-Situ Microwave Casting of Aluminium Alloy 7039 and Cast Microstructure, Materials and Design, 112, 97–106.

[110] Mizuno M, Obata S, Takayama S and Ito S, 2004, Sintering of Alumina by 2.45 GHz Microwave Heating, Journal of the European Ceramic Society, 24, 387–391.

[111] Mohanavel V, Rajan K and Kumar K R S, 2015, Study on Mechanical Properties of AA6351 Alloy Reinforced with Titanium Di-Boride (TiB_2) Composite by In Situ Casting Method, Applied Mechanics and Materials, 787:583–587.

[112] Mondal A, Upadhyaya A and Agrawal D, 2009, Microwave Sintering of W-18Cu and W-7Ni-3Cu Alloys, International Microwave Power Institute, 43 [1], 11–16.

[113] Mondal A, Upadhyaya A and Agrawal D, 2010, Microwave and Conventional Sintering of 90W–7Ni–3Cu Alloys with Premixed and Prealloyed Binder Phase, Materials Science and Engineering: A, 527, 6870–6878.

[114] Mondal A, Upadhyaya A and Agrawal D, 2013, Effect of Heating Mode and Copper Content on the Densification of W-Cu Alloys, Indian Journal of Materials Science, Article ID 603791, 1–7.

[115] Moore A F, Schechter D E and Morrow M S, 2006, Method and Apparatus for Melting Metals, US Patent No. US7011136 B2.

[116] Nadagouda M N, Speth T F and Varma R S, 2011, Microwave-Assisted Green Synthesis of Silver Nanostructures, Accounts of Chemical Research, 44, 469–478.

[117] Narasimhan K S V L, Arvidsson J, Rutz H G and Porter W J, 1995, Methods and Apparatus for Heating Metal Powders, US Patent No. US5397530 A

[118] Narsimhan K S V L, Arvidsson J, Rutz G H, et al., 1995, U.S. Patent No. 5397530.

[119] Nishitani T, 1979, Method for Sintering Refractories and An Apparatus Therefor, US Patent 4,147,911.

[120] Oghbaei M and Mirzaee O, 2010, Microwave Versus Conventional Sintering: A Review of Fundamentals, Advantages and Applications, Journal of Alloys and Compounds, 494, 175–189.

[121] Omrani E, Dorri M A, Menezes P L and Rohatgi P K, 2016, New Emerging Self lubricating Metal Matrix Composites for Tribological Applications BT - Ecotribology: Research Developments. In: Davim JP (ed), Springer International Publishing, Cham, pp 63–103

[122] Ozben T, Kilickap E and Orhan C, 2007, Investigation of Mechanical and Machinability Properties of SiC Particle Reinforced Al-MMC, Journal of Materials Processing Technology, 8, 220–225.

[123] Padmavathi C, Agrawal D, and Upadhayaya A, 2008a, Microwave Sintering of Aluminium Alloys, Ist Global Congress on Microwave Energy Applications, Japan, 153–58.

[124] Panda S S, Singh V, Upadhyaya A and Agrawal D, 2006, Sintering Response of Austenitic (316L) and Ferritic (434L) Stainless Steel Consolidated in Conventional and Microwave Furnaces, Scripta Materialia, 54, 2179–2183.

[125] Pathania A, Singh S, Gupta D, et al., 2015, Development and Analysis of Tribological Behavior of Microwave Processed EWAC + 20% WC10Co2Ni Composite Cladding on Mild Steel Substrate, Journal of Manufacturing Processes, 20 (1), 79–87.

[126] Pauleau Y, Thiery F, Latrasse L, et al., 2004, Characteristics of Copper/Carbon and Nickel/Carbon Composite Films produced by Microwave Plasma-assisted Deposition Techniques from Argon–methane Gas Mixtures. Surface and Coatings Technology, 188, 484–488.

[127] Peelamedu R D, Roy R and Agrawal D K, 2002, Microwave-induced Reaction Sintering of $NiAl_2O_4$, Materials Letters, 55, 234–240.

[128] Pozar D M, 2009, Microwave Engineering, John Wiley & Sons.

[129] Prabhu G., Chakraborty A and Sarma B, 2009, Microwave Sintering of Tungsten, Int. Journal of Refractory Metals & Hard Materials, 27, 545–548.

[130] Prasad S V and Asthana R, 2004, Aluminum Metal-Matrix Composites for Automotive Applications: Tribological Considerations, Tribology Letters, 17, 445–453.

[131] Rajan T P D and Pai B C, 2014, Developments in Processing of Functionally Gradient Metals and Metal–Ceramic Composites: A Review, Acta Metallurgica Sinica (English Letters), 27, 825–838.

[132] Rajkumar K and Aravindan S, 2009, Microwave Sintering of Copper–Graphite Composites, Journal of Materials Processing Technology, 209, 15-16, 5601–5605.

[133] Rajkumar K and Aravindan S, 2011, Tribological Performance of Microwave Sintered Copper–TiC–Graphite Hybrid Composites, Tribology International, 44, 347–358.

[134] Rajkumar K and Aravindan S, 2013, Tribological Behavior of Microwave Processed Copper–Nanographite Composites, Tribology International, 57, 282–296.

[135] Reck B K, Muller D B, Rostkowski K, et al, 2008, Anthropogenic Nickel Cycle : Insights into Use, Trade, and Recycling, Environmental Science & Technology, 42, 3394–3400.

[136] Reddy B S and Ray B K, 2010, Energy for Sustainable Development Decomposition of Energy Consumption and Energy Intensity in Indian Manufacturing Industries, ESD, 14, 35–47.

[137] Rhee S, Shrout T R, Link G, et al., 2003, Investigation of High Frequency (2.45GHz, 30GHz) Sintering of Pb-Based Ferroelectrics, Journal of the Ceramic Society of Japan, 111, 312–317.

[138] Rodiger K, Dreyer K, Willert-Porada M and Gerdes T, 2001, Hard Metal or Cermet Sintered Body and Method for the Production thereof, US Patent No. US6293986.

[139] Roy R, Agrawal D, Cheng J, et al., 1999, Full Sintering of Powdered-Metal Bodies In A Microwave Field, Nature, 399, 668–670.

[140] Sadagopan P, Natarajan H K and J P K, 2017, Study of Silicon Carbide-Reinforced Aluminum Matrix Composite Brake Rotor for Motorcycle Application, International Journal of Advance Manufacturing Technology, 94, 1461–1475.

[141] Saitou K, 2006, Microwave Sintering of Iron, Cobalt, Nickel, Copper and Stainless Steel Powders. Scripta Materialia, 54, 875–879.

[142] Sajjadi S A, Ezatpour H R and Torabi Parizi M, 2012, Comparison of Microstructure and Mechanical Properties of A356 Aluminum Alloy/Al_2O_3 Composites Fabricated by Stir and Compo-Casting Processes, Materials and Design, 34, 106–111.

[143] Sallom Z K, Akselsen O M, and Zhang J, 2005, Brazing of Gamma TiAl with Ag based Filler Metal, Euro mat, 1–30.

[144] Salonitis K, Zeng B, Mehrabi H A, et al., 2016, The Challenges for Energy Efficient Casting Processes, Procedia CIRP, 40, 24–29.

[145] Saltiel C and Datta A K, 1999, Heat and Mass Transfer in Microwave Processing, Advances in Heat Transfer, 33, 1–94.

[146] Scharf T W, Neira A, Hwang J Y, et al., 2010, Self-lubricating Carbon Nanotube Reinforced Nickel Matrix Composites, Journal of Applied Physics, 106, 013508, 1-7.

[147] Seo Y and Kang C, 1995, The Effect of Applied Pressure on Particle-Dispersion Characteristics and Mechanical Properties in Melt-Stirring Squeeze-Cast SiCp / A1 Composites, Journal of Materials Processing Technology, 55, 370–379.

[148] Sethi G, Upadhyaya A and Agrawal D, 2003, Microwave and Conventional Sintering of Premixed and Prealloyed Cu-12Sn Bronze, Science of Sintering, 35, 49–65.

[149] Sharma A K and Krishnamurthy R, 2002, Microwave Processing of Sprayed Alumina Composite for Enhanced Performance, Journal of European Ceramic Society, 22, 2849–2860.

[150] Sharma A K, Aravindhan S and Krishnamurthy R, 2001, Microwave Glazing of Alumina–Titania Ceramic Composite Coatings, Mater Lett, 50, 295–301.

[151] Sharma A K, Srinath M S and Pradeep K, 2009, Microwave Joining of Metallic Materials, Indian Patent No. 1994/Del/2009.

[152] Sheinberg H, Meek T and Blake R, 1990, U.S. Patent No. 4,942,278.

[153] Shi Q, Gu D, Xia M, et al., 2016, Effects of Laser Processing Parameters on Thermal Behavior and Melting / Solidification Mechanism During Selective Laser Melting of TiC/Inconel 718 Composites, Optics and Laser Technology, 84, 9–22.

[154] Shin D J and Min D, 2013, Investigation on the Decomposition of Al_2O_3 Using an Electrochemical Method, ISIJ International, 53:434–440.

[155] Singh S, Singh R, Gupta D, Jain V, 2017, Preliminary Metallurgical and Mechanical Investigations of Microwave Processed Hastelloy Joints, Journal of Manufacturing Science and Engineering, 139, 1–5.

[156] Siores E, and Rego D, 1995, Microwave Applications in Materials Joining, Journal of Materials Processing Technology, 48, 619–25.

[157] Spencer P L, 1945, Method of Treating Foodstuffs, US Patent No. 2495429 A.

[158] Spotz M S, Skamser D J and Johnson D L, 1995, Thermal Stability of Ceramic Materials in Microwave Heating, Journal of the American Ceramic Society, 78, 1041–1048.

[159] Srinath M S and Hebbale A M, 2017, Fuzzy Prediction of Slurry Erosive Behavior of Cobalt Based Clad Developed Through Microwave Energy, Materials Today: Proceedings, 4, 1804–1811.

[160] Srinath M S, Sharma A K and Kumar P, 2011a, A New Approach to Joining of Bulk Copper Using Microwave Energy, Materials and Design, 32, 2685–2694.

[161] Srinath M S, Sharma A K and Kumar P, 2011b, A Novel Route for Joining of Austenitic Stainless Steel (SS-316) Using Microwave Energy, Proceedings of the Institution of Mechanical Engineers, Part B: Journal of Engineering Manufacture, 225, 1083–1091.

[162] Srinath M S, Sharma A K and Kumar P, 2011c, Investigation on Microstructural and Mechanical Properties of Microwave Processed Dissimilar Joints, Journal of Manufacturing Processes, 13, 141–146.

[163] Srivastava M, Grips V K W, Jain A and Rajam K S, 2007, Influence of SiC Particle Size on the Structure and Tribological Properties of Ni – Co Composites, Surface & Coatings Technology, 202,310–318.

[164] Suryanarayanan K, Praveen R and Raghuraman S, 2013, Silicon Carbide Reinforced Aluminium Metal Matrix Composites for Aerospace Applications: A Literature Review,

International Journal of Innovative Research in Science, Engineering and Technology, 2, 6336–6344.

[165] Sutton W H, 1989, Microwave Processing of Ceramic Materials, Ceramic Bulletin, 68, 376–386.

[166] Takayama S, Link G, Sato M and Thumm M, 2004, Sintering of Metal Powder Samples with Millimeter Wave Technology, In: Infrared and Millimeter Waves, Conference Digest of the 2004 Joint 29th International Conference on 2004 and 12th International Conference on Terahertz Electronics, pp 729–730.

[167] Takayama Sadatsugu, Link Guido, Matsubara Akihiro, Sano Saburo, Sato Motoyasu and Thumm Manfred, 2008, Microwave Frequency Effect for Reduction of Magnetite, Plasma and Fusion Research: Regular Articles, 3, S1036-1–4.

[168] Tazegul O, Muhaffel F, Meydanoglu O, et al., 2014, Wear and Corrosion Characteristics of Novel Alumina Coatings Produced by Micro Arc Oxidation on AZ91D Magnesium Alloy, Surface and Coatings Technology, 258, 168–173.

[169] Thakur Sanjay Kumar, Kong Tung Siew and Gupta Manoj, 2007, Microwave Synthesis and Characterization of Metastable (Al/Ti) and Hybrid (Al/Ti + Sic) Composites, Materials Science and Engineering A, 452–453, 61–69.

[170] Thostenson E T and Chou T W, 1999, Microwave Processing: Fundamentals and Applications, Composites: Part A, 30, 1055–71.

[171] Torres F and Jecko B, 1997, Complete FDTD analysis of Microwave Heating Processes in Frequency-Dependent and Temperature-Dependent Media, Microwave Theory and Techniques, IEEE Transactions on Microwave theory and Techniques, 45, 108–117.

[172] Upadhyaya A, Tiwari S K and Mishra P, 2007, Microwave Sintering of W–Ni–Fe Alloy, Scripta Materialia, 56, 5–8.

[173] Venkateswarlu K, Saurabh Suman, Rajinikanth V, Sahu Ranjan Kumar and Ray Ajoy Kumar, 2010, Synthesis of TiN Reinforced Aluminium Metal Matrix Composites through Microwave Sintering, Journal of Materials Engineering and Performance, 19 [2], 231–236.

[174] Veronesi P, Colombini E, Rosa R, et al., 2016, Microwave Assisted Synthesis of Si-Modified Mn25FexNi25Cu(50−x) High Entropy Alloys, Materials Letters, 162, 277–280.

[175] Veronesi P, Colombini E, Rosa R, et al., 2017, Microwave Processing of High Entropy Alloys: A Powder Metallurgy Approach. Chemical Engineering and Processing: Process Intensification, 122, 397-403

[176] Walczak M, Pieniak D and Zwierzchowski M, 2014, The Tribological Characteristics of SiC Particle Reinforced Aluminium Composites, Archives of Civil and Mechanical Engineering, 15, 116–123.

[177] Walkiewicz J W, Kazonich G, and McGill S L, 1988, Microwave Heating Characteristics of Selected Minerals and Compounds, Minerals and Metallurgical Processing, 39–42.

[178] Whittaker A G and Mingos D M P, 1995, Microwave-assisted Solid-state Reactions Involving Metal Powders, Journal of the Chemical Society, Dalton Transactions, 12, 2073–2079.

[179] Wilhelm R, 1990, Method and Apparatus for PCVD Internal Coating a Metallic Pipe by means of a Microwave Plasma, US Patent No. US4897285A.

[180] Willert-Porada MA, Rosin A, Pontiller P, et al., 2015, Additive Manufacturing of Ceramic Composites by Laser Assisted Microwave Plasma Processing, LAMPP. Microwave Symposium (IMS), IEEE MTT-S International, 1–4.

[181] Wong W L E and Gupta M, 2006, Simultaneously Improving Strength and Ductility of Magnesium using Nano-size SiC Particulates and Microwaves. Advanced Engineering Materials, 8, 735–740.

[182] Wong W L E and Gupta M, 2007, Development of Mg/Cu Nanocomposites using Microwave Assisted Rapid Sintering, Composites Science and Technology, 67, 1541–1552.

[183] Xu D, Li J, Meng Q, et al., 2014, Effect of Heating Rate on Microstructure and Mechanical Properties of TRIP-aided Multiphase Steel, Journal of Alloys and Compounds, 614, 94–101.

[184] Ya B, Zhou B, Yang H, et al., 2015, Microstructure and Mechanical Properties of In Situ Casting TiC/Ti6Al4V Composites Through Adding Multi-Walled Carbon Nanotubes. Journal of Alloys and Compounds, 637, 456–460.

[185] Yahaya B, Izman S, Konneh M, Redzuan N, 2014, Microwave Hybrid Heating of Materials Using Susceptors - A Brief Review, Advanced Materials Research, 845, 426–430.

[186] Zafar S and Sharma A K, 2014, Development and Characterisations of WC–12Co Microwave Clad, Materials Characterizations, 96, 241–248.

[187] Zafar S and Sharma A K, 2015, Dry Sliding Wear Performance of Nanostructured WC–12Co Deposited Through Microwave Cladding, Tribology International, 91, 14–22.

[188] Zafar S and Sharma A K, 2016, Abrasive and Erosive Wear Behaviour of Nanometric WC–12Co Microwave Clads, Wear, 346, 29–45.

[189] Zeng C, Tian W, Liao W H and Hua L, 2016, Microstructure and Porosity Evaluation in Laser-Cladding Deposited Ni-Based Coatings, Surface and Coatings Technology, 294, 122–130.

[190] Zhan Y and Zhang G, 2004, Friction and Wear Behavior of Copper Matrix Composites Reinforced with SiC and Graphite Particles, Tribology Letters, 17, 91–98.

[191] Zhao Y, Zhu J, Hong J, et al., 2004, Microwave-Induced Polyol-Process Synthesis of Copper and Copper Oxide Nanocrystals with Controllable Morphology, European Journal of Inorganic Chemistry, 20, 4072–4080.

[192] Zhen J, Li F, Zhu S, et al., 2014, Friction and Wear Behavior of nickel-Alloy-Based High Temperature Self-Lubricating Composites Against Si_3N_4 and Inconel 718. Tribiology International, 75, 1–9.

[193] Zhu J and Zhu Y, 2006, Microwave-Assisted One-Step Synthesis of Polyacrylamide - Metal (M = Ag , Pt , Cu) Nanocomposites in Ethylene Glycol, Journal of Physical Chemistry B, 110 (17) 8593–8597.

[194] Zhu J, Kuznetsov A V and Sandeep K P, 2007, Mathematical Modeling of Continuous Flow Microwave Heating of Liquids (Effects of Dielectric Properties and Design Parameters). International Journal of Thermal Sciences, 46, 328–341.

APPENDIX-A

Fig. A-1: Low speed diamond cutter (Make: DUCOM, Model: MS-10, Courtesy: Microwave materials processing lab, Thapar Institute of Engineering & Technology)

Fig. A-2: X-Ray Diffractometer (XRD) (Courtesy: SAI Labs, Thapar Institute of Engineering & Technology)

Fig. A-3: Optical Microscope (Courtesy: A.M. Lab, Thapar Institute of Engineering & Technology)

Fig. A-4: Scanning Electron Microscope (Courtesy: SAI Labs, Thapar Institute of Engineering & Technology)

Fig. A-5: Vickers Micro-hardness Tester (Courtesy: A.M. Lab, Thapar Institute of Engineering & Technology)

Fig. A-6: Universal tensile testing machine (Courtesy: Mechanical Engg. Dept., IIT Ropar)

Fig. A-7: Pin on disc tribometer **(**wear and friction monitor) (Courtesy: Tribology Lab, Thapar Institute of Engineering & Technology**)**

LIST OF VISIBLE OUTPUT

- **Patent**

1. Singh S, Gupta D, Jain, V and Kumar R, 2015, A method for metal ceramic composite casting through microwave energy. Indian patent no. 2051/DEL/2015 (Applied for).

- **List of SCI/SCIE Papers**

1. Singh S, Gupta D, Jain, V, 2017, Processing of Ni-WC-8Co MMC casting through microwave melting, Materials and Manufacturing Processes, 1-9. *Status: Published Online, Publisher: Taylor & Francis, Impact Factor: 1.41, Category: SCI*
2. Singh S, Gupta D, Jain, V, 2016, Novel microwave composite casting process: Theory, feasibility and characterization, Materials and Design, 111, 51–59. *Status: Published, Publisher: Elsevier, Impact Factor: 4.36, Category: SCI*
3. Singh S, Gupta D, Jain, V, 2016, Microwave melting and processing of metal-ceramic composite castings, Proceedings of the Institution of Mechanical Engineers, Part B: Journal of Engineering Manufacture, 1-9. *Status: Published Online, Publisher: Sage, Impact Factor: 1.366, Category: SCI*
4. Singh S, Gupta D, Jain, V, 2015, Recent applications of microwaves in materials joining and surface coatings, Proceedings of the Institution of Mechanical Engineers, Part B: Journal of Engineering Manufacture, 230; 603-617. *Status: Published, Publisher: Sage, Impact Factor: 1.366, Category: SCI*
5. Singh S, Gupta D, Jain, V and Sharma A K, 2015, Microwave processing of materials and applications in manufacturing industries: A review, Materials and Manufacturing

Processes, 30 [1]; 1-29. *Status: Published, Publisher: Taylor & Francis, Impact Factor: 1.41, Category: SCI*

6. Singh S, Gupta D, Jain, V, 2017. Microwave processing of powdered metal matrix composite castings, Powder Metallurgy. *Status: Under Review, Publisher: Taylor & Francis, Impact Factor: 0.779, Category: SCI*

- **List of International Conference Attended**

1. Singh S, Gupta D, Jain, V, 2016, Some developments on metal-ceramic composite castings through microwave energy. Presented at HES16 (International conference on heating through electromagnetic sources) held in May, 2016 at Padua (Italy).
2. Singh S, Gupta D, Jain, V, 2017, Microwave processing of powdered metal matrix composite castings. Presented at RoPM&AM (5th International Conference on Powder Metallurgy & Advanced Materials) held in September, 2017 at Cluj-Napoca (Romania).

- **List of Book Chapters**

Singh, S., Gupta, D., Jain, V, 2016, An energy efficient processing route for advance ceramic composites using microwaves. In *Advanced Ceramic Materials* (Eds. Ashutosh Tiwari and Rosario A.G.), Willey, 2016, pp. 97-144.